Conserving dynamical mean-field approaches to strongly correlated systems

Dissertation

zur Erlangung des Doktorgrades

des Fachbereichs Physik

der Universität Hamburg

vorgelegt von
Friedrich KRIEN
aus Münster in Westfalen

Hamburg 2018

Gutachter der Dissertation:

Prof. Dr. Alexander Lichtenstein

Prof. Dr. Michael Potthoff

Gutachter der Disputation:

Prof. Dr. Alexander Lichtenstein

Prof. Dr. Michael Potthoff

Prof. Dr. Daniela Pfannkuche

Prof. Dr. Gleb Arutyunov

Prof. Dr. Nils Huse

Datum der Disputation:

Hamburg, den 26. 4. 2018

Vorsitzender des Prüfungsausschusses:

Prof. Dr. Daniela Pfannkuche

Vorsitzender des Promotionsausschusses:

Prof. Dr. Wolfgang Hansen

Dekan des Fachbereichs Physik:

Prof. Dr. Heinrich Graener

"Warum plagen wir einer den andern?
Das Leben zerrinnt, und es versammelt uns nur einmal wie heute die Zeit."

Friedrich von Schiller

Kurzzusammenfassung In dieser Arbeit präsentiere ich numerische Verfahren, deren Ziel es ist die Spektren kollektiver Anregungen in stark korrelierten Elektronensystemen zu bestimmen. Einige qualitative Eigenschaften dieser Spektren hängen mit Erhaltungssätzen zusammen, die nur schwer erfüllbar sind. Im Jahr 1989 wurde eine Theorie entdeckt, die eine realistische Beschreibung kollektiver Anregungen ermöglicht, sogar wenn die elektronischen Wechselwirkungen stark sind: Die dynamische Molekularfeldtheorie. Diese Theorie ist zu einer der wichtigsten Methoden geworden um korrelierte Systeme zu beschreiben, sowie die charakteristischen Phänomene die in ihnen auftreten, wie die Supraleitung, der Magnetismus oder die Mott-Isolatorphase. Große Anstrengungen werden weltweit unternommen, um den Anwendungsbereich dieser Theorie zu vergößern, zum Beispiel auf langreichweitige Wechselwirkungen. In dieser Arbeit präsentiere ich mehrere Anwendungen von Methoden jenseits der dynamischen Molekularfeldtheorie und ich untersuche, aufgrund der Bedeutung der Erhaltungssätze für kollektive Anregungen, ob diese erfüllt werden können. Tatsächlich wurde diese Frage bereits im Jahr 1962 in einer Arbeit von Gordon Baym [15] abschließend beantwortet, aber nicht auf die genaue Weise wie wir sie heute brauchen. Die Aussagen die von G. Baym bewiesen wurden sind so formuliert wie sie damals am nützlichsten erschienen, als Theoretiker noch häufig die Kontinuumsnotation des Viel-Teilchenproblems verwendeten. Heute wird hingegen zumeist die Gitternotation verwandt. Ich glaube, dass häufig übersehen wird, dass einige der wichtigen Aussagen die G. Baym damals für das Kontinuum beweisen konnte auf dem Gitter nicht allgemein gültig sind, darauf möchte ich Aufmerksamkeit lenken und einige Lösungsvorschläge anbieten.

Die Frage nach Erhaltungssätzen ist eng verbunden mit einer fundamentalen Gleichung, der Ward-Identität. Leider wirkt diese Gleichung abstrakt, obwohl sie lediglich eine Umformulierung der Kontinuitätsgleichung darstellt. Wie die Arbeit G. Baym's wird die Ward-Identität häufig im Kontinuum formuliert. Es ist dann nicht offensichtlich, wie nützlich sie im Rahmen von Gitter- und Störstellenmodellen sein kann, was ich detailliert beschreibe. Wenn man die Ward-Identität in der Gitternotation untersucht wird klar an welcher Stelle die Gültigkeit der Baymschen Theorie unterlaufen wird, leider war ich nicht in der Lage diese Lücke zu schließen. Ein Ziel dieser Arbeit ist es daher das vorliegende Problem genau zu dokumentieren, um eine Basis für eine zukünftige Lösung zu schaffen.

Die verbleibende Diskussion bezieht sich auf die dynamische Molekularfeldtheorie. Ich zeige, dass diese Theorie von der Ward-Identität abgeleitet werden kann und dass dies ihre Vorzüge bezüglich der Erhaltungssätze besonders zum Vorschein bringt. Diese Herangehensweise ermöglicht auch einen Einblick wie die dynamische Molekularfeldtheorie für langreichweitige Wechselwirkungen verallgemeinert werden sollte, wobei unerwartete Unterschiede zwischen Wechselwirkungen in den Ladungs- und den Spinkanälen zutage treten. Gleichzeitig komme ich zu dem Schluss, dass das dynamische Molekularfeld nicht verändert werden sollte, wenn die Wechselwirkung kurzreichweitig ist. Begleitend zu diesen Betrachtungen werden vier Anwendungen der dynamischen Molekularfeldtheorie und verwandter Theorien diskutiert. Diese betreffen kollektive Anregungen nahe eines Mott-Übergangs, die Beschreibung von Magnonen in einem Antiferromagneten, langreichweitige Wechselwirkungen und thermodynamische Konsistenz.

Abstract In this thesis I present numerical methods that are designed to calculate the spectra of collective excitations in strongly correlated systems. Several qualitative features of these spectra are related to conservation laws, which are very difficult to satisfy. In 1989 a theory was discovered that is able to describe collective excitations realistically, even when electronic interactions are strong: The dynamical mean-field theory. This theory has become one of the most important tools to understand correlated systems and phenomena that are characteristic for them, such as superconductivity, magnetism, or the Mott-insulating state. Huge efforts are made worldwide to extend the range of applicability of the dynamical mean-field theory, for example, to long-ranged interactions. In this work I present several applications of methods beyond dynamical mean-field theory and, due to the importance of conservation laws for collective excitations, I examine if these can be satisfied. In fact, already in 1962 a work of Gordon Baym [15] answered this question once and for all, but not quite in the exact way that we need today. The statements that were proven by G. Baym are formulated in the form that seemed most useful back then, when theorists were still using the continuum notation of the many-body problem most of the time. Today, however, one usually makes use of the lattice notation. I believe that it is often overlooked that some of the powerful statements that G. Baym was able to derive for the continuum are not in general valid on the lattice, and of this I like to raise awareness and offer some ideas for a solution.

The question of conservation laws is closely related to a fundamental equation, the Ward identity. Unfortunately, this identity seems abstract, while it is merely a reformulation of the continuity equation. Like G. Baym's paper, the Ward identity is often formulated in the continuum. It is then not very obvious how useful it can be in the context of lattice and impurity models, of which I give a detailed account. When one examines the Ward identity in the lattice notation, it becomes clear at which point G. Baym's theory is undercut, but unfortunately I was not able to close this gap. Therefore, a central objective of this text is to document this problem in detail, in order to provide a basis for a future solution.

The remaining discussion concerns the dynamical mean-field theory. I show that this theory can be derived from the Ward identity and that this makes its conserving features very explicit. This approach also gives an idea of how the dynamical mean-field theory should be generalized to long-ranged interactions, where unexpected distinctions occur between interactions in the charge and in the spin channels. On the same note, I also have to conclude that the dynamical mean-field should not be changed when the interaction is short-ranged. Along the way I discuss four applications of the dynamical mean-field theory and its derivatives. These are related to collective excitations near a Mott transition, to the description of magnons in an antiferromagnet, to long-ranged interactions, and to thermodynamic consistency.

Contents

Reading guide

A   A shortened version of the material is marked with Q

B   For results related to physics (no technicalities) follow P

C   Click on section headers to return to the table of contents

Chapter 1

A case for the solid state

A Foreword

Renowned theoretician P.W. Anderson was once asked in an interview by S. Sondhi what he replies to laypeople when they like to know about his field of research. Anderson answered that he had gotten used to the fact that he often encounters bewilderment that such a field as condensed matter physics even exists. Since the interview was conducted in 1999 this situation has changed very little. Reports in the media on physics focus almost exclusively on the subjects of astronomy, cosmology and particle physics. It seems that in the view of many people these fields provide the most complete description of nature. To find the building blocks of matter, and to understand the nature of space and time, presumably implies the completion of physics.

It would not be the first time that claims of this kind were made: In 1874 young student Max Planck was advised not to study physics, since the field was depleted of fundamental questions. Despite his spectacular rebuttal of this viewpoint, it seems that today it is still widely believed that the microscopic laws of physics, now complemented by cosmology, form a theory of everything. The change in this reductionist viewpoint seems to lie only in a rewriting of the fundamental rules. What happens at large is a mere collection of superficial phenomena, which are reducible to some most fundamental building blocks and laws of nature.

To me it seems that this form of reductionism is such a persistent worldview because it is an adequate philosophy around the industrialized production and of the technological innovation that have deeply shaped our societies. Almost all technologies that are and were in widespread use are reducible in the sense that each of their components has a clearly defined purpose. We assume that at least the maker of a machine knows how its components work as a whole. But the solutions for practical problems that are available to us today are biased towards approaches that we find easy to understand. If our brains were made to understand networks more easily than calculus, we would likely have better theories of stock markets than of celestial dynamics. I like to suggest the following interpretation of the widespread (and honest) ignorance towards condensed matter physics: The fields of astronomy, cosmology and fundamental particles seem more essential to us because they remind us of the machinery that surrounds us, and that we find predictable because we have shaped it in ways we understand.

But couldn't we profit greatly from promoting the idea that phenomena found in complex systems can be *independent* from the specifics of their parts? It is well worth knowing for laypeople that condensed matter physics is a field where such questions are addressed, and sometimes understood, in some of the deepest ways known to science.

B   Structure and scope

QP   This thesis is divided into five chapters, where the following one, chapter 2, merely states the definitions of single-band Hamiltonians and of one- and two-particle correlation functions in Sec. A, and of the 1P and 2P self-energies in Sec. B. The integral Schwinger-Dyson equation is derived in Sec. C.

Chapter 3 is devoted to conservation laws. It begins with a short summary of the Baym & Kadanoff theory in Sec. B, which mainly consists of the functional Schwinger-Dyson equation and of the functional Ward identity. Then, the integral Ward identity is derived in Sec. C for lattice and impurity models, including phases with broken symmetry. Sec. D is a comprehensive account of exact statements that follow from the Ward identity. Most of these statements are already known, but often formulated in the continuum, hidden in appendices, and, in any case, scattered over many papers. Derivations are provided for (almost) all statements that are used later in the text, and for a few more that are physically appealing. Probably the most important one is the consistency of zero-field derivatives and fluctuations in Sec. D.6. It is shown in Sec. E that the functional Schwinger-Dyson equation and Ward identity are mirror images of the respective integral relations, provided that the interaction of the considered system conserves the charge and spin densities. Simple conserving approximations, such as the Hartree-Fock approximation in Sec. E.2, are inserted into the Ward identity explicitly, in order to demonstrate the perfect correspondence of the Baym&Kadanoff theory to this type of system. Finally, in Sec. F it is shown that this correspondence ends when the interaction does not conserve the charge or spin densities, which leads to anomalous currents and Ward identities. Before it is proven in Sec. H that the Hartree-Fock approximation violates the Ward identity of such a system, the basics of three-particle irreducibility are introduced in Sec. G, which are necessary for the proof. I recommend to skip this proof, unless it is of immediate interest, and to jump right to the conclusions in Sec. I, which give an intuitive interpretation of this result.

The dynamical mean-field theory (DMFT) is introduced in chapter 4, where it is derived in a novel way from the Ward identities of the Hubbard and of the Anderson impurity model in Sec. A.3. This derivation avoids the Luttinger-Ward functional and instead makes only use of quantities that are known numerically exactly and can be looked at explicitly. For DMFT itself this is a mere sleight of hand, while it proves useful later to validate conservation laws where it is less clear if they hold. The susceptibility of DMFT is formulated in Sec. B, highlighting its relation to the dual fermion and dual boson approaches. The sublime aspects of DMFT in terms of thermodynamic consistency are discussed in Sec. C, followed by some basics regarding the two-particle spectrum in Sec. D. Finally, there follow two applications of DMFT. The low-temperature revival of a collective mode near the

Mott transition is discussed in Sec. E and an approximation of the DMFT susceptibility by single-particle quantities in Sec. F.

In the last chapter 5 two-particle self-consistent dynamical mean-field approaches are motivated in two ways. In Sec. A the dual boson approach is motivated from the Ward identity of an extended Hubbard model with nonlocal charge-charge interactions. It is thus a natural extension of the dynamical mean-field picture to long-ranged interactions. It is found in Sec. A.6 that it is inherently more difficult to derive a similar approximation for a lattice model with exchange interactions. The discussion of long-ranged interactions concludes in Sec. B with the presentation of an exact diagonalization solver for the extended dynamical mean-field theory. Two-particle self-consistency is motivated for short-ranged interactions in Sec. C, as a means to heal the violation of the Mermin-Wagner theorem in DMFT, and to allow a feedback of collective excitations on its impurity model. Unfortunately, in Sec. C.2 I come to the conclusion that approximations to the Hubbard model that establish a two-particle self-consistency condition via retarded interactions in the impurity model have to be refuted on principle grounds. In the conclusions in Sec. C.3 this is related to the earlier findings of chapter 3, which imply that such approximations undermine the applicability of the Baym & Kadanoff formalism. Lastly, Sec. D shows an application of a two-particle self-consistent version of DMFT, highlighting the few benefits and many penalties of modifying the best aspect of DMFT, its dynamical mean-field.

Chapter 2

One- and two-particle correlation functions

"Sooft ich meine Tabakspfeife,
Mit gutem Knaster angefüllt,
Zur Lust und Zeitvertreib ergreife,
So gibt sie mir ein Trauerbild.
Und füget diese Lehre bei,
Dass ich derselben ähnlich sei."

- J. S. Bach

This chapter introduces the definitions and the notation used in the rest of the text. In the discussion of the many-body Hamiltonians the differences between the continuum and the lattice notation are highlighted.

A   Hamiltonians, operators, and correlation functions functions

In the continuum, one defines the Hamiltonian of a many-electron system as follows,

$$
\begin{aligned}
H = \sum_\sigma \int d^3r \Psi_\sigma^\dagger(\mathbf{r}) \left(-\frac{\Delta_\mathbf{r}}{2} + v(\mathbf{r}) \right) \Psi_\sigma(\mathbf{r}) \\
+ \frac{1}{2} \sum_{\sigma\sigma'} \int \int d^3r d^3r' \Psi_\sigma^\dagger(\mathbf{r}) \Psi_{\sigma'}^\dagger(\mathbf{r}') V(|\mathbf{r} - \mathbf{r}'|) \Psi_{\sigma'}(\mathbf{r}') \Psi_\sigma(\mathbf{r}),
\end{aligned}
\tag{A.1}
$$

Here,

$$
H_0 = \sum_\sigma \int d^3r \Psi_\sigma^\dagger(\mathbf{r}) \left(-\frac{\Delta_\mathbf{r}}{2} + v(\mathbf{r}) \right) \Psi_\sigma(\mathbf{r}),
\tag{A.2}
$$

describes the kinetic motion of many non-interacting electrons in a periodic potential of static ions $v(\mathbf{r})$. Electrons of spin σ are created (annihilated) at location $\mathbf{r}$ by the fermionic field operators $\Psi_\sigma^{(\dagger)}(\mathbf{r})$. The Coulomb interaction between the electrons is denoted as

$$H_{\text{int}} = \frac{1}{2} \sum_{\sigma\sigma'} \int\int d^3r\, d^3r'\, \Psi_\sigma^\dagger(\mathbf{r})\Psi_{\sigma'}^\dagger(\mathbf{r}')V(|\mathbf{r}-\mathbf{r}'|)\Psi_{\sigma'}(\mathbf{r}')\Psi_\sigma(\mathbf{r}), \tag{A.3}$$

where $V(|\mathbf{r}-\mathbf{r}'|) = |\mathbf{r}-\mathbf{r}'|^{-1}$ is the Coulomb potential.

A.1 Charge and spin densities of the continuum

Of interest for microscopic conservation laws is the time-evolution of the electronic charges and spins. In the following, $n(\mathbf{r}) = \sum_\sigma \Psi_\sigma^\dagger(\mathbf{r})\Psi_\sigma(\mathbf{r})$ denotes the charge density operator in real space. More generally, one defines the density operators,

$$\varrho^\alpha(\mathbf{r}) = \sum_{\sigma\sigma'} \Psi_\sigma^\dagger(\mathbf{r})s_{\sigma\sigma'}^\alpha\Psi_{\sigma'}(\mathbf{r}), \tag{A.4}$$

where $s_{\sigma\sigma'}^\alpha$ are the Pauli matrices. With $s_{\sigma\sigma'}^c = \delta_{\sigma\sigma'}$ one recovers the charge density, $\varrho^c(\mathbf{r}) = n(\mathbf{r})$, whereas $\alpha = x, y, z$ yield the spin density operators. The operators $S^\alpha = \varrho^\alpha/2$ obey the commutation relations $[S^\alpha, S^\beta] = \sum_\gamma \varepsilon_{\alpha\beta\gamma}S^\gamma$, and one may extend the definition of the Levi-Civita symbol to $\varepsilon_{\alpha\beta\gamma} = 0$ in case one of its labels α, β, γ is equal to the charge flavor c. This reflects the fact that the charge density commutes with all other densities and itself, $[\varrho^c, \varrho^\alpha] = 0$ for each α. Despite the characteristic commutation relations, the spin density operators $\varrho^{x,y,z}$ are not proper spin operators, for reasons explained below.

The above notation is most useful in absence of discrete translational symmetry, such as in the physics of liquid Helium [150]. To approach quantum lattice problems, the continuum notation is rarely used anymore, since it does not make use of the periodicity of the ionic potential $v(\mathbf{r} + \mathbf{R}) = v(\mathbf{r})$. This makes the continuum picture unfavorable in numerical approaches, due to the continuous spatial variable $\mathbf{r}$.

A particular advantage of the continuum over the lattice notation is the simplicity of the Coulomb potential, which is an interaction between charge densities. Such an interaction gives an energetic incentive to electrons to avoid each other in order to minimize their potential energy. However, the Coulomb potential does not contribute to the charge current, which reflects in the commutativity of the Coulomb potential with the charge density, $[n(\mathbf{r}), H_{\text{int}}] = 0$. Likewise, the Coulomb interaction does not cause spin currents either,

$$[\varrho^\alpha, H_{\text{int}}] = 0, \tag{A.5}$$

for the charge and spin densities, $\alpha = c, x, y, z$. These commutation relations also become intuitively clear, considering that the operator combination $\Psi_\sigma^\dagger(\mathbf{r})\Psi_{\sigma'}^\dagger(\mathbf{r}')V(|\mathbf{r}-\mathbf{r}'|)\Psi_{\sigma'}(\mathbf{r}')\Psi_\sigma(\mathbf{r})$ acting on a Fock state $|\Psi\rangle$ annihilates and recreates two electrons at $\mathbf{r}$ and $\mathbf{r}'$ with spins σ and σ'. Taking the double integral over the real space, this operation thus merely counts the total potential energy of the electronic configuration represented by $|\Psi\rangle$, but leaves the

configuration itself unchanged. This feature of the Coulomb interaction is exclusive to the continuum notation and lost when making use of the discrete translational symmetry of the ionic lattice.

A.2 One- and two- particle Green's function in the continuum

Since it is not possible to compute and store all eigenvalues and eigenfunctions of a large electronic system, one aims to approximate electronic correlation functions, which contain greatly compacted information about the thermodynamic, spectral, and critical properties of the many-body system described by H. In most cases it is sufficient to consider the single- and two-particle Green's functions, where

$$G(\mathbf{r}, \mathbf{r}', \tau, \tau', \sigma, \sigma') = -\langle T_\tau \Psi_\sigma(\mathbf{r}, \tau) \Psi_\sigma^\dagger(\mathbf{r}', \tau) \rangle \delta_{\sigma\sigma'}, \tag{A.6}$$

is the single-particle (1P) Green's function[1]. In this work only the notation in imaginary time $\tau \in [0, \beta]$ will be used, where $\beta = 1/T$ is the inverse temperature. The time-dependence of the field-operators is meant in the Heisenberg picture,

$$\Psi^{(\dagger)}(\tau) = e^{\tau \mathcal{H}} \Psi^{(\dagger)}(0) e^{-\tau \mathcal{H}}. \tag{A.7}$$

The brackets $\langle \cdots \rangle = \mathcal{Z}^{-1} \sum_n e^{-\beta E_n} \langle n| \cdots |n \rangle$ denote a thermal average in the system $\mathcal{H} = H - \mu N$ with eigenstates $|n\rangle$ and eigenenergies E_n, where $N = \int d^3r\, n(\mathbf{r})$ is the total particle number operator. $\mathcal{Z} = \sum_n e^{-\beta E_n}$ is the partition sum. $\Psi^{(\dagger)}(0)$ is a time-independent field-operator in the Schrödinger picture. T_τ is the time-ordering operator, which sorts operators at larger times to the left and creation operators to the left of annihilators at equal time, always accounting for as many minus signs as needed for the respective permutation. Therefore, $G(\mathbf{r}, \mathbf{r}, \tau, \tau, \sigma, \sigma) = \langle n_\sigma(\mathbf{r}) \rangle$ yields the average particle number at $\mathbf{r}$, which is time-independent in the equilibrium. Using the fact that the 1P Green's function depends only on time-differences and is diagonal in spin-space, the short-hand notation $G(\mathbf{r}, \mathbf{r}', \tau, \tau', \sigma, \sigma) = G_{\mathbf{rr}'\sigma}(\tau - \tau')$ will be used in the following.

While there is essentially universal agreement on the definition of the 1P Green's function, many different conventions exist for the two-particle (2P) Green's function. In this text variants of the following definition will be used,

$$G^{(2)}(1, 2, 3, 4) = -\langle T_\tau \Psi_1 \Psi_2^\dagger \Psi_3 \Psi_4^\dagger \rangle, \tag{A.8}$$

with superindices $1 = (\mathbf{r}_1, \tau_1, \sigma_1)$.

A.3 The lattice notation

We now turn to the lattice notation for a single-band system, which is introduced by a change to the Wannier basis (time, spin, flavor, ... label will be dropped where it improves

---

[1]The definition of Green's function in Eq. (A.6) assumes paramagnetism or at least collinear magnetic order.

readability),

$$\Psi(\mathbf{r}) = \sum_i \phi_i(\mathbf{r}) c_i, \tag{A.9}$$

where the $\phi_i(\mathbf{r})$ are the Wannier functions and c_i a Wannier operator. They satisfy the orthogonality relation $\int d^3 r \phi_i^*(\mathbf{r}) \phi_j(\mathbf{r}) = \delta_{ij}$. Correspondingly, the density operators of the continuum transform as

$$\varrho^\alpha(\mathbf{r}) = \sum_{\sigma\sigma'} \Psi_\sigma^\dagger(\mathbf{r}) s_{\sigma\sigma'}^\alpha \Psi_\sigma(\mathbf{r}) = \sum_{ij\sigma\sigma'} \phi_i^*(\mathbf{r}) \phi_j(\mathbf{r}) c_{i\sigma}^\dagger s_{\sigma\sigma'}^\alpha c_{j\sigma'}. \tag{A.10}$$

In analogy to the continuum, one defines the charge and spin density operators of the lattice,

$$\rho_i^\alpha = \sum_{\sigma\sigma'} c_{i\sigma}^\dagger s_{\sigma\sigma'}^\alpha c_{i\sigma'}, \tag{A.11}$$

which likewise satisfy the commutation relations $[\rho^\alpha, \rho^\beta] = 2 \sum_\gamma \varepsilon_{\alpha\beta\gamma} \rho^\gamma$. It should be noted here that despite their spin algebra, the $\rho^{x,y,z}/2$ are not proper spin operators, since they act in the Hilbert space spanned by

$$|0\rangle,$$
$$|\uparrow\rangle = c_\uparrow^\dagger |0\rangle,$$
$$|\downarrow\rangle = c_\downarrow^\dagger |0\rangle,$$
$$|\updownarrow\rangle = c_\uparrow^\dagger c_\downarrow^\dagger |0\rangle,$$

which include the vacuum $|0\rangle$ and the doubly occupied state $|\updownarrow\rangle$. Other than proper spin operators, which act only in the space spanned by $|\uparrow\rangle$ and $|\downarrow\rangle$, the ρ^α may be represented by fermionic coherent states in the path integral formalism, rather than by spin coherent states. For spins $\frac{1}{2}$ and 1 a mapping between the ρ^α and proper spin operators exists, leading to a Berry phase [105].

Trivial but nevertheless not intuitive is that the density operator $\varrho(\mathbf{r})$ in Eq. (A.10) is a local operator in the continuum while its Wannier representation is nonlocal. The point charge represented by the charge density $\varrho^c(\mathbf{r})$ in the continuous space, which is most intuitively identified with the electron itself, is hence a complicated superposition of hopping operators $c_i^\dagger c_j$. Likewise, when writing the occupation number $\rho_i^c = \sum_\sigma c_{i\sigma}^\dagger c_{i\sigma}$ in the continuum notation, one sees that the latter is neither identifiable with an electron of the continuum, nor with a simple superposition of several 'direct' electrons,

$$\rho_i^c = \sum_{\sigma\sigma'} \int \int d\mathbf{r} d\mathbf{r}' \phi_i(\mathbf{r}) \phi_i^*(\mathbf{r}') \Psi_\sigma^\dagger(\mathbf{r}) \Psi_\sigma(\mathbf{r}'). \tag{A.12}$$

An identification of lattice and continuum electrons is possible when the system contains only a single site i with one orbital, $\varrho^c(\mathbf{r}) = |\phi(\mathbf{r})|^2 \sum_\sigma c_{i\sigma}^\dagger c_{i\sigma} = |\phi(\mathbf{r})|^2 n_i$, or globally,

$$N = \int d^3 r \varrho(\mathbf{r}) = \sum_{ij\sigma} \int d^3 r \phi_i^*(\mathbf{r}) \phi_j(\mathbf{r}) c_{i\sigma}^\dagger c_{j\sigma} = \sum_{ij\sigma} \delta_{ij} c_{i\sigma}^\dagger c_{j\sigma} = \sum_i n_i, \qquad (A.13)$$

since the total charge (and likewise spin) must be the same in both notations. Hence, classifying the 'direct' electrons of the continuum by the site (and possibly orbital) indices of the ionic lattice is an arbitrary distinction made by the theoretician. This entails complication of the many-body Hamiltonian when transferred to the lattice notation,

$$H = \sum_{ij\sigma} c_{i\sigma}^\dagger t_{ij} c_{j\sigma} + \frac{1}{2} \sum_{\sigma\sigma'} \sum_{ijkl} c_{i\sigma}^\dagger c_{j\sigma'}^\dagger V(ij,kl) c_{l\sigma'} c_{k\sigma}. \qquad (A.14)$$

The hopping amplitude t_{ij} and the matrix elements $V(ij,kl)$ of the Coulomb interaction are overlap integrals of the Wannier functions with the operators of kinetic and potential energies in Eq. (A.1). In the following, they will be treated as free parameters.

A.4 Classification of the Coulomb matrix elements

The price one pays for introducing the lattice notation is a complication of the interaction Hamiltonian. One may classify its matrix elements into charge-charge interactions,

$$n_i V(ij, ij) n_j, \qquad (A.15)$$

spin-spin interactions,

$$-\boldsymbol{\rho}_i V(ij, ji) \boldsymbol{\rho}_j, \qquad (A.16)$$

where $\boldsymbol{\rho} = (\rho^x, \rho^y, \rho^z)$, pair hoppings ($\bar{\sigma} = -\sigma$),

$$c_{i\sigma}^\dagger c_{i\bar{\sigma}}^\dagger V(ii, jj) c_{j\bar{\sigma}} c_{j\sigma}, \qquad (A.17)$$

and processes involving more than two sites i and j. If the interaction is local, spin conservation and Pauli principle allow only for one type of interaction, the Hubbard repulsion $U = V(ii, ii)$. Sometimes, long-ranged charge-charge interactions $V_{ij} = V(ij, ij)$ are taken into account. With respect to the (ferromagnetic) direct exchange interaction $J_{ij} = V(ij, ji)$, the general philosophy is that it should be neglected. This is due to the fact that almost all single-band Hamiltonians are model Hamiltonians, intended to capture effective physics of multi-band systems. The inter- and intra-orbital interactions, such as the Hund's rule exchange, are of much greater importance than the tiny inter-site exchange integral, or should at least be considered alongside. Similarly, one will hardly find discussions of a single-band system with pair hopping, etc.

Considering the matrix elements of the Coulomb interaction without a bias with respect to their physical significance, one finds that some of them are more challenging to treat than others. For instance, the nonlocal charge-charge interaction $n_i V_{ij} n_j$ commutes with all lattice density operators ρ_i^α (since $[\rho^\alpha, n] = 0$). This interaction thus conserves the charge and spin quantum number. The states $|0\rangle, |\uparrow\rangle, |\downarrow\rangle, |\updownarrow\rangle$ of the occupation number basis are eigenstates of this interaction. The direct exchange $\boldsymbol{\rho}_i J_{ij} \boldsymbol{\rho}_j$, on the other hand, commutes only with the charge density $\rho_i^c = n_i$, not with the spin density $\rho_i^{x,y,z}$. Similarly, a pair hopping operator $c_\uparrow^\dagger c_\downarrow^\dagger$ does not conserve the particle number n and as a general statement,

$$[\rho^\alpha, H_{\text{int}}] \neq 0. \tag{A.18}$$

Most of the time, however, the theoretician is getting away in a rather favorable situation: While the Coulomb interaction is diagonal in the continuous basis, $|\mathbf{r}\sigma\rangle = \Psi_\sigma^\dagger(\mathbf{r})|0\rangle$, and off-diagonal in the Wannier basis, $|i\sigma\rangle = c_{i\sigma}^\dagger|0\rangle$, the diagonal elements are in most circumstances dominant, while the rest may be safely neglected. This may be said notwithstanding frequently used effective spin Hamiltonians (Heisenberg model, Kondo lattice model, etc.), which describe localized moments coupled via exchange to other local moments or itinerant electrons. The point here is that in such cases the itinerant nature of the electrons forming the local moments is neglected. In fact, besides the t-J model, one rarely considers magnetic moments that are itinerant *and* coupled via exchange to other itinerant moments.

A.5   Correlation functions on the lattice

We now turn to the definition of the lattice Green's functions, starting with the single-particle Green's function,

$$G_{ij\sigma}(\tau - \tau') = -\langle T_\tau c_{i\sigma}(\tau) c_{j\sigma}^\dagger(\tau')\rangle, \tag{A.19}$$

$$G_{\mathbf{k}\sigma}(\tau - \tau') = -\langle T_\tau c_{\mathbf{k}\sigma}(\tau) c_{\mathbf{k}\sigma}^\dagger(\tau')\rangle, \tag{A.20}$$

which is diagonal in the spin index due to spin conservation, and which depends only on the difference between the time labels. Here, i and j denote sites of the discrete lattice and $\mathbf{k}$ the lattice momentum. These representations are connected via the Fourier transform $G_{\mathbf{k}} = \sum_{ij}' G_{ij} e^{i(\mathbf{r}_i - \mathbf{r}_j)\mathbf{k}}$, where $\mathbf{r}_i, \mathbf{r}_j$ are discrete lattice vectors. The summation $\sum'$ implies a factor of N^{-1}, where N is the number of lattice sites. Similarly, $G_{ij} = \sum_{\mathbf{k}}' G_{\mathbf{k}} e^{-i(\mathbf{r}_i - \mathbf{r}_j)\mathbf{k}}$, this summation as well implies multiplication by N^{-1} (they arise in both the forward and backward transformation due to the double summation over i, j). The Fourier transform may also be applied to the creation and annihilation operators individually, using

$$c_{\mathbf{k}} = \frac{1}{\sqrt{N}} \sum_i c_i e^{i\mathbf{r}_i \mathbf{k}} \quad \text{and} \quad c_i = \frac{1}{\sqrt{N}} \sum_{\mathbf{k}} c_{\mathbf{k}} e^{-i\mathbf{r}_i \mathbf{k}}. \tag{A.21}$$

This is the case, because the thermal average $\langle \cdots \rangle$, as well as the time-ordering operator T_τ, commute with the Fourier transformation between i and $\mathbf{k}$. Matsubara's Green's function

is defined as,

$$G_{ij\nu\sigma} = \int_0^\beta d\tau\, G_{ij\sigma}(\tau - 0)e^{\iota\nu\tau} = " - \langle c_{i\nu\sigma} c_{j\nu\sigma}^\dagger\rangle ", \tag{A.22}$$

where $\nu_n = (2n + 1)\pi/\beta$ are the fermionic Matsubara energies and $\beta = T^{-1}$ is the inverse temperature. The last expression above is put into quotation marks, since it is, strictly speaking, incorrect. The integral $\int_0^\beta d\tau$ of the Matsubara transform commutes with the thermal average but not with the time-ordering operator, the operator $c(\tau)$ may thus not be transformed individually when subjected to time-ordering. Although in certain cases the above notation can lead to incorrect results, it is nevertheless very useful to remind oneself which operators and Matsubara frequencies belong together. In particular with respect to the single-particle Green's function one considers $\langle T_\tau c(\tau)c^\dagger(0)\rangle$ most of the time, where within the interval $0 < \tau < \beta$ the time-ordering operator 'does nothing'. However, it should be stressed that $\langle c_{i\nu\sigma} c_{j\nu\sigma}^\dagger\rangle$ is merely a useful symbolic notation, which also yields formally correct end results 'most of the time'.

The four-point (or two-particle) correlation function is defined as,

$$G_{\mathbf{k}\mathbf{k'}\mathbf{q}}^{(2),\sigma_1\sigma_1'\sigma_2\sigma_2'}(\tau_1,\tau_2,\tau_3,\tau_4) = -\left\langle T_\tau c_{\mathbf{k}\sigma_1}(\tau_1)c_{\mathbf{k}+\mathbf{q},\sigma_1'}^\dagger(\tau_2)c_{\mathbf{k'}+\mathbf{q},\sigma_2}(\tau_3)c_{\mathbf{k'}\sigma_2'}^\dagger(\tau_4)\right\rangle, \tag{A.23}$$

in the particle-hole notation. Only a subset of the possible spin combinations are non-zero due to spin conservation, namely

$$G^{(2),\sigma\sigma\sigma'\sigma'} \equiv G^{(2),\sigma\sigma'}, \tag{A.24}$$

$$G^{(2),\sigma\bar\sigma\bar\sigma\sigma} \equiv G^{(2),\overline{\sigma\sigma}}. \tag{A.25}$$

Under paramagnetism one may flip all spin labels without a change in $G^{(2)}$, $G^{(2),\sigma\sigma'} = G^{(2),\bar\sigma\bar\sigma'}$ and $G^{(2),\overline{\sigma\sigma}} = G^{(2),\overline{\bar\sigma\bar\sigma}}$. Furthermore, under $SU(2)$ symmetry (which of course also implies cylindrical symmetry) there is also a connection between $G^{(2),\sigma\sigma'}$ and $G^{(2),\overline{\sigma\sigma}}$,

$$G^{(2),\overline{\sigma\sigma}} = \frac{1}{2}\sum_\sigma (G^{(2),\sigma\sigma} - G^{(2),\sigma\bar\sigma}) = G^{(2),\uparrow\uparrow} - G^{(2),\uparrow\downarrow} \tag{A.26}$$

For a proof, and an also otherwise comprehensive discussion of n-particle Green's functions, the reader is referred to the thesis of Georg Rohringer [118]. In paramagnetic calculations it is convenient to change to the charge and spin channels, using the Pauli matrices s^α,

$$G_{\mathbf{k}\mathbf{k'}\mathbf{q}}^{(2),\alpha}(\tau_1,\tau_2,\tau_3,\tau_4) = -\frac{1}{2}\sum_{\sigma_1\sigma_1'\sigma_2\sigma_2'} s^\alpha_{\sigma_1'\sigma_1} s^\alpha_{\sigma_2'\sigma_2}\left\langle T_\tau c_{\mathbf{k}\sigma_1}(\tau_1)c_{\mathbf{k}+\mathbf{q},\sigma_1'}^\dagger(\tau_2)c_{\mathbf{k'}+\mathbf{q},\sigma_2}(\tau_3)c_{\mathbf{k'}\sigma_2'}^\dagger(\tau_4)\right\rangle. \tag{A.27}$$

This notation is very convenient, since the Pauli matrices automatically bring $G^{(2)}$ on a diagonal in the case of paramagnetism (or under the stronger $SU(2)$ symmetry). Explicitly,

the Pauli matrices may be conveniently written as,

$$s^c_{\sigma\sigma'} = \delta_{\sigma\sigma'} \tag{A.28}$$

$$s^z_{\sigma\sigma'} = \sigma\delta_{\sigma\sigma'} \tag{A.29}$$

$$s^x_{\sigma\sigma'} = \delta_{\sigma\bar{\sigma}'} \tag{A.30}$$

$$s^y_{\sigma\sigma'} = -\imath\sigma\delta_{\sigma\bar{\sigma}'}. \tag{A.31}$$

The 2P correlation function is therefore given in the charge channel ($\alpha = c$) as,

$$G^{(2),c} = \frac{1}{2}\left(G^{(2),\uparrow\uparrow} + G^{(2),\downarrow\downarrow} + G^{(2),\uparrow\downarrow} + G^{(2),\downarrow\uparrow}\right), \tag{A.32}$$

and in the spin channels ($\alpha = x, y, z$) as,

$$G^{(2),x} = \frac{1}{2}\left(G^{(2),\overline{\uparrow\downarrow}} + G^{(2),\overline{\downarrow\uparrow}}\right), \tag{A.33}$$

$$G^{(2),y} = \frac{1}{2}\left(G^{(2),\overline{\uparrow\downarrow}} + G^{(2),\overline{\downarrow\uparrow}}\right), \tag{A.34}$$

$$G^{(2),z} = \frac{1}{2}\left(G^{(2),\uparrow\uparrow} + G^{(2),\downarrow\downarrow} - G^{(2),\uparrow\downarrow} - G^{(2),\downarrow\uparrow}\right). \tag{A.35}$$

A.6 The susceptibilities

Q The different labels α of $G^{(2),\alpha}$ are referred to as charge ($\alpha = c$) and spin ($\alpha = x, y, z$) channels since the respective susceptibilities can be obtained from them. Introducing the density operator in momentum space,

$$\rho^\alpha_{\mathbf{q}} = \sum_i \rho^\alpha_i e^{i\mathbf{q}\mathbf{r}_i} = \sum_{\mathbf{k}\sigma\sigma'}^{\prime} c^\dagger_{\mathbf{k}\sigma} s^\alpha_{\sigma\sigma'} c_{\mathbf{k}+\mathbf{q},\sigma'}, \tag{A.36}$$

one has at $\tau_1 = \tau_2 = \tau$ and $\tau_3 = \tau_4 = \tau'$,

$$\sum_{\mathbf{k}\mathbf{k}'}^{\prime} G^{(2),\alpha}_{\mathbf{k}\mathbf{k}'\mathbf{q}}(\tau, \tau, \tau'\tau') = -\frac{1}{2}\left\langle T_\tau \rho^\alpha_{-\mathbf{q}}(\tau)\rho^\alpha_{\mathbf{q}}(\tau')\right\rangle, \tag{A.37}$$

this is simply the *disconnected* susceptibility (with a factor of $\frac{1}{2}$). Consistently throughout this text, susceptibilities will be defined with a minus sign in the front. In the spin channels ρ will be used, rather than $\rho/2 = S$, to allow an analogous notation of the charge and spin channels. Most other literature uses S, leading to a factor of 4 in the spin channels. One further defines the *connected* susceptibility as

$$X^\alpha_{\mathbf{q}}(\tau - \tau') = -\left\langle T_\tau \bar{\rho}^\alpha_{-\mathbf{q}}(\tau)\bar{\rho}^\alpha_{\mathbf{q}}(\tau')\right\rangle, \tag{A.38}$$

where $\bar{\rho}_i(\tau) = \rho_i(\tau) - \langle\rho\rangle$ is the density fluctuation ($\bar{\rho}_{\mathbf{q}}(\tau) = \rho_{\mathbf{q}}(\tau) - \langle\rho\rangle\delta_{\mathbf{q}}$). Hence, comparing to Eq. (A.37),

$$X_{\mathbf{q}}^{\alpha}(\tau - \tau') = 2\sum_{\mathbf{k}\mathbf{k}'}' G_{\mathbf{k}\mathbf{k}'\mathbf{q}}^{(2),\alpha}(\tau,\tau,\tau'\tau') + \langle\rho^{\alpha}\rangle\langle\rho^{\alpha}\rangle\delta_{\mathbf{q}}. \tag{A.39}$$

The last step is to introduce the Matsubara transform for the two-particle correlation functions, this will be

$$G^{(2)}(\tau_1,\tau_2,\tau_3,\tau_4) = \sum_{\nu\nu'\omega}' G_{\nu\nu'\omega}^{(2)} e^{-\imath[\nu\tau_1 - (\nu+\omega)\tau_2 + (\nu'+\omega)\tau_3 - \nu'\tau_4]}, \tag{A.40}$$

where $\omega_m = 2m\pi/\beta$ is a bosonic Matsubara energy and the summation symbol $\sum'$ implies a factor β^{-1} for each Matsubara sum (i.e., β^{-3} in this case).

A.7 Four-vector notation

From now on the convenient compact notation will be used, $\textcolor{green}{Q}$

$$k = (\mathbf{k}, \nu) \quad \text{and} \quad q = (\mathbf{q}, \omega), \tag{A.41}$$

for fermionic and bosonic momenta and frequencies, respectively. Summations over these indices imply multiplication by $\beta^{-1}N^{-1}$, e.g., $\sum_k \equiv \sum_{\mathbf{k}\nu}' = \beta^{-1}N^{-1}\sum_{\mathbf{k}\nu}$. Furthermore, in places where Matsubara summations are done on objects with critical convergence radii, an implicit convergence factor $e^{\imath\nu0^+}$ is to be added, that is $\sum_\nu' \hat{=} \frac{1}{\beta}\sum_\nu e^{\imath\nu0^+}$. Throughout, the following convention will be used,

$$\boxed{\sum_k \equiv \sum_{\mathbf{k}\nu}' e^{\imath\nu0^+} = \beta^{-1}N^{-1}\sum_{\mathbf{k}\nu} e^{\imath\nu0^+}.} \tag{A.42}$$

In this notation it will also be written symbolically,

$$G_{kk'q}^{(2),\sigma_1\sigma_1'\sigma_2\sigma_2'} = " - \left\langle c_{k\sigma_1} c_{k+q,\sigma_1'}^{\dagger} c_{k'+q,\sigma_2} c_{k'\sigma_2'}^{\dagger} \right\rangle ", \tag{A.43}$$

and it should be emphasized again that the Fourier transform to Matsubara energies implied in this notation does not commute with the time-ordering operator. This is of importance in particular for four-point correlation functions, since the action of T_τ is almost never trivial here. On the other hand, the notation above is useful to keep track of the indices of the particle-hole pair when translating between algebraic and diagrammatic expressions.

Lastly, applying the compact notation $G_{k\sigma}$ also to the single-particle Green's function, the generalized susceptibility is introduced,

$$X^\alpha_{kk'q} = G^{(2),\alpha}_{kk'q} + \beta\frac{1}{2}\sum_{\sigma\sigma'} s^\alpha_{\sigma\sigma} s^\alpha_{\sigma'\sigma'} G_{k\sigma} G_{k'\sigma'}\delta_q. \tag{A.44}$$

The second term on the right-hand-side (RHS) is non-zero only for $\alpha = 0$ and $\alpha = z$ (since s^x and s^y have no diagonal elements). The factor β in that term stems from the time-independent contribution $\langle\rho\rangle\langle\rho\rangle$ in $X(\tau - \tau')$, Eq. (A.38). Using

$$\sum_\sigma\sum_k s^\alpha_{\sigma\sigma} G_{k\sigma} = \langle\rho^\alpha\rangle, \tag{A.45}$$

one obtains the connected susceptibilities via the simple relation,

$$X^\alpha_q = 2\sum_{kk'} X^\alpha_{kk'q} = -\langle\bar\rho^\alpha_{-q}\bar\rho^\alpha_q\rangle = -\langle\rho^\alpha_{-q}\rho^\alpha_q\rangle + \beta\langle\rho^\alpha\rangle\langle\rho^\alpha\rangle\delta_q. \tag{A.46}$$

A possible source of confusion is the commonly used notation,

$$\sum_{\nu\sigma}{}' G_{\mathbf{k}\nu\sigma} = \sum_\sigma\left\langle c^\dagger_{\mathbf{k}\sigma} c_{\mathbf{k}\sigma}\right\rangle = \sum_\sigma\langle n_{\mathbf{k}\sigma}\rangle = \langle n_{\mathbf{k}}\rangle, \tag{A.47}$$

which is *not* the same as $\rho^c_{\mathbf{q}} = n_{\mathbf{q}}$ when $\mathbf{q}$ goes to $\mathbf{k}$. From the definition of $\rho^c_{\mathbf{q}}$ in Eq. (A.36) one can see that no choice of $\mathbf{q}$ will yield the diagonal operator combination $\sum_\sigma c^\dagger_{\mathbf{k}\sigma} c_{\mathbf{k}\sigma}$. One merely has $\sum'_{\mathbf{k}}\langle n_{\mathbf{k}}\rangle = \langle n_{\mathbf{q}=0}\rangle = \sum_\sigma\sum'_{\mathbf{k}}\langle c^\dagger_{\mathbf{k}\sigma} c_{\mathbf{k}\sigma}\rangle = \langle n\rangle$, which is the average site-local charge density operator. Therefore, a further convention used in this text is to use the label $\mathbf{k}$ when $n_{\mathbf{k}} = \sum_\sigma c^\dagger_{\mathbf{k}\sigma} c_{\mathbf{k}\sigma}$ is meant and to use $\mathbf{q}$ when $n_{\mathbf{q}} = \rho^c_{\mathbf{q}}$ from Eq. (A.36) is meant (i.e., $\mathbf{k}$ is a fermionic vector and $\mathbf{q}$ a bosonic one).

In compact notation the generalized susceptibility is related to $G^{(2)}$ in Eq. (A.23) as follows,

$$X^{\sigma\sigma'}_{kk'q} = G^{(2),\sigma\sigma'}_{kk'q} + \beta G_{k\sigma} G_{k'\sigma'}\delta_q, \tag{A.48}$$

$$X^{\overline{\sigma\bar\sigma}}_{kk'q} = G^{(2),\overline{\sigma\bar\sigma}}_{kk'q}. \tag{A.49}$$

Comparing to Eqs. (A.44) and (A.46), these definitions do not use a factor 2. This is in order to prevent this factor from entering the respective Bethe-Salpeter equations that are

introduced in the following subsection. In the compact notation one obtains the suscepti-
bilities as,

$$X_q^{\sigma\sigma'} = \sum_{kk'} X_{kk'q}^{\sigma\sigma'}, \tag{A.50}$$

$$X_q^{\overline{\sigma\sigma}} = \sum_{kk'} X_{kk'q}^{\overline{\sigma\sigma}}. \tag{A.51}$$

These are related to the charge and spin susceptibilities in Eq. (A.46) via the Pauli matrices,
as in Eq. (A.35). For example, $\sum_{\sigma\sigma'} X_q^{\sigma\sigma'} = X_q^c = - \langle \rho_{-q}^c \rho_q^c \rangle + \beta \langle \rho^c \rangle \langle \rho^c \rangle \delta_q$.

B Self-energies and Dyson equations

The Bethe-Salpeter equation is the analogue of Dyson's equation for two-particle Green's   *Q*
functions. It is introduced here in a matrix notation, which will be used most of the
time, but also a diagrammatic notation is presented. The following definitions assume
paramagnetism, $G_{k\sigma} = G_{k\bar{\sigma}} = G_k$, followed by similar definitions for magnetic solutions.

B.1 Dyson equations

Approximations to the interacting 1P Green's function G_k, diagrammatically denoted as a   *Q*
double line,

$$G_k,$$

are done best at the level of its self-energy Σ_k. This implies the summation of an infinite
set of corrections to the non-interacting Green's function $G_k^0 = [\imath\nu - \varepsilon_{\mathbf{k}} + \mu]^{-1}$ (denoted as
a single line) via the Dyson equation $G^{-1} = [G^0]^{-1} - \Sigma_k$. Diagrammatically this is depicted
as in Fig. 2.1.

FIGURE 2.1: Diagrammatic notation of Dyson's equation. The interacting Green's function
is given by the non-interacting one plus vertex corrections. The self-energy Σ can not be
separated into two parts by cutting one of its internal (noninteracting) lines.

Of interest is a similar equation for the generalized susceptibility $X_{kk'q}^\alpha$:

Throughout the text, labels $k, k', k+q, k'+q$ of four-point objects will consistently refer to the top left, top right, bottom left, and bottom right of the object, respectively. In full analogy to the 1P Dyson equation one writes a 2P Dyson equation, or Bethe-Salpeter equation, for the generalized susceptibility in Eq. (A.44),

$$X_{kk'q}^{\alpha} = G_k G_{k+q} \left[N\beta\delta_{kk'} + \sum_{k''} \Gamma_{kk''q}^{\alpha} X_{k''k'q}^{\alpha} \right], \tag{B.1}$$

which is denoted diagrammatically as in Fig. 2.2.
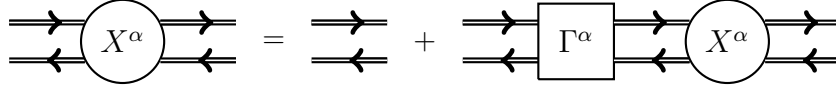
FIGURE 2.2: The Bethe-Salpeter equation for the generalized susceptibility $\hat{X}$ generates all 2P reducible diagrams from the 2P irreducible particle-hole vertex $\hat{\Gamma}$, Since the BSE has a similar form as Dyson's equation in Fig. (2.1), $\hat{\Gamma}$ may be called the 2P self-energy of $\hat{X}$. $\hat{\Gamma}$ can not be separated into two parts by a vertical cut of two of its internal Green's function lines.

Here, one defines the 'bubble' with open ends and closed ends, respectively,

$$X_{kk'q}^0 = N\beta X_{kq}^0 \delta_{kk'} = N\beta G_k G_{k+q}\delta_{kk'}, \tag{B.2}$$

$$X_q^0 = \sum_{kk'} X_{kk'q}^0 = \sum_k X_{kq}^0, \tag{B.3}$$

where X_q^0 is also known as the Lindhard function when $G = G^0$ is the noninteracting Green's function. On the other hand,

$$\Gamma_{kk'q}^{\alpha}, \tag{B.4}$$

is the particle-hole vertex that is irreducible with respect to a vertical cut of a particle and hole pair. In this text this object will be called the 2P self-energy. While this may be unusual to some, it stresses the analogy to the one-particle level and avoids a potential confusion with the *reducible* particle-hole vertex F, which will be called T-matrix.

B.2   Matrix notation of the Bethe-Salpeter equation

It is convenient to introduce a matrix notation with respect to the fermionic indices k, k',

$$C_{kk'} = \sum_{k''} A_{kk''} B_{k''k'}, \tag{B.5}$$

where $\hat{A}, \hat{B}, \hat{C}$ are matrices in the compact indices $k = (\mathbf{k}, \nu)$ and $k' = (\mathbf{k}', \nu')$. Note that the summation implies a factor $(N\beta)^{-1}$. In this notation the Bethe-Salpeter Eq. (B.1) can

FIGURE 2.3: The Bethe-Salpeter equation formulated as a ladder equation for the T-matrix $\hat{F}$. This equation is equivalent to the Bethe-Salpeter equation for the generalized susceptibility, Eq. (B.6).

be formulated as a matrix equation and it is indeed formally solved via matrix inversion ($\hat{1}_{kk'} = \delta_{kk'}$),

$$\hat{X}_q^\alpha = \hat{X}_q^0(\hat{1} + \hat{\Gamma}_q^\alpha \hat{X}_q^\alpha) = (\hat{1} - \hat{X}_q^0 \hat{\Gamma}_q^\alpha)^{-1} \hat{X}_q^0. \tag{B.6}$$

The Bethe-Salpeter equation expresses the repeated application of the matrix,

$$(\hat{X}_q^0 \hat{\Gamma}_q^\alpha)_{kk'} = \sum_{k''} N\beta G_k G_{k+q} \delta_{kk''} \Gamma_{k''k'q}^\alpha = G_k G_{k+q} \Gamma_{kk'q}^\alpha, \tag{B.7}$$

upon itself. Therefore, of physical significance are the eigenvalues of the matrix $(N\beta)^{-1}\hat{X}_q^0\hat{\Gamma}_q^\alpha$, where the factor $(N\beta)^{-1}$ stems from the definition of the matrix multiplication in Eq. (B.5). If the leading eigenvalue approaches unity, $\lambda_{\max} \to 1$, the Bethe-Salpeter equation diverges and with it the generalized susceptibility, possibly signaling a second order phase transition. This may be used to locate critical behavior, such as unconventional superconductivity, [99, 97].

B.3 The T-matrix

Equivalent to the Bethe-Salpeter equation for the generalized susceptibility in Eq. (B.6) is the Bethe-Salpeter equation for the 2P reducible vertex function $F_{kk'q}^\alpha$, which is called T-matrix in this text,

$$\hat{F}_q^\alpha = \hat{\Gamma}_q^\alpha + \hat{\Gamma}_q^\alpha \hat{X}_q^0 \hat{F}_q^\alpha \tag{B.8}$$

$$= (\hat{1} - \hat{\Gamma}_q \hat{X}_q^0)^{-1} \hat{\Gamma}_q. \tag{B.9}$$

The Bethe-Salpeter equation for F is depicted in Fig. 2.3. F contains all diagrams contributing to X, except the bubble X^0, which corresponds to a non-scattering event of a dressed quasi-particle with a dressed quasi-hole, where dressed means that the Green's functions of the bubble contain insertions of the 1P self-energy. The T-matrix F is related to the generalized susceptibility as,

$$\hat{X}_q^\alpha = \hat{X}_q^0 + \hat{X}_q^0 \hat{F}_q^\alpha \hat{X}_q^0. \tag{B.10}$$
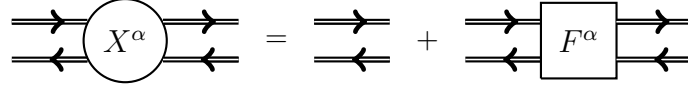
FIGURE 2.4: The generalized susceptibility $\hat{X}$ is given by the sum of the interacting bubble $\hat{X}^0$ and vertex corrections. The 2P reducible vertex function $\hat{F}$ is the T-matrix of $\hat{X}$ and comprises all vertex corrections.

The Bethe-Salpeter equation is a diagrammatic decomposition of F into irreducible building blocks Γ, see Ref. [19] for an analytical derivation. It also has an intuitive interpretation: Considering that Γ contains all diagrams irreducible with respect to a vertical cut of a particle-hole pair, one recovers all diagrams of the T-matrix F by connecting the building block Γ an arbitrary number of times with itself and adding up all of these contributions.

B.4   The Bethe-Salpeter equation in symmetry-broken phases

A formulation of the Bethe-Salpeter equation (BSE) for symmetry-broken phases is needed later. The BSE may be formulated for the generalized susceptibility $X^{\sigma_1\sigma_2\sigma_3\sigma_4}$ defined in Eqs. (A.48) and (A.49). In the longitudinal channel the BSE reads,

$$X_{kk'q}^{\sigma\sigma'} = G_{k\sigma}G_{k+q\sigma}\left[N\beta\delta_{kk'}\delta_{\sigma\sigma'} + \sum_{k''\sigma''}\Gamma_{kk''q}^{\sigma\sigma''}X_{k''k'q}^{\sigma''\sigma'}\right], \tag{B.11}$$

whereas one has in the transversal channel,

$$X_{kk'q}^{\overline{\sigma\bar{\sigma}}} = G_{k\sigma}G_{k+q\bar{\sigma}}\left[N\beta\delta_{kk'} + \sum_{k''}\Gamma_{kk''q}^{\overline{\sigma\bar{\sigma}}}X_{k''k'q}^{\overline{\sigma\bar{\sigma}}}\right]. \tag{B.12}$$

Compared to the BSE in the charge and spin channels, Eq. (B.1), this notation has the disadvantage of Eq. (B.11) being off-diagonal in the spin indices, mixing the components $X^{\sigma\sigma}$ and $X^{\sigma\bar{\sigma}}$. However, away from paramagnetism the change to the charge and spin channels does no longer diagonalize the generalized susceptibility X. There is then no gain in transforming Eqs. (B.11) and (B.12) into the charge and spin notation. The 2P self-energies $\Gamma^{\sigma\sigma'}$ and $\Gamma^{\overline{\sigma\bar{\sigma}}}$ transform between both notations in the same way as $G^{(2)}$ and X

[cf. Eq. (A.32) etc.],

$$\Gamma^c = \frac{1}{2}\left(\Gamma^{\uparrow\uparrow} + \Gamma^{\downarrow\downarrow} + \Gamma^{\uparrow\downarrow} + \Gamma^{\downarrow\uparrow}\right), \tag{B.13}$$

$$\Gamma^x = \frac{1}{2}\left(\Gamma^{\overline{\uparrow\downarrow}} + \Gamma^{\overline{\downarrow\uparrow}}\right), \tag{B.14}$$

$$\Gamma^y = \frac{1}{2}\left(\Gamma^{\overline{\uparrow\downarrow}} + \Gamma^{\overline{\downarrow\uparrow}}\right), \tag{B.15}$$

$$\Gamma^z = \frac{1}{2}\left(\Gamma^{\uparrow\uparrow} + \Gamma^{\downarrow\downarrow} - \Gamma^{\uparrow\downarrow} - \Gamma^{\downarrow\uparrow}\right). \tag{B.16}$$

The Bethe-Salpeter Eqs. (B.11) and (B.12) will also be written in matrix notation,

$$\hat{X}_q^{\sigma\sigma'} = \hat{X}_q^{0,\sigma\sigma}\delta_{\sigma\sigma'} + \hat{X}_q^{0,\sigma\sigma}\sum_{\sigma''}\hat{\Gamma}_q^{\sigma\sigma''}\hat{X}_q^{\sigma''\sigma'}, \tag{B.17}$$

$$\hat{X}_q^{\overline{\sigma\bar{\sigma}}} = \hat{X}_q^{0,\sigma\bar{\sigma}} + \hat{X}_q^{0,\sigma\bar{\sigma}}\hat{\Gamma}_q^{\overline{\sigma\bar{\sigma}}}\hat{X}_q^{\sigma\bar{\sigma}}. \tag{B.18}$$

Here, a spin-dependent bubble was introduced, $\hat{X}_{kk'q}^{0,\sigma\sigma'} = N\beta\delta_{kk'}G_{k\sigma}G_{k+q\sigma'}$. Just like for the charge and spin notation in Eq. (B.10), one defines a T-matrix F that comprises all vertex corrections,

$$\hat{X}_q^{\sigma\sigma'} = \hat{X}_q^{0,\sigma\sigma}\delta_{\sigma\sigma'} + \hat{X}_q^{0,\sigma\sigma}\hat{F}_q^{\sigma\sigma'}\hat{X}_q^{0,\sigma'\sigma'}. \tag{B.19}$$

$$\hat{X}_q^{\overline{\sigma\bar{\sigma}}} = \hat{X}_q^{0,\sigma\bar{\sigma}} + \hat{X}_q^{0,\sigma\bar{\sigma}}\hat{F}_q^{\overline{\sigma\bar{\sigma}}}\hat{X}_q^{0,\sigma\bar{\sigma}}. \tag{B.20}$$

The spin labels of the generalized susceptibility $X^{\sigma_1\sigma_2\sigma_3\sigma_4}$ will be consistently attached counter-clockwise:
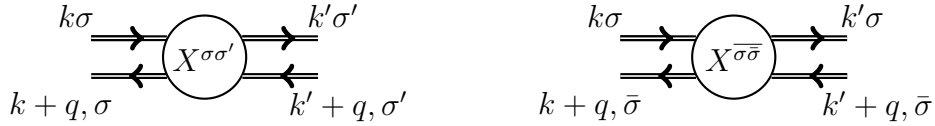
C   Schwinger-Dyson equation and Fierz ambiguity

The T-matrix F is connected to the 1P self-energy via the Schwinger-Dyson equation, which will be derived here. In this context the so-called 'Fierz ambiguity' is discussed, which arises because there are many different ways to denote the Hubbard interaction $Un_\uparrow n_\downarrow$.

C.1   Derivation of the Schwinger-Dyson equation

The Schwinger-Dyson equation can be derived from the equation of motion (EOM) for Green's function,

$$(-\partial_\tau)G_{\mathbf{k}\sigma}(\tau) = \delta(\tau) + \left\langle T_\tau\partial_\tau c_{\mathbf{k}\sigma}(\tau)c_{\mathbf{k}\sigma}^\dagger(0)\right\rangle, \tag{C.1}$$

where the δ-function arises due to non-commutativity of the time-derivative with the time-ordering operator. The time-evolution of the construction operator, $\partial_\tau c = [\mathcal{H}, c]$, is governed by the Hamiltonian $\mathcal{H} = H_0 + H_{\text{int}} - \mu N = H - \mu N$. Let us evaluate this for the following Hamiltonian,

$$H = \sum_{\mathbf{k}\sigma} \varepsilon_{\mathbf{k}} c_{\mathbf{k}\sigma}^\dagger c_{\mathbf{k}\sigma} + \frac{1}{2} \sum_{\mathbf{q}\alpha} \rho_{-\mathbf{q}}^\alpha V_{\mathbf{q}}^\alpha \rho_{\mathbf{q}}^\alpha, \tag{C.2}$$

with $\rho_{\mathbf{q}}^\alpha$ defined as in Eq. (A.36). This is an extended Hubbard model with non-local interactions V^α in the charge and spin channels, $\varepsilon_{\mathbf{k}}$ is the Fourier transform of the hopping t_{ij}. Notwithstanding a shift of the chemical potential, the Hubbard model is recovered for $V_{\mathbf{q}}^c = U, V^{x,y,z} = 0$. It is convenient to separate the contribution of the non-interacting and interacting Hamiltonians, but some care has to be taken,

$$\partial_\tau c = [\mathcal{H}(\tau), c(\tau)] = [\mathcal{H}, c]_\tau = [H_0 - \mu N, c]_\tau + [H_{\text{int}}, c]_\tau. \tag{C.3}$$

Here, $[..., ...]_\tau$ denotes a time-dependence according to the Heisenberg picture, Eq. (A.7). It is important to keep in mind that $[H_{\text{int}}, c]_\tau \neq [H_{\text{int}}, c(\tau)]$, since $H_0 - \mu N$ and H_{int} do not commute (or, in other words, $H_0 - \mu N$ and H_{int} depend on time, while $\mathcal{H}$ does not). Instead, the commutators need to be evaluated at $\tau = 0$. Using $[H_0 - \mu N, c_{\mathbf{k}\sigma}] = -(\varepsilon_{\mathbf{k}} - \mu) c_{\mathbf{k}\sigma}$, the EOM for Green's function takes the form,

$$(-\partial_\tau - \varepsilon_{\mathbf{k}} + \mu) G_{\mathbf{k}\sigma}(\tau) = \delta(\tau) + \left\langle T_\tau [H_{\text{int}}, c_{\mathbf{k}\sigma}]_\tau c_{\mathbf{k}\sigma}^\dagger(0) \right\rangle. \tag{C.4}$$

The commutator involving the interacting part is less appealing[2],

$$[H_{\text{int}}, c_{\mathbf{k}\sigma}] = -\frac{1}{2} \sum_{\alpha\mathbf{q}\sigma'}' V_{\mathbf{q}}^\alpha s_{\sigma\sigma'}^\alpha (\rho_{\mathbf{q}}^\alpha c_{\mathbf{k}-\mathbf{q}\sigma'} + c_{\mathbf{k}+\mathbf{q}\sigma'} \rho_{-\mathbf{q}}^\alpha). \tag{C.5}$$

Inserting this into Eq. (C.4) and using $V_{\mathbf{q}} = V_{-\mathbf{q}}$, both terms on the RHS of Eq. (C.5) can be brought into the same form within the time-ordered product,

$$(-\partial_\tau + \varepsilon_{\mathbf{k}} - \mu) G_{\mathbf{k}\sigma}(\tau) = \delta(\tau) - \sum_{\alpha\mathbf{q}\sigma'}' V_{\mathbf{q}}^\alpha s_{\sigma\sigma'}^\alpha \left\langle T_\tau \rho_{-\mathbf{q}}^\alpha(\tau) c_{\mathbf{k}+\mathbf{q}\sigma'}(\tau) c_{\mathbf{k}\sigma}^\dagger(0) \right\rangle. \tag{C.6}$$

Here it was used that c and ρ commute under the action of the time-ordering operator. Assuming paramagnetism, the sum $\frac{1}{2} \sum_\sigma$ is performed on both sides of Eq. (C.6) and paramagnetism is assumed, $G_\sigma = G_{\bar{\sigma}}$. Further inserting the definition of the density operator

---

[2]Note that no factor N^{-1} is implied by the summation over $\mathbf{q}$ in Eq. (C.2) but that N^{-1} is implied by the respective summation in Eq. (C.5). This factor originates from the density operators in Eq. (C.2).

$$\Sigma \quad = \qquad + \qquad + \qquad F^{\alpha} \tag{C.10}$$

FIGURE 2.5: Diagrammatic representation of the Schwinger-Dyson Eq. (C.12). This relation arises from the EOM of the construction operator, $\partial_\tau c = [\mathcal{H}, c]$, cf. Eq. (C.3).

$\rho_{\mathbf{q}}^{\alpha}$, Eq. (A.36), one finds

$$(-\partial_\tau - \varepsilon_{\mathbf{k}} + \mu)G_{\mathbf{k}}(\tau)$$

$$=\delta(\tau) + \frac{1}{2} \sum_{\alpha \mathbf{k}' \mathbf{q}}{}' \sum_{\sigma_1 \sigma_1' \sigma_2 \sigma_2'} V_{\mathbf{q}}^{\alpha} s_{\sigma_1' \sigma_1}^{\alpha} s_{\sigma_2' \sigma_2}^{\alpha} \left\langle T_\tau c_{\mathbf{k}' \sigma_1}(\tau) c_{\mathbf{k}'+\mathbf{q}\sigma_1'}^{\dagger}(\tau) c_{\mathbf{k}+\mathbf{q}\sigma_2}(\tau) c_{\mathbf{k}\sigma_2'}^{\dagger}(0) \right\rangle \tag{C.7}$$

$$=\delta(\tau) - \sum_{\alpha \mathbf{k}' \mathbf{q}}{}' V_{\mathbf{q}}^{\alpha} G_{\mathbf{k}'\mathbf{k}\mathbf{q}}^{(2),\alpha}(\tau, \tau, \tau, 0),$$

where the definition of the four-point correlation function $G^{(2)}$, Eq. (A.27), was recognized. Using the Fourier transform defined in Eq. (A.40) and the bare Green's function $G_k^0 = [\nu - \varepsilon_{\mathbf{k}} + \mu]^{-1}$, one is left with the Fourier components of Eq. (C.7),

$$[G_k^0]^{-1}G_k = 1 - \sum_{\alpha k' q} V_q^{\alpha} G_{k'kq}^{(2),\alpha}, \tag{C.8}$$

$$\Leftrightarrow \Sigma_k G_k = - \sum_{\alpha k' q} V_q^{\alpha} G_{k'kq}^{(2),\alpha}. \tag{C.9}$$

In the last step, Dyson's equation was used. $G/G^0 = 1 + \Sigma G$. This result still needs to be expressed in terms of the T-matrix F. For the paramagnetic case one has according to Eq. (A.44) and (B.10),

$$G_{kk'q}^{(2),\alpha} = X_{kk'q}^{\alpha} - 2\beta G_k G_{k'} \delta_q \delta_{\alpha,c}$$

$$= G_k G_{k+q} \delta_{kk'} N\beta - 2\beta G_k G_{k'} \delta_q \delta_\alpha + G_k G_{k+q} F_{kk'q}^{\alpha} G_{k'} G_{k'+q}. \tag{C.11}$$

Inserting into Eq. (C.9) and dividing both sides by G_k yields finally,

$$\Sigma_k = 2V_{q=0}^c \sum_{k'} G_{k'} - \sum_{\alpha q} V_q^{\alpha} G_{k+q} - \sum_{\alpha k' q} V_q^{\alpha} G_{k'} G_{k'+q} F_{k'kq}^{\alpha} G_{k+q}. \tag{C.12}$$

This is the Schwinger-Dyson (SD) equation. The first two terms on the RHS correspond to the Hartree and Fock contributions, originating from the uncorrelated parts of $G^{(2)}$.

Diagrammatically one denotes the SD equation as in Fig. 2.5.

C.2   The Fierz ambiguity

Let us consider the Schwinger-Dyson Eq. (C.12) for the Hubbard model, whose interaction potential is $U n_\uparrow n_\downarrow$. Notwithstanding a shift of the chemical potential, this interaction may be fully accounted to the charge channel, using the identity, $\frac{1}{2}\rho^c U \rho^c = \frac{U}{2}(n + 2n_\uparrow n_\downarrow)$, which makes use of the Pauli principle, $n_\sigma^2 = n_\sigma$. Therefore, the Hubbard Hamiltonian may be denoted as in Eq. (C.2), where $V_{\mathbf{q}}^c = U$ and $V^{x,y,z} = 0$. Inserting this interaction into the Schwinger-Dyson Eq. (C.12), the Fock contribution cancels half of the Hartree contribution,

$$\Sigma_k = 2U \sum_{k'} G_{k'} - U \sum_q G_{k+q} - U \sum_{k'q} G_{k'} G_{k'+q} F_{k'kq}^c G_{k+q}. \qquad (C.13)$$

leaving the familiar result for the Hartree part, $\Sigma^{\mathrm{H}} = U \langle n \rangle /2$. On the other hand, one does not immediately see that of the T-matrix $F^c = F^{\uparrow\uparrow} + F^{\uparrow\downarrow}$ only $F^{\uparrow\downarrow}$ is needed to obtain the self-energy Σ. This is the case in the Hubbard model, since due to the Pauli principle its interaction can only act upon two electrons with opposite spins. Therefore, instead of imposing the Pauli principle on the Hubbard interaction $U n_\uparrow n_\downarrow$ from the start, the shift into the charge channel leaves it to the approximation to the T-matrices to somehow cancel out redundant contributions in $F^{\uparrow\downarrow}$ and $F^{\uparrow\uparrow}$. Indeed, many approximations do not satisfy the Pauli principle, such that this cancellation may never occur.

On the other hand, reformulations of the Hubbard interaction that do not shift the chemical potential lead to the desired cancellation of $F^{\uparrow\uparrow}$. To see this, consider the interaction $V^c = \frac{U}{2}, V^z = -\frac{U}{2}$, and $V^{x,y} = 0$. Using $\rho^z = n_\uparrow - n_\downarrow$ one sees that,

$$\frac{1}{2} \sum_{\alpha=c,z} \rho^\alpha V^\alpha \rho^\alpha = \frac{U}{4}[n + 2n_\uparrow n_\downarrow - (n - 2n_\uparrow n_\downarrow)] = U n_\uparrow n_\downarrow. \qquad (C.14)$$

This reformulation does therefore not shift the chemical potential. Inserting the interaction in Eq. (C.14) into the Schwinger-Dyson equation (C.12), one obtains the self-energy,

$$\Sigma_k = 2\frac{U}{2} \sum_{k'} G_{k'} - \sum_q \left(\frac{U}{2} - \frac{U}{2} \right) G_{k+q} - \frac{U}{2} \sum_{k'q} G_{k'} G_{k'+q} (F_{k'kq}^c - F_{k'kq}^z) G_{k+q}. \qquad (C.15)$$

Using $F^c - F^z = F^{\uparrow\uparrow} + F^{\uparrow\downarrow} - (F^{\uparrow\uparrow} - F^{\uparrow\downarrow}) = 2F^{\uparrow\downarrow}$, the T-matrix $F^{\uparrow\uparrow}$ indeed cancels,

$$\Sigma_k = \frac{U \langle n \rangle}{2} - U \sum_{k'q} G_{k'} G_{k'+q} F_{k'kq}^{\uparrow\downarrow} G_{k+q}. \qquad (C.16)$$

Similarly, there are SU(2)-symmetric splittings of the Hubbard interaction, where $V^{x,y,z} \equiv V^s$, making use of the operator identity,

$$\frac{1}{2} \sum_\alpha \rho^\alpha V^\alpha \rho^\alpha = (V^c - 3V^s)n_\uparrow n_\downarrow + (V^c + 3V^s)\frac{n}{2}. \tag{C.17}$$

This yields a Hubbard interaction $Un_\uparrow n_\downarrow$ when the sum rule $U = V^c - 3V^s$ holds, and also a shift of the chemical potential, except for $V^c = \frac{U}{2}, V^s = -\frac{U}{6}$.

The infinity of possible splittings of the Hubbard interaction is sometimes referred to as the 'Fierz ambiguity'. While exact results are left unchanged by the decoupling, the results of approximations may depend on the decoupling ratio between the charge and spin channels. As a general rule it is not desirable to reformulate the Hubbard interaction in a way that causes a shift in the chemical potential [158]. On the other hand, the Fierz ambiguity was used recently as a convergence criterion for the TRILEX approach [10].

C.3   Schwinger-Dyson equation for symmetry-broken phases

It will later be useful to have a more general form of the SD Eq. (C.12) available, which does not make use of the charge and spin diagonalization. To this end, one derives from Eq. (C.6),

$$\Sigma_{k\sigma_4} G_{k\sigma_4} = - \sum_{\alpha k' q \sigma_1 \sigma_2 \sigma_3} s^\alpha_{\sigma_2\sigma_1} V^\alpha_q s^\alpha_{\sigma_4\sigma_3} G^{(2),\sigma_1\sigma_2\sigma_3\sigma_4}_{k'kq}, \tag{C.18}$$

which is similar to Eq. (C.9) but does not assume paramagnetism. Here, $G^{(2),\sigma_1\sigma_2\sigma_3\sigma_4}$ is the four-point correlation function defined in Eq. (A.23). It is convenient to separate the flavors α on the RHS by longitudinal and transversal channels, which allows to drop some of the spin summations (since $s^{c,z}_{\sigma\sigma'} \sim \delta_{\sigma\sigma'}$ and $s^{x,y}_{\sigma\sigma'} \sim \delta_{\sigma\bar\sigma'}$),

$$\Sigma_{k\sigma_4} G_{k\sigma_4} = - \sum_{\alpha=c,z} \sum_{k'q\sigma_1} s^\alpha_{\sigma_1\sigma_1} V^\alpha_q s^\alpha_{\sigma_4\sigma_4} G^{(2),\sigma_1\sigma_4}_{k'kq}$$
$$- \sum_{\alpha=x,y} \sum_{k'q} s^\alpha_{\bar\sigma_4\sigma_4} V^\alpha_q s^\alpha_{\sigma_4\bar\sigma_4} G^{(2),\overline{\sigma_4\sigma_4}}_{k'kq}. \tag{C.19}$$

The four-point functions are now expressed through the generalized susceptibility, according to Eqs. (A.49), (B.19), and (B.20),

$$G^{(2),\sigma\sigma'}_{kk'q} = X^{\sigma\sigma'}_{kk'q} - \beta G_{k\sigma} G_{k\sigma'} \delta_q$$
$$= G_{k\sigma} G_{k+q\sigma} \delta_{kk'} \delta_{\sigma\sigma'} N\beta - \beta G_{k\sigma} G_{k'\sigma'} \delta_q + G_{k\sigma} G_{k+q,\sigma} F^{\sigma\sigma'}_{kk'q} G_{k'\sigma'} G_{k'+q,\sigma'}, \tag{C.20}$$
$$G^{(2),\overline{\sigma\sigma}}_{kk'q} = G_{k\sigma} G_{k+q\bar\sigma} \delta_{kk'} N\beta + G_{k\sigma} G_{k+q,\bar\sigma} F^{\overline{\sigma\sigma}}_{kk'q} G_{k'\sigma} G_{k'+q,\bar\sigma}. \tag{C.21}$$

Inserting into Eq. (C.19) and dividing by $G_{k\sigma_4}$ leaves the Schwinger-Dyson equation ($\sigma_4 \to \sigma'$),

$$
\begin{aligned}
\Sigma_{k\sigma} =& \sum_{k'\sigma'} V^c_{q=0} G_{k'\sigma'} + \sum_{k'\sigma'} \sigma\sigma' V^z_{q=0} G_{k'\sigma'} \\
&- \sum_{\alpha=c,z} \left\{ \sum_q V^\alpha_q G_{k+q\sigma} + \sum_{k'q\sigma'} s^\alpha_{\sigma'\sigma'} V^\alpha_q s^\alpha_{\sigma\sigma} G_{k'\sigma'} G_{k'+q,\sigma'} F^{\sigma'\sigma}_{k'kq} G_{k+q,\sigma} \right\} \\
&- \sum_{\alpha=x,y} \left\{ \sum_q V^\alpha_q G_{k+q\bar\sigma} + \sum_{k'q} s^\alpha_{\bar\sigma\sigma} V^\alpha_q s^\alpha_{\sigma\bar\sigma} G_{k'\sigma} G_{k'+q,\bar\sigma} F^{\overline{\sigma\bar\sigma}}_{k'kq} G_{k+q,\bar\sigma} \right\}.
\end{aligned}
\tag{C.22}
$$

Several symmetries of the Pauli matrices in Eqs. (A.28)-(A.31), as well as spin conservation ($F^{\overline{\sigma\sigma'}} = F^{\overline{\sigma\bar\sigma}} \delta_{\sigma\bar\sigma'}$) were used to derive Eq. (C.22). One recognizes the Hartree-Fock self-energy,

$$
\Sigma^{\text{HF}}_{k\sigma} = V^c_{q=0} \sum_{k'\sigma'} G_{k'\sigma'} + V^z_{q=0} \sum_{k'\sigma'} \sigma\sigma' G_{k'\sigma'} - \sum_{q,\alpha=c,z} V^\alpha_q G_{k+q\sigma} - \sum_{q,\alpha=x,y} V^\alpha_q G_{k+q\bar\sigma}.
\tag{C.23}
$$

D   RPA

Q   As a simple example, the random phase approximation (RPA) to the susceptibility of the Hubbard model is calculated.

D.1   The Hubbard repulsion in the charge and spin channels

To this end, is is convenient to transform the Hubbard interaction $Un_\uparrow n_\downarrow$ into the channels $\alpha = c, x, y, z$. To do this, let us rewrite this interaction in the following way,

$$
n_\uparrow U n_\downarrow = \frac{1}{4} \sum_{\sigma'_1\sigma_1\sigma'_2\sigma_2} c^\dagger_{\sigma'_1} c_{\sigma_1} U^{\sigma'_1\sigma_1\sigma'_2\sigma_2} c^\dagger_{\sigma'_2} c_{\sigma_2},
\tag{D.1}
$$

and transform it using the Pauli matrices [99],

$$
U^{\alpha\beta} = \frac{1}{2} \sum_{\sigma'_1\sigma_1\sigma'_2\sigma_2} s^\alpha_{\sigma'_1\sigma_1} U^{\sigma'_1\sigma_1\sigma'_2\sigma_2} s^\beta_{\sigma'_2\sigma_2}.
\tag{D.2}
$$

It should be stressed that this procedure does *not* imply that the interaction Hamiltonian is decomposed into different channels, which leads to the Fierz ambiguity in Sec. C.2. Instead, one knows from $U^{\alpha\beta}$ how the Hubbard interaction enters the channels $\alpha = c, x, y, z$ of the Bethe-Salpeter Eq. (B.6) in this basis, just like one knows it from $U^{\sigma'_1\sigma_1\sigma'_2\sigma_2}$ with respect to the basis $\sigma'\sigma = \uparrow\uparrow, \downarrow\downarrow, \uparrow\downarrow, \downarrow\uparrow$, Eqs. (B.11) and (B.12). While the operator relation in Eq. (C.17) that gives rise to the Fierz ambiguity implies that the Hubbard interaction can

be split up in infinitely many ways, Eq. (D.2) is an unambiguous transformation from the basis $\{\uparrow\uparrow, \downarrow\downarrow, \uparrow\downarrow, \downarrow\uparrow\}$ to $\{x, y, z, c\}$. Let us apply this transformation according to the RHS of Eq. (D.2) to the interaction matrix $\hat{U}$, whose matrix elements are given as:

$$
\hat{U} = \begin{array}{c|cccc}
 & \uparrow\uparrow & \downarrow\downarrow & \uparrow\downarrow & \downarrow\uparrow \\
\hline
\uparrow\uparrow & 0 & U & 0 & 0 \\
\downarrow\downarrow & U & 0 & 0 & 0 \\
\uparrow\downarrow & 0 & 0 & 0 & -U \\
\downarrow\uparrow & 0 & 0 & -U & 0
\end{array}
$$

The minus signs arise when the operators in (D.1) are brought into the correct order. The transformation to the charge and spin channels is done via the Pauli matrices, which are defined in Eqs. (A.28)-(A.31). These can be comprised into the transformation matrix $\hat{s}$:

$$
\hat{s} = \begin{array}{c|cccc}
 & x & y & z & c \\
\hline
\uparrow\uparrow & 0 & 0 & 1 & 1 \\
\downarrow\downarrow & 0 & 0 & -1 & 1 \\
\uparrow\downarrow & 1 & -\imath & 0 & 0 \\
\downarrow\uparrow & 1 & \imath & 0 & 0
\end{array}
$$

Applying this transformation[3] on the RHS of Eq. (D.2) then yields $U^{\alpha\beta}$,

$$
\frac{1}{2}\hat{s}^T \hat{U}\hat{s} = \begin{pmatrix} -U & 0 & 0 & 0 \\ 0 & -U & 0 & 0 \\ 0 & 0 & -U & 0 \\ 0 & 0 & 0 & U \end{pmatrix}. \tag{D.3}
$$

This corresponds to the transformation of the interaction matrix $U^{\sigma_1'\sigma_1\sigma_2'\sigma_2}$ in Eq. (D.1) into the charge and spin channels. There the interaction is diagonal, $U^{\alpha\beta} = U^\alpha \delta_{\alpha\beta}$, and the diagonal elements are given by $U^x = U^y = U^z = -U$ and $U^c = U$.

D.2   The RPA susceptibility

Now one may perform the RPA approximation to the 1P and 2P self-energies of the paramagnetic Hubbard model:

$$
\Sigma_k = \Sigma^{\mathrm{H}} = \frac{1}{2}U \langle n \rangle, \tag{D.4}
$$

$$
\Gamma^c_{kk'q} = U^c = U, \tag{D.5}
$$

$$
\Gamma^{x,y,z}_{kk'q} = U^{x,y,z} = -U. \tag{D.6}
$$

---

[3] Note that this is not a proper unitary transformation. Although $\hat{s}\hat{s}^\dagger/2 = \hat{1}$, $\hat{s}$ enters Eq. (D.3) not with its hermitian conjugate.

This is inserted into the Bethe-Salpeter equation (B.1),

$$X^\alpha_{kk'q} = G_k G_{k+q} \left[N\beta\delta_{kk'} + \sum_{k''} U^\alpha X^\alpha_{k''k'q} \right], \tag{D.7}$$

where $G^{-1} = [G^0]^{-1} - \Sigma^{\mathrm{H}}$. The susceptibilities are obtained by summing over k, k' and multiplying by two, using $2\sum_{kk'} X^\alpha_{kk'q} = X^\alpha_q$,

$$X^\alpha_q = 2X^0_q + 2X^0_q \sum_{k'k''} U^\alpha X^\alpha_{k''k'q} \tag{D.8}$$

$$= 2X^0_q + X^0_q U^\alpha X^\alpha_q = \frac{2X^0_q}{1 - X^0_q U^\alpha}. \tag{D.9}$$

This is the familiar RPA susceptibility, a geometric series involving the Lindhard function $X^0_q = \sum_k G_k G_{k+q}$. Owing to the convention that all susceptibilities come with a minus sign [cf. Eq. (A.38)], one ends up with an unusual minus sign for the charge channel in the denominator. $X \to -X$ recovers the standard result. The RPA susceptibility diverges when $X^0_q U^\alpha$ approaches unity. This may happen in the spin channels for $U > 0$, and in the charge channel for $U < 0$ (the attractive Hubbard model), signaling transitions to magnetic order or to charge order, respectively.

The RPA is valid only for very small U. However, already the RPA susceptibility has a rich momentum- and energy-dependent structure, with well defined gapless excitations near $q \approx 0$ and a broad excitation spectrum at larger momenta. Examples can be found in Ref. [39]. Other relevant weak- (to intermediate-)coupling approximations are, e.g., the two-particle self-consistent approach (TPSC) [144, 18] and the fluctuation exchange approximation (FLEX) [19]. In these approaches one still recognizes different geometric series in the final expression for the susceptibility. Essentially non-RPA-like approximations to the Hubbard model require non-perturbative starting points or Parquet approaches [119]. Various weak-coupling approximations are currently celebrating a revival within the field of non-equilibrium phenomena [46], where strong-correlation approaches are still in their infancy [29].

The definitions introduced in this section cover only a small fragment of the formalism around 2P correlation functions. In particular, the vertical particle-hole and the particle-particle channel were not discussed. The latter is needed, e.g., for applications to superconductivity [99, 97]. For further reading I recommend the works of Tremblay et al. [143, 157, 146, 144], Bickers et al. [20, 19], as well as papers on DΓA and the dual fermion/boson approaches [119], and the doctoral thesis of H. Hafermann and G. Rohringer [37, 118] are recommended.

Chapter 3

Conservation laws

"Wenn Du Dich mit dem Teufel einlässt, dann ändert sich nicht der Teufel. Der Teufel verändert Dich." - 8mm

It is desirable to construct approximations along physical constraints, however, what *Q* appropriate constraints are depends on the problem at hand. In this text approximations to the two-particle response functions are discussed, several different viewpoints can be taken with respect to the constraints that they should satisfy and in which physical regimes they need to be reliable. Sometimes it is important that an approximation should satisfy microscopic conservation laws, which are of particular importance in the theory of transport [18]. There they guarantee a number of exact statements about transport observables, such as the optical conductivity [87].

However, it is very difficult to construct a conserving approximation, and compromises have to be accepted, since conservation laws do not guarantee that the Pauli principle or the Mermin-Wagner theorem are satisfied. For example, the RPA susceptibility of the Hubbard model in Eq. (D.9) of chapter 2 is conserving but may predict a magnetic phase transition in the two-dimensional Hubbard model. It may be more desirable to study the susceptibility at low temperature than to satisfy microscopic conservation laws. Then, one should rather consider the Mermin-Wagner theorem as an exact constraint on the approximation. Another reason to relinquish conservation laws is that it is difficult to account for the $\mathbf{k}$-dependence of the electronic self-energy. Consequently, conservation laws are often not a feasible requirement when spatial correlations become important.

On the other hand, conservation laws guarantee a high degree of thermodynamic consistency. The latter means very simply that when a quantity can be calculated in several different ways, one should obtain the same result each time. This is always the case for exact solutions, but not necessarily for approximations. For example, a second order phase transition to magnetic order may be found in the susceptibility or in Green's function, which *should* yield the same critical point. While this is most likely not the case in an arbitrary approximation, it is guaranteed when the approximation is conserving. This point and others will be discussed in this section.

A   Global and local conservation

Q   The notion of a 'conserving approximation' is not very clear. On the one hand, if the Hamiltonian H of a system commutes with an operator, $[H, A] = 0$, A is an integral of motion and should be conserved. Here, A may be an observable such as the total energy, total charge, total spin, total momentum or total angular momentum. On the other hand, the time-evolution of a microscopic observable ρ is given in the equilibrium by the equation of motion, $\partial_\tau \varrho + [\varrho, \mathcal{H}] = 0$, which has the form of a continuity equation. If an approximation predicts different values for the LHS and RHS of the continuity equation, ρ is not conserved, which is a problem even when ρ is not an integral of motion. Conservation therefore regards to integrals of motion, $\partial_\tau A = [\mathcal{H}, A] = 0$, or to the proper time-evolution of a microscopic observable $\partial_\tau \varrho = [\mathcal{H}, \varrho]$. Typically, one has a local observable $\varrho(\mathbf{r})$ which can change its value at location $\mathbf{r}$ over time, and a global observable $A = \int d^3\mathbf{r}\rho(\mathbf{r})$, which is an integral of motion.

One therefore distinguishes local conservation, that is the proper time-evolution $\partial_\tau \varrho(\mathbf{r}) + [\varrho(\mathbf{r}), \mathcal{H}] = 0$, from global conservation $\partial_\tau A = 0$, that is the preservation of integrals of motion [36]. Local conservation is a stronger statement and implies global conservation: $\int d^3\mathbf{r}\partial_\tau \rho(\mathbf{r}) = \int d^3\mathbf{r}[\mathcal{H}, \rho(\mathbf{r})] = [\mathcal{H}, A] = 0$. Sometimes, one defines a current operator $\mathbf{j}$, such that $\nabla_\mathbf{r}\mathbf{j} = [\varrho, \mathcal{H}]$, and the continuity equation can be brought into the familiar form,

$$\partial_\tau \varrho(\mathbf{r}) + \nabla_\mathbf{r}\mathbf{j} = 0. \tag{A.1}$$

This needs to be distinguished from the equation of motion for the construction operator c, $\partial_\tau c = [\mathcal{H}, c]$: Continuity equations of microscopic observables lead to Ward identities, which will be discussed in this section. On the other hand, the equation of motion of the construction operator leads to the Schwinger-Dyson equation, as exercised in Sec. C.

B   Recollection of the Baym & Kadanoff theory of conserving approximations

Q   How to construct conserving approximations according to early papers of Luttinger and Ward [86], as well as Baym and Kadanoff [16, 15], is folklore of condensed matter physics: One draws a number of dressed skeleton diagrams with closed Green's function lines, such as in Fig. 3.1, and removes single lines from them, pictorially performing a functional derivative with respect to Green's function. The object to begin with is an approximation to the Luttinger-Ward functional $\Phi[G]$ and the resultant expression is a conserving approximation to the 1P self-energy $\Sigma[G]$. Upon removing a second line the 2P self-energy Γ is obtained. Such an approximation is called Φ-derivable.

Since the initial works of Baym, the Luttinger-Ward functional has become the central object of many a theory. Simple approximations up to some order may be derived from it, the FLEX is obtained from an infinite set of diagrams for Φ [20], it is a central object in the self-energy functional theory [107, 108], and in the bold diagrammatic

$$\Phi \;=\; \vcenter{\hbox{⬭}} \;+\; \vcenter{\hbox{⬭}} \;+\; \vcenter{\hbox{⬭}} \;+\cdots\,,$$

FIGURE 3.1: Within perturbation theory the Luttinger-Ward functional Φ is given by an expansion of bold/dressed skeleton diagrams. Dashed lines denote an interaction matrix element. A truncation of Φ after the first two terms corresponds to the Hartree-Fock approximation [cf. Eq. (C.23)].

Monte Carlo method [112], to name only a few examples. Despite its importance, the exact Luttinger-Ward functional and its dependence on G in an interacting system are never known explicitly, making it a somewhat elusive object. In the following, a few known facts about the Baym & Kadanoff theory and the Luttinger-Ward functional will be summarized and commented on.

B.1   Birth of the Luttinger-Ward functional

The initial idea of the Luttinger-Ward functional was to have it constructed perturbatively, as an expansion of bold skeleton diagrams, this goes back to Luttinger and Ward [86]. The proof that Φ-derivable approximations to the self-energy satisfy the continuity equations stems from G. Baym [15], building on a paper together with L. Kadanoff [16]. In Ref. [15] Baym proved for a many-body system subjected to the Coulomb interaction that Φ-derivable approximations locally conserve the charge, momentum, angular momentum (not the electronic spin) and the energy. The proof was derived for the continuum notation of the many-body Hamiltonian, cf. Eq. (A.1) of chapter 2, but Φ-derivability is nowadays frequently used to derive lattice approximations. It was noted by Baym himself that his proof of momentum conservation breaks down if the interaction is retarded, such as in case of the electron-phonon interaction. The reason for this is that the momentum is then not only carried by the electronic system but also by the phonons. In this sense, the statements in Ref. [15] are constricted to closed systems.

Of central importance in Ref. [15] is the 2P self-energy Γ. This is obtained as the second functional derivative of the Luttinger-Ward functional, $\Gamma = \frac{\delta^2 \Phi}{\delta G^2}$. Together with the relation for the self-energy, $\Sigma = \frac{\delta \Phi}{\delta G}$, one has $\Gamma = \frac{\delta \Sigma}{\delta G}$, making Γ a passive output of Σ (meaning that Γ has no feedback on Σ). However, the importance of Γ for Baym's proof is that in a conserving approximation Σ satisfies a 'vanishing curl condition', which expresses nothing but the crossing symmetry of Γ, which led him to conclude that in conserving theories Σ has a potential. This potential is the Luttinger Ward functional Φ.

B.2   Recent developments

The discovery of the dynamical mean-field theory has led to increased attention to non-perturbative approaches. A non-perturbative construction of the Luttinger-Ward functional was done by M. Potthoff [106]. The importance of this construction is that one may take the relation $\Sigma = \frac{\delta\Phi}{\delta G}$ for granted even in situations where perturbation theory breaks down. Here, Σ and G are the exact self-energy and Green's function of a given system, not approximations. Notably, in Ref. [106] the vanishing curl condition of the 2P self-energy Γ does not play a role in the construction of Φ. This means that the derivation of Φ can be done on the 1P level alone, circumventing the 2P level and its response function.

Restricting oneself to the 1P level, the central benefit of having a conserving theory is the satisfaction of global conservation laws by the 1P quantities Σ and G, as well as consistency of Green's function with the grand potential $\Omega = -T \ln \mathcal{Z}$. This means that in a conserving theory one obtains the same particle number $\langle N \rangle$ from the grand potential and from Green's function,

$$\langle N \rangle = \text{Tr}(G) = -\frac{\partial \Omega}{\partial \mu}. \tag{B.1}$$

The trace $\text{Tr}(\cdots)$ here implies a summation over all dependencies of G. This instance of thermodynamic consistency between the 0P and 1P levels was also a central objective of Baym [15]. However, beneficial aspects of conservation laws go beyond consistency between the 0P and 1P levels, as will be highlighted below.

Notably, Ref. [106] did not prove the uniqueness of Φ. This point has been discussed lately, since non-uniqueness of Φ was indeed verified in several instances [64] and has more recently been investigated in Ref. [35]. Apparently, many unphysical branches of the Luttinger-Ward functional exist next to the physical solution and have intersections with the latter already at moderate strength of the interaction. This poses an issue for bold diagrammatic expansions [112], which perform the expansion in Fig. 3.1 explicitly, and which might converge to the unphysical branches of Φ.

B.3   Hidden perturbations

The pictorial way of obtaining Σ and Γ from Φ by removing Green's function lines from diagrams hides an important element of the Baym & Kadanoff theory, which are implicit symmetry-breaking fields. These are needed in order to obtain a 2P self-energy $\Gamma_{kk'q}$ that indeed depends on three momenta and three frequencies. A clear account of the details was given by N.E. Bickers [19], which will be reiterated here in a very abbreviated form: In the coherent state path integral formalism the grand potential $\Omega = -\beta^{-1} \ln \mathcal{Z}$ may be expressed in the form

$$\Omega = -\beta^{-1} \ln \int \mathcal{D}[c^*, c] e^{-S[c^*, c, \mathcal{U}]}, \tag{B.2}$$

where $c_{i\sigma}^*(\tau), c_{i\sigma}(\tau)$ are anti-commuting Grassmann variables and S is the imaginary time action of the many-body Hamiltonian $\mathcal{H} = H_0 + H_{\text{int}} - \mu N$, cf. Eq. (A.14) of chapter 2. This action is modified by a symmetry-breaking field $\mathcal{U}$, which is set to zero by the end of all calculations,

$$S = \int d\tau \sum_{ij\sigma} c_{i\sigma}^*(\tau)[\delta_{ij}\partial_\tau + t_{ij} - \mu\delta_{ij}]c_{j\sigma}(\tau)$$
$$+ \frac{1}{2} \int d\tau \sum_{\sigma\sigma'} \sum_{ijkl} c_{i\sigma}^*(\tau)c_{j\sigma'}^*(\tau)V(ij,kl)c_{l\sigma'}(\tau)c_{k\sigma}(\tau)$$
$$+ \int\int d\tau d\tau' \sum_{ij\sigma\sigma'} \mathcal{U}^{\sigma\sigma'}(i,j,\tau,\tau')c_{i\sigma}^*(\tau)c_{j\sigma'}(\tau'). \tag{B.3}$$

The perturbation $\mathcal{U}$ is crucial for two reasons: (i) It provides a seed for symmetry-broken phases by explicitly breaking the symmetries of the Hamiltonian. In case a symmetry remains broken in the limit $\mathcal{U} \to 0$ the system is unstable with respect to small perturbations. To be unbiased, one has to break all of the symmetries of the Hamiltonian explicitly, using suitable perturbations $\mathcal{U}$ (see also [19]). The spin-dependence of $\mathcal{U}$ allows for phases with magnetic order. In order to allow transitions to superconducting order one further needs a perturbation coupling to $c^*(\tau)c^*(\tau')$ and $c(\tau)c(\tau')$, etc.

(ii) The non-locality of $\mathcal{U}$ in all quantum numbers makes Green's function,

$$G_{ji\sigma'\sigma}(\tau',\tau) = \mathcal{Z}^{-1} \int \mathcal{D}[c^*,c]c_{i\sigma}^*(\tau)c_{j\sigma'}(\tau')e^{-S[c^*,c,\mathcal{U}]}, \tag{B.4}$$

explicitly dependent on two times, two locations (instead of their relative distance), and two spins [e.g., $G_{\sigma\sigma'}(j,i) \neq G_\sigma(\mathbf{r}_j - \mathbf{r}_i)$ for a finite perturbation $\mathcal{U}$]. It is now easy to convince oneself that one recovers Green's function at $\mathcal{U} = 0$ as

$$\left.\frac{\delta\Omega}{\delta\mathcal{U}^{\sigma\sigma'}(i,j,\tau,\tau')}\right|_{\mathcal{U}=0} = G_{ji\sigma'\sigma}(\tau',\tau), \tag{B.5}$$

keeping in mind that the perturbation $\mathcal{U}$ is set to zero *after* the functional derivative was taken.

It is in this way that one has to think of the derivatives of $\Phi = \Omega - \text{Tr}(\ln G) + \text{Tr}(\Sigma G)$ with respect to G: An infinitesimal perturbation is set to zero after all derivatives have been taken. In this sense, writing $\Gamma = \frac{\delta\Sigma}{\delta G}$ can be misleading, since it suggests that Σ (at $\mathcal{U} = 0$) may be derived first and from it Γ by differentiation. However, if one attempts to do the latter, it is not possible to recover the full frequency and momentum dependence of Γ, since the derivative $\frac{\delta\Sigma_{ij}}{\delta G_{lk}}$, for Σ taken at $\mathcal{U} = 0$, depends only on two spatial coordinates $\mathbf{r}_i - \mathbf{r}_j$ and $\mathbf{r}_l - \mathbf{r}_k$, rather than four, which would be needed in order to obtain a 2P self-energy depending on four spatial labels.

B.4   The Hartree-Fock approximation

Q In some cases the perturbation $\mathcal{U}$ is not needed in order to find the full 2P self-energy, e.g., when the 2P self-energy does not depend on the transferred momentum q anyways, $\Gamma_{kk'q} = \Gamma_{kk'}$. For example, this is the case in the Hartree-Fock approximation to the Luttinger-Ward functional, which corresponds to truncating the perturbative expansion of Φ after the first two terms in Fig. 3.1. To be explicit, the 2P self-energy in Hartree-Fock approximation will now be considered for a single-band extended Hubbard model with nonlocal charge-charge and exchange interactions, i.e., the Hamiltonian in Eq. (C.2) of chapter 2 with the interaction $H_{\text{int}} = \frac{1}{2} \sum_{\mathbf{q}\alpha} \rho^\alpha_{-\mathbf{q}} V^\alpha_{\mathbf{q}} \rho^\alpha_{\mathbf{q}}$, where $\alpha = c, x, y, z$. For this model the Hartree-Fock self-energy is given by the expression in chapter 2, Eq. (C.23),

$$\Sigma^{\text{HF}}_{k\sigma} = \sum_{k''\sigma''} (V^c_{q=0} + \sigma\sigma'' V^z_{q=0}) G_{k''\sigma''} - \sum_{q,\alpha=c,z} V^\alpha_q G_{k+q\sigma} - \sum_{q,\alpha=x,y} V^\alpha_q G_{k+q\bar\sigma}. \qquad (B.6)$$

In order to obtain the 2P self-energy, one takes the functional derivative with respect to G,

$$\begin{aligned}
\Gamma^{\sigma'\sigma}_{k'k} &= \frac{\delta\Sigma_{k\sigma}}{\delta G_{k'\sigma'}} \\
&= \sum_{k''\sigma''} (V^c_{q=0} + \sigma\sigma'' V^z_{q=0}) \delta_{k',k''} \delta_{\sigma'\sigma''} - \sum_{q,\alpha=c,z} V^\alpha_q \delta_{k',k+q} \delta_{\sigma'\sigma} - \sum_{q,\alpha=x,y} V^\alpha_q \delta_{k',k+q} \delta_{\sigma'\bar\sigma} \\
&= (V^c_{q=0} + \sigma\sigma' V^z_{q=0}) - \sum_{\alpha=c,z} V^\alpha_{k'-k} \delta_{\sigma'\sigma} - \sum_{\alpha=x,y} V^\alpha_{k'-k} \delta_{\sigma'\bar\sigma} = \Gamma^{\sigma\sigma'}_{kk'}. \qquad (B.7)
\end{aligned}$$

The last step of flipping the momentum and spin labels assumes the inversion symmetry $V_q = V_{-q}$ and leads to a particularly simple crossing symmetry $\Gamma^{\sigma'\sigma}_{k'k} = \Gamma^{\sigma\sigma'}_{kk'}$ of the 2P self-energy in this approximation. This simple relation only holds when Γ does not depend on q, [$\Gamma^{\sigma\sigma'}_{kk'q} = \Gamma^{\sigma'\sigma}_{k'+q,k+q,-q}$ otherwise, which is seen by examination of Eq. (A.43) in chapter 2]. Assuming paramagnetism one may proceed to calculate the 2P self-energy of the charge and spin channels [cf. chapter 2, Eq. (B.16)],

$$\begin{aligned}
\Gamma^c_{kk'} &= \Gamma^{\uparrow\uparrow}_{k'k} + \Gamma^{\uparrow\downarrow}_{k'k} = 2V^c_{q=0} - V^c_{k'-k} - V^z_{k'-k} - V^x_{k'-k} - V^y_{k'-k}, \\
\Gamma^z_{kk'} &= \Gamma^{\uparrow\uparrow}_{k'k} - \Gamma^{\uparrow\downarrow}_{k'k} = 2V^z_{q=0} - V^c_{k'-k} - V^z_{k'-k} + V^x_{k'-k} + V^y_{k'-k}, \\
\Gamma^x_{kk'} &= \Gamma^y_{kk'} = \Gamma^z_{kk'} = \Gamma^{\overline{\uparrow\downarrow}}_{kk'}, \quad \text{(SU(2) symmetry)}. \qquad (B.8)
\end{aligned}$$

It is thus possible to obtain Γ in this approximation in absence of a perturbation $\mathcal{U}$. However, only the longitudinal components $\Gamma^{\sigma\sigma'}$ can be calculated in this way while the transversal component $\Gamma^{\sigma\bar\sigma}$ follows only indirectly from the assumption of SU(2) symmetry. Away from paramagnetism perturbations $\mathcal{U}$ would be needed in order to obtain this component of the 2P self-energy.

The explicit form of Γ in Eq. (B.8) reveals that it is remarkably difficult to make use of the Hartree-Fock approximation to the 2P self-energy when an interaction V^α depends on q. This is because the Bethe-Salpeter equation $\hat{X}^\alpha_q = \hat{X}^0_q(\hat{1} + \hat{\Gamma}^\alpha \hat{X}^\alpha_q)$ then has to be solved by
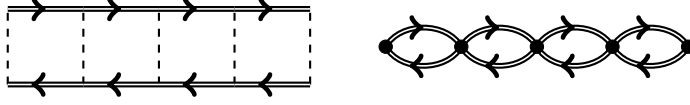
FIGURE 3.2: Collapse of the Hartree-Fock ladder of the extended Hubbard model $H_{\text{int}} = \frac{1}{2}\sum_{\mathbf{q}\alpha}\rho^\alpha_{-\mathbf{q}}V^\alpha_{\mathbf{q}}\rho^\alpha_{\mathbf{q}}$ to the RPA ladder of the Hubbard model $H_{\text{int}} = \frac{U}{2}\sum_{\mathbf{q}}\rho^c_{-\mathbf{q}}\rho^c_{\mathbf{q}}$. Diagrams on the left and right show typical contributions to the T-matrix F. Dashed lines denote the momentum-dependent 2P self-energy $\Gamma^\alpha_{k'-k}$ of the Hartree-Fock approximation in Eq. (B.8). Black dots represent the 2P self-energy $\Gamma^c = -\Gamma^{x,y,z} = U$ of the RPA. In this approximation the momentum summations can be performed in each bubble separately, leading to a mere product of Lindhard bubbles $X^0_q = \sum_k G_k G_{k+q}$.

a $\mathbf{k}, \mathbf{k}'$-matrix inversion. On the other hand, for $V^c = U, V^{x,y,z} = V^s = 0$, i.e., the Hubbard model[1], Eq. (B.8) recovers the RPA, $\Gamma = \pm U$, which was discussed in chapter 2, Sec. D. Then, the Bethe-Salpeter equation yields a simple geometric series for the 2P response, $X^\alpha_q = 2X^0_q/(1 - X^0_q U^\alpha)$. Diagrammatically this simplification can be understood as a collapse of the ladder vertices to single points, due to the convenient q-independence of U [see Fig. (3.2)].

B.5   Functional Schwinger-Dyson equation and functional Ward identity

Having clarified the details of the procedure, one may finally have obtained from an approximate functional Φ the 1P self-energy Σ,

$$\frac{\delta\Phi}{\delta G_{ij\sigma\sigma'}(\tau,\tau')} = \Sigma_{ji\sigma'\sigma}(\tau',\tau), \tag{B.9}$$

and from that a 2P self-energy Γ,

$$\frac{\delta\Sigma_{ji\sigma'_1\sigma_1}(\tau'_1,\tau_1)}{\delta G_{kl\sigma_2\sigma'_2}(\tau_2,\tau'_2)} = \Gamma^{\sigma'_1\sigma_1\sigma'_2\sigma_2}_{jilk}(\tau'_1,\tau_1,\tau'_2,\tau_2). \tag{B.10}$$

After that the perturbation $\mathcal{U}$ is turned to zero (hence $G_{\sigma\sigma'} \to G_\sigma\delta_{\sigma\sigma'}$ and likewise for Σ). Diagrammatically the 1P self-energy will now be given by a number of diagrams via an expression that has the form of a Schwinger-Dyson equation, Eq. (C.12) of chapter 2, i.e., of the Hartree- and Fock- diagrams and corrections. Therefore, one may think of Eq. (B.9) as a functional Schwinger-Dyson equation which is depicted in Fig. 3.3. The second relation, Eq. (B.10), is often called a functional Ward identity.

---

[1] Note that $V^c = U, V^s = 0$ amounts to a complete shift of the Hubbard interaction into the charge channel. Due to the Fierz ambiguity (see Sec. C.2 of chapter 2), all choices of V^c and V^s that satisfy $U = V^c - 3V^s$ recover the Hubbard repulsion, see chapter 2, Eq. (C.17). This choice has no effect on the 2P self-energy of the Hartree-Fock approximation in Eq. (B.8). This can be seen by inserting $V^c = U + 3V^s$ into Eq. (B.8), which leads to $\Gamma^c = U$ and $\Gamma^z = -U$, as it should. The splitting of the Hubbard interaction and the Fierz ambiguity have nothing to do with the transformation into the charge and spin channels in Sec. D of chapter 2, which is unique.

$$G^{-1} = [G^0]^{-1} - \Sigma^1$$

$$\Sigma^1 \quad = \qquad + \qquad + \qquad F^1$$

$$\underbrace{\hspace{6cm}}_{\frac{\delta\Phi}{\delta G}}$$
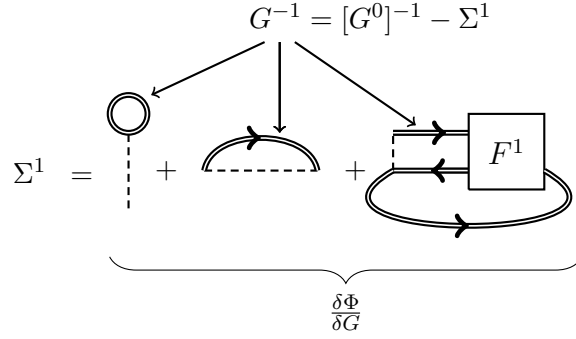
FIGURE 3.3: The functional Schwinger-Dyson Eq. (B.9) of the Baym & Kadanoff theory yields the self-energy Σ^1 as the sum of the Hartree-Fock diagrams and vertex corrections, just like the integral Schwinger-Dyson Eq. (C.12) of chapter 2. Φ-derivable approximations are self-consistent in the sense that the same 1P self-energy Σ^1 appears on the LHS and RHS of the Schwinger-Dyson equation SD1.

B.6   The dilemma of two-particle self-consistency

Q   While microscopic conservation laws guarantee a number of exact statements about the two-particle spectrum and thermodynamic consistency, other relevant statements are left out, such as the Pauli principle or the Mermin-Wagner theorem. This is related to the fact that a conserving approximation need not be two-particle self-consistent. In this sense, Parquet approaches [19] can be seen as complementary to the Baym & Kadanoff theory, since their aim is to establish two-particle self-consistency. On the other hand, Parquet approaches are in general not conserving, theorists therefore have to decide on a case by case basis if they prefer conservation laws or two-particle self-consistency. This central dilemma will be explained in the following.

In the Baym & Kadanoff theory Σ^1 and F^1 are determined self-consistently. This means that the Green's function lines on the RHS of SD1 in Fig. 3.3 are given by $G^{-1} = [G^0]^{-1} - \Sigma^1$, i.e., the same Σ^1 appears on the LHS *and* RHS of SD1. As seen before, Σ^1 yields a 2P self-energy, from now on called Γ^1, via the functional Ward identity, Eq. (B.10). This Γ^1 may be inserted into the Bethe-Salpeter equation for the generalized susceptibility as in Fig. 3.4, $\hat{X} = \hat{X}^0 + \hat{X}^0\hat{\Gamma}^1\hat{X}$. This yields a conserving 2P response function after summation over fermionic labels, $2\sum_{kk'} X_{kk'q} = X_q$ (the label α was dropped). Note that here $X^0_{kk'q} = N\beta G_k G_{k+q}\delta_{kk'}$ is a bubble of *interacting* Green's functions whose self-energy is Σ^1.

This is the output of the Baym & Kadanoff formalism (see Fig. 3.4): $G^{-1} = [G^0]^{-1} - \Sigma^1$ is the thermodynamically consistent Green's function that yields the same particle number
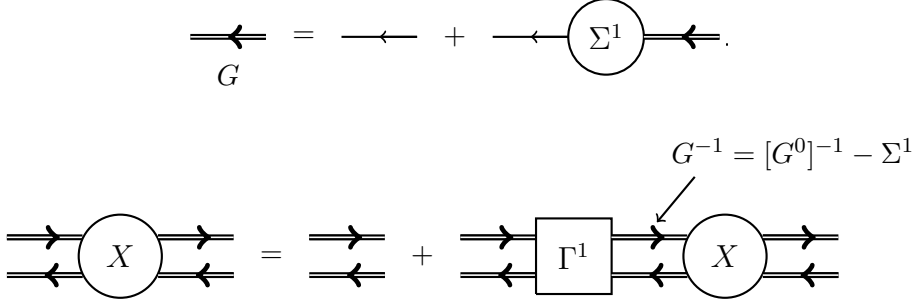
FIGURE 3.4: The conserving one- and two-particle correlation functions of the Baym & Kadanoff theory. Top: Green's function G satisfies thermodynamic consistency with the grand potential Ω, cf. Eq. (B.1). The 1P self-energy Σ^1 is obtained from the functional Schwinger-Dyson equation, Eq. (B.9). Bottom: The generalized susceptibility X satisfies the continuity equation, Eq. (A.1). Its 2P self-energy Γ^1 is the output of the functional Ward identity, Eq. (B.10). The Green's functions that make up the rails of the ladder have the 1P self-energy Σ^1.
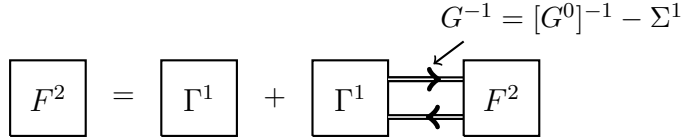
FIGURE 3.5: The T-matrix F^2 is obtained from Γ^1 via the Bethe-Salpeter equation. F^2 is the T-matrix of the conserving 2P response function $\hat{X} = \hat{X}^0 + \hat{X}^0\hat{F}^2\hat{X}^0$, where X^0 is a bubble of Green's functions with self-energy Σ^1.

as the grand potential Ω. X_q on the other hand satisfies the continuity equation $\partial_\tau \rho + [\rho, \mathcal{H}] = 0$.

It is very tempting to go further and use the 2P self-energy Γ^1 to solve the Bethe-Salpeter equation, Eq. (B.9), to obtain the T-matrix F^2, as in Fig. 3.5. In an approximation, however, the new T-matrix F^2 is most likely *not* equal to F^1, which was obtained from the Luttinger-Ward functional. This issue is persistent and can be seen as the central dilemma in the theory of conserving 2P response functions. Let us go a few steps further in order to understand the consequences:

After calculation of F^2, one may use a second Schwinger-Dyson equation, SD2, in order to obtain a new 1P self-energy Σ^2 from F^2. Since F^2 is different from F^1, Σ^2 will consequently not be equal to Σ^1. This is the point where the calculation cycle of a conserving approximation along the lines of Baym & Kadanoff can in general not be closed: If Σ^2 is used to calculate a new 2P self-energy Γ^2, these self-energies are no longer guaranteed to, and most likely will not, yield a conserving Green's function, $G^{-1} = [G^0]^{-1} - \Sigma^2$, and a conserving 2P response, $\hat{X} = \hat{X}^0 + \hat{X}^0\hat{\Gamma}^2\hat{X}$. Likewise, the 2P response function will no longer satisfy the continuity equation when Σ^2 is used in the interacting bubble X^0, even
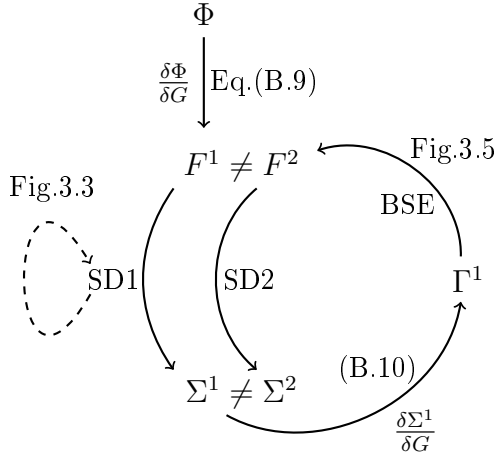
FIGURE 3.6: The 'circle of fifths' of conserving approximations: It just won't close. A functional derivative of Φ yields the self-energy as the Hartree and Fock diagrams plus vertex corrections, comprised in the T-matrix F^1. Self-consistent solution of the Schwinger-Dyson equation (SD1, dashed loop) leads to the 1P self-energy Σ^1, a further functional derivative to the 2P self-energy Γ^1. Solution of the BSE yields F^2, most likely different from F^1. An exact solution closes the circle. See also Fig. 4.5 of chapter 4.

when Γ^1 is kept as the 2P self-energy. Only the combination of Σ^1 for the bubble and Γ^1 as the 2P self-energy yields a conserving 2P response. This is the problem of two-particle self-consistency, which is sketched in Fig. 3.6. At this point I like to thank Vaclav Janiš for a discussion along these lines.

B.7   Is RPA conserving or not?

The discussed inconsistency of $F^1 \neq F^2$ can potentially lead to confusion: For example, the RPA approximation to the susceptibility of the Hubbard model is Φ-derivable, where $\Sigma^1 = U\frac{\langle n \rangle}{2}$ and $\Gamma^1 = \pm U$ are the Hartree self-energy and bare interaction, respectively. However, what is commonly understood to be the 'RPA self-energy' is Σ^2 [87], that is the self-energy obtained from F^2 via the SD2. Obviously, since Σ^2 is obtained from a ladder of Lindhard bubbles, $F^2 = U/(1 \mp X_q^0 U)$, it is not equivalent to the Hartree self-energy Σ^1. Thus, the 'RPA self-energy' is not a conserving approximation to the Hubbard model in the sense of Baym & Kadanoff (it is not Φ-derivable), while the RPA susceptibility and the Hartree self-energy are conserving in this sense.

C   Integral Ward identities

Let us consider the two main ingredients of the Baym & Kadanoff theory: One has a functional Schwinger-Dyson equation $\Sigma = \frac{\delta\Phi}{\delta G}$, Eq. (B.9), and a functional Ward identity

$\Gamma = \frac{\delta \Sigma}{\delta G}$, Eq. (B.10). On the other hand, there is also an integral Schwinger-Dyson equation, namely Eq. (C.12) of chapter 2. The terms 'functional' and 'integral' here are supposed to indicate that Σ and Γ, respectively, are either obtained by functional differentiation or via (one or more than one) $d + 1$-dimensional integral. Obviously, what is missing so far is an integral Ward identity, which will be derived and discussed in this subsection. Readers who are merely interested in the result may skip the following derivation and continue with Sec. D.

C.1   Derivation from the continuity equation

The derivation of the Ward identity on the lattice is done from the continuity equation of the charge and spin density operators, cf. definition Eq. (A.36),

$$\partial_\tau \rho_\mathbf{q}^\alpha(\tau) + [\rho_\mathbf{q}^\alpha(\tau), \mathcal{H}] = 0. \tag{C.1}$$

This is an operator identity but of interest here are approximations to n-point correlation functions. In these the continuity equation becomes manifest in identities such as $\langle \cdots (\partial_\tau \rho_\mathbf{q}(\tau) + [\rho_\mathbf{q}(\tau), \mathcal{H}]) \cdots \rangle = 0$, where arbitrary operators can be put in place of the dots. Such relations are called Ward (or Ward-Takahashi) identities and were first introduced by J.C. Ward in the context of quantum electrodynamics [151]. The most important identities of this kind are those for the 4-point correlation function. In the following, similar to previous derivations [149, 115, 26, 142, 53, 88] or [39], the Ward identities for charge- and spin-correlation functions on a quantum lattice will be derived. There are also Ward identities for the continuum, which can be found in textbooks [74, 126]. The following derivation is independent of the particular form of the non-interacting Hamiltonian $H_0 = \sum_{\mathbf{k}\sigma} \varepsilon_\mathbf{k} c_{\mathbf{k}\sigma}^\dagger c_{\mathbf{k}\sigma}$, valid for lattice and local impurity models, and for now also independent of the interaction Hamiltonian H_{int}. The main results of this section have been published [65].

Let us recall the definition of the generalized susceptibility, Eq. (A.27) of chapter 2,

$$G_{\mathbf{k}\mathbf{k}'\mathbf{q}}^{(2),\alpha}(\tau_1, \tau_2, \tau_3, \tau_4) = -\frac{1}{2} \sum_{\sigma_1 \sigma_1' \sigma_2 \sigma_2'} \langle T_\tau c_{\mathbf{k}\sigma_1}(\tau_1) s_{\sigma_1' \sigma_1}^\alpha c_{\mathbf{k}+\mathbf{q},\sigma_1'}^\dagger(\tau_2) c_{\mathbf{k}'+\mathbf{q},\sigma_2}(\tau_3) s_{\sigma_2' \sigma_2}^\alpha c_{\mathbf{k}'\sigma_2'}^\dagger(\tau_4) \rangle. \tag{C.2}$$

The connection to the continuity equations of the charge- and spin-density operators $\rho_\mathbf{q} = \sum_{\mathbf{k}'\sigma\sigma'}' c_{\mathbf{k}'\sigma'}^\dagger s_{\sigma'\sigma}^\alpha c_{\mathbf{k}'+\mathbf{q},\sigma}$ can be made at equal times $\tau_3 = \tau_4$ from the following equation of motion,

$$\sum_{\mathbf{k}'}' \partial_\tau G_{\mathbf{k}\mathbf{k}'\mathbf{q}}^{(2),\alpha}(\tau_1, \tau_2, \tau, \tau) = \frac{1}{2} \sum_{\sigma_1 \sigma_1'} s_{\sigma_1' \sigma_1}^\alpha \partial_\tau \langle T_\tau c_{\mathbf{k}\sigma_1}(\tau_1) c_{\mathbf{k}+\mathbf{q},\sigma_1'}^\dagger(\tau_2) \rho_\mathbf{q}^\alpha(\tau) \rangle. \tag{C.3}$$

In order to evaluate the time-derivative, one has to make the action of the time-ordering operator T_τ explicit, using the step function,

$$\theta(\tau_1 - \tau_2) = \theta_{12} = \begin{cases} 1 & \text{if } \tau_1 - \tau_2 > 0, \\ 0 & \text{else,} \end{cases} \tag{C.4}$$

whose time-derivatives are given by $\partial_\tau \theta(\tau) = -\partial_\tau \theta(-\tau) = \delta(\tau)$. Dropping momentum and spin labels for the moment and abbreviating the notation as $1 = \tau_1$, $2 = \tau_2$ and $3 = \tau$, one has for the correlation function on the RHS of Eq. (C.3),

$$\begin{aligned} \langle T_\tau c_1 c_2^\dagger \rho_3 \rangle = &\theta_{12}\theta_{23} \left\langle c_1 c_2^\dagger \rho_3 \right\rangle - \theta_{21}\theta_{13} \left\langle c_2^\dagger c_1 \rho_3 \right\rangle \\ &+ \theta_{31}\theta_{12} \left\langle \rho_3 c_1 c_2^\dagger \right\rangle - \theta_{32}\theta_{21} \left\langle \rho_3 c_2^\dagger c_1 \right\rangle \\ &+ \theta_{13}\theta_{32} \left\langle c_1 \rho_3 c_2^\dagger \right\rangle - \theta_{23}\theta_{31} \left\langle c_2^\dagger \rho_3 c_1 \right\rangle. \end{aligned}$$

Applying the derivative $\partial_3 = \partial_\tau$ (note that $\partial_3 \theta_{3i} = -\partial_3 \theta_{i3} = \delta_{i3}$ and $\delta_{ij}\theta_{jk} = \delta_{ij}\theta_{ik}$),

$$\begin{aligned} \partial_3 \langle T_\tau c_1 c_2^\dagger \rho_3 \rangle = &\langle T_\tau c_1 c_2^\dagger (\partial_3 \rho_3) \rangle \\ &- \theta_{12}\delta_{23} \left\langle c_1 c_2^\dagger \rho_3 \right\rangle + \theta_{21}\delta_{13} \left\langle c_2^\dagger c_1 \rho_3 \right\rangle \\ &+ \delta_{31}\theta_{12} \left\langle \rho_3 c_1 c_2^\dagger \right\rangle - \delta_{32}\theta_{21} \left\langle \rho_3 c_2^\dagger c_1 \right\rangle \\ &+ (-\delta_{13}\theta_{12} + \theta_{12}\delta_{32}) \left\langle c_1 \rho_3 c_2^\dagger \right\rangle - (-\delta_{23}\theta_{21} + \theta_{21}\delta_{31}) \left\langle c_2^\dagger \rho_3 c_1 \right\rangle. \end{aligned}$$

The first term on the RHS is the one that arises when neglecting the non-commutativity of ∂_τ and T_τ. The rest can be sorted into a simpler form,

$$\begin{aligned} \partial_3 \langle T_\tau c_1 c_2^\dagger \rho_3 \rangle = &\langle T_\tau c_1 c_2^\dagger (\partial_3 \rho_3) \rangle \\ &+ \theta_{12}\delta_{23} \left\langle c_1 [\rho_2, c_2^\dagger] \right\rangle + \theta_{21}\delta_{31} \left\langle c_2^\dagger [c_1, \rho_1] \right\rangle \\ &+ \delta_{31}\theta_{12} \left\langle [\rho_1, c_1] c_2^\dagger \right\rangle + \delta_{23}\theta_{21} \left\langle [c_2^\dagger, \rho_2] c_1 \right\rangle \\ = &\langle T_\tau c_1 c_2^\dagger (\partial_3 \rho_3) \rangle + \delta_{23} \left\langle T_\tau c_1 [\rho_2, c_2^\dagger] \right\rangle + \delta_{31} \left\langle T_\tau [\rho_1, c_1] c_2^\dagger \right\rangle. \tag{C.5} \end{aligned}$$

One identifies the commutators on the RHS as $[\rho_2, c_2^\dagger] = [\rho_{\mathbf{q}}^\alpha, c_{\mathbf{k+q},\sigma'}^\dagger] = \sum_{\bar{\sigma}} s_{\bar{\sigma}\sigma'}^\alpha c_{\mathbf{k},\bar{\sigma}}^\dagger$ and $[\rho_1, c_1] = [\rho_{\mathbf{q}}^\alpha, c_{\mathbf{k}\sigma}] = -\sum_{\bar{\sigma}} s_{\sigma\bar{\sigma}}^\alpha c_{\mathbf{k+q},\bar{\sigma}}$. Hence,

$$
\begin{aligned}
\delta_{23} \left\langle T_\tau c_1 [\rho_2, c_2^\dagger] \right\rangle &= \delta(\tau_2 - \tau) \sum_{\bar{\sigma}} s_{\bar{\sigma}\sigma'}^\alpha \left\langle T_\tau c_{\mathbf{k}\sigma}(\tau_1) c_{\mathbf{k}\bar{\sigma}}^\dagger(\tau_2) \right\rangle \\
&= -\delta(\tau_2 - \tau) s_{\sigma\sigma'}^\alpha G_{\mathbf{k}\sigma}(\tau_1 - \tau_2), \\
\delta_{31} \left\langle T_\tau [\rho_1, c_1] c_2^\dagger \right\rangle &= -\delta(\tau - \tau_1) \sum_{\bar{\sigma}} s_{\sigma\bar{\sigma}}^\alpha \left\langle T_\tau c_{\mathbf{k+q},\bar{\sigma}}(\tau_1) c_{\mathbf{k+q},\sigma'}^\dagger(\tau_2) \right\rangle \\
&= \delta(\tau - \tau_1) s_{\sigma\sigma'}^\alpha G_{\mathbf{k+q}\sigma'}(\tau_1 - \tau_2),
\end{aligned}
\tag{C.6}
$$

where the definition $G_{\mathbf{k}\sigma}(\tau_1 - \tau_2) = -\langle T_\tau c_{\mathbf{k}\sigma}(\tau_1) c_{\mathbf{k}\sigma'}^\dagger(\tau_2) \rangle \delta_{\sigma\sigma'}$ of Green's function was inserted. We now return to the equation of motion in Eq. (C.3), insert the expressions in Eqs. (C.5) and (C.6), and apply the continuity equation $\partial_\tau \rho^\alpha = -[\rho^\alpha, \mathcal{H}]$. Thus Eq. (C.3) takes the form,

$$
\begin{aligned}
&\partial_\tau \sideset{}{'}\sum_{\mathbf{k}'} G_{\mathbf{k}\mathbf{k}'\mathbf{q}}^{(2)\alpha}(\tau_1, \tau_2, \tau, \tau) + \frac{1}{2} \sum_{\sigma\sigma'} s_{\sigma'\sigma}^\alpha \langle T_\tau c_{\mathbf{k}\sigma}(\tau_1) c_{\mathbf{k+q},\sigma'}^\dagger(\tau_2) [\rho_{\mathbf{q}}^\alpha(\tau), \mathcal{H}] \rangle \\
&= \frac{1}{2} \sum_{\sigma\sigma'} s_{\sigma\sigma'}^\alpha s_{\sigma'\sigma}^\alpha [G_{\mathbf{k+q},\sigma'}(\tau_1 - \tau_2) \delta(\tau - \tau_1) - G_{\mathbf{k}\sigma}(\tau_1 - \tau_2) \delta(\tau - \tau_2)].
\end{aligned}
\tag{C.7}
$$

C.2 The current vertex

At this point, many examples in the literature (e.g., [57], [39], [126]) derive a Ward identity for the so-called current vertex Γ_μ (which should not be confused with the 2P self-energy Γ^α). This will be briefly discussed here for the charge channel ($\alpha = 0$), establishing a connection to this notation: In order to define the charge current vertex, it is necessary to express the commutator $[\varrho_{\mathbf{r}}, \mathcal{H}]$ as the divergence of a charge current operator $\mathbf{j}_{\mathbf{r}}$. Here, $\mathbf{r}$ is a vector in the continuum and $\varrho_{\mathbf{r}}$ is the charge density of the continuum [i.e., Eq. (A.4) of chapter 2 for $\alpha = c$], the case of a quantum lattice will be commented on below. Given the charge current operator $\mathbf{j}_{\mathbf{r}}$, the continuity equation for the charge density may be expressed as $\partial_\tau \varrho_{\mathbf{r}} + \nabla_{\mathbf{r}} \mathbf{j}_{\mathbf{r}} = 0$, or equivalently $(-\imath\omega, \imath\mathbf{q})(\varrho_q, \mathbf{j}_q)^T = 0$ in momentum- and frequency-space, where $\mathbf{q}$ is the 'real' momentum (not the lattice momentum). In the continuum one then derives a Ward identity similar to Eq. (C.7), which is obtained by replacing the lattice construction operators by field operators, $c_{\mathbf{k}\sigma} \to \Psi_{\mathbf{k}\sigma}$. Using $s_{\sigma\sigma'}^c = \delta_{\sigma\sigma'}$ and assuming $G_\uparrow = G_\downarrow$, [with G defined as in chapter 2, Eq. (A.6)] one then has in frequency space the following Ward identity,

$$
-\imath\omega \sum_k G_{kk'q}^{(2),c} + \frac{1}{2} \sum_\sigma \langle T_\tau \Psi_{k\sigma} \Psi_{k+q,\sigma'}^\dagger [\rho^\alpha, \mathcal{H}]_q \rangle = G_{k+q} - G_k.
\tag{C.8}
$$

The aim is now to use the identity $[\varrho_{\mathbf{q}}, \mathcal{H}] = \imath\mathbf{q}\mathbf{j}_{\mathbf{q}}$ to rewrite the LHS of Eq. (C.8) as a four-divergence of the charge current vertex Γ_{kq}^μ, that is $(-\imath\omega, \imath\mathbf{q})(\Gamma_{kq}^0, \mathbf{\Gamma}_{kq})^T$. This is achieved

by defining $\Gamma_{kq}^{\mu} = (\Gamma_{kq}^{0}, \boldsymbol{\Gamma}_{kq})_{\mu}$ in the following way,

$$
\begin{aligned}
\Gamma_{kq}^{0} =& G_{k+q}^{-1} G_{k}^{-1} \frac{1}{2} \sum_{\sigma} \langle T_{\tau} \Psi_{k\sigma}(\tau_{1}) \Psi_{k+q,\sigma}^{\dagger} \varrho_{q} \rangle, \\
=& G_{k+q}^{-1} G_{k}^{-1} \sum_{k'} G_{kk'q}^{(2),c} \\
\boldsymbol{\Gamma}_{kq} =& G_{k+q}^{-1} G_{k}^{-1} \frac{1}{2} \sum_{\sigma} \langle T_{\tau} \Psi_{k\sigma} \Psi_{k+q,\sigma}^{\dagger} \boldsymbol{j}_{q} \rangle.
\end{aligned}
\tag{C.9}
$$

Then, Eq. (C.8) may be written in the compact form,

$$
(-\imath\omega, \imath\mathbf{q})(\Gamma_{kq}^{0}, \boldsymbol{\Gamma}_{kq})^{T} = G_{k}^{-1} - G_{k+q}^{-1}.
\tag{C.10}
$$

Having a current operator $\mathbf{j_q}$ is not only useful to abbreviate notation but it also allows to formulate the current-current correlation function $\left\langle T_{\tau} j_{-\mathbf{q}}^{\mu}(\tau) j_{\mathbf{q}}^{\nu}(\tau') \right\rangle$, which is closely related to the electromagnetic response kernel $K_q^{\mu\nu}$ [126, 154, 39]. From this object one may obtain the resistivity, optical conductivity and other transport properties [18], which is a challenging task, even in exactly solvable systems [27].

On the other hand, the notation using the current operator $\mathbf{j_q}$ is somewhat clumsy to work with in quantum lattice and impurity problems for several reasons: *Firstly*, a current operator $\mathbf{j}$ has to be found, which is a non-trivial task on a quantum lattice. This is because the current is a vector field which depends explicitly on the specific lattice structure, represented by $\varepsilon_{\mathbf{k}}$. The current operator $\mathbf{j}$ therefore has to be determined for each hopping individually. Furthermore, on the discrete quantum lattice the divergence operator "∇" becomes a discrete derivative and has to be defined properly. Already on the simple square lattice this requires some effort, see for example [39], where this is exercised in detail. *Secondly*, when the interaction H_{int} participates in the transport of the density n, that is when $[n_{\mathbf{q}}, H_{\text{int}}] \neq 0$, $\mathbf{j}$ becomes a two-body operator of $\mathcal{O}(c^{\dagger}cc^{\dagger}c)$. In this case the spatial components $\boldsymbol{\Gamma}$ of the current vertex are 6-point correlation functions [cf. Eq. (C.9) with $\Psi \to c$], and finding a proper charge current $\mathbf{j}$ becomes very tedious. One will face a similar issue in the definition of a spin current vertex when $[\mathbf{S}, H_{\text{int}}] \neq 0$. In fact, there are some caveats to defining a proper spin current operator, since the continuity equation $\partial_{\tau} \varrho_{\mathbf{r}}^{x,y,z} + \nabla_{\mathbf{r}} \mathbf{j}_{\mathbf{r}}^{x,y,z} = 0$ specifies only the divergence of the vector field $(\mathbf{j}^{x}, \mathbf{j}^{y}, \mathbf{j}^{z})$ but not its curl [128]. *Thirdly*, it is not obvious how a proper current operator $\mathbf{j}$ and divergence ∇ can be defined for a local quantum impurity problem without spatial degrees of freedom.

C.3   A general notation

Q   The following reformulation of the Ward identity in Eq. (C.7) circumvents the issues pointed out above. Firstly, assuming paramagnetism, $G_{\uparrow} = G_{\downarrow} \equiv G$, one may use $\sum_{\sigma\sigma'} s_{\sigma\sigma'}^{\alpha} s_{\sigma'\sigma}^{\alpha} = 2$

on the RHS of Eq. (C.7),

$$\partial_\tau {\sum_{\mathbf{k}'}}' G^{(2)\alpha}_{\mathbf{k}\mathbf{k}'\mathbf{q}}(\tau_1,\tau_2,\tau,\tau) + \frac{1}{2}\sum_{\sigma\sigma'} s^\alpha_{\sigma'\sigma} \langle T_\tau c_{\mathbf{k}\sigma}(\tau_1) c^\dagger_{\mathbf{k}+\mathbf{q},\sigma'}(\tau_2)[\rho^\alpha_{\mathbf{q}}(\tau),\mathcal{H}]\rangle$$
$$=[G_{\mathbf{k}+\mathbf{q}}(\tau_1-\tau_2)\delta(\tau-\tau_1) - G_{\mathbf{k}}(\tau_1-\tau_2)\delta(\tau-\tau_2)]. \tag{C.11}$$

One further separates the interacting Hamiltonian H_{int} from the non-interacting one, $H_0 - \mu N = {\sum_{\mathbf{k}}}'(\varepsilon_{\mathbf{k}}-\mu)c^\dagger_{\mathbf{k}\sigma}c_{\mathbf{k},\sigma}$,

$$[\rho^\alpha_{\mathbf{q}}(\tau),\mathcal{H}] = [\rho^\alpha_{\mathbf{q}},\mathcal{H}]_\tau = [\rho^\alpha_{\mathbf{q}},H_0-\mu]_\tau + [\rho^\alpha_{\mathbf{q}},H_{\text{int}}]_\tau. \tag{C.12}$$

The first commutator is a one-body operator, $[\rho^\alpha_{\mathbf{q}},H_0-\mu N] = {\sum_{\mathbf{k}\sigma\sigma'}}'(\varepsilon_{\mathbf{k}+\mathbf{q}}-\varepsilon_{\mathbf{k}})c^\dagger_{\mathbf{k}\sigma}s^\alpha_{\sigma\sigma'}c_{\mathbf{k}+\mathbf{q},\sigma'}$, and simply reproduces $G^{(2)}$ in Eq. (C.11), one is left with,

$$\sum_{\mathbf{k}'}'(\partial_\tau + \varepsilon_{\mathbf{k}'+\mathbf{q}} - \varepsilon_{\mathbf{k}'})G^{(2),\alpha}_{\mathbf{k}\mathbf{k}'\mathbf{q}}(\tau_1,\tau_2,\tau,\tau) + \frac{1}{2}\sum_{\sigma\sigma'} s^\alpha_{\sigma'\sigma} \langle T_\tau c_{\mathbf{k}\sigma}(\tau_1)c^\dagger_{\mathbf{k}+\mathbf{q},\sigma'}(\tau_2)[\rho^\alpha_{\mathbf{q}},H_{\text{int}}]_\tau\rangle$$
$$=G_{\mathbf{k}+\mathbf{q}}(\tau-\tau_2)\delta(\tau-\tau_1) - G_{\mathbf{k}}(\tau_1-\tau)\delta(\tau-\tau_2). \tag{C.13}$$

Finally, the Fourier transform to Matsubara frequencies is taken, as defined in Eq. (A.40) of chapter 2. Using the compact notation $k=(\mathbf{k},\nu)$ and $q=(\mathbf{q},\omega)$ one has,

$$\sum_{k'}\left[\varepsilon_{k'+q}-\varepsilon_{k'}-\imath\omega\right]X^\alpha_{kk'q} + \frac{1}{2}\sum_{\sigma\sigma'} s^\alpha_{\sigma'\sigma}\langle c_{k\sigma}c^\dagger_{k+q,\sigma'}[\rho^\alpha,H_{\text{int}}]_q\rangle = G_{k+q} - G_k. \tag{C.14}$$

Here, the generalized susceptibility $X_{kk'q}$ was inserted instead of $G^{(2)}_{kk'q}$. This is possible because these quantities differ merely by a contribution $\sim \delta_q$, which does not contribute to Eq. (C.14), [compare definition Eq. (A.44) of chapter 2]. One should note that the notation $\langle c_{k\sigma}c^\dagger_{k+q,\sigma'}[\rho^\alpha,H_{\text{int}}]_q\rangle$ is symbolic and implies a Fourier transform of the respective correlation function in Eq. (C.13) whose integrals are *outside* of the thermal average. Eq. (C.14) is the Ward identity of the generalized susceptibility for a single-band quantum lattice.

C.4   Ward identity of quantum impurity models

The Ward identity will now be derived for a quantum impurity problem, which requires to perform some steps differently. The Hamiltonian of a local quantum impurity problem be defined as follows,

$$H_{\text{imp}} = -\mu n + H^0_\Delta + H_\Delta + H_{\text{int}}. \tag{C.15}$$

The on-site energy of the impurity is set to $-\mu$, anticipating the later use of the Hamiltonian (C.15) as an *auxiliary* quantum impurity problem. The impurity is coupled to an

uncorrelated bath with the non-interacting Hamiltonian,

$$H_\Delta^0 = \sum_{\boldsymbol{k}\sigma} \epsilon_{\boldsymbol{k}} f_{\boldsymbol{k}\sigma}^\dagger f_{\boldsymbol{k}\sigma}, \tag{C.16}$$

where $f^\dagger, f$ are the bath's construction operators. Furthermore,

$$H_\Delta = \sum_{\boldsymbol{k}\sigma} (v_{\boldsymbol{k}} c_\sigma^\dagger f_{\boldsymbol{k}\sigma} + v_{\boldsymbol{k}}^* f_{\boldsymbol{k}\sigma}^\dagger c_\sigma), \tag{C.17}$$

is the hybridization Hamiltonian, coupling the impurity, represented by the construction operators $c^\dagger, c$, with the bath and $n = \sum_\sigma c_\sigma^\dagger c_\sigma$ in Eq. (C.15). Lastly, H_{int} is a yet unspecified interaction. For the Hamiltonian in Eq. (C.15) one defines the 1P and 2P correlation functions and self-energies in analogy to the lattice. This can simply be done by dropping the momentum labels $\boldsymbol{k}, \boldsymbol{q}$ everywhere, hence $k = (\boldsymbol{k}, \nu) \to \nu$ and $q = (\boldsymbol{q}, \omega) \to \omega$. However, it is convenient to use upper case symbols for lattice quantities and lower case symbols for impurity quantities, (except for the 1P self-energy Σ, where there is little danger of confusion). The conventions used in this text are the following (GF: Green's function, SE: Self-energy):

Quantity	Lattice	Impurity	Chapter, Eq.
Fermionic momentum k	$(\boldsymbol{k}, \nu)$	ν	$2, (\text{A}.41)$
Bosonic momentum q	$(\boldsymbol{q}, \omega)$	ω	$2, (\text{A}.41)$
Hopping	$\varepsilon_{\boldsymbol{k}}$	Δ_ν	$3, (\text{C}.20)$
Bare 1P GF	G_k^0	g_ν^0	$G^0 = [\imath\nu - \varepsilon_{\boldsymbol{k}} + \mu]^{-1}$
Bold 1P GF	G_k	g_ν	$2, (\text{A}.20)$
1P SE	Σ_k	Σ_ν	$2, \text{Fig}.2.1$
2P GF	$G_{kk'q}^{(2),\alpha}$	$g_{\nu\nu'\omega}^{(2),\alpha}$	$2, (\text{A}.27)$
Gen. susc.	$X_{kk'q}^\alpha$	$\chi_{\nu\nu'\omega}^\alpha$	$2, (\text{A}.44)$
Open bubble	$X_{kk'q}^0$	$\chi_{\nu\nu'\omega}^0$	$2, (\text{B}.2)$
Closed bubble	X_q^0	χ_ω^0	$2, (\text{B}.3)$
2P response/Susc.	X_q^α	χ_ω^α	$2, (\text{A}.38)$
2P SE	$\Gamma_{kk'q}^\alpha$	$\gamma_{\nu\nu'\omega}^\alpha$	$2, (\text{B}.4)$
T-matrix	$F_{kk'q}^\alpha$	$f_{\nu\nu'\omega}^\alpha$	$2, (\text{B}.9)$

$$\tag{C.18}$$

Slightly different in definition from the lattice is the non-interacting Green's function g^0 of the impurity via the hybridization function Δ,

$$g_\nu^0 = [\imath\nu - \Delta_\nu + \mu]^{-1}, \tag{C.19}$$

$$\Delta_\nu = \sum_{\boldsymbol{k}} \frac{|v_{\boldsymbol{k}}|^2}{\imath\nu - \epsilon_{\boldsymbol{k}}}. \tag{C.20}$$

The hybridization function Δ arises later upon integrating out the bath operators $f^\dagger, f$ from the path integral of the impurity Hamiltonian (C.15).

Of interest in the following is the Ward identity of the local four-point correlation function of the impurity,

$$g^{(2),\alpha}(\tau_1, \tau_2, \tau_3, \tau_4) = -\frac{1}{2} \sum_{\sigma_1 \sigma_1' \sigma_2 \sigma_2'} s^\alpha_{\sigma_1'\sigma_1} s^\alpha_{\sigma_2'\sigma_2} \langle c_{\sigma_1}(\tau_1) c_{\sigma_1'}^\dagger(\tau_2) c_{\sigma_2}(\tau_3) c_{\sigma_2'}^\dagger(\tau_4) \rangle. \tag{C.21}$$

For the derivation, one may start from Eq. (C.7) for the lattice, omitting momentum indices,

$$\partial_\tau g^{(2),\alpha}(\tau_1, \tau_2, \tau, \tau) + \frac{1}{2} \sum_{\sigma\sigma'} s^\alpha_{\sigma'\sigma} \langle T_\tau c_\sigma(\tau_1) c_{\sigma'}^\dagger(\tau_2) [\rho^\alpha, H_{\mathrm{imp}}]_\tau \rangle$$

$$= \frac{1}{2} \sum_{\sigma\sigma'} s^\alpha_{\sigma\sigma'} s^\alpha_{\sigma'\sigma} [g_{\sigma'}(\tau - \tau_2) \delta(\tau - \tau_1) - g_\sigma(\tau_1 - \tau) \delta(\tau - \tau_2)], \tag{C.22}$$

where $g_\sigma = -\langle c_\sigma(\tau) c_\sigma^\dagger(\tau') \rangle$ is the local Green's function of the impurity ($\langle \cdots \rangle$ denotes an impurity average). Paramagnetism $g_\uparrow = g_\downarrow$ will be assumed for now, simplifying the RHS.

The goal is now again to separate the non-interacting and interacting parts of the Hamiltonian H_{imp}, Eq. (C.15). To this end, the non-interacting part $-\mu n + H_\Delta^0 + H_\Delta$ of the local Hamiltonian H_{imp} needs to be treated somewhat differently compared to the lattice. For the first two operators one has, $[\rho^\alpha, -\mu n] = [\rho^\alpha, H_\Delta^0] = 0$. The commutator with the hybridization yields, $[\rho^\alpha, H_\Delta] = \sum_{\boldsymbol{k}\sigma\sigma'} s^\alpha_{\sigma'\sigma}(v_{\boldsymbol{k}} c_{\sigma'}^\dagger f_{\boldsymbol{k}\sigma} - v_{\boldsymbol{k}}^* f_{\boldsymbol{k}\sigma'}^\dagger c_\sigma)$, which features the bath operators $f^\dagger, f$. Inserting these commutators into Eq. (C.22) and transforming to frequencies yields,

$$g_{\nu+\omega} - g_\nu = -\imath\omega \sum_{\nu'}{}^{\prime} g^{(2),\alpha}_{\nu\nu'\omega} + \frac{1}{2} \sum_{\sigma\sigma'} s^\alpha_{\sigma'\sigma} \langle c_{\nu\sigma} c_{\nu+\omega,\sigma'}^\dagger [\rho^\alpha, H_{\mathrm{int}}]_\omega \rangle \tag{C.23}$$

$$+ \frac{1}{2} \sum_{\sigma_1 \sigma_1' \sigma_2 \sigma_2'} \sum_{\boldsymbol{k}\nu'}{}^{\prime} s^\alpha_{\sigma_1'\sigma_1} s^\alpha_{\sigma_2'\sigma_2} \left\{ v_{\boldsymbol{k}} \langle c_{\nu\sigma_1} c_{\nu+\omega,\sigma_1'}^\dagger c_{\nu'\sigma_2'}^\dagger f_{\boldsymbol{k}\nu'+\omega,\sigma_2} \rangle - v_{\boldsymbol{k}}^* \langle c_{\nu\sigma_1} c_{\nu+\omega,\sigma_1'}^\dagger f_{\boldsymbol{k}\nu'\sigma_2'}^\dagger c_{\nu'+\omega\sigma_2} \rangle \right\}.$$

In order to proceed to a local relation for the correlated site, one needs to integrate out the bath operators in the second line. This can be done in the functional integral formalism,

where the action of the impurity reads,

$$
S_{\mathrm{imp}}[c^*, c, f^*, f, J^*, J] = -\sideset{}{'}\sum_{\nu\sigma} c^*_{\nu\sigma}[\imath\nu + \mu]c_{\nu\sigma} + S_{\mathrm{int}}[c^*, c]
$$

$$
-\sideset{}{'}\sum_{\boldsymbol{k}\nu\sigma} f^*_{\boldsymbol{k}\nu\sigma}[\imath\nu - \epsilon_{\boldsymbol{k}}]f_{\boldsymbol{k}\nu\sigma} + \sideset{}{'}\sum_{\boldsymbol{k}\nu\sigma}([v_{\boldsymbol{k}}c^*_{\nu\sigma} + J^*_{\boldsymbol{k}\nu\sigma}]f_{\boldsymbol{k}\nu\sigma} + f^*_{\boldsymbol{k}\nu\sigma}[v^*_{\boldsymbol{k}}c_{\nu\sigma} + J_{\boldsymbol{k}\nu\sigma}]). \quad \text{(C.24)}
$$

Here, c^*, c, f^*, f are anti-commuting Grassmann numbers and J, J^* are sources, coupling to the bath degrees of freedom. For $J = J^* = 0$ the partition function of the impurity may be obtained as $\mathcal{Z} = \int \mathcal{D}[c^*, c, f^*, f]e^{-S_{\mathrm{imp}}}$. The sources J^*, J were introduced in order to obtain f and f^* as functional derivatives with respect to J^* and J, respectively. Thereby, one may now transfer the four-point correlation functions in Eq. (C.23) to the path integral formalism. For example, one has in short notation,

$$
\langle c_1 c^\dagger_2 c^\dagger_3 f_4 \rangle = -\mathcal{Z}^{-1} \int \mathcal{D}[c^*, c, f^*, f] c_1 c^*_2 c^*_3 \frac{\delta}{\delta J^*_4} e^{-S_{\mathrm{imp}}},
$$

$$
\langle c_1 c^\dagger_2 f^\dagger_3 c_4 \rangle = \mathcal{Z}^{-1} \int \mathcal{D}[c^*, c, f^*, f] c_1 c^*_2 \frac{\delta}{\delta J_3} c_4 e^{-S_{\mathrm{imp}}}. \quad \text{(C.25)}
$$

Now the bath Grassmann numbers f^*, f can be integrated out. The details of this procedure are described in many textbooks, e.g., [96]. In the case at hand the integration leads to the following identity for the impurity's partition function,

$$
\mathcal{Z} = \int \mathcal{D}[c^*, c, f^*, f]e^{-S_{\mathrm{imp}}} = \mathcal{Z}_f \int \mathcal{D}[c^*, c]e^{-S'_{\mathrm{imp}}} = \mathcal{Z}_f \mathcal{Z}_c, \quad \text{(C.26)}
$$

with the effective action

$$
S'_{\mathrm{imp}}[c^*, c, J^*, J] = -\sideset{}{'}\sum_{\nu\sigma} c^*_{\nu\sigma}[\imath\nu + \mu]c_{\nu\sigma} + \sideset{}{'}\sum_{\boldsymbol{k}\nu\sigma}[v_{\boldsymbol{k}}c^*_{\nu\sigma} + J^*_{\boldsymbol{k}\nu\sigma}]\mathcal{G}_{\boldsymbol{k}\nu\sigma}[v^*_{\boldsymbol{k}}c_{\nu\sigma} + J_{\boldsymbol{k}\nu\sigma}] + H_{\mathrm{int}}[c^*, c].
$$

$$
\text{(C.27)}
$$

Here, $\mathcal{G}^{-1}_{\boldsymbol{k}\nu} = \imath\nu - \epsilon_{\boldsymbol{k}}$ denotes the bath Green's function. Now it is possible to perform the functional derivatives in Eq. (C.25) and to set $J^* = J = 0$ subsequently. For the four-point correlation functions in Eq. (C.23) one obtains,

$$
\sum_{\boldsymbol{k}} v_{\boldsymbol{k}} \langle c_{\nu\sigma_1} c^\dagger_{\nu+\omega,\sigma'_1} c^\dagger_{\nu'\sigma'_2} f_{\boldsymbol{k}\nu'+\omega,\sigma_2} \rangle = \sum_{\boldsymbol{k}} |v_{\boldsymbol{k}}|^2 \mathcal{G}_{\boldsymbol{k}\nu'+\omega} \langle c_{\nu\sigma_1} c^*_{\nu+\omega,\sigma'_1} c^*_{\nu'\sigma'_2} c_{\nu'+\omega,\sigma_2} \rangle_c \quad \text{(C.28)}
$$

and

$$
\sum_{\boldsymbol{k}} v^*_{\boldsymbol{k}} \langle c_{\nu\sigma_1} c^\dagger_{\nu+\omega,\sigma'_1} f^\dagger_{\boldsymbol{k}\nu'\sigma'_2} c_{\nu'+\omega\sigma_2} \rangle = \sum_{\boldsymbol{k}} |v_{\boldsymbol{k}}|^2 \mathcal{G}_{\boldsymbol{k}\nu'} \langle c_{\nu\sigma_1} c^*_{\nu+\omega,\sigma'_1} c^*_{\nu'\sigma'_2} c_{\nu'+\omega\sigma_2} \rangle_c. \quad \text{(C.29)}
$$

Here, the averages on the RHSs imply $\langle\cdots\rangle_c = \mathcal{Z}_c^{-1}\int\mathcal{D}[c^*,c]\cdots e^{-S'_{\text{imp}}}$, however, this label will be dropped immediately. One identifies the hybridization function as $\Delta_\nu = \sum_{\boldsymbol{k}}|v_{\boldsymbol{k}}|^2\mathcal{G}_{\boldsymbol{k}\nu}$, according to definition Eq. (C.20). Together with the definition of the four-point correlation function, Eq. (C.21), Eq. (C.23) can finally be cast into the local Ward identity,

$$g_{\nu+\omega} - g_\nu = \sum_{\nu'}{}'[\Delta_{\nu'+\omega} - \Delta_{\nu'} - \imath\omega]\chi^\alpha_{\nu\nu'\omega} + \frac{1}{2}\sum_{\sigma\sigma'}s^\alpha_{\sigma'\sigma}\langle c_{\nu\sigma}c^\dagger_{\nu+\omega,\sigma'}[\rho^\alpha,H_{\text{int}}]_\omega\rangle. \qquad (C.30)$$

Just like on the lattice, $g^{(2)}$ may be freely replaced by χ^α, since they differ merely by a contribution $\sim\delta_\omega$. One immediately recognizes the similarity to the lattice Ward identity, Eq. (C.14). Here, the dynamical hybridization function Δ_ν takes the place of the lattice hopping $\varepsilon_{\mathbf{k}}$.

C.5   Symmetry-broken phases with one atom per unit cell

The Ward identities for symmetry broken phases will be stated with a less detailed deriva- Q
tion, and under the special condition that the commutation relations $[n_{i\sigma},H_{\text{int}}] = 0$ and $[c^\dagger_{i\sigma}c_{i\bar\sigma},H_{\text{int}}] = 0$ hold. This is the case, e.g., in the Hubbard model and in the Anderson impurity model, where $H_{\text{int}} = U\sum_i n_{i\uparrow}n_{i\downarrow}$. If the ordered phase does not break the symmetry of the lattice, as in a simple ferromagnet, one does not have to consider several sublattices. Then, one has for the generalized susceptibility $X^{\sigma\sigma'}_{kk'q}$, defined in Eq. (B.11) of chapter 2,

$$\sum_{k'}\left[\varepsilon_{k'+q,\sigma'} - \varepsilon_{k'\sigma'} - \imath\omega\right]X^{\sigma\sigma'}_{kk'q} = [G_{k+q,\sigma} - G_{k\sigma}]\delta_{\sigma\sigma'}, \qquad (C.31)$$

and the respective identity for $X^{\overline{\sigma\sigma}}_{kk'q}$, Eq. (B.12) of chapter 2,

$$\sum_{k'}\left[\varepsilon_{k'+q,\bar\sigma} - \varepsilon_{k'\sigma} - \imath\omega\right]X^{\overline{\sigma\sigma}}_{kk'q} = G_{k+q,\bar\sigma} - G_{k\sigma}. \qquad (C.32)$$

On the lattice one has $\varepsilon_k \to \varepsilon_{\mathbf{k}}$, the respective relation for an impurity model is obtained for $\varepsilon_k \to \Delta_\nu$, together with the replacements comprised in Eq. (C.18).

C.6   Bipartite ordered phases

If the ordered phase breaks the symmetry of the lattice, several sublattices have to be considered and Fourier transforms can only be performed up to the enlarged unit cell of the ordered state. In the case of an incommensurate charge density wave or spiral order the generalized susceptibility becomes a large matrix, a general discussion of the Ward identity for any type of order becomes very tedious. However, for later reference, the Ward identity for a bipartite ordered state will be discussed in the following, which is useful, e.g., for

bipartite antiferromagnetic or charge ordered phases. The following discussion is part of the publication [137] and follows similar ones in Refs. [114, 32].

In a bipartite ordered state the volume of the Brillouin zone (BZ) is halved, in this reduced Brillouin zone (RBZ) the noninteracting Hamiltonian reads,

$$
H_0 = \sum_{\mathbf{k} \in \text{RBZ}, \sigma} (A_{\mathbf{k}\sigma}^\dagger, B_{\mathbf{k}\sigma}^\dagger) \begin{pmatrix} h_\sigma^A & \varepsilon_{\mathbf{k}} \\ \varepsilon_{\mathbf{k}} & h_\sigma^B \end{pmatrix} \begin{pmatrix} A_{\mathbf{k}\sigma} \\ B_{\mathbf{k}\sigma} \end{pmatrix}, \tag{C.33}
$$

where $A_{\mathbf{k}\sigma}^{(\dagger)}$ and $B_{\mathbf{k}\sigma}^{(\dagger)}$ annihilate (create) a σ-electron with momentum $\mathbf{k}$ in sublattice A and B, respectively. $\varepsilon_{\mathbf{k}}$ is the dispersion of a bipartite lattice, where bipartite means that the lattice can be divided into the two sublattices A and B such that an electron on sublattice A can only hop to atoms of the sublattice B and vice versa. Also introduced is an outer *staggered* field h_σ^a, whose value may depend on the sublattice and spin indices. The outer field may be a staggered chemical potential, $h_\sigma^a = -(\delta_{aA} - \delta_{aB})\tilde{\mu}$, which is the conjugate field of a bipartite charge density wave state (charge order), or a staggered magnetic field $h_\sigma^a = -(\delta_{aA} - \delta_{aB})\sigma h$, the conjugate field of a bipartite antiferromagnet.

In this notation Green's function $G_{k\sigma}^{ab} = -\left\langle a_{k\sigma} b_{k\sigma}^\dagger \right\rangle$ is a two-by-two matrix in the sublattice indices $a, b \in \{A, B\}$,

$$
\hat{G}_{k\sigma} = \begin{pmatrix} G_{k\sigma}^{AA} & G_{k\sigma}^{AB} \\ G_{k\sigma}^{BA} & G_{k\sigma}^{BB} \end{pmatrix} = \begin{pmatrix} -\left\langle A_{k\sigma} A_{k\sigma}^\dagger \right\rangle & -\left\langle A_{k\sigma} B_{k\sigma}^\dagger \right\rangle \\ -\left\langle B_{k\sigma} A_{k\sigma}^\dagger \right\rangle & -\left\langle B_{k\sigma} B_{k\sigma}^\dagger \right\rangle \end{pmatrix}. \tag{C.34}
$$

On the other hand, the two-particle correlation function becomes a tensor in four sublattice indices a, b, c, d. Here, only the transversal spin channel is considered,

$$
G_{kk'q}^{(2),\overline{\sigma\bar{\sigma}},abcd} = -\left\langle a_{k\sigma} b_{k+q,\bar{\sigma}}^\dagger c_{k'+q,\bar{\sigma}} d_{k'\sigma}^\dagger \right\rangle = X_{kk'q}^{\overline{\sigma\bar{\sigma}},abcd}, \tag{C.35}
$$

where the operators labeled with a, b, c, d denote either $A^{(\dagger)}$ or $B^{(\dagger)}$, respectively[2]. The Ward identity for this correlation function is obtained from the equation of motion $\partial_\tau \rho_{\mathbf{q}\bar{\sigma}}^d = [H, \rho_{\mathbf{q}\bar{\sigma}}^d]$ of the local density operator

$$
\rho_{\mathbf{q}\bar{\sigma}}^d = \sum_{\mathbf{k}}' d_{\mathbf{k}\sigma}^\dagger d_{\mathbf{k}+\mathbf{q},\bar{\sigma}}, \tag{C.36}
$$

---

[2] In the transversal spin channel the four-point correlation function is equal to the generalized susceptibility, since they merely differ by an uncorrelated part which vanishes in this channel due to spin conservation [cf. chapter 2, Eq. (A.49)].

where $d \in \{A, B\}$. Similar steps that led to the Ward identity in Eq. (C.11) now yield,

$$\partial_\tau \sum_{\mathbf{k}'}' X^{\overline{\sigma\sigma},abdd}_{\mathbf{k}\mathbf{k}'\mathbf{q}}(\tau_1, \tau_2, \tau, \tau) + \langle T_\tau a_{\mathbf{k}\sigma}(\tau_1) b^\dagger_{\mathbf{k}+\mathbf{q},\bar{\sigma}}(\tau_2)[\rho^d_{\mathbf{q}\bar{\sigma}}(\tau), \mathcal{H}]\rangle$$

$$= [G^{ab}_{\mathbf{k}+\mathbf{q},\bar{\sigma}}(\tau_1 - \tau_2)\delta(\tau - \tau_1)\delta_{ad} - G^{ab}_{\mathbf{k}\sigma}(\tau_1 - \tau_2)\delta(\tau - \tau_2)\delta_{bd}]. \tag{C.37}$$

Despite the complications, the general pattern to obtain the Ward identity remains to impose the continuity equation of a local density on the four-point correlation function. Although derived here for a bipartite lattice, one may use Eq. (C.37) as the starting point for a formulation of the Ward identity in real space or for multi-orbital systems, by viewing the labels a, b, c, d as elements of an arbitrary set of quantum numbers.

Assuming again that the interaction Hamiltonian H_{int} does not contribute to the currents,

$$[\rho^d_{\mathbf{q}\bar{\sigma}}, \mathcal{H}] = [\rho^d_{\mathbf{q}\bar{\sigma}}, H_0 - \mu N]$$

$$= \sum_{\mathbf{k}}'(\varepsilon_{\mathbf{k}+\mathbf{q}}\delta_{Ad} - \varepsilon_{\mathbf{k}}\delta_{Bd})A^\dagger_{\mathbf{k}\sigma}B_{\mathbf{k}+\mathbf{q},\bar{\sigma}} + \sum_{\mathbf{k}}'(\varepsilon_{\mathbf{k}+\mathbf{q}}\delta_{Bd} - \varepsilon_{\mathbf{k}}\delta_{Ad})B^\dagger_{\mathbf{k}\sigma}A_{\mathbf{k}+\mathbf{q},\bar{\sigma}}$$

$$+ (h^A_{\bar{\sigma}} - h^A_\sigma)\sum_{\mathbf{k}}'\delta_{Ad}A^\dagger_{\mathbf{k}\sigma}A_{\mathbf{k}+\mathbf{q},\bar{\sigma}} + (h^B_{\bar{\sigma}} - h^B_\sigma)\sum_{\mathbf{k}}'\delta_{Bd}B^\dagger_{\mathbf{k}\sigma}B_{\mathbf{k}+\mathbf{q},\bar{\sigma}}. \tag{C.38}$$

Inserting this relation into the Ward identity Eq. (C.37) and transforming to Matsubara frequencies leads to

$$-\imath\omega\sum_{k'} X^{\overline{\sigma\sigma},abdd}_{kk'q} + \sum_{k'}(\varepsilon_{k'+q}\delta_{Ad} - \varepsilon_{k'}\delta_{Bd})X^{\overline{\sigma\sigma},abBA}_{kk'q} + \sum_{k'}(\varepsilon_{k'+q}\delta_{Bd} - \varepsilon_{k'}\delta_{Ad})X^{\overline{\sigma\sigma},abAB}_{kk'q}$$

$$+ (h^A_{\bar{\sigma}} - h^A_\sigma)\sum_{k'} X^{\overline{\sigma\sigma},abAA}_{kk'q} + (h^B_{\bar{\sigma}} - h^B_\sigma)X^{\overline{\sigma\sigma},abBB}_{kk'q} = \delta_{ad}G^{ab}_{k+q\bar{\sigma}} - \delta_{bd}G^{ab}_{k\sigma}. \tag{C.39}$$

Evaluating this Ward identity for all possible combinations of the labels a, b and d leads to the following tensor relation for the generalized susceptibility,

$$\sum_{k'} \begin{pmatrix} (h^A_{\bar{\sigma}} - h^A_\sigma) - \imath\omega & (h^A_{\bar{\sigma}} - h^A_\sigma) \\ \varepsilon_{k'+q} & -\varepsilon_{k'} \\ -\varepsilon_{k'} & \varepsilon_{k'+q} \\ (h^B_{\bar{\sigma}} - h^B_\sigma) & (h^B_{\bar{\sigma}} - h^B_\sigma) - \imath\omega \end{pmatrix}^T \hat{X}^{\overline{\sigma\sigma}}_{kk'q} = \begin{pmatrix} G^{AA}_{k+q\bar{\sigma}} - G^{AA}_{k\sigma} & 0 \\ G^{AB}_{k+q\bar{\sigma}} & -G^{AB}_{k\sigma} \\ -G^{BA}_{k\sigma} & G^{BA}_{k+q\bar{\sigma}} \\ 0 & G^{BB}_{k+q\bar{\sigma}} - G^{BB}_{k\sigma} \end{pmatrix}^T,$$

$$\tag{C.40}$$

where the tensor of the generalized susceptibility $X_{kk'q}^{\overline{\sigma\sigma},abcd}$ is given as (spin and momentum labels dropped),

$$
\hat{X} = \begin{pmatrix} X^{AAAA} & X^{ABAA} & X^{BAAA} & X^{BBAA} \\ X^{AABA} & X^{ABBA} & X^{BABA} & X^{BBBA} \\ X^{AAAB} & X^{ABAB} & X^{BAAB} & X^{BBAB} \\ X^{AABB} & X^{ABBB} & X^{BABB} & X^{BBBB} \end{pmatrix}.
$$

(C.41)

Below, several useful statements follow from the Ward identity Eq. (C.40) when summing over the columns on the LHS and RHS, which is equivalent to multiplication with the vector $(1,1)$ from the left on both sides,

$$
\sum_{k'} \begin{pmatrix} 2(h_{\bar{\sigma}}^A - h_{\sigma}^A) - \imath\omega \\ \varepsilon_{k'+q} - \varepsilon_{k'} \\ \varepsilon_{k'+q} - \varepsilon_{k'} \\ 2(h_{\bar{\sigma}}^B - h_{\sigma}^B) - \imath\omega \end{pmatrix}^T \hat{X}_{kk'q}^{\overline{\sigma\sigma}} = \begin{pmatrix} G_{k+q\bar{\sigma}}^{AA} - G_{k\sigma}^{AA} \\ G_{k+q\bar{\sigma}}^{AB} - G_{k\sigma}^{AB} \\ G_{k+q\bar{\sigma}}^{BA} - G_{k\sigma}^{BA} \\ G_{k+q\bar{\sigma}}^{BB} - G_{k\sigma}^{BB} \end{pmatrix}^T.
$$

(C.42)

The mapping of correlation functions from RBZ to those defined in the BZ is the same unitary transformation that diagonalizes the Hamiltonian matrix in Eq. (C.33) for vanishing outer fields $h^A = h^B = 0^3$,

$$
\hat{S} = \frac{1}{\sqrt{2}} \begin{pmatrix} 1 & 1 \\ -1 & 1 \end{pmatrix},
$$

(C.43)

where $\hat{S}^{-1}\hat{S} = \hat{S}^T\hat{S} = \hat{1}$. This maps the susceptibility matrix $X_q^{\overline{\sigma\sigma},ab} = -\left\langle \rho_{-q,\sigma}^a \rho_{q\bar{\sigma}}^b \right\rangle$ to

$$
2\hat{S}^T\hat{X}_q\hat{S} = \begin{pmatrix} X_q^{AA} - X_q^{AB} - X_q^{BA} + X_q^{BB} & X_q^{AA} + X_q^{AB} - X_q^{BA} - X_q^{BB} \\ X_q^{AA} + X_q^{AB} - X_q^{BA} - X_q^{BB} & X_q^{AA} + X_q^{AB} + X_q^{BA} + X_q^{BB} \end{pmatrix}.
$$

(C.44)

In the paramagnet the susceptibility is invariant with respect to the exchange of the labels A and B, such that the offdiagonal elements of the matrix vanish in this case. Hence, the unitary transformation S diagonalizes the susceptibility in the disordered phase and represents the mapping from the RBZ to the BZ. Namely, it maps a wave vector $\mathbf{q}$ of the RBZ to the vectors $\tilde{\mathbf{q}} = \mathbf{q}$ and $\tilde{\mathbf{q}} = \mathbf{q} + \mathbf{Q}$ of the BZ, where $\mathbf{Q}$ is the ordering vector, e.g., $\mathbf{Q} = (\pi, \pi)$ on the square lattice. Fig. 3.7 illustrates the relation between a vector in the

---

[3] Most textbooks do not provide a detailed reformulation of correlation functions in states that do not preserve the lattice symmetry, see the lecture notes on tight-binding models of K. Sun for a comprehensive introduction, http://www-personal.umich.edu/~sunkai/index.html.
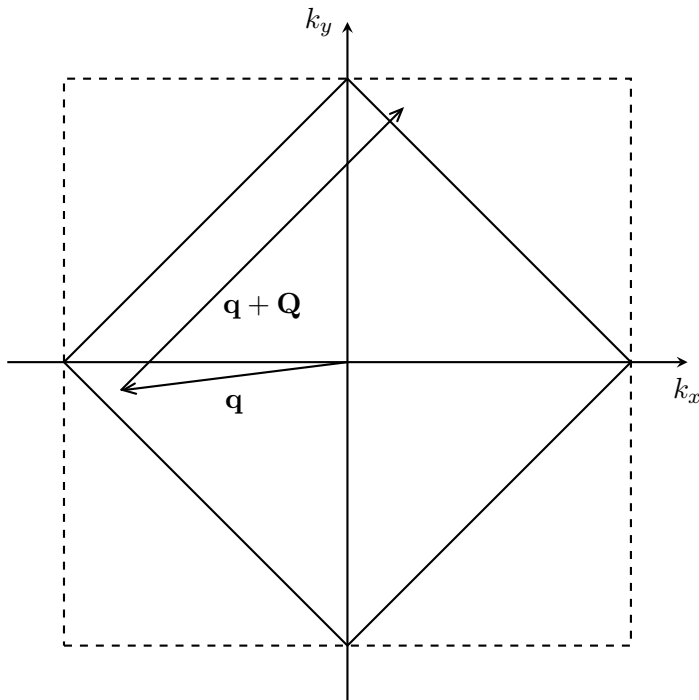
FIGURE 3.7: The Brillouin zone (dashed quadrangle) and the reduced Brillouin zone (solid quadrangle) of the square lattice in bipartite phases. Each vector $\mathbf{q}$ of the reduced Brillouin zone maps to two vectors of the Brillouin zone, $\tilde{\mathbf{q}} = \mathbf{q}$ and $\tilde{\mathbf{q}} = \mathbf{q} + \mathbf{Q}$, where $\mathbf{Q} = (\pi, \pi)$ is the ordering vector.

RBZ and the BZ for this lattice. Using $Q = (\mathbf{Q}, 0)$ one can therefore identify,

$$\hat{X}_{\tilde{q}} = 2\hat{S}^T \hat{X}_q \hat{S} = \begin{pmatrix} X_{q+Q} & X^{\pm}_{q+Q} \\ X^{\pm}_q & X_q \end{pmatrix}, \tag{C.45}$$

where the matrix elements are defined through Eq. (C.44).

D   Remarks on integral Ward identities

Some remarks are in place on the integral Ward identities derived in the last subsection, which imply a number of exact statements regarding the susceptibility.

From the equation of motion for the four-point correlation function, Eq. (C.2), it was possible to derive the Ward identity of the lattice Eq. (C.14) and of a local impurity model, Eq. (C.30). Thanks to their obvious similarity, and using the compact notation $k = (\mathbf{k}, \nu)$,

they can be comprised into

$$G_{k+q} - G_k = \sum_{k'} \left([G^0_{k'}]^{-1} - [G^0_{k'+q}]^{-1}\right) X^\alpha_{kk'q} + \frac{1}{2} \sum_{\sigma\sigma'} s^\alpha_{\sigma'\sigma} \langle c_{k\sigma} c^\dagger_{k+q,\sigma'} [\rho^\alpha, H_{\text{int}}]_q \rangle, \quad \text{(D.1)}$$

where $G^0_k = [\imath\nu + \mu - \varepsilon_{\mathbf{k}}]^{-1}$, $G_k = G_{\mathbf{k}\nu}$ on the lattice and $G^0_k = g^0_\nu = [\imath\nu + \mu - \Delta_\nu]^{-1}$, $G_k = g_\nu$ and $X_{kk'q} = \chi_{\nu\nu'\omega}$ in a local impurity model. The summation only over k' on the RHS of (D.1) seems arbitrary and indeed the whole derivation may be repeated from the equation of motion of $\partial_\tau \sum'_{\mathbf{k}} X^\alpha_{\mathbf{k}\mathbf{k}'\mathbf{q}}(\tau, \tau, \tau_1, \tau_2)$. This leads to a similar expression which reflects the crossing symmetries of the correlation functions in Eq. (D.1), (i.e., $X^\alpha_{kk'q} = X^\alpha_{k'+q,k+q,-q}$ for the generalized susceptibility).

Since in the derivation of Eq. (D.1) the equation of motion was used, any approximation to the 1P and 2P correlation functions G and X that satisfies the EOM must also satisfy the Ward identity (D.1). Then one says that such an approximation satisfies local conservation laws. Global conservation follows immediately and is reflected by satisfaction of Eq. (D.1) at $\mathbf{q} = \mathbf{0}$, since then the EOM yields $\partial_\tau \sum'_i \rho^\alpha_i = \partial_\tau \rho^\alpha_{\mathbf{q}=\mathbf{0}} = [\mathcal{H}, \rho^\alpha_{\mathbf{q}=\mathbf{0}}] = 0$. In the following, several statements will be derived considering the Ward identity in Eq. (D.1) at $\mathbf{q} = \mathbf{0}$. It should be noted that, since most interaction Hamiltonians conserve the total densities, leading to $[\rho^\alpha_{\mathbf{q}=\mathbf{0}}, H_{\text{int}}] = 0$, the second term on the RHS of Eq. (D.1) can usually be neglected in this limit, which is assumed in several places for convenience.

D.1   Global conservation and Goldstone mode

Q The Ward identity in Eq. (D.1) has implications for the spectrum of two-particle excitations, represented by the susceptibilities $X^\alpha_q = 2\sum_{kk'} X^\alpha_{kk'q}$: Summing Eq. (D.1) over k yields zero on the LHS and, therefore,

$$\sum_{kk'} \left([G^0_{k'}]^{-1} - [G^0_{k'+q}]^{-1}\right) X^\alpha_{kk'q} = \frac{1}{2} \langle \rho^\alpha_{-q} [\rho^\alpha, H_{\text{int}}]_q \rangle. \qquad \text{(D.2)}$$

Under the condition that the interaction conserves the total density, $[H_{\text{int}}, \rho^\alpha_{\mathbf{q}=\mathbf{0}}] = 0$, the RHS of (D.2) vanishes at $\mathbf{q} = \mathbf{0}$. The LHS also simplifies due to $[G^0_{\mathbf{k}'\nu'}]^{-1} - [G^0_{\mathbf{k}',\nu+\omega}]^{-1} = -\imath\omega$, and thus Eq. (D.2) yields at $\mathbf{q} = \mathbf{0}$,

$$2\imath\omega \sum_{kk'} X^\alpha_{kk',q=(\mathbf{0},\omega)} = \imath\omega X^\alpha_{\mathbf{q}=\mathbf{0},\omega} = 0. \qquad \text{(D.3)}$$

This statement implies that in the disordered phase ($G_\uparrow = G_\downarrow$ is assumed) the conservation of the total density $\rho^\alpha_{\mathbf{q}=\mathbf{0}}$ requires charge and spin excitations to be gapless at $\mathbf{q} = \mathbf{0}$. This is since $X^\alpha_{\mathbf{q}=\mathbf{0},\omega}$ must vanish for any $\omega \neq 0$, such that excitations at small $\mathbf{q}$ correspond to small energies.

On the other hand, under the influence of a magnetic field $h_\sigma = -\sigma h$ along the z-axis[4], or in a ferromagnetic phase with magnetic moments $\langle m \rangle = \langle n_\uparrow \rangle - \langle n_\downarrow \rangle$ aligned along that direction, one has to consider the Ward identities Eqs. (C.31) and (C.32). With $\varepsilon_{k\sigma} = \varepsilon_{\mathbf{k}} + h_\sigma$, multiplication by two and summation over k' of Eq. (C.32) yields for the transversal susceptibility at $\mathbf{q} = \mathbf{0}$[5],

$$2 \sum_{kk'} (h_{\bar{\sigma}} - h_\sigma - \imath\omega) X^{\overline{\sigma\bar{\sigma}}}_{kk',q=(\mathbf{0},\omega)} = (h_{\bar{\sigma}} - h_\sigma - \imath\omega) X^{\overline{\sigma\bar{\sigma}}}_{q=(\mathbf{0},\omega)} = 2(\langle n_{\bar{\sigma}} \rangle - \langle n_\sigma \rangle),$$

$$\Leftrightarrow X^{\overline{\sigma\bar{\sigma}}}_{\mathbf{q}=\mathbf{0},\omega} = 2 \frac{\langle n_{\bar{\sigma}} \rangle - \langle n_\sigma \rangle}{h_{\bar{\sigma}} - h_\sigma - \imath\omega} = \frac{2\sigma \langle m \rangle}{\imath\omega - 2\sigma h}. \tag{D.4}$$

Hence, in case of a spontaneously broken symmetry with a finite magnetization $\langle m \rangle$ as $h \to 0$, global conservation implies the existence of a gapless Goldstone mode at $\mathbf{q} = \mathbf{0}$. In comparison, the gapless excitations of the disordered phase described by Eq. (D.3) have a vanishing spectral weight at $\mathbf{q} = \mathbf{0}$. The Goldstone mode in Eq. (D.4), on the other hand, has a weight $\sim \langle m \rangle$ at this point. Goldstone excitations of arbitrarily small energy are able to undermine the emergence of an ordered phase in systems of dimensions one and two, as required by the Mermin-Wagner theorem, and other than the gapless modes of the normal state.

An analogous relation follows for a bipartite antiferromagnet with magnetizations $\langle m^A \rangle = -\langle m^B \rangle = \langle m \rangle$ of the two sublattices A and B. For the derivation it is convenient to consider the Ward identity Eq. (C.42) for a vanishing staggered field $h^A = h^B = 0$ and at $q_0 = (\mathbf{q}_0 = 0, \omega)$, where the vector $\mathbf{q}_0$ is the homogeneous wave vector of the reduced Brillouin zone. This leads to the following relation for the tensor of the generalized susceptibility,

$$\sum_{k'} \begin{pmatrix} -\imath\omega \\ 0 \\ 0 \\ -\imath\omega \end{pmatrix}^T \hat{X}^{\overline{\sigma\bar{\sigma}}}_{kk'q} = \begin{pmatrix} G^{AA}_{k\bar{\sigma}} - G^{AA}_{k\sigma} \\ G^{AB}_{k\bar{\sigma}} - G^{AB}_{k\sigma} \\ G^{BA}_{k\bar{\sigma}} - G^{BA}_{k\sigma} \\ G^{BB}_{k\bar{\sigma}} - G^{BB}_{k\sigma} \end{pmatrix}^T. \tag{D.5}$$

---

[4] The single-particle energies of the non-interacting system in an outer magnetic field are defined as $\varepsilon_{k\sigma} = \varepsilon_k + h_\sigma$. The minus sign in the definition of the magnetic field, $h_\sigma = -\sigma h$, implies that the field is aligned with the direction of the $\uparrow$-electrons, such that the energy of these electrons is *lowered* by the magnetic field.

[5] In order to perform the step from the first to the second line in Eq. (D.4) one has to make sure that $h_{\bar{\sigma}} - h_\sigma - \imath\omega \neq 0$. At vanishing magnetic field $h = 0$ this means that the second line of that equation must not be evaluated at $\omega = 0$. However, for an infinitesimal magnetic field this can be done and it leads to Eq. (D.36) for the zero-field derivative $d \langle m \rangle / dh$.

This Ward identity comprises four different relations, the first and the last of which read explicitly,

$$
-\imath\omega \sum_{k'} \left(X_{kk'q_0}^{\overline{\sigma\sigma},AAAA} + X_{kk'q_0}^{\overline{\sigma\sigma},AABB} \right) = G_{k+q_0\bar{\sigma}}^{AA} - G_{k\sigma}^{AA}, \tag{D.6}
$$

$$
-\imath\omega \sum_{k'} \left(X_{kk'q_0}^{\overline{\sigma\sigma},BBBB} + X_{kk'q_0}^{\overline{\sigma\sigma},BBAA} \right) = G_{k+q_0\bar{\sigma}}^{BB} - G_{k\sigma}^{BB}. \tag{D.7}
$$

Summing both relations over k one identifies the susceptibility $X_q^{\overline{\sigma\sigma},ab} = \sum_{kk'} X_{kk'q}^{\overline{\sigma\sigma},aabb}$ and the magnetization using $\sum_k G_{k\sigma}^{aa} = \langle n_\sigma^a \rangle$, as well as $\langle n_{\bar{\sigma}}^a \rangle - \langle n_\sigma^a \rangle = -\sigma \langle m^a \rangle$,

$$
\imath\omega \left(X_{q_0}^{\overline{\sigma\sigma},AA} + X_{q_0}^{\overline{\sigma\sigma},AB} \right) = \sigma \langle m^A \rangle, \tag{D.8}
$$

$$
\imath\omega \left(X_{q_0}^{\overline{\sigma\sigma},BB} + X_{q_0}^{\overline{\sigma\sigma},BA} \right) = \sigma \langle m^B \rangle. \tag{D.9}
$$

Since $\langle m^A \rangle = -\langle m^B \rangle = \langle m \rangle$, addition of these equations leads to

$$
\imath\omega X_{\tilde{q}_0}^{\overline{\sigma\sigma}} = \imath\omega \left(X_{q_0}^{\overline{\sigma\sigma},AA} + X_{q_0}^{\overline{\sigma\sigma},AB} + X_{q_0}^{\overline{\sigma\sigma},BB} + X_{q_0}^{\overline{\sigma\sigma},BA} \right) = 0, \tag{D.10}
$$

where the homogeneous susceptibility $X_{\tilde{q}_0}^{\overline{\sigma\sigma}}$ of the regular Brillouin zone was identified, cf. definition Eq. (C.45), and $\tilde{\mathbf{q}}_0 = \mathbf{0}$ is the homogeneous wave vector of the regular Brillouin zone. Hence, the homogeneous susceptibility of the bipartite antiferromagnet satisfies the same constraint as it does in the disordered phase, Eq. (D.3). On the other hand, subtracting Eq. (D.9) from Eq. (D.8) leads to,

$$
\imath\omega X_{\tilde{q}_0}^{\overline{\sigma\sigma},\pm} = \imath\omega \left(X_{q_0}^{\overline{\sigma\sigma},AA} + X_{q_0}^{\overline{\sigma\sigma},AB} - X_{q_0}^{\overline{\sigma\sigma},BB} - X_{q_0}^{\overline{\sigma\sigma},BA} \right) = 2\sigma \langle m \rangle. \tag{D.11}
$$

The emergence of the order parameter $\langle m \rangle$ in the antiferromagnetic phase can thus be observed in $X_{\tilde{q}_0}^{\overline{\sigma\sigma},\pm}$, rather than in $X_{\tilde{q}_0}^{\overline{\sigma\sigma}}$, where it occurs in the ferromagnet [cf. Eq. (D.4)]. Of course, if the system is ferromagnetic, such that sublattice A and B have the same magnetization $\langle m^A \rangle = \langle m^B \rangle = \langle m \rangle$, the RHSs of Eqs. (D.10) and (D.11) are interchanged and Eq. (D.4) is recovered ($h = 0$).

D.2   Asymptotic relations

The asymptotic behavior of the lattice susceptibility can be determined from the k-integrated Ward identity in Eq. (D.2), which may be recast into

$$
\imath\omega X_q^\alpha = 2 \sum_{kk'} \left[\varepsilon_{k'+q} - \varepsilon_{k'} \right] X_{kk'q}^\alpha - \langle \rho_{-q}^\alpha [\rho^\alpha, H_{\text{int}}]_q \rangle. \tag{D.12}
$$

This relation implies immediately the leading $(\imath\omega)^{-2}$ coefficient of the susceptibility X_q^α, as can be seen by expanding the terms on the RHS up to order $(\imath\omega)^{-1}$. To this end we

remember that the generalized susceptibility is given by the interacting bubble and vertex corrections, $X_{kk'q}^{\alpha} = G_k G_{k+q} \left[N\beta\delta_{kk'} + F_{kk'q}^{\alpha} G_{k'} G_{k'+q} \right]$, comprised in the T-matrix F. Let us examine the $(\imath\omega)^{-1}$ coefficient of the bubble,

$$
\begin{aligned}
G_k G_{k+q} &= \frac{G_k - G_{k+q}}{G_{k+q}^{-1} - G_k^{-1}} \\
&= \frac{1}{\imath\omega} \frac{G_k - G_{k+q}}{1 + (\varepsilon_k - \varepsilon_{k+q} + \Sigma_k - \Sigma_{k+q})/\imath\omega} \\
&= \frac{1}{\imath\omega}(G_k - G_{k+q}) + \mathcal{O}(\omega^{-2}).
\end{aligned}
\tag{D.13}
$$

The term G_{k+q} in the last line needs to be kept, since it is of order $\mathcal{O}(1)$ at $k \approx -q$. While an expansion up to order $(\imath\omega)^{-1}$ of the interacting bubble is trivial, it is difficult to go beyond this order, because this requires some knowledge of the self-energy Σ.

Considering that the T-matrix F does not grow with $\imath\omega$, we can treat it as a constant in the limit and the generalized susceptibility up to order $(\imath\omega)^{-1}$ is hence simply given by the expression in Eq. (D.13),

$$
X_{kk'q}^{\alpha} = N\beta\delta_{kk'} \frac{G_k - G_{k+q}}{\imath\omega} + \mathcal{O}(\omega^{-2}).
\tag{D.14}
$$

On a lattice, where $\varepsilon_k = \varepsilon_{\mathbf{k}}$, one obtains then for the first term on the RHS of Eq. (D.12),

$$
\begin{aligned}
2\sum_{kk'} \left[\varepsilon_{k'+q} - \varepsilon_{k'} \right] X_{kk'q}^{\alpha} &= \frac{2}{\imath\omega} \sum_k \left[\varepsilon_{k+q} - \varepsilon_k \right] (G_k - G_{k+q}) + \mathcal{O}(\omega^{-2}) \\
&= \frac{2}{\imath\omega} {\sum_{\nu\mathbf{k}}}' (G_{\mathbf{k}\nu}\varepsilon_{\mathbf{k+q}} + G_{\mathbf{k+q},\nu}\varepsilon_{\mathbf{k}} - 2G_{\mathbf{k}\nu}\varepsilon_{\mathbf{k}}) + \mathcal{O}(\omega^{-2}) \\
&= \frac{1}{\imath\omega} {\sum_{\mathbf{k}\sigma}}' \langle n_{\mathbf{k}\sigma} \rangle (\varepsilon_{\mathbf{k+q}} + \varepsilon_{\mathbf{k-q}} - 2\varepsilon_{\mathbf{k}}) + \mathcal{O}(\omega^{-2}).
\end{aligned}
\tag{D.15}
$$

For the second term in Eq. (D.12) let us consider the Lehmann representation of a dynamic correlation function $C_\omega = \langle A_{-\omega} B_\omega \rangle$, where A and B are arbitrary bosonic operators, and expand C for large $\imath\omega$,

$$
\begin{aligned}
C_\omega &= \frac{1}{\mathcal{Z}} \sum_{ll'} \frac{\langle l | A | l' \rangle \langle l' | B | l \rangle}{\imath\omega + E_l - E_{l'}} \left(e^{-\beta E_l} - e^{-\beta E_{l'}} \right),
\end{aligned}
\tag{D.16}
$$

$$
= \frac{\langle [A, B] \rangle}{\imath\omega} + \mathcal{O}(\omega^{-2}).
\tag{D.17}
$$

Using this on the second term on the RHS of Eq. (D.12),

$$\langle \rho^\alpha_{-q}[\rho^\alpha, H_{\text{int}}]_q \rangle = \frac{\langle \left[\rho^\alpha_{-\mathbf{q}}, [\rho^\alpha_{\mathbf{q}}, H_{\text{int}}]\right] \rangle}{\imath \omega} + \mathcal{O}(\omega^{-2}). \tag{D.18}$$

Inserting the expressions in Eqs. (D.15) and (D.18) into Eq. (D.12), multiplying by $\imath\omega$ and taking the limit $\omega \to \infty$ yields,

$$\lim_{\omega \to \infty} (\imath \omega)^2 X^\alpha_{\mathbf{q}\omega} = \sum_{\mathbf{k}\sigma}{}' \langle n_{\mathbf{k}\sigma} \rangle \left(\varepsilon_{\mathbf{k}+\mathbf{q}} + \varepsilon_{\mathbf{k}-\mathbf{q}} - 2\varepsilon_{\mathbf{k}} \right) - \left\langle \left[\rho^\alpha_{-\mathbf{q}}, [\rho^\alpha_{\mathbf{q}}, H_{\text{int}}]\right] \right\rangle. \tag{D.19}$$

Hence, the satisfaction of the Ward identity in Eq. (D.1) implies the asymptotic behavior of the susceptibilities in Eq. (D.19). A direct expansion of $X^\alpha_{\mathbf{q}\omega}$ up to $(\imath\omega)^{-2}$ does not straightforwardly yield this result. Instead, it is the factor $\imath\omega$ in Eq. (D.12) that allows to expand its RHS only up to order $(\imath\omega)^{-1}$ to find the asymptotic coefficient of X up to order $(\imath\omega)^{-2}$ in Eq. (D.19). An approximation that does not satisfy local conservation laws is therefore likely to violate this relation. This may be seen on the example of the interacting bubble in Eq. (D.14), which is sometimes used as an approximation to the susceptibility, and which in general violates Eq. (D.19) [39].

D.3   First moment of the spectral weight and relation to the kinetic energy

The correct $(\imath\nu)^{-1}$-coefficient of Green's function, $\langle [c^\dagger, c] \rangle = 1$, is recovered in virtually all approximations. On the other hand, conservation laws are needed to satisfy a similar statement for X, Eq. (D.19). The $(\imath\nu)^{-1}$-coefficient Green's function fixes the total spectral weight of the density of states to unity, while Eq. (D.19) fixes the first spectral moment of the susceptibility. This follows from the relation of the susceptibility on the Matsubara axis to its analytical continuation on the real axis,

$$X^\alpha_{\mathbf{q}\omega} = \int_{-\infty}^{\infty} \frac{dE}{\pi} \frac{\operatorname{Im} X^\alpha_{\mathbf{q}}(E + \imath\delta)}{E - \imath\omega}. \tag{D.20}$$

The imaginary part on the RHS must vanish in a paramagnetic system, therefore[6],

$$\lim_{\omega \to \infty} (\imath \omega)^2 X^\alpha_{\mathbf{q}\omega} = \lim_{\omega \to \infty} (\imath \omega)^2 \int_{-\infty}^{\infty} \frac{dE}{\pi} \frac{E \operatorname{Im} X^\alpha_{\mathbf{q}}(E + \imath\delta)}{E^2 - (\imath\omega)^2} = -\int_{-\infty}^{\infty} \frac{dE}{\pi} E \operatorname{Im} X^\alpha_{\mathbf{q}}(E + \imath\delta). \tag{D.21}$$

---

[6]Interchanging the limit $\omega \to \infty$ with the integral over the real frequency in Eq. (D.21) assumes a certain well-behavedness of $\operatorname{Im} X(E)$ at $E \to \infty$. From a physical point of view it must be possibe for $|\omega|$ to become larger than the largest energy scale of the system at hand, since this effectively provides a finite support for the integral in Eq. (D.21). For this reason, one must not assume that the asymptotic formulae derived in this section remain valid if one of the physical parameters is infinitely large, such as in the Hubbard model in the limit $U \to \infty$.

Therefore, Eq. (D.19) automatically fixes the first spectral moment of the susceptibility on the real axis.

When the interaction conserves the charge and spin densities, i.e., $[\rho_{\mathbf{q}}^\alpha, H_{\text{int}}] = 0$, Eq. (D.19) can be shown to be equivalent to the so-called f-sum rule [157, 65], that is

$$-4 \lim_{\eta \to 0} \frac{1}{\beta} \sum_{n>0}^\infty \omega_n \sin(\eta \omega_n) X_{\mathbf{q}\omega_n}^\alpha = \sum_{\mathbf{k}}' \langle n_{\mathbf{k}} \rangle \left(\varepsilon_{\mathbf{k}+\mathbf{q}} + \varepsilon_{\mathbf{k}-\mathbf{q}} - 2\varepsilon_{\mathbf{k}} \right)$$
$$= \lim_{\omega \to \infty} (\imath\omega)^2 X_{\mathbf{q}\omega}^\alpha. \tag{D.22}$$

This also means that this form of the f-sum rule is not valid for $[\rho_{\mathbf{q}}^\alpha, H_{\text{int}}] \neq 0$, since it does not recover the second term on the RHS of Eq. (D.19). For a numerical evaluation of the f-sum rule the expression $\lim_{\omega \to \infty} (\imath\omega)^2 X_{\mathbf{q}\omega}^\alpha$ is preferable over the LHS of Eq. (D.22), which is ill-behaved [65].

A further implication of the Ward identity is a relation of the susceptibility asymptote to the kinetic energy $E_{\text{kin}} = \sum_{\mathbf{k}\sigma} \langle n_{\mathbf{k}\sigma} \rangle \varepsilon_{\mathbf{k}}$. This can simply be seen by summing the asymptotic relation Eq. (D.19) over $\mathbf{q}$,

$$\lim_{\omega \to \infty} (\imath\omega)^2 \sum_{\mathbf{q}}' X_{\mathbf{q},\omega}^\alpha = \sum_{\mathbf{k}\mathbf{q}\sigma}' \langle n_{\mathbf{k}\sigma} \rangle \left(\varepsilon_{\mathbf{k}+\mathbf{q}} + \varepsilon_{\mathbf{k}-\mathbf{q}} - 2\varepsilon_{\mathbf{k}} \right) - \sum_{\mathbf{q}}' \left\langle \left[\rho_{-\mathbf{q}}^\alpha, [\rho_{\mathbf{q}}^\alpha, H_{\text{int}}] \right] \right\rangle,$$

$$\Leftrightarrow \lim_{\omega \to \infty} (\imath\omega)^2 X_{\text{loc},\omega}^\alpha = -2E_{\text{kin}} - \sum_{\mathbf{q}}' \left\langle \left[\rho_{-\mathbf{q}}^\alpha, [\rho_{\mathbf{q}}^\alpha, H_{\text{int}}] \right] \right\rangle. \tag{D.23}$$

Here, the local part of the susceptibility was defined as $X_{\text{loc}} = \sum_{\mathbf{q}}' X_{\mathbf{q}}$, and it was assumed that $\sum_{\mathbf{k}} \varepsilon_{\mathbf{k}} = 0$. According to Eq. (D.23), an interaction H_{int} manifests in the asymptotic behavior of X_{loc}^α if it does not conserve the density ρ^α.

D.4 Asymptotic relations in an impurity model

The asymptotic relations above can also be derived for an impurity model with the Ward identity in Eq. (C.30). To this end, one may simply set $\varepsilon_k = \Delta_\nu$ in Eq. (D.12), together with the other replacement rules defined in Eq. (C.18). Considering that only the interacting bubble $g_\nu g_{\nu+\omega}$ determines the $(\imath\omega)^{-1}$ coefficient of the generalized susceptibility $\chi_{\nu\nu'\omega}^\alpha$, one performs an expansion of the bubble which is similar to Eq. (D.13), with the result $g_\nu g_{\nu+\omega} = (\imath\omega)^{-1}(g_\nu - g_{\nu+\omega}) + \mathcal{O}(\omega^{-2})$. Then, the first term on the RHS of Eq. (D.12) becomes,

$$= \frac{2}{\imath\omega} \sum_{\nu}' \left[\Delta_{\nu+\omega} - \Delta_\nu \right] (g_\nu - g_{\nu+\omega}) + \mathcal{O}(\omega^{-2})$$

$$= -\frac{4}{\imath\omega} \sum_{\nu}' g_\nu \Delta_\nu + \mathcal{O}(\omega^{-2}), \quad (\omega \to \infty). \tag{D.24}$$

Here it was used that terms of the form $g_\nu \Delta_{\nu+\omega}$ vanish at $\omega \to \infty$. Then, we finally arrive at the asymptotic coefficient of the impurity susceptibility,

$$\lim_{\omega \to \infty} (i\omega)^2 \chi_\omega^\alpha = -4 \sum_\nu{}' g_\nu \Delta_\nu - \langle [\rho^\alpha, [\rho^\alpha, H_{\mathrm{int}}]] \rangle. \tag{D.25}$$

Just like on the lattice, an approximation to the impurity susceptibility is usually required to be conserving in order to satisfy this relation. In full analogy to Eq. (D.19) the asymptote in Eq. (D.25) relates the impurity susceptibility to the kinetic energy, which is $E_{\mathrm{kin}} = 2 \sum_\nu{}' g_\nu \Delta_\nu$ for the impurity model defined in Eq. (C.15) [43].

D.5 Asymptotic equivalence of charge and spin excitations

A remarkable feature of the asymptotic relations in Eqs. (D.25) and (D.19) is that their right-hand-sides are independent of the channel index α, provided that the interaction commutes with the respective density, $[\rho^\alpha, H_{\mathrm{int}}] = 0$. This implies that charge and spin excitations of such models, e.g. of the Hubbard model, are always equivalent at high energies, regardless of the value of the interaction (with the technical exception of an infinite interaction, such that $i\omega$ can not become large). Due to the asymptotic equivalence of charge and spin excitations the mapping of the half-filled Hubbard model to an effective Heisenberg model with $J \sim t^2/U$ for large U must fail for large energies. This is because in the Heisenberg model charge excitations are strictly ruled out, while in the Hubbard model charge and spin excitations are asymptotically equivalent at large energies.

D.6 Consistency of zero-field derivatives and fluctuations

QP One of the key features guaranteed by the Ward identity is thermodynamic consistency between zero-field derivatives of Green's function and fluctuations. This is most straightforwardly seen in the case of simple ferromagnetic order, since it does not lead to a reduction of the Brillouin zone[7]. Some of the steps performed here are inspired by similar discussions in Refs. [54], [100] and [67].

Let us consider a system in a magnetic field $h_\sigma = -\sigma h$ along the z-axis, its non-interacting Green's function reads

$$G_{k\sigma}^0 = [i\nu - \varepsilon_{\mathbf{k}} + \mu - h_\sigma]^{-1}. \tag{D.26}$$

---

[7] To be safe, it is also assumed that $[\rho_q^\alpha, H_{\mathrm{int}}] = 0$ for $\alpha = c, x, y, z$, then the Ward identity in Eq. (D.27) is valid at any q. The discussion in this subsection may nevertheless be valid anyhow, since for the ferromagnetic order the Ward identity is considered at $q = 0$. Here one has $[\rho_{q=0}^\alpha, H_{\mathrm{int}}] = 0$ for most interactions, since they conserve the total density, such that this term does not enter the Ward identity.

The Ward identity in the transversal spin channels for symmetry broken phases was given in Eq. (C.32),

$$G_{k+q,\bar{\sigma}} - G_{k\sigma} = \sum_{k'} \left([G^0_{k'\sigma}]^{-1} - [G^0_{k'+q,\bar{\sigma}}]^{-1}\right) X^{\overline{\sigma\bar{\sigma}}}_{kk'q}. \tag{D.27}$$

The generalized susceptibility can be expressed via the T-matrix F,

$$X^{\overline{\sigma\bar{\sigma}}}_{kk'q} = G_{k\sigma}G_{k+q\bar{\sigma}}\left[N\beta\delta_{kk'} + F^{\overline{\sigma\bar{\sigma}}}_{kk'q}G_{k'\sigma}G_{k'+q\bar{\sigma}}\right]. \tag{D.28}$$

Inserting Eq. (D.28) into the Ward identity and dividing both sides by $G_{k\sigma}G_{k+q\bar{\sigma}}$,

$$G^{-1}_{k\sigma} - G^{-1}_{k+q,\bar{\sigma}} = [G^0_{k\sigma}]^{-1} - [G^0_{k+q,\bar{\sigma}}]^{-1} + \sum_{k'} \left([G^0_{k'\sigma}]^{-1} - [G^0_{k'+q,\bar{\sigma}}]^{-1}\right) F^{\overline{\sigma\bar{\sigma}}}_{kk'q}G_{k'\sigma}G_{k'+q,\bar{\sigma}}. \tag{D.29}$$

Using Dyson's equation $\Sigma = [G^0]^{-1} - G^{-1}$ one finds,

$$\Sigma_{k+q,\bar{\sigma}} - \Sigma_{k\sigma} = \sum_{k'} \left([G^0_{k'\sigma}]^{-1} - [G^0_{k'+q,\bar{\sigma}}]^{-1}\right) F^{\overline{\sigma\bar{\sigma}}}_{kk'q}G_{k'\sigma}G_{k'+q,\bar{\sigma}}. \tag{D.30}$$

This equation relates the 1P self-energy Σ on the LHS to the T-matrix F on the RHS. One can expect that a divergence of the T-matrix at a specific value of a control parameter (e.g., the temperature) results in a corresponding singular behavior of the self-energy at the same point. In case of a ferromagnetic phase transition this means that the divergence of the T-matrix, and thus of the spin susceptibility, coincides with the emergence of a finite magnetization $\langle m \rangle = \langle n_\uparrow \rangle - \langle n_\downarrow \rangle$. As a result, Green's function and the 1P self-energy acquire spin-dependence, evaluating Eq. (D.30) at $q = (\mathbf{q}, \omega) = 0$ then yields a finite value on both sides. Inserting $[G^0_{k\sigma}]^{-1} - [G^0_{k,\bar{\sigma}}]^{-1} = h_{\bar{\sigma}} - h_\sigma = 2\sigma h$ into Eq. (D.30) and dividing by h on both sides one has

$$\frac{\Sigma_{k,\bar{\sigma}} - \Sigma_{k\sigma}}{h} = 2\sigma \sum_{k'} F^{\overline{\sigma\bar{\sigma}}}_{kk',q=0}G_{k'\sigma}G_{k',\bar{\sigma}}. \tag{D.31}$$

Now let us assume that the magnetic field h was very small to begin with, exclude any first order transitions, and suppose that the system is in the *paramagnetic* state when the field h vanishes. Then, as one lets $h \to 0$, the self-energy loses its spin-dependence, $\Sigma_\sigma \overset{h\to 0}{\to} \Sigma(h = 0)$. Adding and subtracting $\Sigma(h = 0)$ on the LHS of Eq. (D.31) one has in

the limit,

$$\frac{\Sigma_{k,\bar{\sigma}} - \Sigma_{k\sigma}}{h} = \frac{\Sigma_{k,\bar{\sigma}} - \Sigma_k(h=0)}{h} - \frac{\Sigma_{k,\sigma} - \Sigma_k(h=0)}{h}$$
$$\stackrel{h\to 0}{=} \frac{d\Sigma_{k\bar{\sigma}}}{dh} - \frac{d\Sigma_{k\sigma}}{dh}$$
$$= -2\frac{d\Sigma_{k\sigma}}{dh}. \tag{D.32}$$

The last equality holds since in the paramagnet near $h \sim 0$ the field acts symmetrically opposed on both spin flavors, implying the relation $\frac{d\Sigma_{k\sigma}}{dh} = -\frac{d\Sigma_{k\bar{\sigma}}}{dh}$. Thus, the LHS of Eq. (D.31) is simply two times the derivative of the self-energy at zero-field and one has

$$\frac{d\Sigma_{k\sigma}}{dh} = -\sigma \sum_{k'} F_{kk',q=0}^{\bar{\sigma}\bar{\sigma}} G_{k'\sigma} G_{k',\bar{\sigma}}. \tag{D.33}$$

Hence, a divergence of the T-matrix at a second order transition to the simple ferromagnet must coincide with a divergence of the zero-field derivative of the self-energy at the same value of the control parameter. Since an outer magnetic field acts in opposite ways on both spin flavors, the zero-field derivatives $\frac{d\Sigma_{k\uparrow}}{dh}$ and $\frac{d\Sigma_{k\downarrow}}{dh}$ diverge in opposite directions. As a consequence, an infinitesimal field h is able to let $\Sigma_\uparrow$ and $\Sigma_\downarrow$ assume different values. The magnitude of this split is given by the magnetization $\langle m \rangle$, i.e., the order parameter. Hence, global conservation, that is the Ward identity taken at $q = 0$, implies that at a second order phase transition to ferromagnetism the order parameter emerges at the same point where the T-matrix diverges.

A similar consideration shows that the Ward identity guarantees the consistency of the zero-field derivative of the magnetization and fluctuations. To see this, one evaluates Eq. (D.27) at $q = 0$, summation over k on both sides and using $\sum_k G_{k\sigma} = \langle n_\sigma \rangle$ yields,

$$\langle n_{\bar{\sigma}} \rangle - \langle n_\sigma \rangle = 2\sigma h \sum_{kk'} X_{kk',q=0}^{\bar{\sigma}\bar{\sigma}}. \tag{D.34}$$

This equation relates the magnetization $\langle m \rangle = \langle n_\uparrow \rangle - \langle n_\downarrow \rangle$ on the LHS, to the transversal spin susceptibility $\sum_{kk'\sigma} X_{kk'q}^{\bar{\sigma}\bar{\sigma}} = X_q^{x,y}$ on the RHS [see definitions in Eqs. (A.35) and (A.46) of chapter 2]. Assuming again that the system is paramagnetic in the limit $h \to 0$ one has by virtue of SU(2) symmetry that $\sum_{kk'\sigma} X_{kk',q}^{\bar{\sigma}\bar{\sigma}} = 2\sum_{kk'} X_{kk',q}^{\bar{\sigma}\bar{\sigma}} = X_q^{x,y} = X_q^z \equiv X_q^s$. Dividing Eq. (D.34) by h on both sides and letting $h \to 0$ one has,

$$\frac{\langle n_{\bar{\sigma}} \rangle - \langle n_{\bar{\sigma}}(h=0) \rangle}{h} - \frac{\langle n_\sigma \rangle - \langle n_\sigma(h=0) \rangle}{h} \to -\sigma \frac{d\langle m \rangle}{dh} \tag{D.35}$$
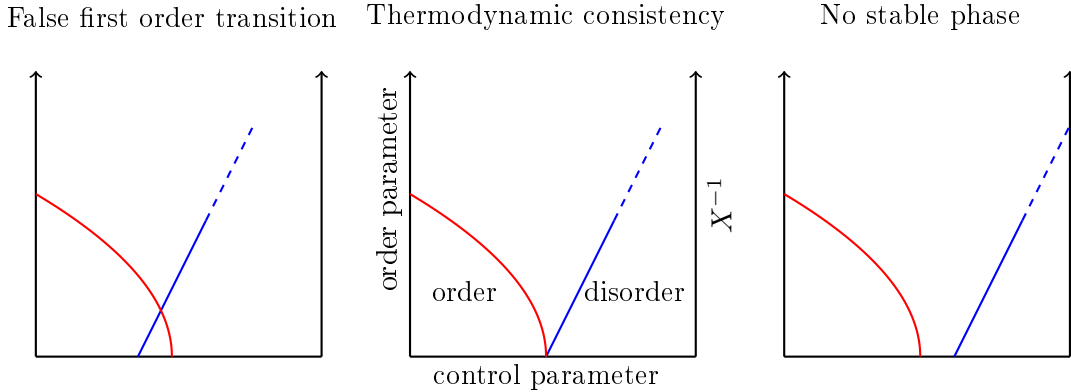
FIGURE 3.8: Three scenarios of thermodynamic (in-)consistency at a second order critical point. In the thermodynamically consistent scenario (middle) the order parameter (red) of the ordered phase and the inverse susceptibility (blue) of the disordered phase vanish at the same value of the control parameter. A thermodynamically inconsistent approximation may either predict a region with two stable phases (left), or with no stable phase at all (right). The former scenario may be interpreted as a false first order transition, while the latter scenario is physically unsound. Note that the units of order parameter and inverse susceptibility are different.

on the LHS of Eq. (D.34), where it was used that $\langle n_{\bar{\sigma}}(h=0) \rangle = \langle n_{\sigma}(h=0) \rangle$. It follows the usual relation between the zero-field derivative and the spin susceptibility,

$$\frac{d \langle m \rangle}{dh} = -X_{q=0}^{s}. \tag{D.36}$$

Although this relation may seem trivial, the equivalence of the zero-field derivative $\frac{d\langle m \rangle}{dh}$ to the homogeneous susceptibility expressed by Eq. (D.36) can not be taken for granted in an arbitrary approximation. In the derivation of Eq. (D.36) the Ward identity at $q = 0$ was used. Hence, global conservation is a sufficient criterion for this equivalence, while a violation of global conservation laws will most likely be accompanied by a violation of Eq. (D.36).

The thermodynamic consistency of zero-field derivatives and fluctuations at second order phase transitions is of great importance. To illustrate this point, let us consider briefly the consequence of a violation of the Ward identity, in particular at $q = 0$. In this case one can not expect that the spin-dependence of the self-energy emerges at the same point where the T-matrix diverges, as expressed by Eq. (D.33). Hence, a violation of global conservation will most likely lead to an inconsistency of the critical points predicted by the susceptibility in the normal phase and by the direct calculation of the order parameter in the ordered phase. In such a thermodynamically inconsistent approximation it may become impossible to distinguish between first and second order phase transitions. In the worst

case an approximation predicts that in some region neither the ordered nor the normal phase are stable. These scenarios are depicted in Fig. 3.8.

An example of a thermodynamically inconsistent approximation has been discussed with the spin-DMFT in Ref. [100], where the violation of Eq. (D.36) has been linked to a violation of the Ward identity. In this work it is also shown that the spin-DMFT predicts a gapped magnon spectrum in the ordered phase, which indicates a violation of Goldstone's theorem. This relates to the discussion after Eq. (D.4), where global spin conservation was shown to imply a gapless magnon spectrum in the ordered phase. Thermodynamic inconsistency of second order critical points and a violation of Goldstone's theorem are thus directly linked via a violation of the Ward identity at $q = 0$.

D.7   Broken lattice symmetry

Although only the special case of simple ferromagnetism was considered above, the Ward identity guarantees in general the consistency of zero-field derivatives and susceptibilities. To illustrate this, let us consider a bipartite antiferromagnet, whose conjugate field is the staggered magnetic field $h_\sigma^a = -(\delta_{aA} - \delta_{aB})\sigma h$, which points in different directions on sublattice A and B. The Ward identity of this system is Eq. (C.42), which needs to be evaluated at the homogeneous wave vector $\mathbf{q} = 0$ of the reduced Brillouin zone and at $\omega = 0$,

$$
\sum_{k'} \begin{pmatrix} 2(h_{\bar\sigma}^A - h_\sigma^A) \\ 0 \\ 0 \\ 2(h_{\bar\sigma}^B - h_\sigma^B) \end{pmatrix}^T \hat{X}_{kk',q=0}^{\overline{\sigma\sigma}} = \begin{pmatrix} G_{k\bar\sigma}^{AA} - G_{k\sigma}^{AA} \\ G_{k\bar\sigma}^{AB} - G_{k\sigma}^{AB} \\ G_{k\bar\sigma}^{BA} - G_{k\sigma}^{BA} \\ G_{k\bar\sigma}^{BB} - G_{k\sigma}^{BB} \end{pmatrix}^T .
\tag{D.37}
$$

Considering the first and the last of the four relations implied by this Ward identity and using $h_{\bar\sigma}^A - h_\sigma^A = -(h_{\bar\sigma}^B - h_\sigma^B) = 2\sigma h$ one has,

$$
4\sigma h \sum_{k'} \left(X_{kk',q=0}^{\overline{\sigma\sigma},AAAA} - X_{kk',q=0}^{\overline{\sigma\sigma},AABB} \right) = -\sigma \left\langle m^A \right\rangle,
\tag{D.38}
$$

$$
4\sigma h \sum_{k'} \left(X_{kk',q=0}^{\overline{\sigma\sigma},BBAA} - X_{kk',q=0}^{\overline{\sigma\sigma},BBBB} \right) = -\sigma \left\langle m^B \right\rangle.
\tag{D.39}
$$

Subtracting the second from the first relation, summing over k and using $\sum_{kk'q} X_{kk',q}^{\overline{\sigma\sigma},aabb} = X_q^{\overline{\sigma\sigma},ab}$ it follows

$$
4\sigma h \left(X_{q=0}^{\overline{\sigma\sigma},AA} - X_{q=0}^{\overline{\sigma\sigma},AB} - X_{q=0}^{\overline{\sigma\sigma},BA} + X_{q=0}^{\overline{\sigma\sigma},BB} \right) = -2\sigma \left\langle m \right\rangle,
\tag{D.40}
$$

where it was also used that $\left\langle m^A \right\rangle = -\left\langle m^B \right\rangle = \left\langle m \right\rangle$. As discussed earlier, a vector $\mathbf{q}$ of the reduced Brillouin maps to the vectors $\tilde{\mathbf{q}} = \mathbf{q}$ and $\tilde{\mathbf{q}} = \mathbf{q} + \mathbf{Q}$ of the regular Brillouin

zone, where $\mathbf{Q}$ is the ordering vector of the bipartite lattice. Therefore, $\mathbf{q} = 0$ maps to $\tilde{\mathbf{q}} = \mathbf{0}$ and to $\tilde{\mathbf{q}} = \mathbf{Q}$. Indeed, on the LHS of Eq. (D.40) one recognizes the definition of the susceptibility $X^{\overline{\sigma}\overline{\sigma}}_{\mathbf{Q},\omega=0}$ of the regular Brillouin zone, cf. definition Eq. (C.45). Therefore, Eq. (D.40) simply yields $2\sigma h X^{\overline{\sigma}\overline{\sigma}}_{\mathbf{Q},\omega=0} = -\sigma \langle m \rangle$. In analogy to Eq. (D.36) this leads to

$$\frac{d \langle m \rangle}{dh} = -X^s_Q, \tag{D.41}$$

where $X^s_{\tilde{q}}$ is the spin susceptibility of the paramagnet in the regular Brillouin zone and $Q = (\mathbf{Q}, 0)$. Consequently, the Ward identity also guarantees the thermodynamic consistency of zero-field derivatives that belong to phases whose ordering vector is not $\tilde{\mathbf{q}} = \mathbf{0}$. While here only a bipartite ordered state was discussed, it is reasonable to assume that similar considerations hold for many other types of ordered phases. However, for a general discussion one needs to introduce arbitrarily complex unit cells, as well as appropriate staggered conjugate fields and tensor Ward identities. In the case of superconductivity a conjugate pairing field is needed, while a staggered chemical potential corresponds to the charge order. In the latter case the Ward identity can be expected to guarantee thermodynamic consistency of the zero-field derivative $\frac{d\langle n \rangle}{d\mu}$ with the charge susceptibility X^c. The consistency of the charge response has been shown to hold exactly within the dynamical mean-field theory [83]. In accord with the discussion above, this consistency holds owing to the fact that the susceptibility of the dynamical mean-field theory satisfies the Ward identity of the Hubbard model, which will be shown in a later section.

D.8   Zero-field derivatives and criticality in an impurity model

The discussion of the zero-field derivative $\frac{d\langle m \rangle}{dh}$ above may be extended to an impurity model with the non-interacting Green's function

$$g^0_{\nu\sigma} = [\imath\nu - \Delta_{\nu\sigma} + \mu - h_\sigma]^{-1}. \tag{D.42}$$

Importantly, this Green's function potentially depends on the amplitude of the magnetic field h in *two* ways: Explicitly through the term $h_\sigma = -\sigma h$ itself, and implicitly through a dependence of the hybridization function $\Delta(h)$. When considering solutions to the impurity model at fixed Δ, the latter dependence need not be considered. However, in the case of a self-consistently determined hybridization function this dependence on the magnetic field must be accounted for.

In analogy to the lattice, cf. Eq. (D.30), the Ward identity is considered in the transversal spin channels, expressed through the T-matrix of the impurity model,

$$\Sigma_{\nu+\omega,\bar{\sigma}} - \Sigma_{\nu\sigma} = \sum_{\nu'}{}' \left([g^0_{\nu'\sigma}]^{-1} - [g^0_{\nu'+\omega,\bar{\sigma}}]^{-1}\right) f^{\overline{\sigma}\overline{\sigma}}_{\nu\nu'\omega} g_{\nu'\sigma} g_{\nu'+\omega,\bar{\sigma}}. \tag{D.43}$$

Here, Σ, g^0, f, and g are the local 1P self-energy, non-interacting Green's function, T-matrix, and interacting Green's function of the impurity model, respectively, cf. also the correspondence to the lattice in Eq. (C.18). Evaluating this Ward identity at $\omega = 0$, using $[g^0_{\nu'\sigma}]^{-1} - [g^0_{\nu',\bar\sigma}]^{-1} = \Delta_{\nu'\bar\sigma} - \Delta_{\nu'\sigma} + 2\sigma h$, and dividing by the amplitude h of the magnetic field on both sides one has,

$$\frac{\Sigma_{\nu,\bar\sigma} - \Sigma_{\nu\sigma}}{h} = \sum_{\nu'}' \left(2\sigma + \frac{\Delta_{\nu'\bar\sigma} - \Delta_{\nu'\sigma}}{h} \right) f^{\overline{\sigma\bar\sigma}}_{\nu\nu',\omega=0} g_{\nu'\sigma} g_{\nu',\bar\sigma}. \tag{D.44}$$

In the limit $h \to 0$, similar considerations that led to Eq. (D.33) now lead to the following zero-field derivative of the impurity self-energy[8],

$$\frac{d\Sigma_{\nu\sigma}}{dh} = -\sum_{\nu'}' \left(\sigma - \frac{d\Delta_{\nu'\sigma}}{dh} \right) f^{\overline{\sigma\bar\sigma}}_{\nu\nu',\omega=0} g_{\nu'\sigma} g_{\nu',\bar\sigma}. \tag{D.45}$$

Using $g_{\nu\sigma} = [\imath\nu - \Delta_{\nu\sigma} + \mu - h_\sigma - \Sigma_{\nu\sigma}]^{-1}$ one has for the zero-field derivative of the magnetization,

$$\begin{aligned}
\frac{d\langle m \rangle}{dh} &= \sum_\sigma \sigma \frac{d\langle n_\sigma \rangle}{dh} = \sum_{\nu\sigma}' \sigma \frac{dg_{\nu\sigma}}{dh} \\
&= -\sum_{\nu\sigma}' \sigma g_{\nu\sigma}^2 \left(\sigma - \frac{d\Delta_{\nu\sigma}}{dh} - \frac{d\Sigma_{\nu\sigma}}{dh} \right) \\
&= -\sum_{\nu\nu'\sigma}' \left(1 - \frac{d\Delta_{\nu\sigma}}{dh} \right) \chi^{\overline{\sigma\bar\sigma}}_{\nu\nu',\omega=0}.
\end{aligned} \tag{D.46}$$

In the last step Eq. (D.45) and the definition of the generalized susceptibility of the impurity model were inserted,

$$\chi^{\overline{\sigma\bar\sigma}}_{\nu\nu',\omega} = g_{\nu\sigma} g_{\nu+\omega,\bar\sigma} \left(\beta \delta_{\nu\nu'} + f^{\overline{\sigma\bar\sigma}}_{\nu\nu',\omega} g_{\nu'\sigma} g_{\nu'+\omega,\bar\sigma} \right). \tag{D.47}$$

It was further used that $\frac{d\Delta_\sigma}{dh} = -\frac{d\Delta_{\bar\sigma}}{dh}$, $\frac{d\Sigma_\sigma}{dh} = -\frac{d\Sigma_{\bar\sigma}}{dh}$, and that $g_\sigma = g_{\bar\sigma}$ at $h = 0$.

---

[8] To be explicit, assuming that the system is paramagnetic at $h = 0$ the hybridization function must not depend on the spin in this limit, that is $\Delta_\sigma \to \Delta(h = 0)$. This is analogous to the considerations regarding the self-energy in Eq. (D.32). Then,

$$\begin{aligned}
\frac{\Delta_{\nu,\bar\sigma} - \Delta_{\nu\sigma}}{h} &= \frac{\Delta_{\nu,\bar\sigma} - \Delta_\nu(h = 0)}{h} - \frac{\Delta_{\nu,\sigma} - \Delta_\nu(h = 0)}{h} \\
&\stackrel{h\to 0}{=} \frac{d\Delta_{\nu\bar\sigma}}{dh} - \frac{d\Delta_{\nu\sigma}}{dh} = -2\frac{d\Delta_{\nu\sigma}}{dh}.
\end{aligned}$$

In the last step it was assumed that the dependence of the hybridization function on the magnetic field is such that a small magnetic field acts symmetrically opposed in both spin directions, allowing the identification $\frac{d\Delta_\sigma}{dh} = -\frac{d\Delta_{\bar\sigma}}{dh}$.

At least at finite temperature an impurity model can not have a spontaneous magnetic phase transition, therefore its T-matrix f and generalized susceptibility χ do not diverge. At vanishing magnetic field $h = 0$ the symmetry can therefore only be broken via the dependence of the hybridization function $\Delta(h)$ on the magnetic field. Like on the lattice it can be expected that the discussion here can be repeated for other symmetry-breaking fields, such as a pairing field. A generalization to an impurity model with a pairing potential seems also possible [160]. For a detailed discussion regarding criticality of impurity models along similar lines the reader is referred to [76].

D.9 Remarks on non-commuting limits and zero-field derivatives

In this section one comes along several occasions where the (generalized) susceptibility or the T-matrix are evaluated at $\mathbf{q} = 0$ and/or $\omega = 0$, in some cases coming with a side note that one or the other has to be set to zero first. A short comment is in place to avoid confusion regarding these limits: **QP**

Whenever considering the limit $q = 0$ one has to keep in mind that the bubble $X^0_{kq} = G_k G_{k+q}$ has singular analytic properties at this point, because the poles of the two Green's functions merge at this combination of ω and $\mathbf{q}$. Therefore, the limits $|\mathbf{q}| \to 0$ and $\omega \to 0$ do not commute, the bubble assumes different values when one or the other limit is taken first. It does so at least as long as the considered system is a Fermi liquid, such that G has a coherent contribution (a pole) proportional to the quasiparticle weight Z at the Fermi level. However, the bubble is also the building block of the Bethe-Salpeter equation and therefore the T-matrix F and eventually the (generalized) susceptibility X inherit the property of non-commuting limits as a consequence.

The problem of non-commuting limits disappears when considering zero-field derivatives: The role of the conjugate field h in the derivation of, e.g., Eq. (D.36) for the zero-field derivative $\frac{d\langle m \rangle}{dh}$ is to *shift the poles* of the Green's functions in the bubble $X^{0,\sigma\bar{\sigma}}_{kq} = G_{k\sigma} G_{k+q,\bar{\sigma}}$ away from each other at $q = 0$. These would otherwise merge in the paramagnet where $G_\uparrow = G_\downarrow$. Then $X^{0,\sigma\bar{\sigma}}_q$ can be evaluated at $q = 0$ without ambiguity and the Ward identity in Eq. (D.27), which is used to relate the zero-field derivative $\frac{d\langle m \rangle}{dh}$ to the susceptibility $X^{\sigma\bar{\sigma}}_q$, can be evaluated at $q = 0$. What makes the concept of conjugate fields so useful in this context is that they can be set to infinitesimal values that lead to unambiguous differential expressions. This is possible because the limits $\omega \to 0$ and $\mathbf{q} \to 0$ *do* commute as long as the limit $h \to 0$ is taken last. To see this, let us consider the spin-dependent Lindhard function $L^\sigma_q = \sum_k X^{0,\sigma\bar{\sigma}}_{kq}$ of a non-interacting system subjected to a magnetic field h,

$$L^\sigma_q = \sum_k \frac{G^0_{k+q,\bar{\sigma}} - G^0_{k,\sigma}}{G^{0,-1}_{k\sigma} - G^{0,-1}_{k+q,\bar{\sigma}}} = \sum_{\mathbf{k}}' \frac{f^0(\varepsilon_{\mathbf{k}+\mathbf{q},\bar{\sigma}}) - f^0(\varepsilon_{\mathbf{k}\sigma})}{\varepsilon_{\mathbf{k}+\mathbf{q},\bar{\sigma}} - \varepsilon_{\mathbf{k}\sigma} - \imath\omega}, \qquad (D.48)$$

where it was used that in the non-interacting system the average occupation number $\langle n_{\mathbf{k}\sigma} \rangle = \sum_\nu' G^0_{k\sigma} = f^0(\varepsilon_{\mathbf{k}\sigma})$ is given by the Fermi function f^0. The spin-dependence of the single particle energies $\varepsilon_{\mathbf{k}\sigma} = \varepsilon_{\mathbf{k}} + h_\sigma$ is given by the conjugate field $h_\sigma = -\sigma h$. Hence, for *finite*

h, such that $\varepsilon_{\mathbf{k}\sigma} \neq \varepsilon_{\mathbf{k}\bar{\sigma}}$, it is irrelevant how the limits of ω and $\mathbf{q}$ are taken,

$$
\lim_{|\mathbf{q}|\to 0} \lim_{\omega\to 0} L_q^\sigma = \lim_{\omega\to 0} \lim_{|\mathbf{q}|\to 0} L_q^\sigma = -\sum_{\mathbf{k}}{}' \frac{f^0(\varepsilon_{\mathbf{k},\bar{\sigma}}) - f^0(\varepsilon_{\mathbf{k}\sigma})}{2h\sigma}, \quad (h \neq 0). \tag{D.49}
$$

Taking the limit $h \to 0$ subsequently leads to a zero-field derivative of f^0. Instead, if one were to begin with $h = 0$, it is readily verified that $\lim_{|\mathbf{q}|\to 0} \lim_{\omega\to 0} L_q \sim \frac{\partial f^0}{\partial \varepsilon_{\mathbf{k}}}$, while $\lim_{\omega\to 0} \lim_{|\mathbf{q}|\to 0} L_q = 0$. In an interacting system the situation is similar, the limits do *not* commute when taken on the interacting bubble of a Fermi liquid. This is discussed in chapter 13 of Ref. [1] by M. Fabrizio.

D.10   Divergence of the T-matrix at a zero-temperature Mott transition

P As mentioned above, it is reasonable to assume that the Ward identity relates in general the divergence of zero-field derivatives, such as of $\frac{d\Sigma}{dh}$, to the divergence of a T-matrix at a second order phase transition. The Ward identity therefore relates certain scattering processes of quasiparticles, which are described by the T-matrix, directly to a corresponding conjugate field. It is a very intriguing question what may be the conjugate field and associated T-Matrix of the Mott transition and if they exist at all.

In the following, I point at some peculiarities of the Mott metal-to-insulator transition at zero temperature $T \to 0$, which follow from the Ward identity. To this end, one has to make sure first that the phase transition at hand is of second order, so it is reasonable to consider the divergence of a T-Matrix as a signal. While in finite dimensions there exists the scenario of a first order transition line down to $T = 0$ [12], a second order Mott transition occurs at $T = 0$ in the infinite dimensional Hubbard model, see [32] and references therein.

Let us begin with the Ward identity in Eq. (D.1) for a paramagnetic system. Assuming that the interaction does not contribute to the currents, $[\rho^\alpha, H_{\text{int}}] = 0$, and expressing the generalized susceptibility via the T-matrix F,

$$
X_{kk'q}^\alpha = G_k G_{k+q} \left[N\beta\delta_{kk'} + F_{kk'q}^\alpha G_{k'} G_{k'+q} \right], \tag{D.50}
$$

the Ward identity Eq. (D.1) can be expressed in the following form[9],

$$
\Sigma_{k+q} - \Sigma_k = \sum_{k'} \left([G_{k'}^0]^{-1} - [G_{k'+q}^0]^{-1} \right) F_{kk'q}^\alpha G_{k'} G_{k'+q}. \tag{D.51}
$$

Let us consider this relation at $k_{-1} = (\mathbf{k}, \nu_{-1})$ and $q_1 = (\mathbf{0}, \omega_1)$, where $\nu_{-1} = -\pi T$ is the largest negative fermionic Matsubara frequency and $\omega_1 = 2\pi T$ is the smallest positive bosonic Matsubara frequency. Hence, $k_{-1} + q_1 = (\mathbf{k}, \nu_0) \equiv k_0$, where $\nu_0 = \nu_{-1} + \omega_1 = \pi T$, is the smallest positive fermionic Matsubara frequency. Evaluating Eq. (D.51) at $k = k_{-1}$

---

[9] Also Dyson's equation was used, the steps are similar to the ones that led to Eq. (D.30).

and $q = q_1$ one has

$$\Sigma_{k_0} - \Sigma_{k_{-1}} = \sum_{k'} \left([G^0_{k'}]^{-1} - [G^0_{k'+q_1}]^{-1} \right) F^\alpha_{k_{-1}k'q_1} G_{k'} G_{k'+q_1}. \tag{D.52}$$

Using $\Sigma_{\mathbf{k}\nu} = \Sigma^*_{\mathbf{k},-\nu}$ and $[G^0_{k'}]^{-1} - [G^0_{k'+q_1}]^{-1} = -\imath\omega_1$ and dividing both sides by $\omega_1 = 2\nu_0$ this simplifies to

$$\frac{2\imath \operatorname{Im}\Sigma_{k_0}}{2\nu_0} = -\imath \sum_{k'} F^\alpha_{k_{-1}k'q_1} G_{k'} G_{k'+q_1}. \tag{D.53}$$

On the LHS one recognizes a commonly used approximation to the scattering rate [130, 3],

$$\frac{\operatorname{Im}\Sigma_{\mathbf{k}\nu_0}}{\nu_0} \approx \left.\frac{\partial \Sigma'_{\mathbf{k}}(E)}{\partial E}\right|_{E=0}. \tag{D.54}$$

Here, Σ' is the real part of the self-energy on the real axis, $\Sigma(E) = \Sigma'(E) + \imath\Sigma''(E)$, and E is the real energy. The relation (D.54) becomes exact in the limit $T \to 0$. Hence, at $T = 0$ it follows from Eq. (D.53) that

$$\left.\frac{\partial \Sigma'_{\mathbf{k}}(E)}{\partial E}\right|_{E=0} = -\lim_{T\to 0} \sum_{k'} F^\alpha_{k_{-1}k'q_1} G_{k'} G_{k'+q_1}. \tag{D.55}$$

The LHS of this expression is related to the quasiparticle weight Z,

$$Z_{\mathbf{k}} = \frac{1}{1 - \left.\frac{\partial \Sigma'_{\mathbf{k}}(E)}{\partial E}\right|_{E=0}}. \tag{D.56}$$

The resulting relationship

$$1 - Z_{\mathbf{k}}^{-1} = -\lim_{T\to 0} \sum_{k'} F^\alpha_{k_{-1}k'q_1} G_{k'} G_{k'+q_1}, \tag{D.57}$$

is well known as part of the Landau theory of Fermi liquids[10], cf. Sec. II §19 of [68]. Approaching the Mott transition at $T = 0$ the quasiparticle weight vanishes, hence the derivative of the self-energy and thus the LHS of Eq. (D.57) diverges. However, according to Eq. (D.57) this divergence should be accompanied by the divergence of the T-matrix F^α in the limit $\lim_{T\to 0} F^\alpha_{k_{-1}k'q_1}$ at least for one value of k'. Since Eq. (D.57) is valid for any α, the divergence should occur in the charge and in the spin channels at the homogeneous wave vector $\mathbf{q} = \mathbf{0}$.

According to Eq. (D.55) the Mott transition stands out among other phase transitions due to the very peculiar situation that the real energy E in Eq. (D.55) appears

---

[10] Note that in Ref. [68] a relation similar to Eq. (D.57) is obtained in the limit $\frac{|\mathbf{q}|}{\omega_1} \to 0$. This is consistent with the steps performed here, where $\mathbf{q}$ is assumed to be zero from the start.
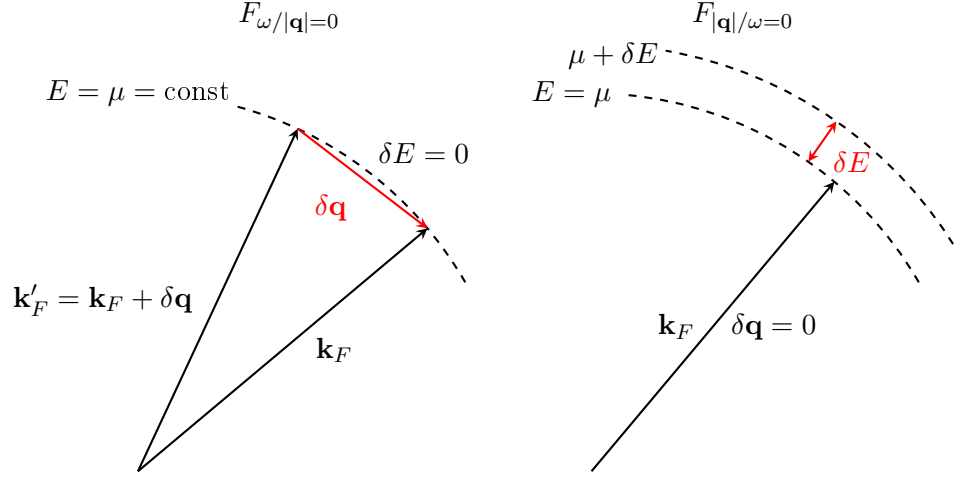
FIGURE 3.9: Sketch of the scattering processes on the Fermi surface at $T = 0$ that are described by the T-matrices $F_{\omega/|\mathbf{q}|=0}$ and $F_{|\mathbf{q}|/\omega=0}$. The limit $F_{\omega/|\mathbf{q}|=0}$ (left) corresponds to scatterings with a small transferred momentum $\delta\mathbf{q} = \mathbf{k}'_F - \mathbf{k}_F$, while the transferred energy δE is strictly zero. In case of $F_{\omega/|\mathbf{q}|=0}$ (right) the energy may be varied but the transferred momentum is zero. However, in a Fermi liquid at $T = 0$ scatterings can only happen from one point on the Fermi surface to another. At the Mott transition $F_{|\mathbf{q}|/\omega=0}$ diverges [cf. Eq. (D.55)], which seems to imply an infinitely strong tendency towards the unphysical scatterings that would remove the quasiparticles from the Fermi surface.

in the place where one usually finds the conjugate field, e.g., the magnetic field h in case of the transition to the simple ferromagnet in Eq. (D.33). Furthermore, the divergence does *not* occur at vanishing energy $\omega_0 = 0$, which corresponds to the static homogeneous limit $F_{\omega/|\mathbf{q}|=0} = \lim_{|\mathbf{q}|\to 0} \lim_{\omega\to 0} F_q$. Instead, F diverges at $\omega_1 = 2\pi T$ for $T \to 0$, which is a different limit [see remarks on non-commuting limits above], namely $F_{|\mathbf{q}|/\omega=0} = \lim_{\omega\to 0} \lim_{|\mathbf{q}|\to 0} F_q$. Indeed, it has been seen early that in the half-filled Hubbard model on an infinite dimensional hypercubic lattice the static homogeneous susceptibility $X_{q=0} = \lim_{|\mathbf{q}|\to 0} \lim_{\omega\to 0} X_q$ does *not* diverge at the Mott transition at zero temperature. Instead, it approaches a finite value, which is consistent with analytical considerations [55, 32].

Peculiar is also the physical meaning of the diverging T-matrix $F_{|\mathbf{q}|/\omega=0}$, which is best explained paraphrasing Landau&Lifshitz, see Sec. II §17 of [68]: In case of $F_{\omega/|\mathbf{q}|=0}$ one takes the limit $\omega \to 0$ first, the resulting T-matrix corresponds to scatterings of quasiparticles for which the transferred energy is strictly zero. This limit of the T-matrix may be used to describe scatterings that transfer small momenta but no energy[11]. On the other hand, the T-matrix that relates to the Mott transition in Eq. (D.57) is $F_{|\mathbf{q}|/\omega=0}$. In this case the limit

---

[11] This is to be understood such that one can expand $F_{q=(\delta\mathbf{q},\omega=0)}$ around $F_{\omega/|\mathbf{q}|=0}$ for small $\delta\mathbf{q}$. This limit is not suitable in order to consider small energy transfers $\delta\omega$.

$|\mathbf{q}| \to 0$ is taken first. The resulting T-matrix corresponds to scatterings of quasiparticles that transfer small energies while the transferred momentum is strictly zero. However, in a Fermi liquid at zero temperature the situation described by $F_{|\mathbf{q}|/\omega=0}$ is unphysical. This is because the only allowed scatterings then happen at the Fermi level $E = \mu = \text{const}$, such that no energy transfer is possible. A sketch of the scattering events corresponding to $F_{\omega/|\mathbf{q}|=0}$ and $F_{|\mathbf{q}|/\omega=0}$ is drawn in Fig. 3.9. Notably, the other second order transitions discussed in this text are related to the physical limit $F_{\omega/|\mathbf{q}|=0}$ [cf. Eq. (D.33)].

An order parameter and a conjugate field for the Mott transition of the Hubbard model on an infinite dimensional lattice have recently been derived within the slave spin formalism [161]. Remarkably, the proposed conjugate field is not a physical observable and the associated order parameter is finite in the Fermi liquid phase, marking the Fermi liquid as the 'ordered' phase in usual terms.

D.11 Luttinger's theorem

An exact statement about the ground state of an interacting Fermi liquid is Luttinger's theorem [86], which states that at $T = 0$ the volume enclosed by the Fermi surface is given by the particle number. The standard derivation of Luttinger's theorem starts from the simple observation that Green's function may be rewritten in terms of its own derivative with respect to the Matsubara frequency, $G_{k\sigma} = \imath \frac{\partial \ln G_{k\sigma}}{\partial \nu} - \imath G_{k\sigma} \frac{\partial \Sigma_{k\sigma}}{\partial \nu}$. Calculating the average occupation number from this expression, $\langle n_\sigma \rangle = \sum_k G_{k\sigma}$, one encounters the sum, $\sum_k G_{k\sigma} \frac{\partial \Sigma_{k\sigma}}{\partial \nu}$, which in the limit $T \to 0$ is also called Luttinger's integral. Along a frequently used line of argument one considers Φ-derivable approximations to G and Σ, and shows in a few steps that Luttinger's integral vanishes due to the stationarity of the Luttinger-Ward functional Φ upon a small variation δG, see, e.g., [104]. Luttinger's theorem is a statement about the Fermi liquid, while in other phases Luttinger's integral may assume nonzero values. This is the case, e.g., in the local moment phase of an Anderson impurity model, where it is a rather subtle task to reconcile the finite value of Luttinger's integral with the (universal) stationarity of Φ [76, 77]. Luttinger's theorem also follows from the Ward identity if one makes explicitly use of the assumption that the considered system is a Fermi liquid [68].

D.12   Merits of the Ward identity

QP A number of exact statements follow from the Ward identity, some of which are tabulated below.

Feature	See text
Ungapped collective excitations at the Γ-point in the *disordered* phase.	Eq. (D.3).
Ungapped spectra of Goldstone excitations in *ordered* phases.	FM: Eq. (D.4), AFM: Eq. (D.11).
Asymptotic coefficient of X_ω, first spectral moment of $X(E + \imath\delta)$, f-sum rule.	Eqs. (D.19), (D.21), and (D.22), respectively.
Consistency of X_{loc} with kinetic energy.	Lattice: Eq. (D.23), Impurity: Eq. (D.25).
Consistency of zero-field derivatives and fluctuations.	FM: Eq. (D.36), AFM: Eq. (D.41), and Fig. 3.8.
Relation of quasiparticle weight to T-matrix.	Eq. (D.57).
Luttinger's theorem.	Sec. D.11.

E   Relation to Baym & Kadanoff theory

Q So far, the Ward identity was discussed with an unspecified interaction Hamiltonian H_{int} In this subsection an important special case will be discussed, namely that the interaction does not contribute to the charge and spin currents,

$$[\rho^\alpha, H_{\mathrm{int}}] = 0. \tag{E.1}$$

Under this condition the Ward identity in Eq. (D.1) simplifies,

$$G_{k+q} - G_k = \sum_{k'} \left([G^0_{k'}]^{-1} - [G^0_{k'+q}]^{-1} \right) X^\alpha_{kk'q}. \tag{E.2}$$

This is the Ward identity of, e.g., the Hubbard model, the extended Hubbard model with charge-charge couplings ($n_{-\mathbf{q}}V_{\mathbf{q}}n_{\mathbf{q}}$), or of the Anderson impurity model. A diagrammatic representation of this Ward identity is shown in Fig. 3.10. The RHS of Eq. (E.2) features the channel index α, whereas the LHS does not. Since in an interacting system the physics of charge- and spin-excitations are entirely different for not too small interaction, this identity expresses a remarkable symmetry of the two-particle spectrum. It can be seen as a weaker
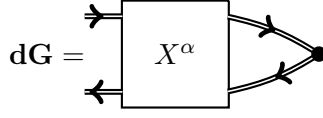
FIGURE 3.10: Diagrammatic representation of the integral Ward identity Eq. (E.2). The full circle represents $[G^0_{k'}]^{-1} - [G^0_{k'+q}]^{-1}$. The expression $\mathbf{dG}_q$ on the LHS of the Ward identity is a vector with respect to the four-momentum k, $(\mathbf{dG}_q)_k = G_{k+q} - G_k$.

version of an integral of motion, an 'integral of interaction', since $[\rho^\alpha, H_{\text{int}}]$ rather than $[\rho^\alpha, H]$ vanishes. This symmetry is due to the fact that the models in question do not offer channels for the independent propagation of charge and spin. This conjoint movement is reflected by the independence of the LHS of Eq. (E.2) from the channel index α.

E.1 Ward identity of the self-energies

The simplified Ward identity Eq. (E.2) for the generalized susceptibility X can be recast into a Ward identity for the 1P and 2P self-energies Σ and Γ: To this end, one inserts the Bethe-Salpeter equation $X_{kk'q}$,

$$X^\alpha_{kk'q} = G_k G_{k+q} \left[N\beta\delta_{kk'} + \sum_{k''} \Gamma^\alpha_{kk''q} X^\alpha_{k''k'q} \right], \tag{E.3}$$

into Eq. (E.2). This yields

$$G_{k+q} - G_k = \left([G^0_k]^{-1} - [G^0_{k+q}]^{-1}\right) G_k G_{k+q}$$
$$+ G_k G_{k+q} \sum_{k''} \Gamma^\alpha_{kk''q} \sum_{k'} \left([G^0_{k'}]^{-1} - [G^0_{k'+q}]^{-1}\right) X^\alpha_{k''k'q}. \tag{E.4}$$

By dividing both sides by $G_k G_{k+q}$, bringing the first term on the RHS to the LHS and using Dyson's equation, $[G^0_k]^{-1} - G^{-1}_k = \Sigma_k$, one obtains,

$$\Sigma_{k+q} - \Sigma_k = \sum_{k''} \Gamma^\alpha_{kk''q} \sum_{k'} \left([G^0_{k'}]^{-1} - [G^0_{k'+q}]^{-1}\right) X^\alpha_{k''k'q}. \tag{E.5}$$

Here one recognizes that the expression on the RHS that is summed over k' is simply the RHS of the Ward identity Eq. (E.2). Therefore, the infinite series that arises from the ladder-like Bethe-Salpeter Eq. (E.3) can be summed up exactly by making use of the Ward identity, leading to the compact statement,

$$\Sigma_{k+q} - \Sigma_k = \sum_{k'} \Gamma^\alpha_{kk'q} \left[G_{k'+q} - G_{k'} \right]. \tag{E.6}$$

This relation holds for lattice and impurity models that satisfy Eq. (E.1), in the latter case one performs the replacements by the respective local quantities, $\Sigma_k \to \Sigma_\nu$, $G_k \to g_\nu$, and $\Gamma_{kk'q} \to \gamma_{\nu\nu'\omega}$. Eq. (E.6) involves the 1P and 2P self-energies and therefore offers itself for approximations, which are best done at the low level of irreducible self-energies. In a compact notation one may also write,

$$\mathbf{d\Sigma}_q = \hat{\Gamma}_q^\alpha \mathbf{dG}_q, \tag{E.7}$$

where $\mathbf{d\Sigma}_q$ is a vector with components $(\mathbf{d\Sigma}_q)_k = \Sigma_{k+q} - \Sigma_k$, and $\mathbf{dG}_q$ is defined likewise. As in Eq. (E.2), one recognizes in Eq. (E.7) the remarkable property that the same LHS is recovered for each channel index $\alpha = c, x, y, z$ on the RHS, a consequence of the special assumption $[\rho^\alpha, H_{\text{int}}] = 0$. For completeness, the respective relations for symmetry-broken phases will also be stated. In analogous steps that led to Eq. (E.7), one obtains from Eq. (C.31),

$$\mathbf{d\Sigma}_q^{\sigma'\sigma} \delta_{\sigma\sigma'} = \hat{\Gamma}_q^{\sigma\sigma'} \mathbf{dG}_q^{\sigma'\sigma}, \tag{E.8}$$

and likewise from Eq. (C.32),

$$\mathbf{d\Sigma}_q^{\bar{\sigma}\sigma} = \hat{\Gamma}_q^{\overline{\sigma\bar{\sigma}}} \mathbf{dG}_q^{\bar{\sigma}\sigma}, \tag{E.9}$$

where, $(\mathbf{d\Sigma}_q^{\sigma'\sigma})_k = \Sigma_{k+q,\sigma'} - \Sigma_{k\sigma}$.

E.2   Relation between the integral and functional Ward identities

Q Now the relation of the integral Ward identities in Eqs. (E.2) and (E.6)-(E.9) to the Baym & Kadanoff approach to conserving approximations will be discussed. Firstly, let us insert two prominent Φ-derivable approximations into the integral Ward identity. For the Hubbard model a trivial example of an approximation that satisfies the Ward identity Eq. (E.6), and thereby also local conservation laws, is the RPA, where $\Sigma^{\text{H}} = \frac{U\langle n\rangle}{2}$ and $\Gamma^c = -\Gamma^{x,y,z} = U$. This approximation satisfies Eq. (E.6) in a trivial way, since both sides of the equation vanish. Not coincidentally, the RPA is also the simplest approximation to the Hubbard model (notwithstanding $\Sigma = \Gamma = 0$) that is Φ-derivable and which corresponds to a Luttinger-Ward functional given by the first diagram in Fig. 3.1.

Somewhat less trivial is the Hartree-Fock approximation to the extended Hubbard model with non-local charge-charge interactions, i.e., $H_{\text{int}} = \frac{1}{2}\sum_{\mathbf{q}} \rho_{-\mathbf{q}}^c V_{\mathbf{q}}^c \rho_{\mathbf{q}}^c$, where $V_{\mathbf{q}}^c = U + V_{\mathbf{q}}$ and $V_{ii} = \sum_{\mathbf{q}}' V_{\mathbf{q}} = 0$. The Hartree-Fock self-energy is then given by the first two terms of the Schwinger-Dyson Eq. (C.12) of chapter 2 [also cf. Eq. (B.6)],

$$\begin{aligned}
\Sigma_k^{\text{HF}} &= 2V_{q=0}^c \sum_{k'} G_{k'} - \sum_q V_q^c G_{k+q} \\
&= \frac{(U + V_{\mathbf{q}=0})\langle n\rangle}{2} - {\sum_{\mathbf{q}}}' \frac{V_{\mathbf{q}} \langle n_{\mathbf{k}+\mathbf{q}}\rangle}{2}.
\end{aligned} \tag{E.10}$$

The 2P self-energy $\Gamma^c_{kk'q} = U - V_{\mathbf{k'-k}}$ of the charge channel, together with the Hartree-Fock self-energy above, yields a conserving 2P response function. Γ^c may be derived from a Luttinger Ward functional corresponding to the first two terms in Fig. 3.1, i.e., by taking the functional derivative $\delta\Sigma^{\mathrm{HF}}_{\mathbf{k}}/\delta G_{\mathbf{k'}}$ [cf. Eq. (B.8)]. Since the extended Hubbard model with charge-charge interactions satisfies the condition $[\rho^\alpha_{\mathbf{q}}, H_{\mathrm{int}}] = 0$, its Ward identity takes the form of Eq. (E.6), as discussed above. We can convince ourselves that Σ^{HF} and Γ^c satisfy the Ward identity: Inserting the Hartree-Fock self-energy Eq. (E.10) and $\Gamma^c_{kk'q}$ into the left- and right-hand-side of Eq. (E.6), respectively, one sees that this approximation is indeed conserving,

$$\Sigma^{\mathrm{HF}}_{k+q} - \Sigma^{\mathrm{HF}}_k = \sum_{k'} \Gamma^c_{kk'q} \left[G_{k'+q} - G_{k'} \right],$$

$$\Leftrightarrow -\sideset{}{'}\sum_{\mathbf{p}} V_{\mathbf{p}} \frac{\langle n_{\mathbf{k+p+q}}\rangle - \langle n_{\mathbf{k+p}}\rangle}{2} = \sideset{}{'}\sum_{\mathbf{k'}\nu'} (U - V_{\mathbf{k'-k}}) \left[G_{\mathbf{k'+q},\nu'+\omega} - G_{\mathbf{k'}\nu'} \right]. \qquad (E.11)$$

The expressions on the LHS and RHS are equal, as can be seen by a shift $\mathbf{p} \to \mathbf{k'-k}$ on the LHS and inserting $\sum'_\nu G_{\mathbf{k}\nu} = \langle n_{\mathbf{k}}\rangle /2$ on the RHS. The same consideration holds in the spin channels, where $\Gamma^z_{kk'q} = -U - V_{\mathbf{k'-k}}$ [cf. Eq. (B.8)]. Hence, the Hartree-Fock approximation to the extended Hubbard model with charge-charge interactions satisfies local conservation laws, as expected.

As discussed above, it is much more challenging to obtain the 2P response from the Bethe-Salpeter equation in Hartree-Fock approximation than in the RPA, which corresponds to the Hartree approximation (cf. Fig. 3.2). At least it is possible to show that the 2P response in Hartree-Fock approximation satisfies the correct asymptotic behavior given in Eq. (D.22)[12]. These examples illustrate that Φ-derivable approximations are destined to satisfy the integral Ward identity $\mathbf{d\Sigma} = \hat{\Gamma}\mathbf{dG}$, whose similarity to the functional Ward identity $\delta\Sigma = \Gamma\delta G$ seems obvious. Indeed, both equations reflect the fact that the exact 1P and 2P self-energies satisfy the continuity Eq. (C.1).

However, the functional Ward identity Eq. (B.10) is a more powerful statement than the integral Ward identity in Eq. (E.7). This is because the functional form allows to obtain the complete dynamical 2P self-energy Γ (depending on three momenta k, k', q) *from* the 1P self-energy Σ, while the integral form contains only 'integrated' information about Γ.

---

[12]This can be seen by expanding the Bethe-Salpeter Eq. (E.3) up to $\mathcal{O}(\omega)^{-2}$,

$$X^c_{kk'q} = G_k G_{k+q} \left[N\beta\delta_{kk'} + \sum_{k''} \Gamma^c_{kk''q} X^c_{k''k'q} \right] = (G_k - G_{k+q})N\beta\delta_{kk'} \left[(\imath\omega)^{-1} - (\imath\omega)^{-2}(\varepsilon_k - \varepsilon_{k+q} + \Sigma_k - \Sigma_{k+q}) \right]$$

$$+ (\imath\omega)^{-2}(G_k - G_{k+q})(U - V_{k'-k})(G_{k'} - G_{k'+q}) + \mathcal{O}(\omega)^{-3}. \qquad (E.12)$$

From the first to the second line the bubble was expanded up to $\mathcal{O}(\omega^{-2})$ and the vertex corrections up to $\mathcal{O}(\omega^{-1})$. Inserting the Hartree-Fock self-energy Eq. (E.10) and summing over k, k' one sees that the term $\sim (\imath\omega)^{-1}$ and those depending on U and V cancel out, multiplication by two then leaves the correct result Eq. (D.22).

In case of a lattice problem this can be seen by expanding the Ward identity Eq. (E.7) at vanishing bosonic frequency and infinitesimal momentum, i.e., $\delta q = (\delta \mathbf{q}, \omega = 0)$,

$$(\nabla_{\mathbf{k}} \Sigma_{\mathbf{k}\nu}) \delta \mathbf{q} = \sum_{\mathbf{k}'\nu'} \Gamma^{\alpha}_{\mathbf{k}\mathbf{k}'\nu\nu'}(\mathbf{q} = 0, \omega = 0)(\nabla_{\mathbf{k}'} G_{\mathbf{k}'\nu'}) \delta \mathbf{q}. \qquad (\text{E.13})$$

Now one has in fact a small variation $\nabla_{\mathbf{k}} \Sigma_{\mathbf{k}\nu} \delta \mathbf{q} = \delta \Sigma_{\mathbf{k}\nu}$ of the self-energy that is given by the variation $\nabla_{\mathbf{k}} G_{\mathbf{k}\nu} \delta \mathbf{q} = \delta G_{\mathbf{k}\nu}$ of Green's function and by the 2P self-energy $\Gamma^{\alpha}_{\mathbf{k}\mathbf{k}'\nu\nu'}(\mathbf{q} = 0, \omega = 0)$. However, the variation of Green's function on the RHS of Eq. (E.13) can not be done individually for each $\mathbf{k}'$, it is therefore not possible to obtain Γ from this relation. The functional relation $\delta \Sigma = \Gamma \delta G$ allows this, due to the perturbations $\mathcal{U}$ [see Eq. (B.3)] that are implied in the Baym & Kadanoff framework. They serve as free variational parameters, of which there are none in Eq. (E.13). In the Baym & Kadanoff theory a suitable variational parameter $\mathcal{U}$ allows to vary $G_{\mathbf{k}\nu}$ only in a single point $(\mathbf{k}, \nu)$.

E.3   Six central relations

Q   The Ward identity $\mathbf{d}\Sigma_q = \hat{\Gamma}^{\alpha}_q \mathbf{d}\mathbf{G}_q$ completes the set of basic equations that underlie the framework of local conservation laws in lattice and quantum impurity models: (i) The equation of motion of the construction operator, $\partial_\tau c = [\mathcal{H}, c]$, which is reflected in the functional and integral Schwinger-Dyson equations. (ii) The EOM of the density, $\partial_\tau \rho = [\mathcal{H}, \rho]$, also called continuity equation, which has its counterparts in the functional and integral Ward identities. These are summarized in Eq. (E.14), (Σ^{HF} denotes the Hartree-Fock part of the self-energy, $X^0_{kq} = G_{k+q} G_k$).

	Schwinger-Dyson equation		Ward identity	
EOM	$\partial_\tau c = [\mathcal{H}, c]$	$2, (\text{C.3})$	$\partial_\tau \rho = [\mathcal{H}, \rho]$	$3, (\text{C.1})$
Functional	$\Sigma = \frac{\delta \Phi}{\delta G}$	$3, (\text{B.9})$	$\Gamma = \frac{\delta \Sigma}{\delta G}$	$3, (\text{B.10})$
Integral	$\Sigma_k = \Sigma^{\text{HF}}_k - \sum_{k'q} V_q X^0_{k'q} F_{k'kq} G_{k+q}$	$2, (\text{C.12})$	$\mathbf{d}\Sigma_q = \hat{\Gamma}_q \mathbf{d}\mathbf{G}_q$	$3, (\text{E.7})$

$$(\text{E.14})$$

F   The ugly companion of the integral Ward identity: $[\rho, H_{\mathbf{int}}]$

Q   So far, the discussion of the integral Ward identity did not address the contribution of the interaction H_{int},

$$G_{k+q} - G_k = \sum_{k'} \left([G^0_{k'}]^{-1} - [G^0_{k'+q}]^{-1}\right) X^{\alpha}_{kk'q} + \frac{1}{2} \sum_{\sigma\sigma'} s^{\alpha}_{\sigma'\sigma} \left\langle c_{k\sigma} c^{\dagger}_{k+q,\sigma'} [\rho^{\alpha}, H_{\text{int}}]_q \right\rangle. \quad (\text{F.1})$$

The second term on the RHS corresponds to the currents created by the interaction, its significance will be discussed in this section.

F.1 When the interaction transports the spin

Depending on the physical situation, a significant part of the charge and, in particular, of the spin currents may originate from the interaction. Let us consider two scenarios where this term is relevant: Q

(i) A lattice Hamiltonian with vanishing hopping $H_0 = 0$ and nonlocal exchange interactions,

$$H = H_{\text{int}} = \frac{1}{2} \sum_{\mathbf{q}, \alpha = x, y, z} \rho^\alpha_{-\mathbf{q}} V^\alpha_{\mathbf{q}} \rho^\alpha_{\mathbf{q}}. \tag{F.2}$$

With $V^{x,y,z}_{\mathbf{q}} = J_{\mathbf{q}}/4$ as the isotropic exchange coupling (a factor 4 comes in due to $S = \rho/2$) and at half-filling this model becomes *almost* a spin-$\frac{1}{2}$ Heisenberg model but not quite an exact one. This is since the operators ρ^α_i act in the enlarged local Hilbert space $\{|0\rangle, |\uparrow\rangle, |\downarrow\rangle, |\updownarrow\rangle\}$. Although for vanishing hopping $\varepsilon_k = 0$ there is no direct way for the electrons to move from site to site, the empty and doubly occupied states allow for minuscule charge fluctuations, thanks to the thermal bath of the grand canonical potential. However, at the cost of introducing a Berry phase, the contribution of the empty and doubly occupied states may be canceled out via introduction of an imaginary chemical potential $\tilde{\mu}$ (the details of this procedure are not relevant here, see Refs. [105, 100]). Then, there are no more charge fluctuations and the model in Eq. (F.2) indeed maps exactly to the spin-$\frac{1}{2}$ Heisenberg Hamiltonian. For this model the single-particle correlation function G_k becomes obsolete and one may sum the Ward identity Eq. (F.1) on both sides over k, without a loss in physically relevant information. Using $\sum_k (G_{k+q} - G_k) = 0$, $G^0_k = [\imath\nu + \tilde{\mu}]^{-1}$, and $X^\alpha_q = 2 \sum_{kk'} X^\alpha_{kk'q}$ one obtains,

$$\imath\omega X^\alpha_q = \left\langle \rho^\alpha_{-q} [\rho^\alpha, H_{\text{int}}]_q \right\rangle. \tag{F.3}$$

This is the Ward identity of a spin-$\frac{1}{2}$ Heisenberg model, which may also be derived directly from its Hamiltonian $H = \frac{1}{2} \sum_{\mathbf{q}} \mathbf{S}_{-\mathbf{q}} J_{\mathbf{q}} \mathbf{S}_{\mathbf{q}}$ (where $\mathbf{S}$ acts in the local Hilbert space $\{|\uparrow\rangle, |\downarrow\rangle\}$) by making use of the continuity equation $\partial_\tau \mathbf{S}_{\mathbf{q}} + [\mathbf{S}_{\mathbf{q}}, H] = 0$. Obviously, the only current present in the Heisenberg model is the spin current generated by the exchange interaction, represented by the RHS of Eq. (F.3).

(ii) The second relevant scenario is the *t-J*-model. This model arises from a Hamiltonian with finite hopping H_0 and interactions $V^c = U \to \infty$ and $V^{x,y,z}_{\mathbf{q}} = J_{\mathbf{q}}/4$ (there is also a nonlocal charge-charge coupling that is often neglected). This model formally has the Ward identity in Eq. (F.1), although analytical properties of the correlation functions change drastically in the limit $U \to \infty$. For example, the asymptotic formulae in Sec. D become invalid. Usually, a projection operator is applied to the hopping in order to eliminate double

occupancies [111] but one may as well take the limit $U \to \infty$ explicitly, starting from a formulation with finite U [42].

F.2   Ward identity of the extended Hubbard model

Let us evaluate the Ward identity of an extended Hubbard Hamiltonian explicitly. In the following, a model with nonlocal charge-charge and nonlocal exchange interactions will be considered, $\mathcal{H} = H_0 - \mu N + \frac{1}{2} \sum_{\mathbf{q}, \alpha = c, x, y, z} \rho^\alpha_{-\mathbf{q}} V^\alpha_{\mathbf{q}} \rho^\alpha_{\mathbf{q}}$. In this model the commutator in the Ward identity Eq. (F.1) evaluates to,

$$
\begin{aligned}
[\rho^\alpha_{\mathbf{q}}, H_{\text{int}}] =& \imath \sum_{\mathbf{p}\beta\gamma} \varepsilon_{\alpha\beta\gamma} \rho^\beta_{\mathbf{p}} (V^\beta_{\mathbf{p}} + V^\beta_{-\mathbf{p}}) \rho^\gamma_{\mathbf{q}-\mathbf{p}} + (1 - \delta_{\alpha,c}) \frac{(2\imath)^2}{2} \left(\sum^{'}_{\mathbf{p}, \beta \neq \alpha} V^\beta_{\mathbf{p}} \right) \rho^\alpha_{\mathbf{q}} \\
=& 2\imath \sum_{\mathbf{p}\beta\gamma} \varepsilon_{\alpha\beta\gamma} \rho^\beta_{\mathbf{p}} V^\beta_{\mathbf{p}} \rho^\gamma_{\mathbf{q}-\mathbf{p}}.
\end{aligned}
\tag{F.4}
$$

It was used that $[\rho^\alpha_{\mathbf{q}}, \rho^\beta_{\mathbf{p}}] = 2\imath \sum_\gamma \varepsilon_{\alpha\beta\gamma} \rho^\gamma_{\mathbf{q}+\mathbf{p}}$. From the first to the second line it was assumed that $\sum'_{\mathbf{q}} V^{x,y,z}_{\mathbf{q}} = V^{x,y,z}_{ii} = 0$ and $V_{\mathbf{q}} = V_{-\mathbf{q}}$. The commutator $[\rho^\alpha_{\mathbf{q}}, H_{\text{int}}]$ may be interpreted as the divergence of a current, ∇j^α [cf. discussion after Eq. (C.7)]. Therefore, Eq. (F.4) expresses that none of the interactions in H_{int} generate a charge current, $[\rho^c, H_{\text{int}}] = 0$, while an exchange interaction $V^{x,y,z}$ will generate currents of the perpendicular spin components[13]. Inserting the expression in Eq. (F.4) into the Ward identity Eq. (F.1) leads to,

$$
G_{k+q} - G_k = \sum_{k'} \left([G^0_{k'}]^{-1} - [G^0_{k'+q}]^{-1} \right) X^\alpha_{kk'q} + \imath \sum_{\sigma\sigma'} s^\alpha_{\sigma'\sigma} \sum_{p\beta\gamma} \varepsilon_{\alpha\beta\gamma} V^\beta_p \left\langle c_{k\sigma} c^\dagger_{k+q,\sigma'} \rho^\beta_p \rho^\gamma_{q-p} \right\rangle.
\tag{F.5}
$$

In the Heisenberg limit with the Ward identity in Eq. (F.3), and with isotropic exchange couplings $V^{x,y,z} = J/4$, the spin currents reveal their peculiar contribution as a coupling of the exchange interaction J to the dynamical spin chirality [152],

$$
\imath\omega \langle \mathbf{S}_{-q} \mathbf{S}_q \rangle = \imath \sum_p J_p \langle \mathbf{S}_{-q} (\mathbf{S}_p \times \mathbf{S}_{q-p}) \rangle.
\tag{F.6}
$$

Here, Eq. (F.3) was written as a vector equation, the definitions of the spin operators $S = \rho/2$, of the spin susceptibility $\imath\omega X^\alpha_q = 4\imath\omega \langle S^\alpha_{-q} S^\alpha_q \rangle$, and of the vector product were used, $(\mathbf{A} \times \mathbf{B})_\alpha = \sum_{\beta\gamma} \varepsilon_{\alpha\beta\gamma} A_\beta B_\gamma$.

---

[13] The spin components should not to be confused with the spatial direction of the current $\mathbf{j}^\alpha$. Quanta of the x component may flow in y direction etc.

According to Eqs. (F.5) and (F.6) the contribution of the interaction to the spin currents enters the Ward identity in the form of a six-point correlation function[14],

$$X^{\alpha\beta\gamma}_{kk'k''qp} = -\imath\varepsilon_{\alpha\beta\gamma} \sum_{\sigma_i} s^{\alpha}_{\sigma'_1\sigma_1} s^{\beta}_{\sigma'_2\sigma_2} s^{\gamma}_{\sigma'_3\sigma_3} \left\langle c_{k\sigma_1} c^{\dagger}_{k+q,\sigma'_1} c_{k'+p,\sigma_2} c^{\dagger}_{k',\sigma'_2} c_{k''+q-p,\sigma_3} c^{\dagger}_{k'',\sigma'_3} \right\rangle. \quad \text{(F.8)}$$

Except for a prefactor one obtains the spin chirality in Eq. (F.6) by connecting ends of equal flavor, i.e., summing $\sum_{kk'k''} X^{\alpha\beta\gamma}_{kk'k''qp}$ [see Fig. 3.11 left]. Due to the Levi-Civita symbol in its definition this correlation function vanishes whenever any one of its labels α, β, γ is the charge flavor c, or if two of these labels are the same. The latter property is related to the fact that the vector product in Eq. (F.6) is always perpendicular to its multiplicands, $\mathbf{A}(\mathbf{A} \times \mathbf{B}) = \mathbf{B}(\mathbf{A} \times \mathbf{A}) = \mathbf{0}$. For $X^{\alpha\beta\gamma}$ the diagrammatic representation on the left of Fig. 3.11 is appropriate. Using the definition in Eq. (F.8), the Ward identity of the extended Hubbard model can be brought into the form,

$$G_{k+q} - G_k = \sum_{k'} \left([G^0_{k'}]^{-1} - [G^0_{k'+q}]^{-1}\right) X^{\alpha}_{kk'q} - \sum_{k'k''p\beta\gamma} V^{\beta}_p X^{\alpha\beta\gamma}_{kk'k''qp}, \quad \text{(F.9)}$$

which merely hides the mess created in the spin channels by the exchange couplings V^{β}_p. A diagrammatic representation of the Ward identity in Eq. (F.9) is depicted in Fig. 3.11. In the spirit of Eqs. (E.4) and Eqs. (E.5), one may expand the generalized susceptibility X in the Ward identity Eq. (F.9) using the Bethe-Salpeter equation and divide both sides by $G_k G_{k+q}$,

$$G_k^{-1} - G_{k+q}^{-1} = \left([G^0_k]^{-1} - [G^0_{k+q}]^{-1}\right) + \sum_{\underline{k}} \Gamma^{\alpha}_{k\underline{k}q} \sum_{k'} \left([G^0_{k'}]^{-1} - [G^0_{k'+q}]^{-1}\right) X^{\alpha}_{\underline{k}k'q}$$
$$- G_k^{-1} G_{k+q}^{-1} \sum_{k'k''p\beta\gamma} V^{\beta}_p X^{\alpha\beta\gamma}_{kk'k''qp} \quad \text{(F.10)}$$

Using Dyson's equation, $[G^0]^{-1} - G^{-1} = \Sigma$, one has

$$\Sigma_{k+q} - \Sigma_k = \sum_{\underline{k}} \Gamma^{\alpha}_{k\underline{k}q} \sum_{k'} \left([G^0_{k'}]^{-1} - [G^0_{k'+q}]^{-1}\right) X^{\alpha}_{\underline{k}k'q} - G_k^{-1} G_{k+q}^{-1} \sum_{k'k''p\beta\gamma} V^{\beta}_p X^{\alpha\beta\gamma}_{kk'k''qp}. \quad \text{(F.11)}$$

---

[14] A six-point correlation function always appears when $[H_{\text{int}}, \rho^{\alpha}] \neq 0$: The commutator of operators $\mathcal{O}(c^{\dagger}c)$ and $\mathcal{O}(c^{\dagger}cc^{\dagger}c)$ is given as

$$[c^{\dagger}_a c_b, c^{\dagger}_{\alpha} c_{\beta} c^{\dagger}_{\gamma} c_{\delta}] = (c^{\dagger}_a c_{\beta} \delta_{b\alpha} - c^{\dagger}_{\alpha} c_b \delta_{a\beta}) c^{\dagger}_{\gamma} c_{\delta} + c^{\dagger}_{\alpha} c_{\beta} (c^{\dagger}_a c_{\delta} \delta_{b\gamma} - c^{\dagger}_{\gamma} c_b \delta_{a\delta}). \quad \text{(F.7)}$$

Either the Kronecker symbols lead to a cancellation, or the result is of order $\mathcal{O}(c^{\dagger}cc^{\dagger}c)$. Insertion into the Ward identity Eq. (F.1) then leads to a six-point correlation function.
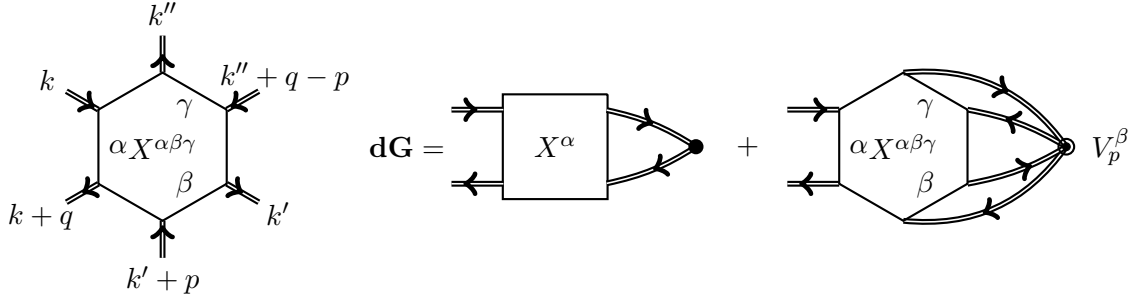
FIGURE 3.11: Left: Diagrammatic representation of the six-point correlation function $X^{\alpha\beta\gamma}$, which is similar to the spin-chirality [see Eq. (F.6)] but with open ends. Right: The integral Ward identity of the extended Hubbard model with exchange couplings, Eq. (F.9). The full circle represents the expression $[G^0_{k'}]^{-1} - [G^0_{k'+q}]^{-1}$. The concentric circles represent the exchange interaction $V^{x,y,z}$. Connecting Green's function lines of $X^{\alpha\beta\gamma}$ implies summation over momentum k and spin flavor α.

The first term on the RHS can be simplified by inserting the Ward identity Eq. (F.9), in order to remove the non-interacting Green's function G^0 from this relation,

$$
\begin{aligned}
\Sigma_{k+q} - \Sigma_k &= \sum_{\underline{k}} \Gamma^\alpha_{k\underline{k}q}[G_{\underline{k}+q} - G_{\underline{k}}] + \sum_{\underline{k}k'k''p\beta\gamma} V^\beta_p (\Gamma^\alpha_{k\underline{k}q} - G^{-1}_k G^{-1}_{k+q}\delta_{k\underline{k}})X^{\alpha\beta\gamma}_{\underline{k}k'k''qp} \\
&= \sum_{\underline{k}} \Gamma^\alpha_{k\underline{k}q}[G_{\underline{k}+q} - G_{\underline{k}}] - \sum_{\underline{k}k'k''p\beta\gamma} V^\beta_p (\hat{X}^{\alpha,-1})_{k\underline{k}q}X^{\alpha\beta\gamma}_{\underline{k}k'k''qp}.
\end{aligned} \tag{F.12}
$$

From the first to the second line the inverted Bethe-Salpeter equation was inserted, $\hat{\Gamma} - \hat{X}^{0,-1} = -\hat{X}^{-1}$. From the LHS and the first term on the RHS one recognizes the familiar relation $\mathbf{d\Sigma} = \hat{\Gamma}\mathbf{dG}$ that was discussed above. However, due to the presence of the chiral 3P correlation function $X^{\alpha\beta\gamma}$ in Eq. (F.12), further progress can not be made without knowledge about its diagrammatic structure.

F.3   Bose-Fermi-Kondo model - The extended Hubbard model in zero dimensions

Above, the Ward identity of the extended Hubbard model with the interaction Hamiltonian $H_{\text{int}} = \frac{1}{2}\sum_{\mathbf{q}\alpha}\rho^\alpha_{-\mathbf{q}}V^\alpha_{\mathbf{q}}\rho^\alpha_{\mathbf{q}}$ was derived. In the limit of infinite coordination number this model maps to an impurity model when the nonlocal interaction is scaled with $z^{-1/2}$ [136]. This impurity model is known as a Bose-Fermi-Kondo model. The interaction $\Lambda^\alpha(\tau - \tau')$ of this model is nonlocal in time, i.e., retarded, rather than nonlocal in space. The analogy

between these interactions is obvious in the imaginary time path integral,

$$S_{\text{int}} = \frac{1}{2} \sum_\alpha \int \int d\tau d\tau' \rho^\alpha(\tau) \Lambda^\alpha(\tau - \tau') \rho^\alpha(\tau'). \tag{F.13}$$

In the following the Ward identities of such an impurity model will be derived. As before, the derivation starts from the Hamiltonian formulation of the Bose-Fermi-Kondo model,

$$H_{\text{imp}} = H_{\text{at}} + H_\Delta^0 + H_\Delta + H_\Lambda^0 + H_\Lambda. \tag{F.14}$$

Here, $H_{\text{at}} = -\mu n + U n_\uparrow n_\downarrow$ is the Hamiltonian of a single-orbital Hubbard atom. It is coupled to a fermionic bath, the hybridization, via the Hamiltonians H_Δ^0 and H_Δ that were discussed earlier, see Eqs. (C.15), (C.16), and (C.17). The Hamiltonian $H_{\text{at}} + H_\Delta^0 + H_\Delta$ thus corresponds to the Anderson impurity model, with the on-site interaction U.

The remaining components H_Λ^0 and H_Λ represent the retarded interactions. In the Hamiltonian picture such interactions are mediated by bosons ϕ^α. For each channel of the retarded interaction, one charge and three spin channels, respectively, there is one flavor α of bosons. The non-interacting bosonic systems are comprised in the Hamiltonian $H_\Lambda^0 = \sum_\alpha H_\Lambda^{0,\alpha}$, where

$$H_\Lambda^{0,\alpha} = \sum_q \Omega_q^\alpha (b_q^\alpha)^\dagger b_q^\alpha. \tag{F.15}$$

Here, each bosonic flavor has a spectrum of energies Ω_q^α, where q labels the quantum numbers of the bosons. The construction operators $(b_q^\alpha)^\dagger$ and b_q^α create and annihilate a boson of the flavor α with the quantum number q, respectively. The free system of bosons, not coupled to the impurity, has the non-interacting bosonic Green's function,

$$\mathcal{D}_{q\omega}^\alpha = \frac{2\Omega_q^\alpha}{(\imath\omega)^2 - (\Omega_q^\alpha)^2}. \tag{F.16}$$

The four reservoirs of bosons with flavors $\alpha = c, x, y, z$ mediate four retarded interactions via couplings to the charge and spin densities ρ^α, comprised in the operator $H_\Lambda = \sum_\alpha H_\Lambda^\alpha$. The individual coupling operators read

$$H_\Lambda^\alpha = \sum_q w_q^\alpha \rho^\alpha \phi_q^\alpha, \qquad \phi_q^\alpha = (b_q^\alpha)^\dagger + b_q^\alpha. \tag{F.17}$$

Here, w_q^α is a matrix element coupling a boson with flavor α and the quantum number q to the respective density ρ^α.

The operator $\rho^\alpha = \sum_{\sigma\sigma'} c_\sigma^\dagger s_{\sigma\sigma'}^\alpha c_{\sigma'}$ is the density of the correlated impurity. In the Bose-Fermi-Kondo model the impurity is coupled to two baths, the fermionic hybridization on the one hand and the bosons mediating the retarded interactions on the other. Although the physics described by the two baths is entirely different, there exists a formal analogy between them: The matrix elements v_k (w_q^α) couple the correlated fermions $c^\dagger, c$ (density
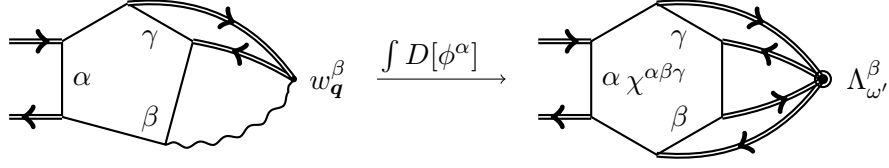
FIGURE 3.12:   (Left) Diagrammatic representation of the mixed fermion-boson correlation function in Eq. (F.20). The wiggly line connects two bosonic end points. The boson and two fermions couple to w^β, which is represented by a small dot. Integrating out the bosons ϕ^α, the mixed fermion-boson vertex takes the form of the chiral 3P correlation function $\chi^{\alpha\beta\gamma}$ defined in Eq. (F.32), whereas the fermion-boson coupling w^β gives rise to the retarded interaction Λ^β. The resulting Ward identity is analogous to that of the extended Hubbard model in Fig. 3.10.

ρ^α) to a bath of non-interacting fermions $f^\dagger, f$ (bosons ϕ^α) with the spectrum $\epsilon_{\bm{k}}$ ($\Omega_{\bm{q}}^\alpha$). More information on the fermionic bath is given above, see Sec. C near Eq. (C.15).

The derivation of the Ward identity starts from Eq. (C.30), where the commutator $[\rho^\alpha, H_{\text{int}}]$ was left unspecified. In the Bose-Fermi-Kondo model the interaction is given by the Hubbard interaction and the retarded interactions, $H_{\text{int}} = U n_\uparrow n_\downarrow + H_\Lambda^0 + H_\Lambda$. Since the Hubbard interaction $U n_\uparrow n_\downarrow$ commutes with the densities ρ^α, one only needs to account for the bosonic baths, making use of the fact that all fermionic operators commute with all bosonic ones, $[f, \phi^\alpha] = [c, \phi^\alpha] = 0$. Hence, the non-interacting bosonic Hamiltonian Eq. (F.15) commutes with the densities, $[\rho^\alpha, H_\Lambda^0] = 0$ for $\alpha = c, x, y, z$. This leaves the coupling operators in Eq. (F.17) comprised in H_Λ, leading to the Ward identity,

$$g_{\nu+\omega} - g_\nu = \sideset{}{'}\sum_{\nu'} [\Delta_{\nu'+\omega} - \Delta_{\nu'} - \imath\omega] \chi_{\nu\nu'\omega}^\alpha + \frac{1}{2} \sum_{\sigma\sigma'} s_{\sigma'\sigma}^\alpha \langle c_{\nu\sigma} c_{\nu+\omega,\sigma'}^\dagger [\rho^\alpha, H_\Lambda]_\omega \rangle. \qquad (\text{F.18})$$

Like in the extended Hubbard model the charge density ρ^c commutes with all interactions, including the one in the charge channel that arises from the couplings $w_{\bm{q}}^c$. The spin densities $\rho^{x,y,z}$, on the other hand, do not commute with the retarded interactions of a perpendicular flavor,

$$[\rho^\alpha, H_\Lambda] = 2\imath \sum_{\beta\gamma} \varepsilon_{\alpha\beta\gamma} \sum_{\bm{q}} w_{\bm{q}}^\beta \phi_{\bm{q}}^\beta \rho^\gamma. \qquad (\text{F.19})$$

The second term on the RHS of Eq. (F.18) is hence given as,

$$\imath \sum_{\sigma\sigma'} s_{\sigma'\sigma}^\alpha \sum_{\beta\gamma} \varepsilon_{\alpha\beta\gamma} \sideset{}{'}\sum_{\omega'\bm{q}} w_{\bm{q}}^\beta \langle c_{\nu\sigma} c_{\nu+\omega,\sigma'}^\dagger \phi_{\bm{q}\omega'}^\beta \rho_{\omega-\omega'}^\gamma \rangle. \qquad (\text{F.20})$$

Diagrammatically this contribution to the Ward identity may be depicted as shown on the left of Fig. 3.12. The remaining task is to integrate out the bosons from the Ward identity

Eq. (F.18) to obtain a relation involving only impurity correlation functions. To this end, one needs to introduce the path integral formulation of the BFK model with the action,

$$S'_{\text{BFK}} = S_{\text{AIM}} + S^0_\Lambda + S^\phi_\Lambda, \tag{F.21}$$

where the components of the BFK that correspond to the Anderson impurity model are separated off as

$$S_{\text{AIM}}[c^*, c] = -\sum_{\nu\sigma}{}' c^*_{\nu\sigma}[\imath\nu + \mu - \Delta_\nu]c_{\nu\sigma} + U\sum_\omega{}' n_{\uparrow,-\omega}n_{\downarrow\omega}. \tag{F.22}$$

Here, Δ_ν is the hybridization function Eq. (C.20) that arises upon integrating out the fermionic bath operators $f^\dagger, f$, as exercised below Eq. (C.24) in Sec. C. The bosonic part of the action, S'_{BFK}, comprises S^0_Λ, originating from the non-interacting bosonic Hamiltonian H^0_Λ in Eq. (F.15), and of the fermion-boson coupling S^ϕ_Λ, which corresponds to the Hamiltonian in Eq. (F.17). A source term J^α is added to S^ϕ_Λ, which allows to represent bosonic operators in impurity correlation functions via functional derivatives,

$$S^\phi_\Lambda[\rho^\beta, \phi^\beta, J^\beta] = \sum_{\omega\boldsymbol{q}\beta}{}' [w^\beta_{\boldsymbol{q}}\rho^\beta_{-\omega} + J^\beta_{\boldsymbol{q},-\omega}]\phi^\beta_{\boldsymbol{q}\omega}. \tag{F.23}$$

In the path integral formalism the operators $c^\dagger, c$ and ϕ are transferred to Grassmann numbers c^*, c and complex numbers $\phi = b^* + b$, respectively. Making use of the source term J^α in Eq. (F.23) the bosonic operators in the correlation function in Eq. (F.20) can be replaced by functional derivatives,

$$\sum_{\boldsymbol{q}} w^\beta_{\boldsymbol{q}} \langle c_{\nu\sigma}c^\dagger_{\nu+\omega,\sigma'}\phi^\beta_{\boldsymbol{q}\omega'}\rho^\gamma_{\omega-\omega'}\rangle = \mathcal{Z}'^{-1}_{\text{BFK}} \sum_{\boldsymbol{q}} w^\beta_{\boldsymbol{q}} \int D[c^*, c, \phi] c_{\nu\sigma}c^*_{\nu+\omega,\sigma'}\phi^\beta_{\boldsymbol{q}\omega'}\rho^\gamma_{\omega-\omega'}e^{-S'_{\text{BFK}}}$$

$$= \mathcal{Z}'^{-1}_{\text{BFK}} \sum_{\boldsymbol{q}} w^\beta_{\boldsymbol{q}} \int D[c^*, c, \phi] c_{\nu\sigma}c^*_{\nu+\omega,\sigma'} \left(-\frac{\delta}{\delta J^\beta_{\boldsymbol{q},-\omega'}}\bigg|_{J^\beta=0}\right) \rho^\gamma_{\omega-\omega'}e^{-S'_{\text{BFK}}}. \tag{F.24}$$

Here, $\mathcal{Z}'^{-1}_{\text{BFK}} = \int D[c^*, c]e^{-S'_{\text{BFK}}}$ is the partition sum of the BFK model defined in Eq. (F.21). In this form the bosons ϕ^α may now be integrated out from the path integral in Eq. (F.24). This procedure is done in a slightly different way than for fermions, some details are provided in Appendix A. The result amounts to the following identity,

$$\int D[\phi]e^{-S^0_\Lambda - S^\phi_\Lambda} = \mathcal{Z}_\phi e^{-S_\Lambda}, \tag{F.25}$$

where $\mathcal{Z}_\phi = \int D[\phi] e^{-S_\Lambda^0}$ is the partition sum of the non-interacting bosonic system. The effective action representing the retarded interaction is then given by

$$S_\Lambda[\rho^\beta, J^\beta] = \frac{1}{2} \sum_{\omega\boldsymbol{q}\beta}{}' [w_{\boldsymbol{q}}^\beta \rho_{-\omega}^\beta + J_{\boldsymbol{q},-\omega}^\beta] \mathcal{D}_{\boldsymbol{q}\omega}^\beta [w_{\boldsymbol{q}}^\beta \rho_\omega^\beta + J_{\boldsymbol{q}\omega}^\beta]. \tag{F.26}$$

Here, $\mathcal{D}^\beta$ is the non-interacting Green's function of the bosons defined in Eq. (F.16), it was used that $\mathcal{D}_\omega^\beta = \mathcal{D}_{-\omega}^\beta$. One may now perform the functional derivative in Eq. (F.24), with the result

$$\sum_{\boldsymbol{q}} w_{\boldsymbol{q}}^\beta \langle c_{\nu\sigma} c_{\nu+\omega,\sigma'}^\dagger \phi_{\boldsymbol{q}\omega'}^\beta \rho_{\omega-\omega'}^\gamma \rangle = \mathcal{Z}_{\mathrm{BFK}}^{-1} \sum_{\boldsymbol{q}} (w_{\boldsymbol{q}}^\beta)^2 \mathcal{D}_{\boldsymbol{q}\omega'}^\beta \int D[c^*, c] c_{\nu\sigma} c_{\nu+\omega,\sigma'}^* \rho_{\omega'}^\beta \rho_{\omega-\omega'}^\gamma e^{-S_{\mathrm{BFK}}}$$

$$= \Lambda_{\omega'}^\beta \left\langle c_{\nu\sigma} c_{\nu+\omega,\sigma'}^* \rho_{\omega'}^\beta \rho_{\omega-\omega'}^\gamma \right\rangle_\Lambda. \tag{F.27}$$

Here, three abbreviations were introduced. Firstly, the effective action of the BFK model was introduced,

$$S_{\mathrm{BFK}} = S_{\mathrm{AIM}} + S_\Lambda[J^\beta = 0]$$

$$= S_{\mathrm{AIM}} + \frac{1}{2} \sum_{\omega\alpha} \rho_{-\omega}^\alpha \Lambda_\omega^\alpha \rho_\omega^\alpha. \tag{F.28}$$

Secondly, the brackets $\langle \cdots \rangle_\Lambda = \mathcal{Z}_{\mathrm{BFK}}^{-1} \int D[c^*, c] \cdots e^{-S_{\mathrm{BFK}}}$ denote an average in the effective action of the BFK. Here, $\mathcal{Z}_{\mathrm{BFK}}^{-1} = \mathcal{Z}_\phi \mathcal{Z}_{\mathrm{BFK}}'^{-1} = \int D[c^*, c] e^{-S_{\mathrm{BFK}}}$ is the effective partition sum of the BFK, where $\mathcal{Z}_{\mathrm{BFK}}'^{-1}$ and $\mathcal{Z}_\phi$ are defined below Eqs. (F.24) and (F.25), respectively. The subscript $\langle \cdots \rangle_\Lambda$ will be dropped in the following. And thirdly, the retarded interaction was defined as,

$$\Lambda_\omega^\alpha = \sum_{\boldsymbol{q}} (w_{\boldsymbol{q}}^\alpha)^2 \mathcal{D}_{\boldsymbol{q}\omega}^\alpha = \sum_{\boldsymbol{q}} \frac{2(w_{\boldsymbol{q}}^\alpha)^2 \Omega_{\boldsymbol{q}}^\alpha}{(\imath\omega)^2 - (\Omega_{\boldsymbol{q}}^\alpha)^2}. \tag{F.29}$$

As a result of integrating out the bosons from Eq. (F.27) one can deduce the following replacement rule for bosonic operators inside impurity averages of the BFK model[15],

$$" \sum_{\boldsymbol{q}} w_{\boldsymbol{q}}^\beta \phi_{\boldsymbol{q}\omega}^\beta \to \Lambda_\omega^\beta \rho_\omega^\beta ". \tag{F.30}$$

---

[15] For further details with regard to integrating out bosons the reader is referred to Appendix A, as well as [65] and [61]. As usual, the notation in Eq. (F.27) must not mislead to interpret the Fourier transform to Matsubara frequencies to be done within the brackets $\langle \cdots \rangle$. See also the comment after Eq. (A.43) in chapter 2.

Performing this replacement in Eq. (F.20) and inserting the result into the Ward identity Eq. (F.18) it takes the form,

$$g_{\nu+\omega} - g_\nu = \sum_{\nu'}^{\prime} [\Delta_{\nu'+\omega} - \Delta_{\nu'} - \imath\omega]\chi_{\nu\nu'\omega}^\alpha + \imath \sum_{\sigma\sigma'} s_{\sigma'\sigma}^\alpha \sum_{\beta\gamma} \varepsilon_{\alpha\beta\gamma} \sum_{\omega'}^{\prime} \Lambda_{\omega'}^\beta \left\langle c_{\nu\sigma}c_{\nu+\omega,\sigma'}^* \rho_{\omega'}^\beta \rho_{\omega-\omega'}^\gamma \right\rangle.$$

(F.31)

In full analogy to the extended Hubbard model a chiral 3P or six-point correlation function arises on the RHS of the Ward identity of the BFK. This will be abbreviated as

$$\chi_{\nu\nu'\nu''\omega\omega'}^{\alpha\beta\gamma} = -\imath\varepsilon_{\alpha\beta\gamma} \sum_{\sigma_i} s_{\sigma_1'\sigma_1}^\alpha s_{\sigma_2'\sigma_2}^\beta s_{\sigma_3'\sigma_3}^\gamma \left\langle c_{\nu\sigma_1} c_{\nu+\omega,\sigma_1'}^\dagger c_{\nu'+\omega',\sigma_2} c_{\nu',\sigma_2'}^\dagger c_{\nu''+\omega-\omega',\sigma_3} c_{\nu'',\sigma_3'}^\dagger \right\rangle.$$

(F.32)

The contribution of this correlation function to the Ward identity is denoted diagrammatically on the RHS of Fig. 3.12. Integrating out the bosons from the impurity model transfers the mixed fermion-boson vertex in Eq. (F.20) to the chiral 3P correlation function in Eq. (F.32). Connecting ends of equal flavor of $\chi^{\alpha\beta\gamma}$ by summation over fermionic frequencies and using the definition of the spin density operators $S^\alpha = 2\rho^\alpha$ leaves behind a local analogue of the spin chirality in Eq. (F.6),

$$\sum_{\nu\nu'\nu''}^{\prime} \chi_{\nu\nu'\nu''\omega\omega'}^{\alpha\beta\gamma} = 8\imath\varepsilon_{\alpha\beta\gamma} \left\langle S_{-\omega}^\alpha S_{\omega'}^\beta S_{\omega-\omega'}^\gamma \right\rangle.$$

(F.33)

In case of an isotropic retarded spin-spin interaction $\Lambda^{x,y,z} = \Lambda^s$ the contribution of the dynamical spin chirality to the Ward identity Eq. (F.32) may be written as $\int_0^\beta \Lambda_{\tau_2-\tau_3}^s \langle T_\tau[\mathbf{S}_{\tau_1}(\mathbf{S}_{\tau_2} \times \mathbf{S}_{\tau_3})]\rangle d\tau_2$ [cf. Eq. (F.6) and related discussion]. The local spin chirality vanishes whenever two of the times τ_1, τ_2, τ_3 are equal. The contribution of this correlation function to the Ward identity vanishes if Λ^s is static, $\Lambda^s(\tau - \tau') \to \Lambda^s \delta_{\tau,\tau'}$ [16].

F.4 Interpretation of the Ward identity of the BFK model

Apparently, the dynamical spin chirality arises in the Ward identity Eq. (F.31) as a peculiar effect of a time-dependent spin-spin interaction, a similar contribution does not occur in the charge channel. This is due to the fact that a retarded spin-spin interaction leads to spin currents, whereas a retarded charge-charge interaction conserves both the charge and spin quantum numbers.

The spin currents generated by the 'spin-bosons' can be understood intuitively in the segment picture, which is used to solve the BFK in a continuous-time quantum Monte Carlo (CTQMC) algorithm [98]. There the retarded spin-spin interactions are represented

---

[16]Strictly speaking, this is not possible here, since an interaction of the form given in Eq. (F.29) which originates from a bosonic bath can not be static. However, in the effective action of the BFK model Eq. (F.28) one might regard to Λ^α as a free parameter that need not be associated to a bosonic bath.
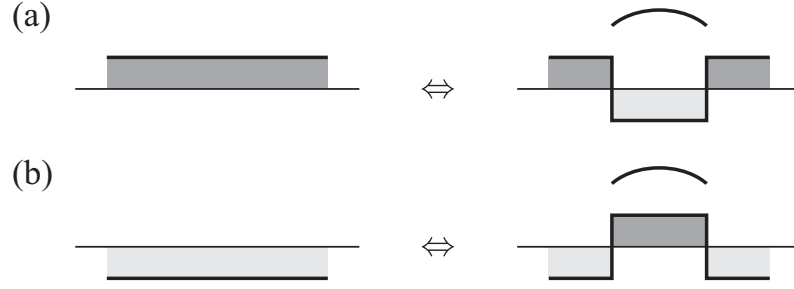
FIGURE 3.13:   Illustration of the spin-flip events that are taken into account in the segment picture [98]. (a) A spin-↑ electron resides on the impurity (left). An update of this world-line may flip the impurity spin into the ↓-state (right), in turn creating a spin-boson that is denoted by an arc. The boson carries a spin +1, until after some time it is annihilated, flipping the impurity spin back from ↓ to ↑. (b) The inverse situation in case of a ↓-spin. Here, the spin-boson carries a spin quantum −1. The spin-bosons contribute to the spin currents and introduce the chiral 3P correlation function $\chi^{\alpha\beta\gamma}$ into the Ward identity in Eq. (F.31). The charge quantum number is conserved by the spin-bosons, such that they do not contribute to the charge current. I kindly thank J. Otsuki for allowing me to use this figure, Fig. 2 of [98].

by spin-flip updates, which correspond to the action of spin-1/2 ladder operators S^+ and S^- upon the impurity spin. This is shown in Fig. 3.13. Each of these spin-flips creates or annihilates a spin-boson, which trade spin quanta with the fermionic system. During the time of its existence, the spin-boson carries the spin quantum ± 1, which represents a spin current. This spin current is independent of the charge current, spin quanta may enter and leave the impurity while the charge remains in place.

F.5   Ward identity of the extended Hubbard model and of the BFK

Comparing to the Ward identity of the extended Hubbard model Eq. (F.5) one can see that the Ward identity of the Bose-Fermi-Kondo model takes a fully analogous form. Both identities may be comprised in a common notation as

$$G_{k+q} - G_k = \sum_{k'} \left([G_{k'}^0]^{-1} - [G_{k'+q}^0]^{-1} \right) X_{kk'q}^{\alpha} - \sum_{k'k''p\beta\gamma} V_p^{\beta} X_{kk'k''qp}^{\alpha\beta\gamma}, \qquad (\text{F.34})$$

This Ward identity may be denoted diagrammatically as in Fig. 3.10. Likewise, a Ward identity for the irreducible self-energies Σ and Γ of the BFK model may be derived, in full analogy to Eq. (F.12),

$$\Sigma_{k+q} - \Sigma_k = \sum_{\underline{k}} \Gamma_{k\underline{k}q}^{\alpha} [G_{\underline{k}+q} - G_{\underline{k}}] - \sum_{\underline{k}k'k''p\beta\gamma} V_p^{\beta} (\hat{X}^{\alpha,-1})_{k\underline{k}q} X_{\underline{k}k'k''qp}^{\alpha\beta\gamma}. \qquad (\text{F.35})$$

From Eqs. (F.34) and (F.35) the respective Ward identities of the BFK model are obtained by performing the replacements in Eq. (C.18), as well as the following additional ones:

Quantity	Lattice	Impurity	See definition
Bosonic momentum p	$(\mathbf{p}, \omega')$	ω'	
Interaction	V_p^α	$\Lambda_{\omega'}^\alpha$	(F.29)
Chiral 3P GF	$X_{kk'k''qp}^{\alpha\beta\gamma}$	$\chi_{kk'k''qp}^{\alpha\beta\gamma}$	(F.8)

$$(F.36)$$

Here, a chiral 3P correlation function $\chi^{\alpha\beta\gamma}$ was introduced in analogy to Eq. (F.8).

F.6 Susceptibility asymptotes

As has been seen earlier in Eq. (D.19), the non-commutativity of a density ρ^α with the interaction Hamiltonian H_{int} manifests itself in the high frequency asymptote of the susceptibility X^α with a contribution,

$$\left\langle \left[\rho_{-\mathbf{q}}^\alpha, [\rho_{\mathbf{q}}^\alpha, H_{\text{int}}] \right] \right\rangle. \tag{F.37}$$

This contribution to the asymptote will be considered here for the extended Hubbard model and for the BFK model.

For the extended Hubbard model with the interaction operator $H_{\text{int}} = \frac{1}{2} \sum_{\mathbf{q}\beta}' \rho_{-\mathbf{q}}^\beta V_{\mathbf{q}}^\beta \rho_{\mathbf{q}}^\beta$ the commutator $[\rho_{\mathbf{q}}^\alpha, H_{\text{int}}] = 2i \sum_{\mathbf{p}\beta\gamma}' \varepsilon_{\alpha\beta\gamma} \rho_{\mathbf{p}}^\beta V_{\mathbf{p}}^\beta \rho_{\mathbf{q}-\mathbf{p}}^\gamma$ has been calculated in Eq. (F.4). Inserting this into Eq. (F.37) yields

$$2i \sum_{\mathbf{p}\beta\gamma}' \varepsilon_{\alpha\beta\gamma} V_{\mathbf{p}}^\beta \left\langle [\rho_{-\mathbf{q}}^\alpha, \rho_{\mathbf{p}}^\beta \rho_{\mathbf{q}-\mathbf{p}}^\gamma] \right\rangle$$

$$= (2i)^2 \sum_{\mathbf{p}\beta\gamma}' \varepsilon_{\alpha\beta\gamma}^2 \left(V_{\mathbf{q}-\mathbf{p}}^\beta \langle \rho_{-\mathbf{p}}^\gamma \rho_{\mathbf{p}}^\gamma \rangle - V_{\mathbf{p}}^\beta \langle \rho_{-\mathbf{p}}^\beta \rho_{\mathbf{p}}^\beta \rangle \right) \tag{F.38}$$

This contribution vanishes in the charge channel $\alpha = c$ and the charge-charge interaction V^c does not contribute to this expression. In the derivation of Eq. (F.38) inversion symmetry $V_{\mathbf{q}} = V_{-\mathbf{q}}$ was assumed and that the local part of the exchange interactions vanishes, $\sum_{\mathbf{q}}' V_{\mathbf{q}}^{x,y,z} = 0$. Further assuming paramagnetism, where $\langle \rho^{x,y,z} \rangle = 0$, one can substitute the equal-time susceptibility $-\sum_\omega' X_{\mathbf{q}\omega}^\beta = \langle \rho_{-\mathbf{p}}^\beta \rho_{\mathbf{p}}^\beta \rangle$ in Eq. (F.38), see definition Eq. (A.46). Inserting Eq. (F.38) into the expression Eq. (D.19) for the susceptibility asymptote one

finally has for the extended Hubbard model,

$$\lim_{\omega \to \infty} (\imath\omega)^2 X_{\mathbf{q}\omega}^\alpha = \sum_{\mathbf{k}}{}' \langle n_{\mathbf{k}} \rangle \left(\varepsilon_{\mathbf{k}+\mathbf{q}} + \varepsilon_{\mathbf{k}-\mathbf{q}} - 2\varepsilon_{\mathbf{k}} \right) - 4 \sum_{\mathbf{p}\beta\gamma\omega}{}' \varepsilon_{\alpha\beta\gamma}^2 \left(V_{\mathbf{q}-\mathbf{p}}^\beta X_{\mathbf{p}\omega}^\gamma - V_{\mathbf{p}}^\beta X_{\mathbf{p}\omega}^\beta \right).$$

$$(\text{F.39})$$

Apparently, considering a susceptibility in the spin channel $\alpha \in \{x, y, z\}$, the Levi-Civita symbol on the RHS sorts out the flavors $\beta \neq \alpha$ in the summation on the RHS of Eq. (F.38). As a consequence, the asymptote X^α of that channel depends on the susceptibilities $X^{\beta \neq \alpha}$ in the perpendicular channels but not on X^α itself. This can be seen as a consequence of the fact that the interaction V^β in a given spin channel β contributes only to the currents of the spin components perpendicular to β. The asymptote of the local susceptibility is obtained by summation over $\sum_{\mathbf{q}}'$. As in Eq. (D.23) the first term on the RHS of Eq. (F.39) then yields the kinetic energy,

$$\lim_{\omega \to \infty} (\imath\omega)^2 X_{\mathrm{loc},\omega}^\alpha = -2E_{\mathrm{kin}} + 4 \sum_{\mathbf{p}\omega\beta\neq\alpha}{}' V_{\mathbf{p}}^\beta X_{\mathbf{p}\omega}^\beta. \qquad (\text{F.40})$$

Here, the exchange interaction V^β appears next to the kinetic energy, which highlights its role as a propagation channel for spin quanta of flavor $\alpha \neq \beta$. In absence of exchange interactions the spin is merely transported via the electronic hopping $\varepsilon_{\mathbf{k}}$. In the Heisenberg model the situation is reversed: The electronic hopping vanishes, the spin is only transported via the interaction [cf. discussion near Eq. (F.6)]. In this case the susceptibility asymptotes in Eqs. (F.39) and (F.40) are determined entirely be the second contribution on their RHS, respectively.

Lastly, the asymptote of the susceptibility will also be derived for the BFK model in Eq. (F.14), which features a retarded spin-spin interaction mediated by bosons. In this case one has to calculate the local expression,

$$\langle [\rho^\alpha, [\rho^\alpha, H_{\mathrm{int}}]] \rangle. \qquad (\text{F.41})$$

The commutator with the interaction H_{int} of the BFK model is given in Eq. (F.19),

$$[\rho^\alpha, H_{\mathrm{int}}] = 2\imath \sum_{\beta\gamma} \varepsilon_{\alpha\beta\gamma} \sum_{\mathbf{q}} w_{\mathbf{q}}^\beta \phi_{\mathbf{q}}^\beta \rho^\gamma. \qquad (\text{F.42})$$

On the RHS the fermion-boson couplings w^β and the bosons ϕ^β appear. Calculating the second commutator one has,

$$
\begin{aligned}
\langle[\rho^\alpha,[\rho^\alpha,H_{\text{int}}]]\rangle =& 2\imath \sum_{\beta\gamma} \varepsilon_{\alpha\beta\gamma} \sum_{\boldsymbol{q}} w^\beta_{\boldsymbol{q}} \langle\phi^\beta_{\boldsymbol{q}}[\rho^\alpha,\rho^\gamma]\rangle \\
=& -(2\imath)^2 \sum_{\beta\gamma} \varepsilon^2_{\alpha\beta\gamma} \sum_{\boldsymbol{q}} w^\beta_{\boldsymbol{q}} \langle\phi^\beta_{\boldsymbol{q}}\rho^\beta\rangle \\
=& -(2\imath)^2 \sum_{\beta\gamma} \varepsilon^2_{\alpha\beta\gamma} \sum_{\boldsymbol{q}\omega'} w^\beta_{\boldsymbol{q}} \langle\phi^\beta_{\boldsymbol{q},-\omega'}\rho^\beta_{\omega'}\rangle.
\end{aligned}
\tag{F.43}
$$

In the last step the static average $\langle\phi^\beta\rho^\beta\rangle$ was expressed through the dynamical correlation function $\langle\phi^\beta_{-\omega'}\rho^\beta_{\omega'}\rangle$ via a summation over bosonic Matsubara energies ω'. As discussed above, integrating out the bosons ϕ^β from the BFK leads to the replacement rule given in Eq. (F.30), giving rise to the retarded spin-spin interaction Λ^β. Performing this replacement in Eq. (F.43) and inserting the result into the expression in Eq. (D.25) for the asymptote one is left with,

$$
\begin{aligned}
\lim_{\omega\to\infty} (\imath\omega)^2 \chi^\alpha_\omega =& -4 \sum_\nu{}' g_\nu\Delta_\nu - 4 \sum_{\omega',\beta\neq\alpha}{}' \Lambda^\beta_{\omega'} \langle\rho^\beta_{-\omega'}\rho^\beta_{\omega'}\rangle \\
=& -4 \sum_\nu{}' g_\nu\Delta_\nu + 4 \sum_{\omega',\beta\neq\alpha}{}' \Lambda^\beta_{\omega'} \chi^\beta_{\omega'}
\end{aligned}
\tag{F.44}
$$

In the last step the impurity susceptibility, $-\chi^\alpha_\omega = \langle\rho^\beta_{-\omega}\rho^\beta_\omega\rangle$, was substituted for the paramagnetic case where $\langle\rho^{x,y,z}\rangle = 0$. Eq. (F.44) parallels the expression for the asymptote of the local susceptibility in the extended Hubbard model, Eq. (F.40).

G   Three-particle irreducible contributions to the integral Ward identity

In the last section a lattice model and an impurity model were introduced, whose Ward identities feature a six-point- or 3P-correlation function. Here the diagrammatic structure of this correlation function will be discussed.

G.1   Loss of similarity to the noninteracting system

The appearance of the six-point correlation function $X^{\alpha\beta\gamma}$ in the integral Ward identity Eq. (F.12) due to the exchange couplings $V^{x,y,z}$ obviously marks a substantial complication. This contribution can be seen as a loss in similarity of the exchange-coupled system to the non-interacting one. This is because an interacting system that satisfies $[\rho^\alpha, H_{\text{int}}] = 0$ has the same Ward identity in the channel α as the non-interacting system. This in turn is the

case because then the non-interacting and the interacting system obey the same continuity equation: $\partial_\tau \rho = [H_0 - \mu N, \rho]_\tau$.

However, if $[\rho^\alpha, H_{\text{int}}] \neq 0$, this is not the case anymore, the Ward identities of interacting and noninteracting system are different (compare Figs. 3.10 and 3.11). The same is the case for the continuity equations, which are $\partial_\tau \rho = [H_0 - \mu N, \rho]_\tau + [H_{\text{int}}, \rho]_\tau$ in the interacting system, instead of $\partial_\tau \rho = [H_0 - \mu N, \rho]_\tau$ in the non-interacting one. This makes it seem that the satisfaction of the Ward identity must be inherently more difficult when $[\rho^\alpha, H_{\text{int}}] \neq 0$. Is it really guaranteed that Φ-derivable theories satisfy the Ward identity in Eq. (F.12)?

G.2 Does $\delta\Sigma = \Gamma\delta G$ still guarantee local conservation?

Q Let us consider an argument why the framework of Baym & Kadanoff is most likely not sufficient to satisfy such a Ward identity: The six-point correlation function $X^{\alpha\beta\gamma}$ in this relation contains essentially three-particle irreducible components. Therefore, it is not possible to bring this Ward identity into the form $\mathbf{d\Sigma} = \hat{\Gamma}\mathbf{dG}$, which features only the 1P and 2P irreducible self-energies Σ and Γ, this was noted earlier by W. Metzner [91]. However, it was seen above that the integral Ward identity $\mathbf{d\Sigma} = \hat{\Gamma}\mathbf{dG}$ is closely related to the functional Ward identity $\delta\Sigma = \Gamma\delta G$ [see discussion after Eq. (E.13)]. It seems that due to the chiral 3P correlation function in Eq. (F.12) this correspondence between the functional and integral Ward identities is not there anymore.

G.3 Diagrammatic structure of the six-point correlation function

In order to find out if a Φ-derivable approximation guarantees local conservation in a system with the Ward identity in Eq. (F.12), the diagrammatic structure of the chiral six-point correlation function $X^{\alpha\beta\gamma}$ needs to be examined. It will then be shown in Sec. H that the Φ-derivable Hartree-Fock approximation indeed violates such a Ward identity. The reader is advised to skip the following derivations on a first reading and jump to the conclusions in Sec. I.

Diagrammatic decompositions of n-particle correlation functions with $n > 2$ are rarely performed, Ref. [47] gives a clear account how this should be approached. Furthermore, the importance of three-particle vertices in the dual fermion approach was analyzed in Ref. [116]. In the following, the three-particle (3P) correlation function in Eq. (F.12) will be decomposed diagrammatically in a similar way as in Refs. [47, 116].

In order to make progress, the 3P connected contributions need to be peeled out of $X^{\alpha\beta\gamma}$ in Eq. (F.12). This is comparable to the calculation of the T-matrix from the four-point correlation function $G^{(2)}$ by subtracting the uncorrelated parts and dividing by the 4 legs (i.e. Green's functions),

$$F_{kk'q}^{\sigma\sigma'} = \frac{G_{kk'q}^{(2),\sigma\sigma'} + \beta G_{k\sigma}G_{k'\sigma'}\delta_q - G_{k\sigma}G_{k+q\sigma}\delta_{kk'}\delta_{\sigma\sigma'}N\beta}{G_{k\sigma}G_{k+q,\sigma}G_{k'\sigma'}G_{k'+q,\sigma'}}. \tag{G.1}$$
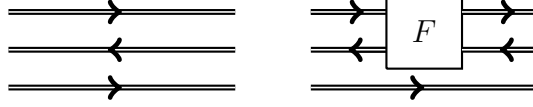
FIGURE 3.14: Typical three-particle reducible building blocks of the six-point correlation function $X^{\alpha\beta\gamma}$.

Similarly, first the 'uncorrelated parts' of $X^{\alpha\beta\gamma}$ have to be separated. However, uncorrelated with respect to the 3P level need not mean that these parts are uncorrelated at the 2P level. Therefore, some uncorrelated parts of $X^{\alpha\beta\gamma}$ are merely a product of three 1P reducible Green's functions, others are a product of one Green's function and the 2P reducible vertex F and its legs. Two typical contributions to the uncorrelated part of $X^{\alpha\beta\gamma}$ are shown in Fig. 3.14.

Let us denote $X^{\alpha\beta\gamma}$ from Eq. (F.8) in the following short notation,

$$X^{\alpha\beta\gamma}_{11'22'33'} = -\imath \varepsilon_{\alpha\beta\gamma} \sum_{\sigma_i} s^{\alpha}_{1'1} s^{\beta}_{2'2} s^{\gamma}_{3'3} \left\langle c_1 c^{\dagger}_{1'} c_2 c^{\dagger}_{2'} c_3 c^{\dagger}_{3'} \right\rangle, \tag{G.2}$$

where

$$
\begin{aligned}
1 &= (k, \sigma_1), & 1' &= (k+q, \sigma'_1), \\
2 &= (k'+p, \sigma_2), & 2' &= (k', \sigma'_2), \\
3 &= (k''+q-p, \sigma_3), & 3' &= (k'', \sigma'_3).
\end{aligned}
\tag{G.3}
$$

Fortunately, what is needed is not a completely general six-point correlation function with any spin labels, but only $X^{\alpha\beta\gamma}$ in Eq. (G.2), which has the factor $\varepsilon_{\alpha\beta\gamma} s^{\alpha} s^{\beta} s^{\gamma}$ attached. This may be considered as a 'chiral' channel, since the symmetries of these prefactors are responsible for $X^{\alpha\beta\gamma}_{kk'k''qp}$ becoming the spin chirality when closing ends of equal spin flavor (i.e., summing over k, k', k'', cf. Fig. 3.11).

The symmetries of $X^{\alpha\beta\gamma}_{kk'k''qp}$ imply the following simplifications: (i) The Levi-Civita symbol in Eq. (G.2) yields zero whenever two flavors α, β, γ are equal, or if one of them is the charge flavor c. Therefore, the labels α, β, γ will always be a permutation of the set x, y, z. (ii) Since s^x and s^y are zero on the diagonal, they lead to zero whenever their indices are equal, i.e., $s^x_{aa'} = s^y_{aa'} = 0$ when $\sigma_a = \sigma_{a'}$. (iii) Assuming paramagnetism and using that Green's function is diagonal in the spin indices, an expression of the form $G_{aa'} s^z_{aa'} = G_a \delta_{aa'} s^z_{aa}$ will lead to zero under the summation over all spin indices σ_i in Eq. (G.2).

First, let us find the 3P reducible parts of $X^{\alpha\beta\gamma}$ that are merely a product of three Green's functions. For this one may pretend that Wick's theorem is valid and decompose the chiral 3P correlation function in Eq. (G.2) into all possible triples of Green's functions.
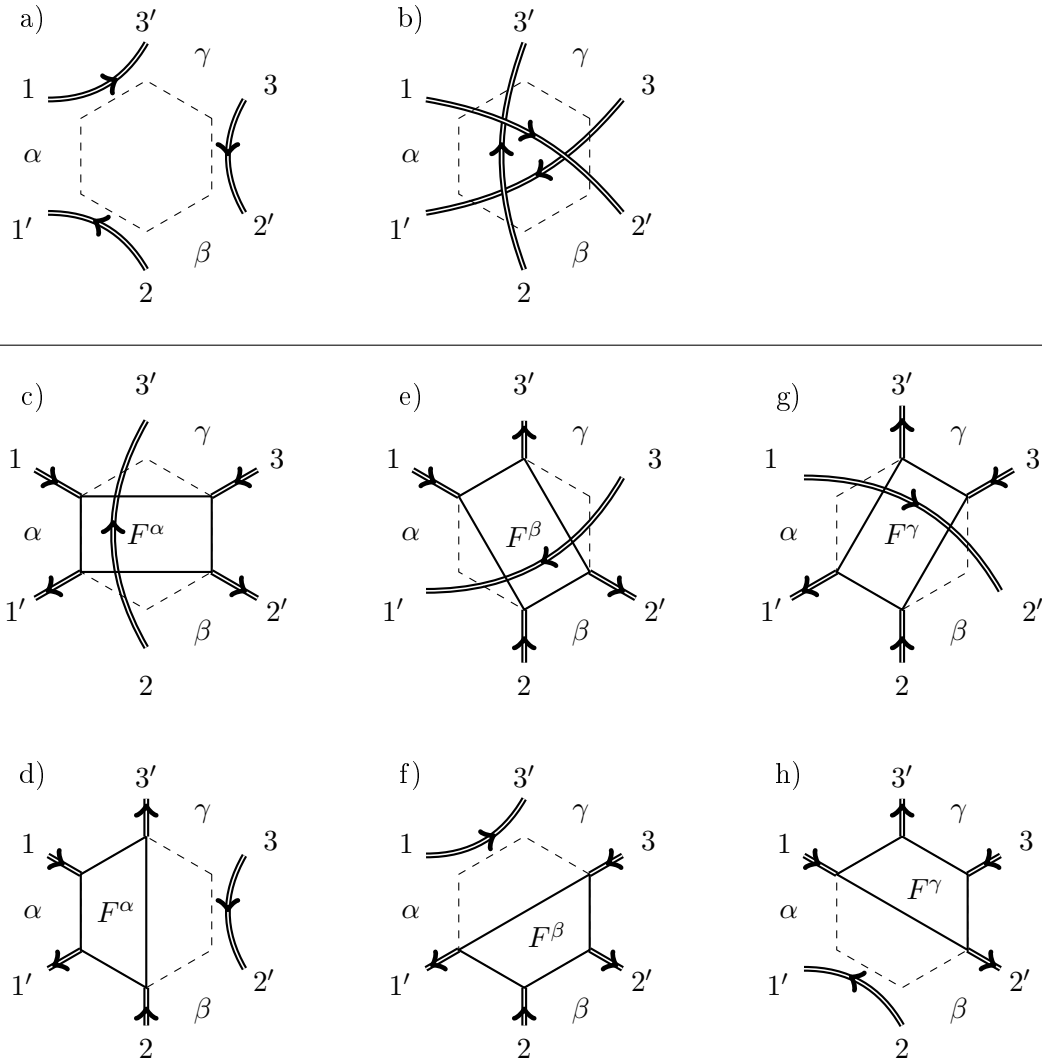
FIGURE 3.15: Lowest order 3P reducible diagrams of the chiral 3P correlation function $X^{\alpha\beta\gamma}_{11'22'33'}$. Top: The only two surviving fully uncorrelated contributions, which are 3-fold 1P reducible. Other combinations vanish due to symmetries of the Levi-Civita symbol $\varepsilon_{\alpha\beta\gamma}$, of the Pauli matrices $s^{x,y,z}$, and due to paramagnetism. Bottom: The six surviving contributions to $X^{\alpha\beta\gamma}$ that consist of a 2P reducible (F) and a 1P reducible part (G). Note that the shapes drawn with bold black lines are a guide to the eye to help spotting the 2P reducible contributions of F, while entry and exit points are not in the appropriate order.

Of such diagrams, only the two on the top of Fig. 3.15 survive, due to the symmetries of $X^{\alpha\beta\gamma}$. In particular, no single Green's function can connect entry and exit points with the same flavor α, β, γ, since then the summation over all spin labels in Eq. (G.2) leads to zero due to the Pauli matrices. Thus, only two such "GGG" combinations remain, diagrams a) and b) in Fig. 3.15.

The second type of lowest order 3P reducible diagrams in $X^{\alpha\beta\gamma}$ are those that have one Green's function line and one 2P reducible contribution of the vertex F. The latter can not be separated by cutting one line but by cutting two lines. Again, the single Green's function line must not connect end points of the same flavor, whereas F may connect any flavors, see diagrams c) to h). In fact, since there are three entry and three exit points, F has to connect an entry and an exit of the same flavor. This flavor 'wins' over the other two, as will be shown below, and the 2P reducible contribution attains the flavor of the majority labels [thus the respective flavor labels in diagrams c) to h)]. Six of these diagrams survive. The diagrams in Fig. 3.15 are all diagrams that do not have 3P irreducible parts. In the following, the diagrams in Fig. 3.15 will be evaluated in detail and expressed through the susceptibilities and T-matrices X^{α} and F^{α}.

G.4   Diagrams a) and b)

From the two diagrams a) and b) on the left of Fig. (3.15) one deduces the 3-fold 1P reducible parts of $X^{\alpha\beta\gamma}$ as follows [permutation of the labels yields a minus sign, cf. Eq. (G.2)],

$$\imath\varepsilon_{\alpha\beta\gamma}\sum_{\sigma_i}s^{\alpha}_{1'1}s^{\beta}_{2'2}s^{\gamma}_{3'3}[G_{21'}G_{32'}G_{13'}+G_{12'}G_{23'}G_{31'}]$$

$$=\imath\varepsilon_{\alpha\beta\gamma}\sum_{\sigma_i}G_1G_2G_3[s^{\alpha}_{21}s^{\beta}_{32}s^{\gamma}_{13}\delta_{21'}\delta_{32'}\delta_{13'}+s^{\alpha}_{31}s^{\beta}_{12}s^{\gamma}_{23}\delta_{12'}\delta_{23'}\delta_{31'}]$$

$$=\imath\varepsilon_{\alpha\beta\gamma}G_1G_2G_3[\mathrm{Tr}(\hat{s}^{\alpha}\hat{s}^{\gamma}\hat{s}^{\beta})\delta_{21'}\delta_{32'}\delta_{13'}+\mathrm{Tr}(\hat{s}^{\alpha}\hat{s}^{\beta}\hat{s}^{\gamma})\delta_{12'}\delta_{23'}\delta_{31'}]. \tag{G.4}$$

From the first to the second line it was used that $G_{ab'} = G_a\delta_{ab'}$[17] and the Kronecker symbols were used to perform the summations $\sum_{\sigma'_1\sigma'_2\sigma'_3}$. Going from the second to the third line paramagnetism was assumed, such that G_{σ} does not depend on σ, allowing to perform the remaining spin summations $\sum_{\sigma_1\sigma_2\sigma_3}$ independently of the Green's functions. For the Pauli matrices one has the identity $\hat{s}^{\alpha}\hat{s}^{\beta} = \delta_{\alpha\beta}\hat{1} + \imath\sum_{\epsilon}\varepsilon_{\alpha\beta\epsilon}\hat{s}^{\epsilon}$. Since α, β, γ have to be different in pairs due to the Levi-Civita symbol in the front, the traces simplify to $\mathrm{Tr}(\hat{s}^{\alpha}\hat{s}^{\gamma}\hat{s}^{\beta}) = \imath\sum_{\epsilon}\varepsilon_{\gamma\beta\epsilon}\mathrm{Tr}(\hat{s}^{\alpha}\hat{s}^{\epsilon}) = 2\imath\varepsilon_{\gamma\beta\alpha}$ and likewise $\mathrm{Tr}(\hat{s}^{\alpha}\hat{s}^{\beta}\hat{s}^{\gamma}) = 2\imath\varepsilon_{\beta\gamma\alpha}$. In both cases it was used that necessarily $\alpha = \epsilon$ and $\mathrm{Tr}(\hat{s}^{\alpha}\hat{s}^{\alpha}) = 2$. The fully uncorrelated part of the chiral 3P Green's function therefore simplifies to,

$$-2\varepsilon_{\alpha\beta\gamma}G_1G_2G_3[\varepsilon_{\gamma\beta\alpha}\delta_{21'}\delta_{32'}\delta_{13'}+\varepsilon_{\beta\gamma\alpha}\delta_{12'}\delta_{23'}\delta_{31'}]$$

$$=-2\varepsilon^2_{\alpha\beta\gamma}G_1G_2G_3[-\delta_{21'}\delta_{32'}\delta_{13'}+\delta_{12'}\delta_{23'}\delta_{31'}]$$

---

[17]In order not to clutter the formulae any further, the short notation on the Kronecker symbol δ_{ab} will later imply a factor $N\beta$ where needed.

From the first to the second line the (anti-)cyclic property of the Levi-Civita symbol was used, $\varepsilon_{\gamma\beta\alpha} = -\varepsilon_{\alpha\beta\gamma}$, and likewise, $\varepsilon_{\beta\gamma\alpha} = \varepsilon_{\alpha\beta\gamma}$.

G.5   Diagram c)

Now to the 1-fold 1P and 1-fold 2P reducible diagrams on the right of Fig. 3.15. Let us consider the four-point correlation function and its relation to the T-matrix F, in abbreviated notation,

$$- \left\langle c_1 c_{1'}^\dagger c_2 c_{2'}^\dagger \right\rangle = -G_1 G_2 \delta_{11'}\delta_{22'} + G_1 G_2 \delta_{12'}\delta_{21'} + G_1 G_{1'} F_{11'22'} G_{2'} G_2. \tag{G.5}$$

The indices of F on the RHS correspond to the order of the construction operators on the LHS. Looking at diagram c) in Fig. 3.15, it corresponds to a 1P reducible contribution of $G_2\delta_{23'}$ and a 2P reducible contribution stemming from the four-point correlation function $\left\langle c_1 c_{1'}^\dagger c_3 c_{2'}^\dagger \right\rangle$. The 2P reducible part of that correlation function is some $G_1 G_{1'} F_{11'32'} G_{2'} G_3$. Therefore, the contribution of diagram c) to the uncorrelated part of $X^{\alpha\beta\gamma}$ is [a minus sign arises due to permutation of the labels, cf. Eq. (G.2)],

$$\imath\varepsilon_{\alpha\beta\gamma} \sum_{\sigma_i} s_{1'1}^\alpha s_{2'2}^\beta s_{3'3}^\gamma G_1 G_{1'} F_{11'32'} G_{2'} G_3 G_2 \delta_{23'}$$

$$=\imath\varepsilon_{\alpha\beta\gamma} \sum_{\sigma_i} s_{1'1}^\alpha \imath\varepsilon_{\beta\gamma\alpha} s_{2'3}^\alpha G_1 G_{1'} F_{11'32'} G_{2'} G_3 G_2 \delta_{23'}. \tag{G.6}$$

From the first to the second line the summation over σ_3' was performed, then $\sum_{\sigma_2} s_{2'2}^\beta s_{23}^\gamma = \delta_{2'3}\delta_{\beta\gamma} + \imath \sum_\epsilon \varepsilon_{\beta\gamma\epsilon} s_{2'3}^\epsilon = \imath\varepsilon_{\beta\gamma\alpha} s_{2'3}^\alpha$ was inserted, (this holds since α, β, γ are always different in pairs, such that $\epsilon = \alpha$). Now one recognizes that Green's function G does not depend on the spin labels and that

$$\frac{1}{2} \sum_{\sigma_i} s_{1'1}^\alpha F_{11'32'} s_{2'3}^\alpha = F_{11'32'}^\alpha. \tag{G.7}$$

This explains the label α on F in diagram c) of Fig. 3.15. Hence, one is left with the following contribution of diagram c) to the chiral 3P correlation function,

$$- 2\varepsilon_{\alpha\beta\gamma}^2 G_1 G_{1'} F_{11'32'}^\alpha G_{2'} G_3 G_2 \delta_{23'}$$

G.6 Diagrams d) to h)

In the following, the respective results for all diagrams in Fig. 3.15 will be listed:

$$
\begin{aligned}
\text{Diagram a):} \quad & 2\varepsilon_{\alpha\beta\gamma}^2 G_1 G_2 G_3 \delta_{21'} \delta_{32'} \delta_{13'} \\[4pt]
\text{Diagram b):} \quad & -2\varepsilon_{\alpha\beta\gamma}^2 G_1 G_2 G_3 \delta_{12'} \delta_{23'} \delta_{31'} \\[4pt]
\text{Diagram c):} \quad & -2\varepsilon_{\alpha\beta\gamma}^2 G_1 G_{1'} F_{11'32'}^{\alpha} G_{2'} G_3 G_2 \delta_{23'} \\[4pt]
\text{Diagram d):} \quad & 2\varepsilon_{\alpha\beta\gamma}^2 G_1 G_{1'} F_{11'23'}^{\alpha} G_{3'} G_2 G_3 \delta_{32'} \\[4pt]
\text{Diagram e):} \quad & -2\varepsilon_{\alpha\beta\gamma}^2 G_1 G_{3'} F_{13'22'}^{\beta} G_{2'} G_2 G_3 \delta_{31'} \\[4pt]
\text{Diagram f):} \quad & 2\varepsilon_{\alpha\beta\gamma}^2 G_3 G_{1'} F_{31'22'}^{\beta} G_{2'} G_2 G_1 \delta_{13'} \\[4pt]
\text{Diagram g):} \quad & -2\varepsilon_{\alpha\beta\gamma}^2 G_2 G_{1'} F_{21'33'}^{\gamma} G_{3'} G_3 G_1 \delta_{12'} \\[4pt]
\text{Diagram h):} \quad & 2\varepsilon_{\alpha\beta\gamma}^2 G_1 G_{2'} F_{12'33'}^{\gamma} G_{3'} G_3 G_2 \delta_{21'}
\end{aligned}
\tag{G.8}
$$

The contributions of diagrams a)-d) may be in terms of the generalized susceptibility $X_{11'22'}^{\alpha} = G_1 G_{1'} (\delta_{12'} \delta_{21'} + F_{11'22'}^{\alpha} G_{2'} G_2)$. Adding together diagrams a) and d), as well as b) and c) one gets,

$$
\begin{aligned}
\text{Diagram a)+d):} \quad & 2\varepsilon_{\alpha\beta\gamma}^2 X_{11'23'}^{\alpha} G_3 \delta_{32'}, \\[4pt]
\text{Diagram b)+c):} \quad & -2\varepsilon_{\alpha\beta\gamma}^2 X_{11'32'}^{\alpha} G_2 \delta_{23'}.
\end{aligned}
\tag{G.9}
$$

G.7 The three-particle bubble

Now all the contributions of the diagrams in Fig. 3.15 will be collected to form the 'three-particle bubble'. This consists of all diagrams that are 3P reducible and have no 3P irreducible parts. First, collecting Eqs. (G.9) and (G.8), the 3P reducible vertex $P^{\alpha\beta\gamma}$ is isolated,

$$
P_{11'22'33'}^{\alpha\beta\gamma} = \frac{X_{11'22'33'}^{\alpha\beta\gamma} - X_{11'22'33'}^{0,\alpha\beta\gamma}}{G_1 G_{1'} G_2 G_{2'} G_3 G_{3'}}.
\tag{G.10}
$$

This object is 3P reducible but it *does* have 3P irreducible contributions. $P^{\alpha\beta\gamma}$ is defined in full analogy to the 2P reducible vertex in Eq. (G.1). On the RHS there is the full chiral 3P correlation function $X^{\alpha\beta\gamma}$, from it all diagrams in Fig. 3.15 are subtracted. These are
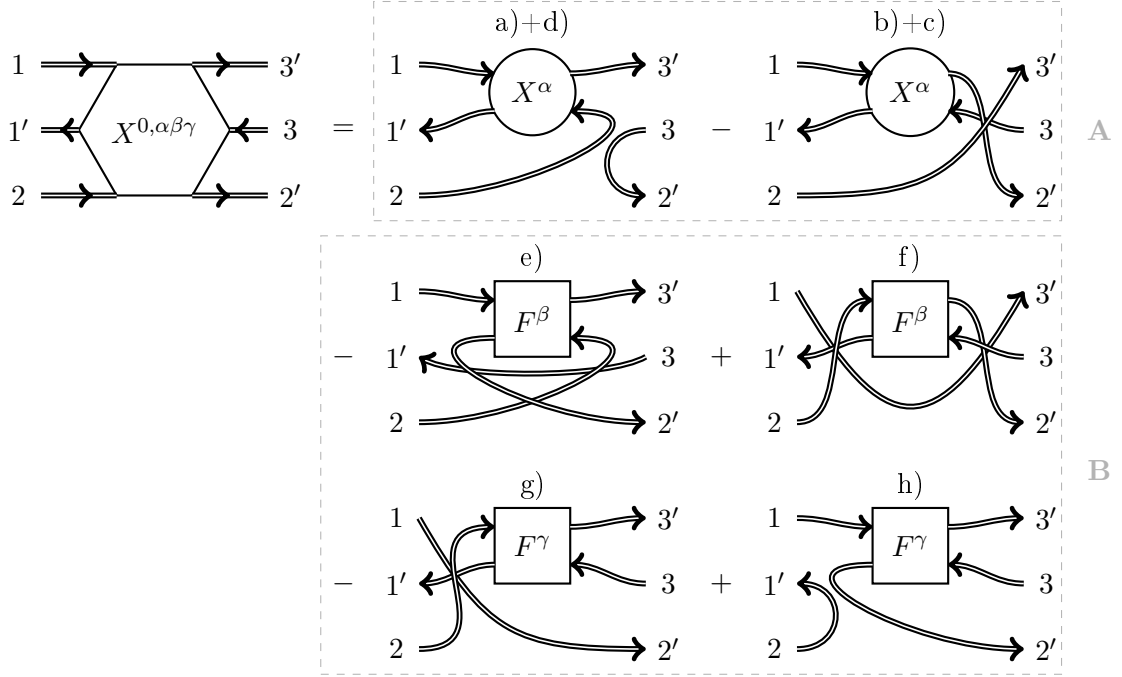
FIGURE 3.16:   The 'three-particle bubble' $X^{0,\alpha\beta\gamma}$, expressed through the (2P) generalized susceptibility X^α and the 2P reducible T-matrices F^β and F^γ. On the RHS are all diagrams of $X^{\alpha\beta\gamma}$ that are 3P reducible and do not contain 3P irreducible parts. The small letters correspond to the diagrams in Fig. (3.15) where the respective contribution stems from, compare also Eq. (G.11). Note that in this figure the entry and exit points are consistent with the definition of X^α, F^β, and F^γ, cf. Sec. B of chapter 2.

all comprised into the three-particle bubble $X^{0,\alpha\beta\gamma}$,

$$
\begin{aligned}
X^{0,\alpha\beta\gamma}_{11'22'33'} &= 2\varepsilon^2_{\alpha\beta\gamma}\left[X^\alpha_{11'23'}G_3\delta_{32'} - X^\alpha_{11'32'}G_2\delta_{23'}\right] \\
&+ 2\varepsilon^2_{\alpha\beta\gamma}G_1 G_{1'}\left\{(G_3 F^\beta_{31'22'}\delta_{13'} - G_{3'}F^\beta_{13'22'}\delta_{31'})G_{2'}G_2\right. \\
&+ \left.(G_{2'}F^\gamma_{12'33'}\delta_{21'} - G_2 F^\gamma_{21'33'}\delta_{12'})G_{3'}G_3\right\}.
\end{aligned}
\tag{G.11}
$$

This is the sum of all contributions in Eq. (G.8). The symbol $\varepsilon^2_{\alpha\beta\gamma}$ is unity when α, β, γ are a permutation of the set $\{x, y, z\}$ and zero otherwise. A diagrammatic depiction of $X^{0,\alpha\beta\gamma}$ is shown in Fig. 3.16.

H Violation of local spin conservation by the Hartree-Fock approximation

In the following, it will be shown that the Hartree-Fock approximation to the extended Hubbard model with exchange interactions is incapable to satisfy the Ward identity in Eq. (F.12) in the spin channels. This Φ-derivable approximation was also considered by Baym & Kadanoff [16] for the Coulomb interaction in the continuum. In the extended Hubbard model one has $H_{\text{int}} = \frac{1}{2} \sum_{q\alpha} \rho^\alpha_{-q} V^\alpha_q \rho^\alpha_q$, where $\alpha = c, x, y, z$ runs over all channels, including the spin channels x, y, z. For simplicity, paramagnetism will be assumed.

In order to show that the Hartree-Fock approximation violates the Ward identity, three ingredients are needed: (i) The Hartree-Fock 1P self-energy, which was derived earlier in chapter 2, Eq. (C.23),

$$\Sigma^{\text{HF}}_k = \quad V^c_{p=0} \langle n \rangle - \sum_{p\beta} V^\beta_p G_{k+p}. \tag{H.1}$$

(ii) The 2P self-energy of the channel $\alpha = z$, this was determined in Eq. (B.8) as a functional derivative of Σ^{HF},

$$\Gamma^z_{k\underline{k}} = \quad 2V^z_{q=0} - V^c_{\underline{k}-k} - V^z_{\underline{k}-k} + V^x_{\underline{k}-k} + V^y_{\underline{k}-k}. \tag{H.2}$$

(iii) Also the 3P correlation function $X^{\alpha\beta\gamma}$ needs to be approximated, since it contributes to the Ward identity,

$$\Sigma_{k+q} - \Sigma_k = \quad \sum_{\underline{k}} \Gamma^\alpha_{k\underline{k}q}[G_{\underline{k}+q} - G_{\underline{k}}] - \sum_{\underline{k}k'k''p\beta\gamma} V^\beta_p (\hat{X}^{\alpha,-1})_{k\underline{k}q} X^{\alpha\beta\gamma}_{\underline{k}k'k''qp}. \tag{H.3}$$

A 3P self-energy or correlation function is not defined in the Baym & Kadanoff theory. However, the Hartree-Fock approximation violates the Ward identity when setting $X^{\alpha\beta\gamma} = 0$, which can be seen by inserting this approximation into Eq. (H.3),

$$\Sigma^{\text{HF}}_{k+q} - \Sigma^{\text{HF}}_k = \sum_{\underline{k}} \Gamma^z_{k\underline{k}q}[G_{\underline{k}+q} - G_{\underline{k}}] \tag{H.4}$$

$$\Leftrightarrow -\sum_{p\beta} V^\beta_p[G_{k+p+q} - G_{k+p}] = \sum_{\underline{k}}(2V^z_{q=0} - V^c_{\underline{k}-k} - V^z_{\underline{k}-k} + V^x_{\underline{k}-k} + V^y_{\underline{k}-k})[G_{\underline{k}+q} - G_{\underline{k}}].$$

All Hartree contributions cancel out. Setting $p \to \underline{k} - k$ on the LHS one has,

$$-\sum_{\underline{k}\beta} V^\beta_{\underline{k}-k}[G_{\underline{k}+q} - G_{\underline{k}}] = \sum_{\underline{k}}(2V^z_{q=0} - V^c_{\underline{k}-k} - V^z_{\underline{k}-k} + V^x_{\underline{k}-k} + V^y_{\underline{k}-k})[G_{\underline{k}+q} - G_{\underline{k}}]$$

$$\Leftrightarrow -\sum_{\underline{k}}(V^x_{\underline{k}-k} + V^y_{\underline{k}-k})[G_{\underline{k}+q} - G_{\underline{k}}] = +\sum_{\underline{k}}(V^x_{\underline{k}-k} + V^y_{\underline{k}-k})[G_{\underline{k}+q} - G_{\underline{k}}]. \tag{H.5}$$

From the first to the second line, the contributions of V^c and V^z were canceled out. What remains is certainly a false statement, since the respective contibutions of V^x and V^y do

not cancel.   Apparently, one is forced to make an approximation at the 3P level.   The next best reasonable guess is therefore to consider only the lowest order (i.e., 3P reducible) diagrams of the 3P correlation function[18].   These are all comprised in the three-particle bubble $X^{0,\alpha\beta\gamma}$ in Fig. 3.16,

$$X^{\alpha\beta\gamma}_{\underline{k}k'k''qp} \equiv X^{0,\alpha\beta\gamma}_{\underline{k}k'k''qp}. \tag{H.6}$$

This approximation corresponds to neglecting vertex corrections on the 3P level in Eq. (G.10). Inserting this together with the Hartree-Fock approximation into the Ward identity Eq. (H.3) one has,

$$\Sigma^{\mathrm{HF}}_{k+q} - \Sigma^{\mathrm{HF}}_{k} = \quad \sum_{\underline{k}} \Gamma^{z}_{k\underline{k}q}[G_{\underline{k}+q} - G_{\underline{k}}] - \sum_{\underline{k}k'k''p\beta\gamma} V^{\beta}_{p}(\hat{X}^{z,-1})_{kkq}X^{0,z\beta\gamma}_{\underline{k}k'k''qp}. \tag{H.7}$$

Next, the three-particle bubble from Eq. (G.11) will be inserted, going back to the momentum notation, $1 = \underline{k}, 1' = \underline{k} + q, 2 = k' + p, 2' = k', 3 = k'' + q - p, 3' = k''$, and setting $\alpha = z$. After some simplifications, which are detailed in Appendix B, and assuming $SU(2)$-symmetry, $F^{x} = F^{y} = F^{z} \equiv F^{s}$, the Ward identity then takes the form,

$$\begin{aligned}
\Sigma^{\mathrm{HF}}_{k+q} - \Sigma^{\mathrm{HF}}_{k} = &\sum_{\underline{k}} \Gamma^{z}_{k\underline{k}q}[G_{\underline{k}+q} - G_{\underline{k}}] \\
&- 2 \sum_{\underline{k}k'p\beta\gamma} \varepsilon^{2}_{z\beta\gamma} V^{\beta}_{p}(\hat{X}^{z,-1})_{k\underline{k}q} X^{z}_{\underline{k},k',q}(G_{k'+q+p} - G_{k'+p}) \\
&- \sum_{\underline{k}} (\hat{X}^{z,-1})_{k\underline{k}q} G_{\underline{k}+q} G_{\underline{k}} T^{z}_{\underline{k}q},
\end{aligned} \tag{H.8}$$

where T^{z} abbreviates the following expression,

$$T^{\alpha}_{\underline{k}q} = 2 \sum_{k'p\beta\gamma} \varepsilon^{2}_{\alpha\beta\gamma} G_{\underline{k}+p} G_{k'}(V^{\beta}_{q-p} - V^{\beta}_{p}) \left\{ G_{k'+q-p} F^{s}_{\underline{k}+p,k',q-p} + G_{k'+p} F^{s}_{\underline{k},k',p} \right\}. \tag{H.9}$$

The second line of Eq. (H.8) orginates from the diagrams in box A of Fig. 3.16. The term in the third line involving T^{z} corresponds to box B in that figure. Let us look at the second line of Eq. (H.8). Firstly, one can see that the susceptibility X^{z} is divided out exactly from this term, since $\sum_{\underline{k}}(\hat{X}^{z,-1})_{kkq}X^{z}_{\underline{k},k',q} = \delta_{k,k'}$. Secondly, the Levi-Civita symbol filters out only the contributions of the interactions V^{β} where $\beta \neq z$. This simplifies the second line

---

[18]Obviously, it is not entirely clear which approximation to the 3P correlation function corresponds to the Hartree-Fock level. However, the three-particle bubble seems to be the only straightforward choice, since this corresponds to setting the "3P self-energy" to zero, i.e., 3P irreducible contributions are neglected. Since in the Hartree-Fock approximation the 2P self-energy does not depend on Green's function [cf. Eq. (H.2)], a functional derivative with respect to the latter indeed leads to zero.

of Eq. (H.8) to,

$$
\begin{aligned}
-2 \sum_{\underline{k}k'p\beta\gamma} &\varepsilon_{z\beta\gamma}^2 V_p^\beta (\hat{X}^{z,-1})_{k\underline{k}q} X_{\underline{k},k',q}^z (G_{k'+q+p} - G_{k'+p}) \\
&= -2 \sum_p (V_p^x + V_p^y)[G_{k+q+p} - G_{k+q}] \\
&= -2 \sum_{\underline{k}} (V_{\underline{k}-k}^x + V_{\underline{k}-k}^y)[G_{\underline{k}+q} - G_{\underline{k}}].
\end{aligned}
\tag{H.10}
$$

Inserting this into Eq. (H.8), together with the explicit expressions for Σ^{HF} and Γ^z from Eqs. (H.1) and (H.2),

$$
\begin{aligned}
-\sum_{\underline{k}\beta} V_{\underline{k}-k}^\beta [G_{\underline{k}+q} - G_{\underline{k}}] = &\sum_{\underline{k}} (-V_{\underline{k}-k}^c - V_{\underline{k}-k}^z + V_{\underline{k}-k}^x + V_{\underline{k}-k}^y)[G_{\underline{k}+q} - G_{\underline{k}}] \\
&-2 \sum_{\underline{k}} (V_{\underline{k}-k}^x + V_{\underline{k}-k}^y)[G_{\underline{k}+q} - G_{\underline{k}}] \\
&-\sum_{\underline{k}} (\hat{X}^{z,-1})_{k\underline{k}q} G_{\underline{k}+q} G_{\underline{k}} T_{\underline{k}q}^z.
\end{aligned}
\tag{H.11}
$$

All terms in the first and in the second line cancel, merely leaving behind,

$$
0 = \sum_{\underline{k}} (\hat{X}^{z,-1})_{k\underline{k}q} G_{\underline{k}+q} G_{\underline{k}} T_{\underline{k}q}^z.
\tag{H.12}
$$

Again, no complete cancelation occurs, since the approximation is unable to account for the contribution on the RHS of Eq. (H.12), which originates from the diagrams in box B of Fig. 3.16. These diagrams represent the current of the spin density ρ^z that is caused by the interactions V^x and V^y. Therefore, regardless of whether one neglegts $X^{\alpha\beta\gamma}$ or accounts for its lowest order diagrams, contributions by the interactions $V^{x,y}$ lead to a violation of the Ward identity in the considered spin channel $\alpha = z$. Apparently, the simplest Φ-derivable approximation violates the continuity equation of the spin density ρ^z, due to the exchange interactions V^x and V^y. On the other hand, one shows in the same way as in Sec. E.2 that the Ward identity holds in the charge channel $\alpha = c$.

I   Conclusions

QP The calculation in Sec. H reveals a violation of the Ward identity by the most simple Φ-derivable approximation. I attempt an intuitive explanation for this rather technical result:

The canonical reference for conserving approximations is Ref. [15], which proved that Φ-derivable approximations to a many-electron system subjected to the Coulomb potential satisfy the continuity equation. However, this proof is formulated in the continuum, where the Coulomb potential commutes with the charge and the spin densities, $\varrho^\alpha(\mathbf{r}) = \sum_{\sigma\sigma'} \Psi_\sigma^\dagger(\mathbf{r}) s_{\sigma\sigma'}^\alpha \Psi_{\sigma'}(\mathbf{r})$, which is a rather special case. On the lattice the Coulomb interaction generates many terms that do not commute with one or more than one of the densities $\rho_i^\alpha = \sum_{\sigma\sigma'} c_{i\sigma}^\dagger s_{\sigma\sigma'}^\alpha c_{i\sigma'}$ (see also chapter 2, Sec. A). To say that the continuity equation of $\varrho^\alpha(\mathbf{r})$ is satisfied in the continuum is, very simply, a different statement than that the continuity equation of ρ_i^α holds on the lattice. In fact, the local densities ρ_i^α of the lattice are *nonlocal* operators in the continuum [see Eq. (A.12) in chapter 2], such that on the lattice the notion of 'local conservation' refers to an entirely different observable than in the continuum. It would be surprising if the statements made in Ref. [15] were valid in a more general context than was considered. Indeed, the Hartree-Fock approximation to an extended Hubbard model with exchange interactions violates the Ward identity, the spin-dependent interaction of this model is not covered by Ref. [15]. On the other hand, in an extended Hubbard model with nonlocal charge-charge potential the Ward identity holds [see discussion near Eq. (E.10)]. This seems logical, since this interaction commutes with the lattice densities ρ_i^α, analogous to the Coulomb potential which commutes with the densities $\varrho^\alpha(\mathbf{r})$ of the continuum.

In quantum lattice models the picture of conservation laws is more fragmented than is sometimes suggested. It was already mentioned in Ref. [15] that Φ-derivable approximations to the electron-phonon problem need not conserve the electronic momentum. This exception may serve as an incentive to examine the role that the interaction plays for conservation laws. It turns out that the functional Ward identity,

$$\delta\Sigma = \Gamma^\alpha \delta G,$$

only guarantees local conservation when the interaction H_{int} conserves the density ρ^α, that is

$$[\rho^\alpha, H_{\mathrm{int}}] = 0.$$

Then, the integral Ward identity $\mathbf{d\Sigma} = \hat{\Gamma}^\alpha \mathbf{dG}$ is valid and has a one-to-one correspondence to the functional Ward identity $\delta\Sigma = \Gamma\delta G$ of the Baym & Kadanoff theory. This makes it seem that Φ-derivable approximations may satisfy the Ward identity in one channel, where $[\rho^\alpha, H_{\mathrm{int}}] = 0$ is satisfied, but not in another one, where $[\rho^\beta, H_{\mathrm{int}}] \neq 0$.

This is indeed the situation that is encountered in the case of the Φ-derivable Hartree-Fock approximation to the extended Hubbard model with exchange interactions, as discussed in Secs. F and H: The charge density $n = \rho^c$ commutes with the interaction of this

model, the Hartree-Fock approximation indeed satisfies the integral Ward identity in the charge channel. The spin density $S^{x,y,z} = \rho^{x,y,z}/2$, on the other hand, does not commute with the exchange interaction, hence the Ward identity is violated in the spin channel. This violation happens in a characteristic way, due to the properties of the exchange interaction,

$$J_{ij}^x S_i^x S_j^x + J_{ij}^y S_i^y S_j^y + J_{ij}^z S_i^z S_j^z.$$

The exchange interaction in a given channel, w.l.o.g. the z-channel, commutes with the respective component of the spin density, $[S_k^z, J_{ij}^z S_i^z S_j^z] = 0$. However, the interactions in the x- and y-channels do not commute with S^z. Consequently, it turned out that the violation of the Ward identity in the z-channel is not related to the interaction J^z, but only to the perpendicular components J^x and J^y [cf. discussion after Eq. (H.12)] [19]. On the same note, the interaction J^z not only assigns a potential energy to the z-components of two spins at sites i and j. It also serves as a channel for the x- and y-components of the spins to propagate from site i to site j and vice versa. J^z creates a current of S^x and S^y that becomes manifest in their continuity equations. This situation is sketched in Fig. 3.17.

Likewise, the interactions J^x and J^y generate a current of S^z. This kinetic aspect of exchange interactions becomes manifest in the asymptote of the local spin susceptibility, Eq. (F.40) in the text,

$$\lim_{\omega \to \infty} (\imath\omega)^2 X_{\text{loc},\omega}^z = -2E_{\text{kin}} + \sum_{\mathbf{p}\omega}' (J_{\mathbf{p}}^x X_{\mathbf{p}\omega}^x + J_{\mathbf{p}}^y X_{\mathbf{p}\omega}^y). \tag{I.1}$$

Here, the kinetic energy E_{kin} stands side-by-side with the exchange interactions J^x and J^y. This reflects the fact that the z-component of the spin is transported by the hopping *and* by the interactions J^x and J^y. J^z, on the other hand, does not contribute to the asymptote of X^z. This interaction does not cause a current of S^z, since it commutes with this observable. Likewise, exchange interactions do not contribute to the asymptote of the charge susceptibility X^c, since the charge density commutes with all components of the exchange interaction, $[n_k, J_{ij}\mathbf{S}_i\mathbf{S}_j] = 0$. It seems plausible that an interaction that does not commute with the charge density, such as a pair-*hopping* $c_{i\uparrow}^\dagger c_{i\downarrow}^\dagger V_{ij}^p c_{j\uparrow} c_{j\downarrow}$, contributes with a similar term to the asymptote of the charge susceptibility.

The asymptotic formula in Eq. (I.1) follows directly from the Ward identity (cf. Sec. D), which takes account of all currents. In the Ward identity the propagation of densities through the interaction manifests as an anomaly. In the case of the extended Hubbard model with exchange couplings this identity reads in a lazy notation,

$$\mathbf{d\Sigma}_q = \hat{\Gamma}_q^\alpha \mathbf{dG}_q - \tfrac{1}{4}\sum_{p\beta\gamma} J_p^\beta (\hat{X}^{\alpha,-1})_q \mathbf{X}_{qp}^{\alpha\beta\gamma}. \tag{I.2}$$

The anomaly is the second term on the RHS, which involves a 'chiral' three-particle correlation function $\mathbf{X}^{\alpha\beta\gamma}$. Such a Ward identity is also called an anomalous Ward identity [22].

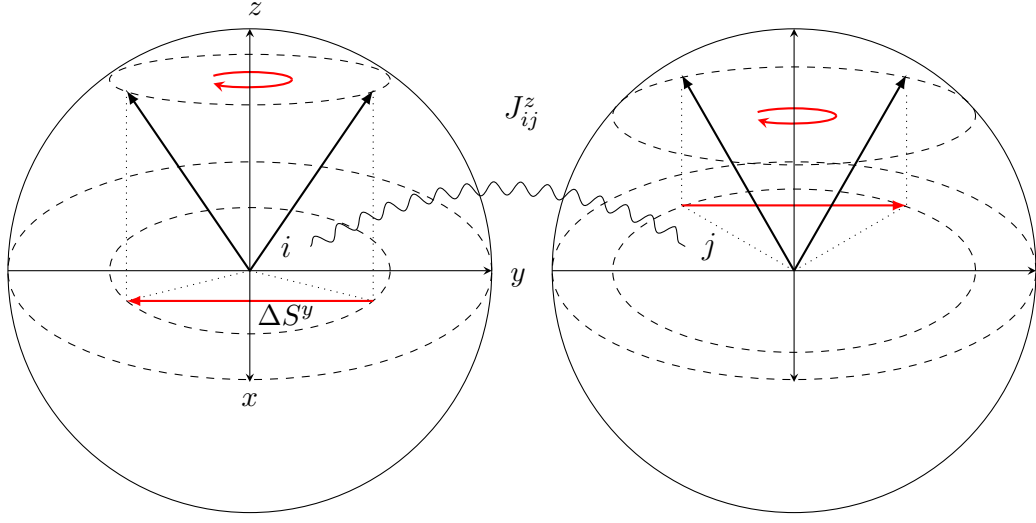[19] The exchange interactions were called V^x and V^y in Sec. H, $J = 4V$.

FIGURE 3.17: A sketch of spins at lattice sites i and j that rotate around the z-axis under the action of the exchange interaction J_{ij}^z (wiggly line). This interaction weighs the configuration $S_i^z S_j^z$ with a potential energy J^z, but also leads to currents of the spin components $S^{x,y}$, since they do not commute with J^z (for simplicity, only S^y changes here). Local spin conservation of S^y is satisfied if the change ΔS^y on lattice site i is exactly compensated by a change $-\Delta S^y$ at lattice site j (straight red arrows). The contribution of the exchange interaction to the spin currents leads to the anomaly in the Ward identity Eq. (I.2). Φ-derivable approximations are not guaranteed to conserve anomalous currents. Since classical spins are depicted, this sketch should not be understood as an accurate representation of an exchange interaction or of a spin current.

The situation can therefore be summarized as follows: There is nothing to a Φ-derivable approximation that prevents it from violating an anomalous Ward identity. Therefore, Φ-derivable approximations in general violate the Ward identity in a channel α if $[\rho^\alpha, H_{\text{int}}] \neq 0$. This is because this commutator leads to the anomaly in the associated Ward identity.

On the lattice most matrix elements of the Coulomb interaction do not commute with the charge or spin densities. For this reason, the Baym & Kadanoff theory is fully applicable only to a very narrow range of lattice Hamiltonians, of which the Hubbard model and the extended Hubbard model with charge-charge couplings are exemplary. Remarkably, a number of important quantum lattice models are not covered, such as the Kondo-lattice model, multi-orbital models featuring the intra-atomic Hund's rule exchange[20], the t-J model, and any other kind of exchange model. It should be noted, however, that these severe limitations concern *local* conservation, the Ward identity, and the conserving properties of the 2P response, which were discussed in this section. On the other hand, none of statements

---

[20] In case of an intra-atomic exchange interaction the anomalous currents are local. It seems that in the dynamical mean-field theory these currents should not pose a problem for conservation laws when the local reference system is solved numerically exactly.
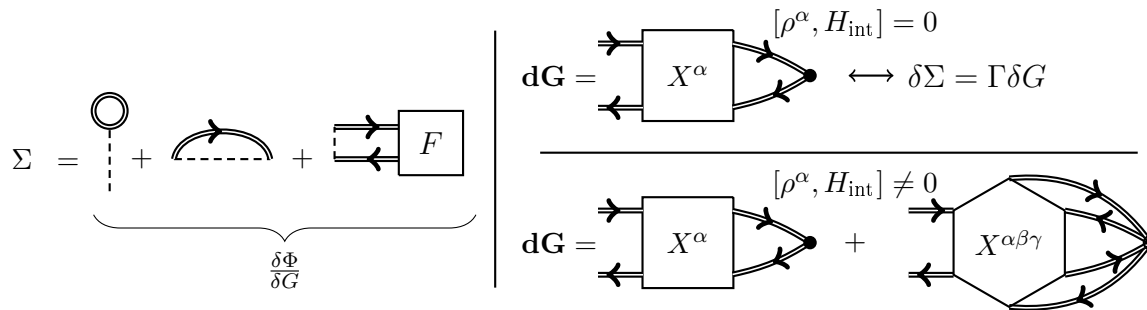
FIGURE 3.18: The integral Schwinger-Dyson equation [left, Eq. (C.12) in the text] is always given by the Hartree and Fock diagrams plus T-matrix corrections, whereas the integral Ward identity [right, cf. Eq. (F.9)] either relates correlation functions of the 1P and 2P levels, or of the 1P, 2P, and 3P levels due to anomalous currents. The anomaly is the second diagram in the bottom right. The functional Ward identity $\delta\Sigma = \Gamma\delta G$ in general only yields a conserving 2P self-energy when there is no anomaly. Regarding the correspondence of the integral and functional relations see also Eq. (E.14).

above is at odds with *global* conservation of a Φ-derivable 1P self-energy: It may well be that an approximation $\Sigma = \frac{\delta\Phi}{\delta G}$ to the 1P self-energy satisfies global conservation laws and is thermodynamically consistent with the grand potential (see Sec. B), while at the same time the 2P self-energy $\Gamma = \frac{\delta^2\Phi}{\delta G^2}$ violates the continuity equation.

In fact, it seems plausible that of the two functional relations of the Baym & Kadanoff theory only the value of the functional Ward identity is undermined by anomalous currents. This is because the Schwinger-Dyson equation is universal, whereas the Ward identity is not: The integral Schwinger-Dyson equation can be derived from the equation of motion of the construction operator,

$$\partial_\tau c + [c, H_0 - \mu N + H_{\text{int}}] = 0.$$

This derivation was exercised in Sec. B. The construction operator never commutes with the interaction and given a quartic interaction potential $H_{\text{int}} \propto \mathcal{O}(c^\dagger c c^\dagger c)$ the Schwinger-Dyson equation always has the same form. Namely, it yields the 1P self-energy Σ as the Hartree and Fock diagrams plus vertex corrections comprised in the T-matrix F, as on the left of Fig. 3.18. A higher vertex than F (such as a six-point vertex) does not appear in the integral Schwinger-Dyson equation, it is therefore of universal structure[21].

However, the shape of the integral Ward identity depends on the interaction, since it is derived from the continuity equation,

$$\partial_\tau \rho + [\rho, H_0 - \mu N + H_{\text{int}}] = 0.$$

---

[21] Note that higher vertices *do* occur in the Schwinger-Dyson equation when the interaction potential is of higher order than $\mathcal{O}(c^\dagger c c^\dagger c)$, as in the dual fermion formalism [116].

This equation either comes with a finite anomaly $[\rho, H_{\text{int}}]$ of order $\mathcal{O}(c^\dagger c c^\dagger c)$, or without, then the whole equation is of order $\mathcal{O}(c^\dagger c)$. Consequently, the integral Ward identity either comes with an anomaly in the form of a six-point vertex on its RHS, or it comes without an anomaly, both cases are shown on the right of Fig. 3.18.

Chapter 4

Dynamical mean-field theory

"Elvis has left the building." - Unknown

The dynamical mean-field theory (DMFT) is beautiful. Since it was understood that the Hubbard model can be mapped exactly to the Anderson impurity model in the limit of large coordination number [92], DMFT has become one of the most important tools for the study of strongly correlated electrons [32]. Amongst others, two aspects have contributed to this success: (i) It is numerically feasible to apply DMFT in the context of real materials. (ii) This allowed two formerly separate communities of condensed matter physicists, those interested in the exact solution of model systems and those working in the context of real materials, to combine their efforts and to create synergies.

The first point relies on the fact that the DMFT approximation maps the Hubbard model to a local impurity model, which can nowadays be solved efficiently by means of continuous-time quantum Monte-Carlo (CTQMC) solvers [33]. Although the computational expense of solving an impurity model grows drastically with the number of orbitals, optimizations of CTQMC algorithms have made an application of DMFT to systems with up to five or seven orbitals numerically feasible [102, 131]. Another step towards realistic applications is the unification of the density functional theory (DFT) with DMFT (DFT+DMFT) [2, 70].

The second point regards a former fault line within condensed matter physics. A persistent dilemma of the field has been that one is either forced to accept making very coarse approximations to real materials, or to employ model systems, which may not describe the salient physics of the real material. DMFT and its embedding into the DFT has bridged this gap: Nowadays, physicists interested in real materials and those interested in model systems often share their insights during the same scientific sessions [148].

DMFT has first been applied to infinite-dimensional systems, where it becomes exact. In particular the existence of the Mott metal-to-insulator transition in this limit is an established fact [32]. Although applications to lattices with an infinite coordination number have become more rare, improvements in the development of impurity solvers open up new possibilities occasionally. For example, although DMFT solves the Hubbard model on a lattice with infinite coordination number formally exactly, it becomes difficult in certain

extreme regimes to obtain reliable results on the real axis, such as in a minutely doped Mott insulator. While the quasi-particle peak vanishes in the Mott phase, tiny dopings revive resilient quasi-particles with a very small coherence temperature and spectral weight [27]. In order to resolve such residual evidence of Fermi liquid behavior, highly accurate real axis data is needed, such as from improved Numerical Renormalization group (NRG) solvers [28]. This has revealed the exact resistivity curve of a doped Mott insulator [27], which shows no less than four distinct temperature regimes that range from the Fermi liquid over the bad and strange to the high-T metal.

A   Derivation of DMFT

Q DMFT has in common with other beautiful theories that it has many derivations. Some are sketched below.

A.1   The limit of infinite coordination number/dimensionality

The first derivation of DMFT was done in the limit of infinite dimensions [92]. Nevertheless, a straightforward expansion around this limit is not the best way to introduce DMFT as an approximation for a lattice in finite dimensions. A standard method to derive DMFT and other dynamical mean-field theories in finite dimensions is the cavity construction [32]. In this approach one separates a representative site from the rest of the lattice and describes the coupling between them via a retarded hybridization function. Corrections to this local effective medium description, which is equivalent to the Anderson impurity model, vanish in the limit of large coordination number.

    The reason for this is essentially that at any given moment the further time-evolution of the representative lattice site depends less and less on the particular configuration of its neighbors the more neighbors there are. This becomes clear when considering the opposite limit, the Hubbard model on a one-dimensional chain with nearest neighbor hoppings: A spin-↑ electron on a given lattice site may be temporarily locked in place by two other spin-↑ electrons to the left and right, as on the left of Fig. 4.1. Such situations are highly likely to occur on a low-dimensional lattice and thus there are strong short-range correlations between neighboring lattice sites, an effective single-site description is a bad starting point. On the other hand, the chance that a non-generic situation is created spontaneously becomes very small when the reference site has many neighbors. Then it is difficult for them to coordinate a similar conspiracy against an electron on the reference site. In the limit of infinitely many neighbors, $z \to \infty$, the time-evolution of the reference site is affected by its environment only on average, which can be described by a hybridization of the reference site with an effective dynamical bath. In this sense the cavity construction is a formal way to express the separation of the lattice into a representative site and the rest. This separation becomes exact in the limit of infinite coordination number. Another way to derive DMFT
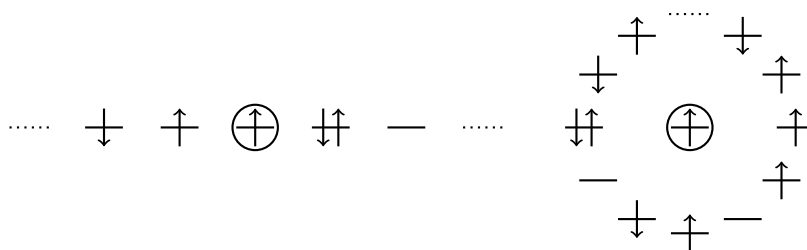
FIGURE 4.1: Two momentary electronic configurations of a one-dimensional chain (left) and of an infinite dimensional lattice (right) around a reference site (circles). In the case of the chain with coordination number $z = 2$ the mobility of an electron on a given site strongly depends on states of electrons occupying the neighboring sites. Here, the ↑-electron on the reference site is locked in place due to the Pauli principle, unable to move unless one of the neighboring ↑-electrons vacates its position. This corresponds to strong short-range correlations. In the limit $z \to \infty$ the configuration of the neighboring sites is always an exact representation of the average occupancy, magnetization, ..., etc., of the whole crystal. The chance for a momentary deviation of this environment from the mean is zero: The surrounding sites become an effective, dynamical bath and nonlocal correlations vanish.

in the limit of large coordination number is to perform a dimensional analysis of the self-energy diagrams of the Hubbard model, where only local contributions survive the limit to infinite dimensions [32].

Other ways to DMFT have been found later: For example, in the dual fermion approach DMFT arises as the lowest level approximation to the self-energy of the dual fermions [122]. An embedding of DMFT into a wider context of approximations was done in the self-energy functional theory [109]. The latter is based on the observation that two systems with the same interaction Hamiltonian H_{int} but different noninteracting Hamiltonians H_0 share the same functional dependence of the Luttinger-Ward functional $\Phi[G]$ on Green's function G. This serves as a bridge between, e.g., the Hubbard model in the thermodynamic limit and a small cluster of Hubbard atoms, that both have the same interaction $U n_\uparrow n_\downarrow$. The self-energy functional theory therefore comprises a large number of 'self-consistent cluster' approximations, in which the hopping of a cluster, optionally also a hybridization with a non-interacting bath, is fixed self-consistently. DMFT arises in the limit of the smallest cluster size of one atom, coupled to a continuous (i.e., infinite) noninteracting bath.

A.2   Derivation from the Luttinger-Ward functional

The derivation of DMFT from the Luttinger-Ward functional is probably the most compact and thence a frequently cited one: The Luttinger-Ward functional of the Hubbard model $\Phi[G_{ij}]$ is a functional of Green's function. In DMFT this functional is approximated by considering only the subset $\phi[G_{ii}]$ of diagrams that contribute to Φ in which all propagators are local, $\Phi[G_{ij}] \approx \sum_i \phi[G_{\text{loc},i} = G_{ii}]$. As a consequence, the self-energy of DMFT is local, $\Sigma_{ij} = \delta\Phi[G_{i'j'}]/\delta G_{ji} = \delta\phi[G_{\text{loc}}]/\delta G_{\text{loc}}\delta_{ji}$. In practice it is not possible to evaluate

$\Sigma = \delta\phi[G_{\rm loc}]/\delta G_{\rm loc}$ exactly, since $\phi[G_{ii}]$ is unknown. The evaluation of Σ from ϕ is therefore circumvented by solving the Anderson impurity model, whose Green's function and Luttinger-Ward functional are g and $\phi[g]$, respectively. By imposing the self-consistency condition $G_{\rm loc} = g$ one makes sure that the impurity model sums up all local diagrams of the lattice model.

The downside of this derivation is its abstraction, while it does not put DMFT into a wider context of approximations, as the self-energy functional theory does. Since the calculation of the Luttinger-Ward functional $\phi[g]$ must be circumvented, the critical recipient of this argument is faced with a claim that is very difficult to verify in practice (i.e., numerically): That the converged solutions for Green's function and for the self-energy indeed satisfy $\Sigma = \delta\phi[G_{\rm loc}]/\delta G_{\rm loc}$, which is the central point of the derivation. Furthermore, this approach implicitly makes use of the fact that the Hubbard model and the Anderson impurity model share the same interaction Hamiltonian. While this may be the case in DMFT, it is not so in a number of related dynamical mean-field approaches (e.g. in EDMFT). However, these are frequently motivated in the same way, i.e., as a local approximation to the Luttinger-Ward functional. In these cases it is not obvious how the interactions of lattice and local reference model ought to be related.

In this chapter and the following chapter 5 it will be clarified that if the goal is to obtain a conserving approximation, that is, an approximation that satisfies the Ward identity of the lattice model, the interaction Hamiltonian of the effective impurity model can not be chosen in an arbitrary way. This is because it must be guaranteed that lattice system and impurity model share the same type of Ward identity (this notion will be made explicit later). It seems plausible that the main observation of the self-energy functional theory, the universality of Φ for systems that share *the same* interaction Hamiltonian, may on a deeper level be related to the fact that the Ward identities of the lattice and of the reference system are then similar as well.

Lastly, the main practical implication of a derivation of DMFT from the Luttinger-Ward functional are explicit bold-line expansions of the Luttinger-Ward functional, that may be truncated at some order (i.e., methods that perform the expansion in Fig. 3.1 explicitly). Although it was pointed out in Ref. [32] that these are rather impractical, significant progress has been made in this respect [112]. At the same time, bold-line expansions have also led to the discovery of the non-uniqueness of Φ [64], revealing a whole new set of deep questions to grapple with away from the weak-coupling regime.

On the other hand, the derivation of DMFT from the Luttinger-Ward functional has the advantage that it directly relates to the framework of conserving approximations by Baym&Kadanoff. As a consequence, DMFT satisfies the Ward identity of the Hubbard model, which comes with all the beneficial aspects discussed in chapter 3. In order to accommodate the conserving aspects of DMFT within a more practical approach, one which comes without the conceptual difficulties of its functional formulation, it will be suggested in the following that it is advantageous to derive DMFT, and potentially other approximations, directly from a Ward identity. The main results of this section were published in Ref. [65].

A.3 Derivation from the Ward identity

The interaction Hamiltonian of the single-band Hubbard model conserves the local charge
and spin densities, $[H_{\text{int}}, \rho^\alpha] = [U n_\uparrow n_\downarrow, \rho^\alpha] = 0$. Therefore, Green's function G and the 1P
and 2P self-energies Σ_k and $\Gamma^\alpha_{kk'q}$ of the Hubbard model have to satisfy the *lattice Ward
identity*, Eq. (E.6) of chapter 3,

$$\Sigma_{k+q} - \Sigma_k = \sum_{k'} \Gamma^\alpha_{kk'q} \left[G_{k'+q} - G_{k'} \right]. \tag{A.1}$$

DMFT corresponds to approximating $\Sigma_k \approx \Sigma_\nu$ and $\Gamma^\alpha_{kk'q} \approx \gamma^\alpha_{\nu\nu'\omega}$ by their local counterparts
$\Sigma_\nu, \gamma^\alpha_{\nu\nu'\omega}$ of an Anderson impurity model with a yet unspecified hybridization function Δ_ν,
cf. definition in chapter 3, Eq. (C.15). The interaction $U n_\uparrow n_\downarrow$ of the Anderson impurity
model is the local counterpart of the lattice interaction and thus as well commutes with
the charge and spin densities. Therefore, a local analogue of Eq. (A.1), the *impurity Ward
identity*, is satisfied by the respective quantities of the impurity model,

$$\Sigma_{\nu+\omega} - \Sigma_\nu = \sum_{\nu'} \gamma^\alpha_{\nu\nu'\omega} \left[g_{\nu'+\omega} - g_{\nu'} \right], \tag{A.2}$$

where g_ν is the impurity Green's function. Inserting the local approximation into the lattice
Ward identity in Eq. (A.1), it follows that the latter is satisfied if and only if,

$$\Sigma_{\nu+\omega} - \Sigma_\nu = \sum_{\mathbf{k}\nu}' \gamma^\alpha_{\nu\nu'\omega} \left[G_{\mathbf{k}'+\mathbf{q},\nu+\omega} - G_{\mathbf{k}'\nu'} \right]$$

$$= \sum_{\nu}' \gamma^\alpha_{\nu\nu'\omega} \left[G_{\text{loc},\nu+\omega} - G_{\text{loc},\nu'} \right]. \tag{A.3}$$

By comparison to Eq. (A.2) it follows immediately that this criterion is exactly satisfied
if the self-consistency condition $G_{\text{loc}} = g$ holds, which can be achieved by self-consistent
adjustment of the hybridization function Δ. In order to allow symmetry-broken phases, the
derivation may be repeated from suitable Ward identities that are valid in the given phase,
such as Eqs. (E.8) and (E.9) of chapter 3 in case of broken SU(2) symmetry.

A trivial outcome of this approach to DMFT is that it satisfies the Ward identity
Eq. (A.1). Whether or not this is the case has been, in fact, an open question for some
time and it was eventually validated numerically in Ref. [39]. As expected, Eq. (A.3)
holds in converged DMFT calculations[1]. According to the derivation given above, the
lattice Ward identity Eq. (A.1) holds by virtue of, and is equivalent to, the impurity Ward
identity Eq. (A.2), provided that the DMFT self-consistency condition is satisfied. As a
consequence, all statements that can be derived from the lattice Ward identity Eq. (A.1)

---

[1]Note that the local Ward identity Eq. (A.2) always holds when the impurity correlation functions are
obtained numerically exactly, since it is an exact statement, whereas Eq. (A.3) in general only holds by
virtue of the self-consistency condition.

hold in DMFT, combined with those that follow from the impurity Ward identity Eq. (A.2). The simultaneous satisfaction of *two* Ward identities, one on the lattice and one on the impurity, entails a number of appealing synergies, which will be discussed below. As another side effect it is clear from the derivation that next to the 1P self-energy Σ, also the 2P self-energy Γ is a central object of DMFT. In fact, one may view the introduction of Γ into the derivation of DMFT as the price one has to pay for removing the Luttinger-Ward functional Φ from the scene[2]. Fortunately, neither Γ nor Φ need to be known in order to complete the DMFT cycle, which is certainly one of the assets that have made DMFT so successful. In contrast to Φ, however, Γ *can* be evaluated numerically exactly.

B   Four formulations of the DMFT susceptibility

In the following, four equivalent formulations of the DMFT susceptibility will be introduced for later reference. It will also be shown that two of these formulations can be seen as formal precursors to the dual fermion and dual boson approaches, which emerge as natural extensions of DMFT. A number of key facts concerning the DMFT susceptibility will be explained along the way. Paramagnetism is assumed throughout, although all formulae can be generalized to ordered phases.

B.1   Explicit use of the 2P self-energy Γ

The most straightforward way to formulate the susceptibility in DMFT is to make use of its approximation to the 2P self-energy explicitly. The Bethe-Salpeter equation, Eq. (B.1) of chapter 2, in DMFT approximation then reads in k, k'-matrix notation,

$$\hat{X}_q^\alpha = \hat{X}_q^0 + \hat{X}_q^0 \hat{\gamma}_\omega^\alpha \hat{X}_q^\alpha, \tag{B.1}$$

where X^0 is a bubble of DMFT Green's functions, $G_k^{-1} = [G_k^0]^{-1} - \Sigma_\nu$, and the approximation $\Gamma^\alpha \approx \gamma^\alpha$ for the 2P self-energy has been inserted. Often the Bethe-Salpeter equation is formulated equivalently for the T-matrix,

$$\boxed{\hat{F}_q^\alpha = \hat{\gamma}_\omega^\alpha + \hat{\gamma}_\omega^\alpha \hat{X}_q^0 \hat{F}_q^\alpha,} \tag{B.2}$$

A crucial simplification of the DMFT approximation to the susceptibility is that due to the locality of the 2P self-energy γ the T-matrix F does not depend on the momenta $\mathbf{k}$ and $\mathbf{k}'$ (it does depend on the transferred momentum $\mathbf{q}$ in which the BSE is diagonal). Therefore, all objects in Eq. (B.2) are merely matrices in the fermionic frequencies ν and ν'[3]. Only this simplification makes the storage and handling of the matrices involved in the

---

[2]Cf. chapter motto.

[3] Since the $\mathbf{k}, \mathbf{k}'$-dependencies drop out of Eq. (B.2), the momentum summation implied by matrix multiplications [see Eq. (B.5) of chapter 2] will be dropped on a case by case basis, such that $\hat{C} = \hat{A}\hat{B}$ may either imply $C_{kk'} = \sum'_{k''} A_{kk''} B_{k''k'}$ or $C_{\nu\nu'} = \sum'_{\nu''} A_{\nu\nu''} B_{\nu''\nu'}$. Note that the generalized susceptibility in Eq. (B.1) *does* depend on $\mathbf{k}$ and $\mathbf{k}'$.

Bethe-Salpeter equation numerically feasible when considering a reasonably large number of **k**-points to reach the thermodynamic limit $N \to \infty$.

Although the direct use of the 2P self-energy γ is the most obvious way to proceed, it has several downsides. Firstly, γ is, probably without exception, not the 2P quantity that is obtained by a quantum impurity solver. Instead, the local four-point correlation function

$$g^{(2),\sigma\sigma'}_{\nu\nu'\omega} = - \left\langle c_{\nu\sigma} c^{\dagger}_{\nu+\omega,\sigma} c_{\nu'+\omega,\sigma'} c^{\dagger}_{\nu'\sigma'} \right\rangle \tag{B.3}$$

is measured by impurity solvers [$g^{(2),\overline{\sigma\sigma}}$ is defined analogously, cf. also definition in imaginary time in chapter 2, Eq. (A.23)]. From this the local generalized susceptibilities $\chi^{\sigma\sigma'}_{\nu\nu'\omega} = g^{(2),\sigma\sigma'}_{\nu\nu'\omega} + \beta g_{\nu\sigma} g_{\nu'\sigma'} \delta_{\omega}$ and $\chi^{\overline{\sigma\sigma}}_{\nu\nu'\omega} = g^{(2),\overline{\sigma\sigma}}_{\nu\nu'\omega}$ are obtained [cf. chapter 2, Eq. (A.49)], and optionally brought into the channels $\alpha = c, x, y, z$ via the Pauli matrices [cf. chapter 2, Eq. (A.27)]. One may then proceed by inverting the local Bethe-Salpeter equation for the generalized susceptibility in order to solve for γ,

$$\hat{\chi}^{\alpha}_{\omega} = \hat{\chi}^{0}_{\omega} + \hat{\chi}^{0}_{\omega} \hat{\gamma}^{\alpha}_{\omega} \hat{\chi}^{\alpha}_{\omega}, \tag{B.4}$$

$$\Leftrightarrow \hat{\chi}^{0,-1}_{\omega} = \hat{\chi}^{\alpha,-1}_{\omega} + \hat{\gamma}^{\alpha}_{\omega}, \tag{B.5}$$

where $\chi^{0}_{\nu\nu'\omega} = g_{\nu} g_{\nu+\omega} \beta \delta_{\nu\nu'} = \chi^{0}_{\nu\omega} \beta \delta_{\nu\nu'}$ is the local impurity bubble. Alternatively, one solves $\hat{\chi}^{\alpha}_{\omega} = \hat{\chi}^{0}_{\omega} + \hat{\chi}^{0}_{\omega} f^{\alpha}_{\omega} \hat{\chi}^{0}_{\omega}$ for the local T-matrix f, explicitly [cf. chapter 2, Eq. (B.10)],

$$f^{\alpha}_{\nu\nu'\omega} = \frac{\chi^{\alpha}_{\nu\nu'\omega} - g_{\nu} g_{\nu+\omega} \beta \delta_{\nu\nu'}}{g_{\nu} g_{\nu+\omega} g_{\nu'} g_{\nu'+\omega}}. \tag{B.6}$$

The 2P self-energy is then obtained by inverting the Bethe-Salpeter equation for f,

$$\hat{f}^{\alpha}_{\omega} = \hat{\gamma}^{\alpha}_{\omega} + \hat{\gamma}^{\alpha}_{\omega} \hat{\chi}^{0}_{\omega} \hat{f}^{\alpha}_{\omega}, \tag{B.7}$$

$$\Leftrightarrow \hat{\gamma}^{\alpha,-1}_{\omega} = \hat{f}^{\alpha,-1}_{\omega} + \hat{\chi}^{0}_{\omega}. \tag{B.8}$$

Regardless of whether Eq. (B.5) or Eq. (B.8) is used to compute γ, in both cases a local Bethe-Salpeter equation has to be inverted. Since either the generalized susceptibility χ or the T-matrix f are typically known only at a limited number of Matsubara frequencies, this inversion introduces a cutoff error. In particular at low temperature it can be a numerically intense task to measure these objects in CTQMC solvers at a sufficient number of frequencies in order to make the error introduced by the inversion small enough. The error of χ and f in Monte-Carlo calculations is furthermore larger at large Matsubara frequencies, such that in the calculation of γ the error of the larger frequencies then propagates also to the smaller ones due to the Matrix inversion. A further issue when working directly with the irreducible 2P self-energy γ is that it is known to diverge in regimes of intermediate to strong coupling in DMFT applications to the Hubbard model and to the Falicov-Kimball model [125, 117], although the reducible objects χ and f typically show perfectly non-singular behavior. These divergences have, in fact, recently been linked to the existence of unphysical branches of the Luttinger-Ward functional [35]. For these reasons it is advantageous in practical

calculations to avoid the explicit use of the local 2P self-energy γ.

B.2   Reformulation in terms of the local T-matrix - Dual fermions

A frequently used reformulation of the T-matrix of DMFT relies on the simple observation that one may invert the Bethe-Salpeter Eq. (B.2) and eliminate γ by making use of the local Bethe-Salpeter Eq. (B.8),

$$
\begin{aligned}
\hat{\gamma}_\omega^{\alpha,-1} &= \hat{F}_q^{\alpha,-1} + \hat{X}_q^0 \\
&= \hat{f}_\omega^{\alpha,-1} + \hat{\chi}_\omega^0, & \text{(B.9)} \\
\Rightarrow \hat{F}_q^{\alpha,-1} &+ \hat{X}_q^0 - \hat{\chi}_\omega^0 = \hat{f}_\omega^{\alpha,-1}. & \text{(B.10)}
\end{aligned}
$$

Multiplication of this equation by F from the right and by f from the left yields,

$$
\boxed{\hat{F}_q^\alpha = \hat{f}_\omega^\alpha + \hat{f}_\omega^\alpha \hat{\tilde{X}}_q^0 \hat{F}_q^\alpha,} \qquad\qquad \text{(B.11)}
$$

where $\tilde{X}_q^0$ denotes the nonlocal bubble,

$$
\tilde{X}_{kk'q}^0 = X_{kk'q}^0 - \chi_{\nu\nu'\omega}^0 N\delta_{\mathbf{k},\mathbf{k}'} = (G_k G_{k+q} - g_\nu g_{\nu+\omega})\delta_{kk'} N\beta = \tilde{X}_{kq}^0 \delta_{kk'} N\beta. \qquad \text{(B.12)}
$$

The Bethe-Salpeter Eq. (B.11) is now formulated in terms of the local T-matrix f and an inversion of a local Bethe-Salpeter equation is no longer required. This avoids the issues pointed out after Eq. (B.8) and comes with the additional benefit that the nonlocal bubble $\tilde{X}^0$ decays faster in the Matsubara frequencies than the bubble X^0. This makes the handling of its high frequency asymptote more accurate or even unnecessary in numerical applications.

Eq. (B.11) also draws a connection between DMFT and the dual fermion approach, which is seen as follows: The nonlocal bubble has the favorable property that it can be factorized into nonlocal Green's functions $\tilde{\mathcal{G}}_k = G_k - g_\nu$ when it is summed over the momentum $\mathbf{k}$. Making use of the DMFT self-consistency condition $G_{\text{loc}} = \sum_{\mathbf{k}}' G_{\mathbf{k}} = g$ one has,

$$
\begin{aligned}
\sum_{\mathbf{k}}' \tilde{\mathcal{G}}_k \tilde{\mathcal{G}}_{k+q} &= \sum_{\mathbf{k}}' (G_k - g_\nu)(G_{k+q} - g_{\nu+\omega}) \\
&= \sum_{\mathbf{k}}' (G_k G_{k+q} - G_k g_{\nu+\omega} - g_\nu G_{k+q} + g_\nu g_{\nu+\omega}) \\
&= \sum_{\mathbf{k}}' (G_k G_{k+q} - g_\nu g_{\nu+\omega}) = \sum_{\mathbf{k}}' \tilde{X}_{kq}^0 \equiv \tilde{X}_{\nu q}^0. \qquad \text{(B.13)}
\end{aligned}
$$

Furthermore, also by virtue of self-consistency, the local part of this expression vanishes,

$$\sum_{\mathbf{q}}' \tilde{X}^0_{\nu q} = \sum_{\mathbf{q}}' \sum_{\mathbf{k}}' (G_k G_{k+q} - g_\nu g_{\nu+\omega}) = (g_\nu g_{\nu+\omega} - g_\nu g_{\nu+\omega}) = 0. \tag{B.14}$$

Making the momentum and frequency summations $\sum_k = \sum_{\mathbf{k}\nu}'$ explicit and using Eq. (B.13), the Bethe-Salpeter Eq. (B.11) can be expressed as,

$$
\begin{aligned}
F^\alpha_{\nu\nu'q} &= f^\alpha_{\nu\nu'\omega} + \sum_{\mathbf{k}''\nu''}' f^\alpha_{\nu\nu''\omega} \tilde{X}^0_{k''q} F^\alpha_{\nu''\nu'q}, \\
&= f^\alpha_{\nu\nu'\omega} + \sum_{\nu''}' f^\alpha_{\nu\nu''\omega} \tilde{X}^0_{\nu''q} F^\alpha_{\nu''\nu'q}.
\end{aligned}
\tag{B.15}
$$

Here, the definition in Eq. (B.13) was inserted, making use of the fact that f and F do not depend on $\mathbf{k}$ or $\mathbf{k}'$.

The Bethe-Salpeter Eq. (B.15) is now formulated in terms of the $\mathbf{k}$-summed nonlocal bubble in Eq. (B.13). Since the latter is equivalent to the $\mathbf{k}$-summed bubble of nonlocal Green's functions, $\tilde{X}^0_{\nu''q} = \sum_{\mathbf{k}}' \tilde{\mathcal{G}}_k \tilde{\mathcal{G}}_{k+q}$, it is tempting to view the nonlocal Green's function $\tilde{\mathcal{G}}$ as the fundamental building block of the DMFT susceptibility, as an alternative to the DMFT Green's function G. In fact, this viewpoint is put on solid ground within the dual fermion approach [122], and Eq. (B.15) can be seen as a precursor to the Bethe-Salpeter equation of the dual fermions, whose *noninteracting* Green's function is the nonlocal DMFT Green's function $\tilde{\mathcal{G}}_k = G_k - g_\nu$. In the dual fermion approach one progresses beyond DMFT by dressing $\tilde{\mathcal{G}}$ with a $\mathbf{k}$-dependent self-energy $\tilde{\Sigma}$, $\tilde{G}_k^{-1} = \tilde{\mathcal{G}}_k^{-1} - \tilde{\Sigma}_k$, where $\tilde{G}$ is the interacting Green's function of the dual fermions.

B.3 Exact summation of all local diagrams

While the reformulation in Eq. (B.15) of the Bethe-Salpeter equation already improves upon Eq. (B.2), further progress can be made by summing up all purely local diagrams in the Bethe-Salpeter equation exactly. It was presumably first noted by Pruschke et al.[4] that such a procedure leads to superior quality of final results in numerical calculations of the DMFT susceptibility [113]. A suitable formulation of the DMFT susceptibility is obtained as follows: The Bethe-Salpeter Eq. (B.1) is inverted and the 2P self-energy γ eliminated by inserting Eq. (B.5), this leads to

$$
\begin{aligned}
\hat{X}^{\alpha,-1}_q - \hat{X}^{0,-1}_q &= \hat{\chi}^{\alpha,-1}_\omega - \hat{\chi}^{0,-1}_\omega, \\
\Leftrightarrow \hat{X}^{\alpha,-1}_q + \hat{\xi}_q &= \hat{\chi}^{\alpha,-1}_\omega,
\end{aligned}
\tag{B.16}
$$

---

[4] I like to recommend to the reader the many great papers on DMFT of T. Pruschke, who unfortunately passed away much too early in 2016, that are among the best papers on the method, and which may serve as instructive examples of clarity and readability.

where the expression involving the impurity bubble χ^0 and the DMFT bubble X^0 was abbreviated as $\hat{\xi}_q = (\hat{\chi}_\omega^{0,-1} - \hat{X}_q^{0,-1})$. Multiplying Eq. (B.16) by χ^α from the right and by X^α from the left, as well as doing this vice versa, one obtains two alternative ladder equations for X^α,

$$\begin{aligned}
\hat{X}_q^\alpha &= \hat{\chi}_\omega^\alpha + \hat{\chi}_\omega^\alpha \hat{\xi}_q \hat{X}_q^\alpha \\
&= \hat{\chi}_\omega^\alpha + \hat{X}_q^\alpha \hat{\xi}_q \hat{\chi}_\omega^\alpha.
\end{aligned} \tag{B.17}$$

Inserting the second relation on the RHS of the first it follows that,

$$\hat{X}_q^\alpha = \hat{\chi}_\omega^\alpha + \hat{\chi}_\omega^\alpha (\hat{\xi}_q + \hat{\xi}_q \hat{X}_q^\alpha \hat{\xi}_q) \hat{\chi}_\omega^\alpha. \tag{B.18}$$

Using Eq. (B.16) the expression in brackets can be reformulated as $\hat{\xi}_q + \hat{\xi}_q \hat{X}_q^\alpha \hat{\xi}_q = \hat{\xi}_q \hat{X}_q^\alpha \hat{\chi}_\omega^{\alpha,-1}$. On the other hand, Eq. (B.16) can also be solved for $\hat{X}_q^\alpha = (\hat{1} - \hat{\chi}_\omega^\alpha \hat{\xi}_q)^{-1} \hat{\chi}_\omega^\alpha$. The expression in brackets in Eq. (B.18) is therefore given as $\hat{\xi}_q + \hat{\xi}_q \hat{X}_q^\alpha \hat{\xi}_q = \hat{\xi}_q (\hat{1} - \hat{\chi}_\omega^\alpha \hat{\xi}_q)^{-1}$. Inserting this into Eq. (B.16) it follows,

$$\boxed{\hat{X}_q^\alpha = \hat{\chi}_\omega^\alpha + \hat{\chi}_\omega^\alpha \left[\hat{\xi}_q (\hat{1} - \hat{\chi}_\omega^\alpha \hat{\xi}_q)^{-1} \right] \hat{\chi}_\omega^\alpha.} \tag{B.19}$$

This is the relation derived in Ref. [113]. It has favorable properties for numerical applications, since one can make use of the fact that in practice the goal is rarely to explicitly evaluate the generalized susceptibility but the susceptibility, $X_q^\alpha = 2 \sum_{kk'} X_{kk'q}^\alpha$. Performing the trace over k and k' in Eq. (B.19) one can identify the impurity susceptibility, $\chi_\omega^\alpha = 2 \sum_{\nu\nu'}' \chi_{\nu\nu'\omega}^\alpha$, and it is therefore possible to rewrite the susceptibility of DMFT as the sum of the local impurity susceptibility $\chi_\omega^\alpha = - \langle \rho_{-\omega}^\alpha \rho_\omega^\alpha \rangle + \beta \langle \rho^\alpha \rangle \langle \rho^\alpha \rangle \delta_\omega$ and nonlocal corrections X',

$$X_q^\alpha = \chi_\omega^\alpha + X_q'^\alpha. \tag{B.20}$$

The great advantage of this reformulation over Eqs. (B.2) and (B.15) is that the impurity susceptibility χ_ω^α can be measured directly in Monte Carlo calculations, which typically has a rather small statistical error compared to fermionic variables. Eq. (B.20) yields numerical results of superior quality because all diagrams comprised in the local Bethe-Salpeter Eq. (B.4) are summed up exactly into this directly measurable object. In Eqs. (B.2) and (B.15) this is not the case and the local BSE is then implicitly summed numerically, introducing large cutoff errors, since all quantities are only known at a finite number of Matsubara frequencies.

B.4   Dual bosons

The fourth formulation of the DMFT susceptibility was found in the context of the dual boson approach [121], it is explicitly shown to be equivalent to the DMFT susceptibility in Ref. [39]. The dual boson formulation is equivalent to Eq. (B.19) and can be derived by

reformulating

$$
\begin{aligned}
\hat{\xi}_q &= (\hat{\chi}_\omega^{0,-1} - \hat{X}_q^{0,-1}) \\
&= \hat{\chi}_\omega^{0,-1} (\hat{X}_q^0 - \hat{\chi}_\omega^0) \hat{X}_q^{0,-1} \\
&= \hat{\chi}_\omega^{0,-1} \hat{\tilde{X}}_q^0 \hat{X}_q^{0,-1},
\end{aligned}
\tag{B.21}
$$

where the definition of the nonlocal bubble $\hat{\tilde{X}}^0$ in Eq. (B.12) was used. In the same way one shows that $\hat{\xi}_q = \hat{X}_q^{0,-1} \hat{\tilde{X}}_q^0 \hat{\chi}_\omega^{0,-1}$. Using this in Eq. (B.18) and expressing the generalized susceptibility by the T-matrix, $\hat{X}_q^\alpha = \hat{X}_q^0 + \hat{X}_q^0 \hat{F}_q^\alpha \hat{X}_q^0$, one obtains

$$
\hat{X}_q^\alpha = \hat{\chi}_\omega^\alpha + \hat{\chi}_\omega^\alpha (\hat{\xi}_q + \hat{\xi}_q \hat{X}_q^0 \hat{\xi}_q) \hat{\chi}_\omega^\alpha + \hat{\chi}_\omega^\alpha \hat{\chi}_\omega^{0,-1} \hat{\tilde{X}}_q^0 \hat{F}_q^\alpha \hat{\tilde{X}}_q^0 \hat{\chi}_\omega^{0,-1} \hat{\chi}_\omega^\alpha.
\tag{B.22}
$$

The second term on the RHS of this relation simplifies, since $\hat{\xi}_q + \hat{\xi}_q \hat{X}_q^0 \hat{\xi}_q = \hat{\chi}_\omega^{0,-1} \hat{\tilde{X}}_q^0 \hat{\chi}_\omega^{0,-1}$. Abbreviating $\hat{\lambda}_\omega^{\alpha,l} = \hat{\chi}_\omega^\alpha \hat{\chi}_\omega^{0,-1}$ and $\hat{\lambda}_\omega^{\alpha,r} = \hat{\chi}_\omega^{0,-1} \hat{\chi}_\omega^\alpha$ one finally has

$$
\boxed{\hat{X}_q^\alpha = \hat{\chi}_\omega^\alpha + \hat{\lambda}_\omega^{\alpha,l} \left[\hat{\tilde{X}}_q^0 + \hat{\tilde{X}}_q^0 \hat{F}_q^\alpha \hat{\tilde{X}}_q^0 \right] \hat{\lambda}_\omega^{\alpha,r}.}
\tag{B.23}
$$

Multiplication by two and summation over the outer fermionic frequencies leads to the formula derived in Ref. [39]. The matrix elements of λ are given as,

$$
\begin{aligned}
\lambda_{\nu\nu'\omega}^{\alpha,r} &= {\sum_{\nu''}}' \chi_{\nu\nu''\omega}^{0,-1} \chi_{\nu''\nu'\omega}^\alpha = {\sum_{\nu''}}' (g_\nu g_{\nu+\omega})^{-1} \delta_{\nu\nu''} \chi_{\nu''\nu'\omega}^\alpha \\
&= \beta \delta_{\nu\nu'} + f_{\nu\nu'\omega}^\alpha g_{\nu'} g_{\nu'+\omega},
\end{aligned}
\tag{B.24}
$$

where from the first to the second line the generalized susceptibility χ was expressed through the T-matrix f.

One should note that the newly introduced vertices λ^l and λ^r have a clear physical interpretation as the three-leg vertices of the impurity model, as depicted in Fig. 4.2. λ^r is hence related to the generalized susceptibility χ by the amputation of the left pair of legs $g_\nu g_{\nu+\omega}$. Tracing out the fermionic frequencies ν and ν' from Eq. (B.23) in order to obtain the susceptibility, $X_q = 2 {\sum_{\nu\nu'}}' X_{\nu\nu'q}$, implies connecting the remaining pair of legs of λ^r,

$$
\lambda_{\nu\omega}^{\alpha,r} \equiv {\sum_{\nu'}}' \lambda_{\nu\nu'\omega}^{\alpha,r} = 1 + {\sum_{\nu'}}' f_{\nu\nu'\omega}^\alpha g_{\nu'} g_{\nu'+\omega}.
\tag{B.25}
$$

After closing the legs of the matrix $\lambda_{\nu\nu'\omega}^{\alpha,r}$ on the right by summing over ν' there remains a vector $\lambda_{\nu\omega}^{\alpha,r}$ in the fermionic frequency ν, which will therefore be denoted without a hat. One likewise defines $\lambda_{\nu\nu'\omega}^{\alpha,l}$ by amputating the right legs of the generalized susceptibility and $\lambda_{\nu'\omega}^{\alpha,l} = {\sum_\nu}' \lambda_{\nu\nu'\omega}^{\alpha,l}$. The three-leg vertices λ^l and λ^r are related due to the crossing
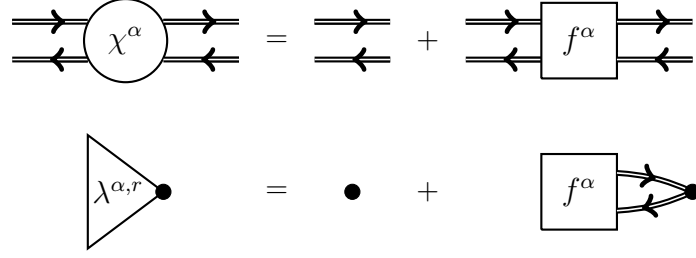
FIGURE 4.2: The three-leg vertex λ^r of the impurity model is obtained by amputating the pair of legs on the left side of the generalized susceptibility $\hat{\chi}$ and closing those on the right side. Similarly, λ^l is constructed by removing the legs on the right but is related to λ^r due to the crossing symmetry of the T-matrix f [see Eq. (B.26)]. Black dots symbolize bosonic end points and come with a factor of 1.

symmetry $f_{\nu,\nu',\omega} = f_{\nu'+\omega,\nu+\omega,-\omega}$ of the T-matrix, which follows from the definition of the local four-point correlation function in Eq. (B.3),

$$
\begin{aligned}
\lambda^{\alpha,r}_{\nu\omega} &= 1 + \sum_{\nu'}{}' f^{\alpha}_{\nu'+\omega,\nu+\omega,-\omega} g_{\nu'} g_{\nu'+\omega} \\
&= 1 + \sum_{\nu'}{}' g_{\nu'} g_{\nu'-\omega} f^{\alpha}_{\nu',\nu+\omega,-\omega} \\
&= \lambda^{\alpha,l}_{\nu+\omega,-\omega}.
\end{aligned}
\tag{B.26}
$$

Performing the trace over fermionic frequencies in Eqs. (B.19) and (B.23) defines the non-local corrections X' in Eq. (B.20) that carry the dependence of the DMFT susceptibility on the transferred momentum $\mathbf{q}$,

$$
\begin{aligned}
X'^{\alpha}_q &= 2\mathrm{Tr}\left(\hat{\chi}^{\alpha}_{\omega} \left[\hat{\xi}_q (\hat{1} - \hat{\chi}^{\alpha}_{\omega}\hat{\xi}_q)^{-1} \right] \hat{\chi}^{\alpha}_{\omega} \right) \\
&= 2\mathrm{Tr}\left(\hat{\lambda}^{\alpha,l}_{\omega} \left[\hat{\tilde{X}}^0_q + \hat{\tilde{X}}^0_q \hat{F}^{\alpha}_q \hat{\tilde{X}}^0_q \right] \hat{\lambda}^{\alpha,r}_{\omega} \right).
\end{aligned}
\tag{B.27}
$$

In the first line is the formulation of Pruschke et al. in Eq. (B.19), the second line shows the formulation as used in the dual boson approach. It should be noted that taking the trace in the second line merely amounts to leaving out the hat on top of λ^l and λ^r, implying summations as in Eq. (B.25).

In the dual boson approach the DMFT susceptibility is formulated in terms of the nonlocal bubble $\tilde{X}^0$, which was seen in Eq. (B.13) to be a bubble of bare dual fermion propagators $\tilde{\mathcal{G}}$. In contrast to the dual fermion approach one not only introduces a fermionic self-energy $\tilde{\Sigma}$ for the dual fermions but also a bosonic self-energy $\tilde{\Pi}$ and bare and dressed bosonic propagators $\tilde{\mathcal{X}}$ and $\tilde{X}$, respectively, that are related via a Dyson equation, $\tilde{X}^{\alpha,-1}_q = \tilde{\mathcal{X}}^{\alpha,-1}_q - \tilde{\Pi}^{\alpha}_q$. In the simplest approximation to the Hubbard model, which amounts to

DMFT, one sets $\tilde{\Sigma} = 0$, whereas $\tilde{\Pi}$ is given as,

$$\tilde{\Pi}_q^{\alpha} = \chi_{\omega}^{\alpha,-1} X_q'^{\alpha} \chi_{\omega}^{\alpha,-1} = 2\chi_{\omega}^{\alpha,-1} \lambda_{\omega}^{\alpha,l} \left[\hat{\tilde{X}}_q^0 + \hat{\tilde{X}}_q^0 \hat{F}_q^{\alpha} \hat{\tilde{X}}_q^0 \right] \lambda_{\omega}^{\alpha,r} \chi_{\omega}^{\alpha,-1}. \tag{B.28}$$

In the notation introduced in Refs. [121] and [85] the factors $\chi_{\omega}^{\alpha,-1}$ are absorbed into the definition of λ. Expressing the nonlocal corrections X' in Eq. (B.20) via the bosonic self-energy $\tilde{\Pi}$ in Eq. (B.28), the DMFT susceptibility is thence given as,

$$X_q^{\alpha} = \chi_{\omega}^{\alpha} + \chi_{\omega}^{\alpha} \tilde{\Pi}_q^{\alpha} \chi_{\omega}^{\alpha}. \tag{B.29}$$

A qualitative difference between the fermionic and the bosonic degrees of freedom is that in the simplest approximation, i.e., DMFT, the self-energy $\tilde{\Sigma}$ of the dual fermions is zero, whereas $\tilde{\Pi}$, the one of the dual bosons, is finite and large. Since DMFT satisfies the Ward identity, its susceptibility is subjected to a number of exact constraints derived in chapter 3, such as $\imath\omega X_{\mathbf{q}=0,\omega}^{\alpha} = 0$ as a consequence of global charge and spin conservation [cf. chapter 3, Eq. (D.3)]. The impurity susceptibility χ_{ω}^{α}, the first term on the RHS of Eq. (B.29), does not have this property, therefore, $\tilde{\Pi}$ is required to reconcile this constraint. Explicitly, $\chi_{\omega}^{\alpha} \tilde{\Pi}_{\mathbf{q}=0,\omega}^{\alpha} = -1$ has to be satisfied for any finite $\omega \neq 0$. It is therefore clear that neglecting $\tilde{\Pi}$, or its momentum dependence, leads to a violation of global conservation laws.

Although the dual boson formulation of the DMFT susceptibility in Eq. (B.29) is eventually equivalent to the formula of Pruschke et al. in Eq. (B.19), it can be interpreted in a more straightforward way as a ladder of nonlocal DMFT bubbles $\tilde{X}^0$, i.e., as a ladder of bare dual fermions. It is worth noting that, next to the exact summation of all local diagrams into χ_{ω}^{α}, an added benefit of Eqs. (B.19) and (B.29) is that the arising three-leg vertices with one closed pair of legs, $\sum_{\nu'}' \chi_{\nu\nu'\omega}^{\alpha}$ in the formulation of Pruschke et al., and equivalently $\lambda_{\nu\omega}^{\alpha} = (g_{\nu} g_{\nu+\omega})^{-1} \sum_{\nu'}' \chi_{\nu\nu'\omega}^{\alpha}$ in the dual boson approach, can be measured directly in CTQMC implementations [38]. The correlation function that needs to be measured then, e.g., in the longitudinal channel, is $\sum_{\nu'}' g_{\nu\nu'\omega}^{(2),\sigma\sigma'} = \langle c_{\nu\sigma} c_{\nu+\omega,\sigma}^{\dagger} n_{\omega\sigma'} \rangle$. This further reduces the numerical noise and allows an analytical continuation of the DMFT susceptibility to the real axis, examples are shown, e.g., in Refs. [78] and [39], as well as below.

B.5   Conclusions

The DMFT susceptibility may be formulated in a number of equivalent ways, four of them are given in Eqs. (B.2), (B.11), (B.19), and (B.23). Despite their equivalence, the third and the fourth of these formulae should be favored in practical applications, since they sum up all local diagrams exactly into objects that can be measured directly in CTQMC calculations. This greatly reduces the statistical noise and makes an analytical continuation of the DMFT susceptibility to the real axis feasible. Eq. (B.11) draws a connection to the dual fermion approach [122] by reformulating the Bethe-Salpeter equation in terms of a ladder of bare dual fermions, whereas Eq. (B.23) relates the DMFT susceptibility to the bosonic self-energy of the dual boson approach [121].

C Synergies of 1P self-consistency and local conservation laws
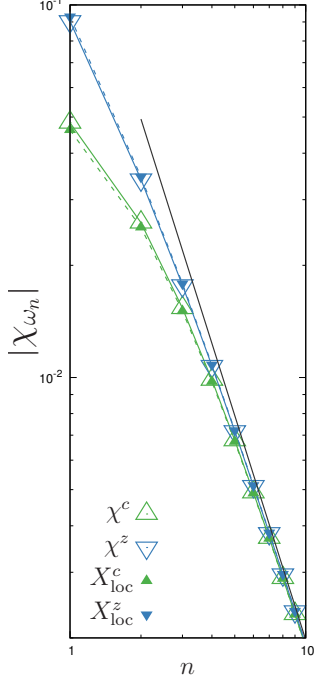
FIGURE 4.3:   High fre-
quency   behavior   of χ
(open triangles, bold line)
and X_{loc} (filled triangles,
dashed line) in a DMFT
calculation for the half-
filled Hubbard model on the
square lattice (n.n. hopping
$t = 1$, $U = 6$, $\beta = 2$). The
charge (green) and spin
(blue) susceptibility ap-
proach the same asymptote
$-2E_{\mathrm{kin}}/\omega^2$ (black line).

According to the derivation of DMFT given in Sec. A it satisfies
the Ward identity, which comes with all of the benefits that were
discussed in chapter 3. At the same time, DMFT is one-particle
self-consistent, meaning that it is subject to the self-consistency
condition $G_{\mathrm{loc}} = g$, where g is the exact Green's function of the
Anderson impurity model. While the self-consistency eventu-
ally guarantees the satisfaction of the lattice Ward identity in
Eq. (A.1), it also implies that DMFT satisfies the Ward identity
of the impurity model, Eq. (A.2). The simultaneous satisfaction
of these two Ward identities comes with a number of additional
benefits that go beyond those discussed in chapter 3, which as-
sume that only either an impurity or a lattice Ward identity is
satisfied, respectively. These additional benefits can be viewed
as synergies of local conservation laws in combination with the
1P self-consistency condition $G_{\mathrm{loc}} = g$, which will be highlighted
in this section.

C.1   1P and 2P consistency of the kinetic energy

The kinetic energy of the Hubbard model is given as

$$E_{\mathrm{kin}}^{\mathrm{lat}} = \sum_{\mathbf{k}\sigma}' \varepsilon_{\mathbf{k}} \langle n_{\mathbf{k}\sigma} \rangle, \qquad (\mathrm{C.1})$$

where the superscript 'lat' denotes that this is the kinetic en-
ergy of the lattice. Since DMFT satisfies the Ward identity of
the Hubbard model, the high frequency asymptote of the local
DMFT susceptibility, $\sum_{\mathbf{q}}' X_{\mathbf{q},\omega}^{\alpha} = X_{\mathrm{loc},\omega}^{\alpha}$, must yield the kinetic
energy [cf. Eq. (D.23) of chapter 3],

$$\lim_{\omega \to \infty} (\imath\omega)^2 X_{\mathrm{loc},\omega}^{\alpha} = -2E_{\mathrm{kin}}^{\mathrm{lat}}. \qquad (\mathrm{C.2})$$

On the other hand, the local DMFT susceptibility can be calcu-
lated from Eq. (B.20) as the impurity susceptibility plus nonlo-
cal corrections X', which are given as in Eq. (B.27). The local
part of X is hence

$$X_{\mathrm{loc},\omega}^{\alpha} = \chi_{\omega}^{\alpha} + \lambda_{\omega}^{\alpha,l} \sum_{\mathbf{q}}' \left[\hat{\tilde{X}}_{q}^{0} + \hat{\tilde{X}}_{q}^{0} \hat{F}_{q}^{0} \hat{\tilde{X}}_{q}^{0} \right] \lambda_{\omega}^{\alpha,r}. \qquad (\mathrm{C.3})$$

While the local part of the nonlocal bubble is zero, $\sum_{\mathbf{q}}' \tilde{X}_q^0 = 0$, according to Eq. (B.14), the vertex corrections introduced by F in general *do* have a local part. Therefore, the local DMFT susceptibility is in general not equal to the impurity susceptibility, $X_{\mathrm{loc},\omega}^\alpha \neq \hat{\chi}_\omega^\alpha$, because DMFT is not two-particle self-consistent. However, a high frequency expansion of Eq. (C.3) shows that the impurity and local lattice susceptibility share the same ω^{-2}-asymptote[5],

$$\lim_{\omega\to\infty} (\imath\omega)^2 X_{\mathrm{loc},\omega}^\alpha = \lim_{\omega\to\infty} (\imath\omega)^2 \chi_\omega^\alpha. \tag{C.4}$$

Fig. 4.3 shows on the example of a numerical calculation that on the one hand X_{loc} and χ are not identical but that their asymptotes are indeed the same.

Therefore, the asymptote of χ must likewise equal the kinetic energy of the lattice according to Eq. (C.2). However, since DMFT also satisfies the Ward identity of the impurity, the impurity susceptibility must satisfy a further constraint, namely Eq. (D.25) from chapter 3,

$$\lim_{\omega\to\infty} (\imath\omega)^2 \chi_\omega^\alpha = -2E_{\mathrm{kin}}^{\mathrm{imp}}, \tag{C.5}$$

where the superscript 'imp' denotes that the kinetic energy of the impurity is meant,

$$E_{\mathrm{kin}}^{\mathrm{imp}} = 2\sum_\nu' \Delta_\nu g_\nu, \tag{C.6}$$

which *a priori* need not have anything to do with the kinetic energy of the lattice. However, thanks to the satisfaction of the lattice Ward identity, which implies Eq. (C.2), and simultaneous satisfaction of the impurity Ward identity, implying Eq. (C.5), the kinetic energies of lattice and local reference system are exactly equal,

$$E_{\mathrm{kin}}^{\mathrm{imp}} = E_{\mathrm{kin}}^{\mathrm{lat}}. \tag{C.7}$$

Furthermore the kinetic energy may be obtained from the *1P level*, via Eqs. (C.1) and (C.6), or from the *2P level* (that is from the respective susceptibility), via Eqs. (C.2) and (C.5). These are four distinct ways to obtain the kinetic energy, belonging to two different levels of the DMFT approximation, which are nevertheless fully consistent by virtue of the 1P self-consistency combined with the satisfaction of local conservation laws.

It is often stressed that a conserving theory guarantees consistency between Green's function and thermodynamic potentials, which may be thought of as thermodynamic consistency of the 1P to the 0P level. Here the Ward identity guarantees to some extent also the thermodynamic consistency of the 1P to the 2P level by virtue of the Eqs. (C.2)

---

[5] Since $\sum_{\mathbf{q}}' \hat{\tilde{X}}_q^0 = 0$, a difference in the ω^{-2}-asymptotes of X_{loc}^α and χ^α must be due to the local vertex corrections, $\lambda_\omega^{\alpha,l} \sum_{\mathbf{q}}' \left(\hat{\tilde{X}}_q^0 \hat{F}_q^0 \hat{\tilde{X}}_q^0 \right) \lambda_\omega^{\alpha,r}$. These decay with ω^{-4} such that $\lim_{\omega\to\infty} (\imath\omega)^2 X_{\mathrm{loc}}^\alpha$ and $\lim_{\omega\to\infty} (\imath\omega)^2 \chi^\alpha$ are the same constant in Eq. (C.2).

and (C.5), which relate the kinetic energy to the susceptibility. However, one can not assume in general that thermodynamic observables computed from the 1P and from the 2P level need to be the same in conserving theories. This is clear, because local conservation laws do not guarantee two-particle self-consistency, which was explained in the introduction of chapter 3 (cf. Fig. 3.6) and which will be discussed for the case of DMFT below C.5. Likewise, the potential energy need not be consistent between 1P and 2P level, which will be discussed below. It is the consistency of the *kinetic* energy that is guaranteed by the Ward identity because it accounts for the currents the system is subjected to. Furthermore, the Ward identity guarantees the highly valuable consistency of zero-field derivatives and fluctuations, as discussed in Sec. D of chapter 3 (see also Fig. 3.8), allowing an unambiguous determination of second order critical points from the 1P and from the 2P level.

C.2 1P consistency of the potential energy

Q The potential energy of the Hubbard model is given as

$$E_{\text{pot}}^{\text{lat}} = U d^{\text{lat}}, \tag{C.8}$$

where $d_{\text{lat}} = \langle n_\uparrow n_\downarrow \rangle$ is the double occupancy of the lattice. Although d is a two-particle quantity, it can be calculated from 1P quantities via the Migdal Galitzkii formula. The latter is obtained in a similar way as the Schwinger-Dyson equation[6],

$$d_{\text{1P}}^{\text{lat}} = \frac{1}{U} \sum_k G_k \Sigma_k. \tag{C.9}$$

Here, the subscript 'lat' denotes again that the double occupancy of the lattice and the superscript '1P' implies that it is obtained from the 1P quantities Σ and G. An analogous formula can be derived for the Anderson impurity model,

$$d_{\text{1P}}^{\text{imp}} = \frac{1}{U} \sum_\nu{}' g_\nu \Sigma_\nu. \tag{C.10}$$

Since the self-energy of DMFT is local and equal to Σ_ν the momentum summation in Eq. (C.9) can be performed, which yields $d_{\text{1P}}^{\text{lat}} = \frac{1}{U} \sum_\nu' G_{\text{loc},\nu} \Sigma_\nu$. By virtue of the self-consistency condition $G_{\text{loc}} = g$ one therefore has $d_{\text{1P}}^{\text{lat}} = d_{\text{1P}}^{\text{imp}}$. As a consequence, the potential energies of lattice and impurity are consistent, provided they are calculated from the 1P level, i.e., the Migdal-Galitzkii formulae Eqs. (C.9) and (C.10),

$$E_{\text{pot}}^{\text{lat}} = E_{\text{pot}}^{\text{imp}} = \sum_\nu{}' g_\nu \Sigma_\nu. \tag{C.11}$$

---

[6] Namely, from the equation of motion of Green's function, i.e., when evaluating Eq. (C.6) of chapter 2 at $\tau = 0$ and for $V_{\mathbf{q}}^c = U, V^{x,y,z} = 0$, and making use of $\langle n^2 \rangle = \langle n \rangle + 2 \langle n_\uparrow n_\downarrow \rangle$. The contribution of $\langle n \rangle$ needs to be shifted into the chemical potential.

In combination with Eq. (C.6) for the kinetic energy one obtains an appealing formula for the total energy of the Hubbard model in DMFT approximation,

$$E_{\text{tot}} = E_{\text{kin}} + E_{\text{pot}} = \sum_{\nu}' g_\nu [\Sigma_\nu + 2\Delta_\nu], \qquad (C.12)$$

which is the total energy of the lattice *and* of the impurity model. Unfortunately, the consistency of the potential energy of DMFT only holds at the 1P level. This is because the double occupancy is also related to the local susceptibility at equal time, $X_{\text{loc},\tau=0} = \sum_\omega' X_{\text{loc},\omega}$,

$$X_{\text{loc},\tau=0}^c = -\langle \bar\rho^c \bar\rho^c \rangle = -(\langle n \rangle + 2d_{\text{lat}}^{2\text{P}} - \langle n \rangle^2), \qquad (C.13)$$

$$X_{\text{loc},\tau=0}^z = -\langle \bar\rho^z \bar\rho^z \rangle = -(\langle n \rangle - 2d_{\text{lat}}^{2\text{P}}), \qquad (C.14)$$

where $\bar\rho^\alpha = \rho^\alpha - \langle \rho^\alpha \rangle$ is the density fluctuation (note that $\rho^c = n_\uparrow + n_\downarrow$ and $\rho^z = n_\uparrow - n_\downarrow$). Here, the superscript '2P' denotes that d is obtained from the 2P quantity X. Above equations may be solved for d, which leads to

$$d_{2\text{P}}^{\text{lat}} = -\frac{1}{4}\left[X_{\text{loc},\tau=0}^0 - X_{\text{loc},\tau=0}^z - \langle n \rangle_{\text{lat}}^2\right]. \qquad (C.15)$$

The occupation number $\langle n \rangle$ was denoted with a label 'lat' here to distinguish it from the one of the impurity. Similarly, d may be obtained from the impurity susceptibility as,

$$d_{2\text{P}}^{\text{imp}} = -\frac{1}{4}\left[\chi_{\tau=0}^0 - \chi_{\tau=0}^z - \langle n \rangle_{\text{imp}}^2\right]. \qquad (C.16)$$

The self-consistency condition implies that $\langle n \rangle_{\text{lat}} = \langle n \rangle_{\text{imp}}$. The remaining quantities in Eqs. (C.15) and (C.16) need not be identical, since in general $X_{\text{loc}} \neq \chi$. As a consequence, the potential energy of DMFT is not thermodynamically consistent on the 2P level [84], except in the limit of infinite coordination number[7]. While this may seem like a minuscule flaw of the DMFT approximation, it is actually related to the much more significant drawback that the DMFT susceptibility violates the Mermin-Wagner theorem in two dimensions. If X_{loc} was indeed equal to χ then it would follow from a theorem by Vilk and Tremblay that the Mermin-Wagner theorem must hold [157]. This can be seen as one among several motivations to make DMFT two-particle self-consistent, which will be the subject of chapter 5.

---

[7] Thermodynamic consistency is recovered in the limit of infinite coordination number. This is because the nonlocal vertex corrections X_q' in Eq. (B.20) vanish at any 'generic' vector $\mathbf{q}$ of the Brillouin zone [32], where the notion 'generic' may be understood as 'randomly chosen from'. Since non-generic vectors represent only a zero-dimensional subset of the Brillouin zone in infinite dimensions, they do not contribute when the sum over $\mathbf{q}$ is taken, $\sum_{\mathbf{q}}' X_{\mathbf{q}}' = 0$. Consequently, one has $X_{\text{loc}} = \chi + \sum_{\mathbf{q}}' X_{\mathbf{q}}' = \chi$.
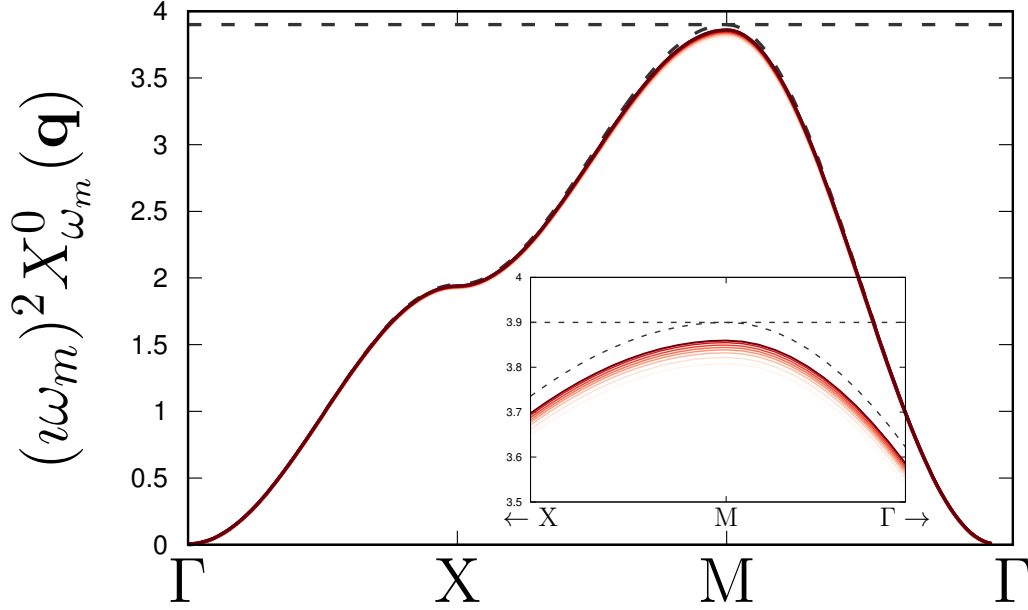
FIGURE 4.4: The asymptote of the charge susceptibility of the Hubbard model on the square lattice in DMFT (red lines) as a function of $\mathbf{q}$. Darker red indicates a larger Matsubara index $m \leq 20$. The dashed curve marks the analytical expression for $\lim_{m \to \infty} (\imath\omega_m)^2 X^c_{\mathbf{q}\omega_m}$, Eq. (C.18). The dashed straight line indicates the value $-4E_{\mathrm{kin}}$, (half-filling, $U = 6, \beta = 2$). The inset shows a closeup of the region around the M point. The agreement with Eq. (C.18) also holds for the spin susceptibility (not shown).

C.3   Asymptote of the lattice susceptibility and f-sum rule

The consistency of the kinetic energy between 1P and 2P level in DMFT manifests not only in the local susceptibility but also in its momentum dependence, since the Ward identity determines the ω^{-2}-asymptote of the susceptibility, see chapter 3, Eq. (D.19),

$$\lim_{\omega \to \infty} (\imath\omega)^2 X^\alpha_{\mathbf{q}\omega} = \sideset{}{'}\sum_{\mathbf{k}\sigma} \langle n_{\mathbf{k}\sigma} \rangle \, (\varepsilon_{\mathbf{k}+\mathbf{q}} + \varepsilon_{\mathbf{k}-\mathbf{q}} - 2\varepsilon_{\mathbf{k}}). \tag{C.17}$$

In the Hubbard model on a square lattice with nearest neighbor hoppings the $\mathbf{q}$-dependence of this expression can be peeled out, leading to [65],

$$\lim_{\omega \to \infty} (\imath\omega)^2 X^\alpha_{\mathbf{q}\omega} = (\cos q_x + \cos q_y - 2) \, E_{\mathrm{kin}}. \tag{C.18}$$

The amplitude of this function is therefore entirely determined by the kinetic energy defined in Eq. (C.1), which has been seen above to be the same on the lattice as on the impurity. We can convince ourselves in Fig. 4.4 that Eq. (C.18) is indeed satisfied in a DMFT calculation.

It should be noted that Eq. (C.17) is equivalent to the f-sum rule, Eq. (D.22) of chapter 3, see also [65]. DMFT satisfies the f-sum rule, since it follows from the lattice Ward identity Eq. (A.1), while its consistency with the kinetic energy of the impurity is a consequence of the self-consistency condition $G_{\text{loc}} = g$.

C.4 Phase transitions in DMFT - a matter of the bath

A physically very significant synergy of the Ward identity and 1P self-consistency is the exact relation of a second order phase transition in the lattice approximation to a broken symmetry in the hybridization function of the impurity model. This will be illustrated on the example of a transition to ferromagnetic order but the discussion can be repeated for other phase transitions. $\color{green}{QP}$

It was shown in chapter 3, Eq. (D.34), that the Ward identity implies that the zero-field derivative of the magnetization is consistent with the susceptibility,

$$\frac{d \langle m \rangle}{dh} = -X^s_{q=0}. \tag{C.19}$$

Here, $X^s = X^{x,y,z}$ is the spin susceptibility of the paramagnet and h is a homogeneous magnetic field, the conjugate field of a ferromagnetic phase transition[8]. It should be stressed again that, while Eq. (C.19) may seem trivial because it is often used to *define* the susceptibility, it is in general not guaranteed to hold when global spin conservation is violated. This is because both on the LHS and on the RHS of Eq. (C.19) an approximation is inserted, here that is the magnetization $\langle m \rangle = \sum_k (G_{k\uparrow} - G_{k\downarrow})$ of the *lattice* on the LHS, where G is the DMFT Green's function, and X on the RHS, which is the DMFT susceptibility. Fortunately, the lattice Ward identity Eq. (A.1) guarantees that Eq. (C.19) holds.

However, in DMFT the zero-field derivative of $\langle m \rangle$ is subject to a second constraint, due to the impurity Ward identity Eq. (A.2) also Eq. (D.46) from chapter 3 must hold,

$$\frac{d \langle m \rangle}{dh} = - \sum_{\nu\nu'\sigma}' \left(1 - \frac{d\Delta_{\nu\sigma}}{dh} \right) \chi^{\overline{\sigma}\overline{\sigma}}_{\nu\nu',\omega=0}, \tag{C.20}$$

where χ and Δ on the RHS are the generalized susceptibility and the self-consistent hybridization function of the impurity model, respectively. Likewise, $\langle m \rangle = \sum_\nu' (g_{\nu\uparrow} - g_{\nu\downarrow})$ is the magnetization of the *impurity*.

The crucial point is now that the LHS of Eq. (C.20) and the LHS of Eq. (C.19) must be equal by virtue of the self-consistency condition $G_{\text{loc}} = g$, consequently their RHSs must

---

[8] Likewise, one may consider a bipartite antiferromagnet with the sublattice magnetization $\langle m \rangle$ where $\frac{d\langle m \rangle}{dh} = -X^s_Q$ holds, see chapter 3, Eq. (D.41). In this case h is a staggered magnetic field and $Q = (\mathbf{Q}, \omega = 0)$ is the ordering vector.

be equal as well, which implies

$$X^s_{q=0} = \sum_{\nu\nu'\sigma}{}' \left(1 - \frac{d\Delta_{\nu\sigma}}{dh} \right) \chi^{\overline{\sigma\overline{\sigma}}}_{\nu\nu',\omega=0}. \tag{C.21}$$

This equation relates exactly the DMFT susceptibility of the lattice on the LHS to the (generalized) susceptibility of the impurity on the RHS. In the Hubbard model the spin susceptibility X^s may diverge, most commonly considered is the antiferromagnetic phase, where $X^s_{\mathbf{Q},\omega=0}$ diverges at the ordering vector Q, but also Nagaoka ferromagnetism is possible at very large interaction $U \to \infty$, which is signaled by the divergence of $X^s_{q=0}$ [95, 114]. According to Eq. (C.21) the divergence of the DMFT susceptibility on the LHS is inevitably accompanied by a divergence of the RHS. However, χ on the RHS is the generalized susceptibility of a zero-dimensional impurity model, which can not diverge at finite temperature since this model has at most *quantum* phase transitions at $T = 0$. Therefore, the only place where a divergence can happen on the RHS of Eq. (C.21) is in the zero-field derivative of the hybridization function, $\frac{d\Delta}{dh}$. As a consequence, a magnetic phase transition at finite temperature can occur within DMFT only due to a broken symmetry in the bath Δ, which is determined according to the self-consistency condition $G_{\text{loc}} = g$. Since the Ward identity in general guarantees the consistency of zero-field derivatives and susceptibilities, it seems that similar considerations hold for other phase transitions as well.

It should be noted that a somewhat comparable situation arises in case of the Mott transition, where it is likewise the hybridization function that is responsible for the phase transition on the lattice by developing a gap, this is discussed in, e.g., chapter 13 of Ref. [1].

C.5   The problem of two-particle self-consistency in DMFT

Despite the great aspects of DMFT with respect to thermodynamic consistency, it suffers like many other conserving theories from the dilemma of two-particle self-consistency, which was illustrated in Sec. B.6 of chapter 3. In DMFT this unfolds as follows: The approximate Luttinger Ward functional is the one of the Anderson impurity model, $\Phi \approx \phi$. The functional Schwinger-Dyson equation yields the conserving 1P self-energy $\Sigma^1 = \delta\phi/\delta g = \Sigma_\nu$, which is the local self-energy of the AIM, and which is then given as the Hartree (and Fock) diagrams plus vertex corrections. In DMFT the latter are given by the T-matrix $F^1 = f_{\nu\nu'\omega}$, which is the local T-matrix of the impurity. A crucial aspect in DMFT is that Σ and f are numerically exact, which means that f contains all vertex corrections to Σ. If the 2P self-energy $\Gamma^1 = \delta\Sigma/\delta g = \gamma_{\nu\nu'\omega}$ and Σ_ν are used to solve the local Bethe-Salpeter equation, it leads to F^2,

$$\hat{F}^2 = \hat{\gamma}_\omega + \hat{\gamma}_\omega \hat{\chi}^0_\omega \hat{F}^2. \tag{C.22}$$

Here, $\chi^0_{\nu\omega} = g_\nu g_{\nu+\omega}$ is the bubble of impurity Green's functions. Due to the numerical exactness, however, one has $F^2 = F^1 = f_{\nu\nu'\omega}$. This means that the dilemma of two-particle self-consistency is not there on the impurity: When using the integral Schwinger-Dyson
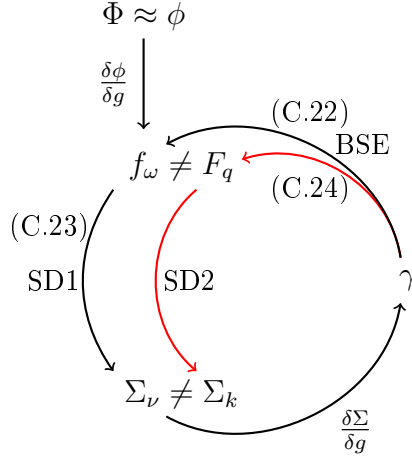
FIGURE 4.5: The problem of two-particle self-consistency in DMFT. The impurity model is solved exactly, such that Σ, γ, and f form a two-particle self-consistent sequence via the Bethe-Salpeter and integral Schwinger-Dyson equation of the impurity. In the DMFT approximation the T-matrix F is finally constructed by replacing the impurity bubble χ_ω^0 by a bubble X_q^0 of DMFT Green's functions [cf. Eqs. (C.22) and (C.24)], which lifts the consistency (red lines). See also Sec. B.6 and Fig. 3.6 of chapter 3.

equation (SD1) of the impurity [cf. Eq. (C.16)], one obtains

$$\Sigma^2 = \frac{U \langle n \rangle}{2} - U \sum_{\alpha\nu'\omega} g_{\nu'} g_{\nu'+\omega} f_{\nu'\nu\omega}^{\uparrow\downarrow} g_{\nu+\omega}, \tag{C.23}$$

which is the same 1P self-energy one started with, $\Sigma^2 = \Sigma^1 = \Sigma_\nu$. This is represented by the closed sequence drawn in black lines in Fig. 4.5. In DMFT the dilemma of two-particle self-consistency comes in because one uses the exact self-energy of the AIM as an approximation for a different system, the Hubbard model. Then, instead of the local Bethe-Salpeter Eq. (C.22), one solves,

$$\hat{F}^2 = \hat{\gamma}_\omega + \hat{\gamma}_\omega \hat{X}_q^0 \hat{F}^2, \tag{C.24}$$

where $X_{kq}^0 = G_k G_{k+q}$ is a bubble of DMFT Green's functions, $G_k^{-1} = \imath\nu + \mu - \varepsilon_{\mathbf{k}} - \Sigma_\nu$. Instead of the local T-matrix f of the impurity, the Bethe-Salpeter Eq. (C.24) yields $F^2 = F_{\nu\nu'q}$, which is the $\mathbf{q}$-dependent T-matrix of DMFT. Therefore, $F^1 \neq F^2$ in DMFT. If F^2 was now used to calculate a new $\Sigma^2 = \Sigma_k$ from the Schwinger-Dyson equation (SD2) again, it is $\mathbf{k}$-dependent, and evidently $\Sigma^1 \neq \Sigma^2$. These steps are depicted by the red lines in Fig. 3.6.

D   The two-particle spectrum

QP One of the consequences of global charge and spin conservation in the disordered phase is that the 2P spectrum in both sectors must be ungapped at the homogeneous wave vector $\mathbf{q} = 0$, see chapter 3, Eq. (D.3),

$$\imath\omega X^\alpha_{\mathbf{q}\omega} = 0. \tag{D.1}$$

An explicit calculation of the electromagnetic response kernel shows that this collective mode behaves as $\frac{|\mathbf{q}|^2}{\omega^2}$ at small wave vectors $|\mathbf{q}| \sim 0$. For the Hubbard model on the square lattice this calculation was done in Ref. [39]. The collective mode is the lattice counterpart of the zero-sound that was predicted by L. Landau as part of his theory of Fermi liquids, which was observed in liquid Helium in the experiment. On the lattice, however, this collective mode is always damped above $T = 0$ [110].

It is intriguing to observe the fate of the collective excitations at different values of the interaction and near the Mott crossover of the Hubbard model. Here DMFT is a viable approach, since it provides a non-perturbative *and* conserving description of the intermediate coupling range of the Hubbard model. While a non-perturbative starting point allows to observe Mott physics, it is necessary to obey at least Eq. (D.1), which follows from global conservation, in order to achieve a physically sound description of the collective mode.

Fig. 4.6 shows the two-particle spectrum of DMFT for the half-filled Hubbard model on the square lattice with nearest neighbor hopping $t = 1$ at the inverse temperature $\beta = 2$ for different values of the interaction $U = 1, 4, 8$. This is obtained by an analytical continuation via a pade approximant of $X^{\alpha=c,z}_{\mathbf{q}\omega}$ from the Matsubara to the real axis and plotting $\operatorname{Im} X^\alpha_{\mathbf{q}}(E + \imath\delta)$, where E is the real energy and $\delta = 0.1$ the distance to the real axis (see also implementation notes below). The momentum $\mathbf{q}$ follows the high-symmetry path of the Brillouin zone, $\Gamma \to X \to M$.

The considered values of the interaction are all below the critical interaction $U_c \sim 9.4$ of the Mott transition, which is roughly the value predicted by DMFT. However, at the rather large temperature of $T = \beta^{-1} = 0.5$ there is only a Mott crossover with a steep decline of the quasiparticle weight. At the smallest interaction $U = 1$ the spectra of charge and spin excitations are very similar, with a rather sharp collective mode at small $\mathbf{q}$ and a broad and incoherent excitation spectrum around the M-point[9]. The similarity between charge and spin excitations at small U is due to the vicinity of the non-interacting limit $U \to 0$, where DMFT becomes exact and where its susceptibility is given by the Lindhard function [cf. (D.48) of chapter 3 for $h = 0$]. The latter is also the non-interacting limit of the RPA and corresponds to $X^\alpha_q = 2 \sum_k G^0_k G^0_{k+q}$, which is independent of the channel index α, hence the similarity of the spectra for $\alpha = c$ and $\alpha = z$ at small U.

---

[9]Since the system is paramagnetic, the spin susceptibility is the same in all spin channels, $X^z = X^x = X^y$. The channel X^z is shown, since the CTQMC solver used to produce Fig. 4.6 measures the T-matrix of the impurity only in the longitudinal channel $f^{\sigma\sigma'}$ (not $f^{\sigma\bar{\sigma}}$). One has $f^z = f^{\uparrow\uparrow} - f^{\uparrow\downarrow}$, see also Eq. (B.16) of chapter 2.

An increase of the interaction highlights one of the key features of the DMFT description of the Hubbard model, which is the separation of the energy scales of charge and spin excitations: While the main spectral features of the charge excitations migrate to larger values of $E \sim U$, their overall weight shrinks drastically, in particular in the vicinity of the Mott transition (compare the maxima of the color scales in the left column of Fig. 4.6). At the same time, the spin excitations move to small $E \sim t^2/U$, where at $U = 8$ their spectral weight is mainly centered at the M point, $\mathbf{Q} = (\pi, \pi)$, the direction in which the spin susceptibility of DMFT develops its instability.

It should be noted that the total spectral weight of the charge and spin excitations is not fixed to a specific value, such as the total spectral weight of the density of states, which must always be equal to unity. Instead, only the first moment of the spectral weight of the collective excitations is fixed by Eq. (D.21) of chapter 3,

$$\lim_{\omega \to \infty} (\imath\omega)^2 X_{\mathbf{q}\omega}^{\alpha} = -\int_{-\infty}^{\infty} \frac{dE}{\pi} E \operatorname{Im} X_{\mathbf{q}}^{\alpha}(E + \imath\delta) = (\cos q_x + \cos q_y - 2) E_{\text{kin}}, \qquad \text{(D.2)}$$

where the expression on the RHS is found using Eq. (C.18), which is valid in the Hubbard model on the square lattice with nearest neighbor hoppings. Hence, the first spectral moment of the collective excitations is apparently completely determined by the kinetic energy E_{kin}. One can therefore understand the reduction in the total spectral weight of the charge excitations in the left column of Fig. 4.6 for increasing interaction as a requirement of Eq. (D.2): The integral in that relation puts a stronger weight on spectral weight at high energies. Therefore, as the charge excitations are shifted to higher energies, their total weight must decrease, so the value of the first spectral moment remains in agreement with the RHS of Eq. (D.2). Since the latter is given by the kinetic energy, which is reduced at large interactions, this effect is emphasized even further.

Although the similarity of the charge and spin excitations in the non-interacting limit seems to be completely lifted at large interaction $t \ll U < \infty$, the high frequency asymptotes of $X_{\mathbf{q}\omega}^c$ and $X_{\mathbf{q}\omega}^z$ on the LHS of Eq. (D.2) remain always *equivalent*, and so do the first spectral moments of $\operatorname{Im} X^c(E + \imath\delta)$ and $\operatorname{Im} X^z(E + \imath\delta)$, since they have to be equal to the same RHS. These equivalences between the charge and spin sectors can be traced back to the Ward identity of the Hubbard model, Eq. (A.1), whose LHS is independent of the channel index α. The Ward identity implies that the susceptibilities are asymptotically given by Eq. (D.2), which was shown to hold in DMFT in Fig. 4.4, and which inherits the feature that it is independent of the channel. The same can be observed in the local susceptibility shown in Fig. 4.3, where both X_{loc}^c and X_{loc}^z approach the same asymptote at large ω. This is a consequence of the fact that charge and spin are only transported via the hopping and *not* by the interaction [see Sec. D.5 and below Eq. (E.2) in chapter 3]. If this was not so the interaction would manifest itself in an additional term in the susceptibility asymptote [cf. chapter 3, Eq. (D.19)], which typically *does* depend on the channel index α. However, since the Hubbard interaction $U n_\uparrow n_\downarrow$ conserves both the charge and the spin densities, this term is absent, hence the equivalence in the asymptotes. Following this reasoning backwards, this means that approximations to the Hubbard model which

$$\mathrm{Im}\, X_{\mathbf{q}}^{c}(E + \imath\delta) \qquad\qquad \mathrm{Im}\, X_{\mathbf{q}}^{z}(E + \imath\delta)$$
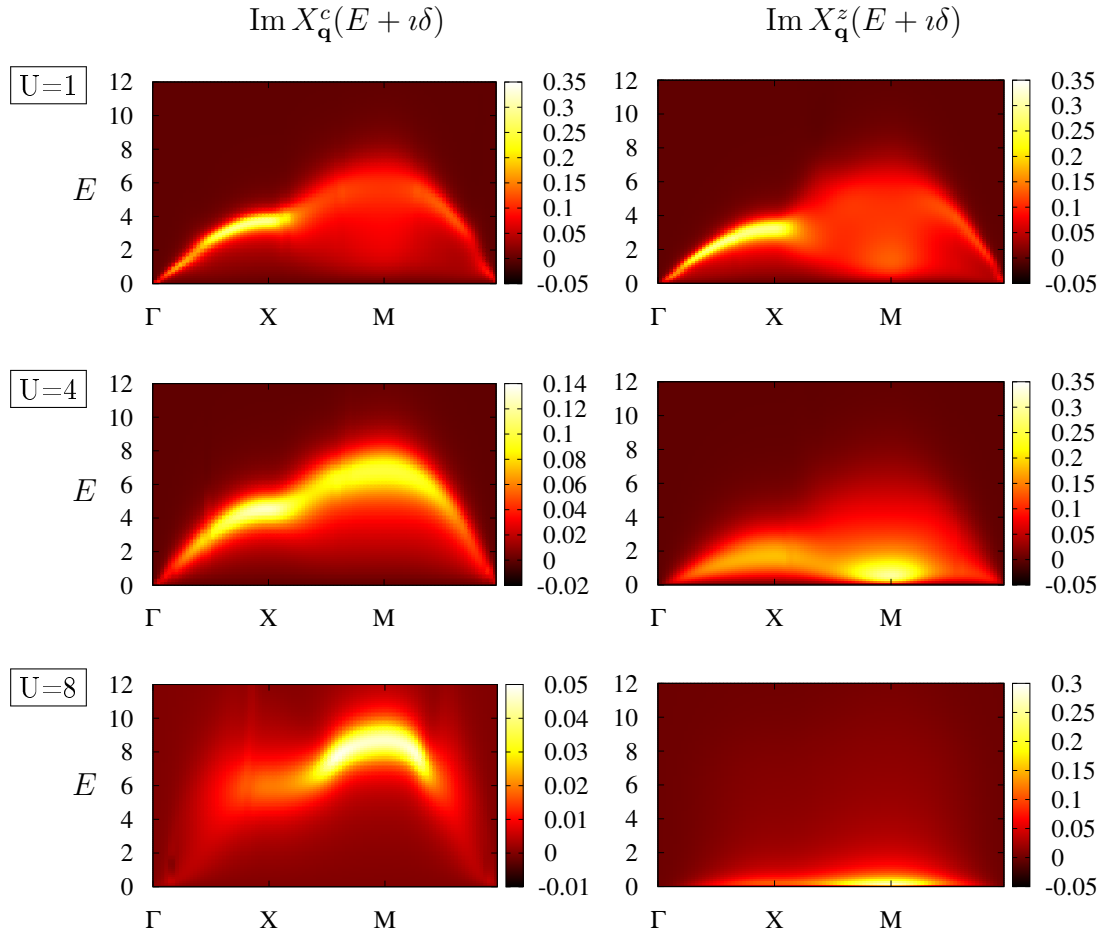

FIGURE 4.6: Spectra of the charge (left) and spin (right) excitations in the half-filled Hubbard model on the square lattice with nearest neighbor hoppings for different values of the interaction. At small U charge and spin excitations show similar spectra, that are well described by the Lindhard function [cf. chapter 3, Eq. (D.48)]. At large interaction the energy scales of charge and spin excitations separate into U and t^2/U, respectively. Both channels show a collective mode at the Γ-point that vanishes in the charge channel as the Mott transition is approached.

assign different asymptotes to the susceptibilities in the charge and in the spin channel, respectively, can not be conserving, since they violate this requirement. DMFT correctly reproduces this feature of the Hubbard model and its Ward identity.

Likewise in agreement with the latter, Fig. 4.6 shows that the collective modes at the Γ-point are ungapped in both channels, as required by Eq. (D.1). In the charge channel, however, the collective mode disappears completely as the Mott transition is approached (not shown). It is demonstrated in detail in Ref. [39] that its disappearance is accompanied by a vanishing compressibility, which is proportional to $\frac{d\langle n\rangle}{d\mu}$. The latter must vanish in the Mott phase, since the density of states is gapped, and therefore the occupation number at the Fermi level remains unchanged by a small variation of μ. Although the collective mode of the charge channel becomes faint close to the Mott boundary, it emerges again at low temperature, as will be seen in the following subsection, since the system retrieves more of the characteristics of a Fermi liquid at low T.

The instability of the DMFT susceptibility in the spin channel is the reason that the high temperature $T = 0.5$ is considered, since it diverges already at moderate temperatures and interaction, which in the present case implies a violation of the Mermin-Wagner theorem. Below the antiferromagnetic instability a calculation of the *paramagnetic* spin susceptibility leads to divergences in more and more points $\mathbf{q} \approx \mathbf{Q}$. Near such a divergence at some point $\mathbf{q}$, an eigenvalue of the matrix $(N\beta)^{-1}\hat{X}^0_{\mathbf{q},\omega=0}\hat{\gamma}^z_{\omega=0}$ approaches unity, which leads to a divergence of the Bethe-Salpeter equation in this point [cf. Sec. B.2 in chapter 2]. When lowering the temperature even further, the eigenvalue exceeds unity and the susceptibility at this value of $\mathbf{q}$ becomes positive, which is unphysical[10]. The paramagnetic spin susceptibility of DMFT can therefore only be considered at large temperature or at small $\mathbf{q}$, which is a severe drawback to the applicability of DMFT as a means to observe the spectrum of spin excitations, except if the instability is suppressed, e.g., by frustration. The instability also constitutes a delicate obstacle for extensions of DMFT that aim at incorporating a $\mathbf{k}$-dependence into the fermionic self-energy [119]. This is because the latter needs to be calculated via the Schwinger-Dyson equation, Eq. (C.12) of chapter 2, from the T-matrix F, which diverges in the spin channel. The charge channel is not affected by this and it is possible to study charge excitations at low temperature using DMFT.

E Application I: Low-temperature revival of a collective mode near the Mott phase

As mentioned above, the collective mode of the charge excitations described by DMFT disappears at the Mott transition with the compressibility. When the interaction is increased, the collective mode becomes faint and incoherent already in the vicinity of the Mott phase (or near the Mott crossover), as seen in the bottom left panel of Fig. 4.6. Since the approach of the Mott transition with the interaction is also accompanied by a departure from Fermi

QP

---

[10] This change in the sign is to be understood in the same way as it happens at a divergence of the RPA susceptibility in chapter 2, Eq. (D.9), where the denominator of $2X^0_q/(1 - X^0_q U^\alpha)$ changes sign.

liquid physics, it is interesting to follow the behavior of the collective mode upon lowering the temperature, where Fermi liquid features are then more pronounced again. One may expect that at low temperature the collective mode shows more of the characteristics that it has at smaller interaction. It will be shown here on the example of the half-filled Hubbard model on the isotropic *triangular* lattice with nearest neighbor hoppings that DMFT indeed predicts such a revival of the collective mode at low temperature in the vicinity of the Mott phase. The following results are unpublished, but may serve as a starting point for a larger study in the future.

E.1   The Hubbard model on the triangular lattice

QP   The bare dispersion relation of the single-band Hubbard model on the anisotropic triangular lattice with nearest neighbor hoppings has the dispersion relation,

$$\varepsilon_{\mathbf{k}} = -2\left[t_2\cos(k_x) + 2t_1\cos\left(\frac{k_x}{2}\right)\cos\left(\frac{k_y\sqrt{3}}{2}\right)\right],\tag{E.1}$$

where the ratio t_1/t_2 controls the anisotropy. This model is of some relevance as an effective Hamiltonian for the organic charge transfer salts, which are possible candidates for the realization of a spin liquid phase [132]. An application of the finite temperature Lanzcos method reveals properties characteristic of a bad metal [62], which shows the eponymous feature that the resistivity follows a $\propto T$-dependence that extrapolates to a finite value at $T = 0$. This behavior is observed frequently in systems close to the Mott insulating phase, both at half-filling near the critical interaction, $U \lesssim U_c$, as well as in doped Mott insulators [28, 52, 159]. At temperatures below the bad metal regime lies a Fermi liquid with a low coherence temperature T_{coh}, where quasiparticles are formed and where the resistivity finally follows a $\propto T^2$-dependence that leads to zero.

In the following, a bad metal and a Fermi liquid regime will be identified near the Mott transition of the Hubbard model on the triangular lattice. Unfortunately, it is rather difficult to calculate the resistivity accurately from the Matsubara axis, but other markers may be used to identify a bad metal: One of them is the existence of local magnetic moments, which emerge at elevated temperature because thermal excitations undermine the Kondo screening of the spins. In the DMFT picture the local impurity spin is then decoupled from the bath, a situation which has more options to be realized than the Kondo state, leading to a large entropy. At the same time, the impurity spin is then available to align itself with an outer magnetic field, instead of being entangled with the bath in the Kondo state, which has no net magnetic moment. This leads to a Curie-Weiss law in the temperature dependence of the local spin susceptibility above T_{coh}, where $X^z_{\text{loc},\omega=0} \sim (T + \text{const})^{-1}$. Below T_{coh}, on the other hand, the local moments are screened by the bath and thus the local spin susceptibility, which describes the response to an outer magnetic field, saturates at low temperature (i.e., Pauli paramagnetism).
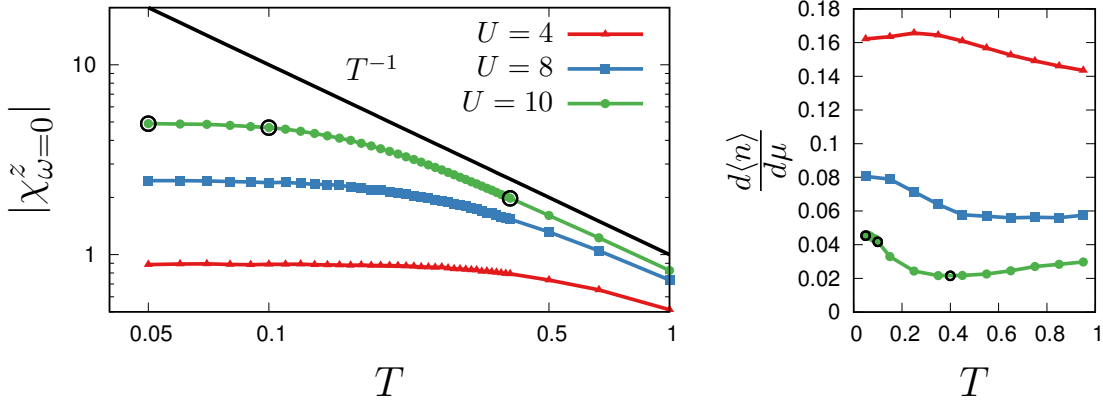
FIGURE 4.7: Left: Local spin susceptibility χ^z of the half-filled Hubbard model on the triangular lattice in DMFT approximation. At $U = 10$ (green), close to the Mott phase, χ^z shows a Curie-Weiss law $\propto (T + \text{const})^{-1}$ already at $T \gtrsim 0.4$ [cf. Curie law (black)], signaling the existence of local moments. χ^z saturates towards the Pauli paramagnetism of the Kondo state below $T \sim 0.2$. Right: $d\langle n\rangle/d\mu$, which is proportional to the compressibility, shows for $U = 10$ a minimum near $T \sim 0.4$ and an upturn at $T \sim 0.2$, while a first sign of saturation is visible at $T \sim 0.05$. The magnitude of $d\langle n\rangle/d\mu$ determines the spectral weight of the collective mode of the charge excitations, they vanish together in the Mott phase [39].

E.2   Identification of the bad metal and of the Fermi liquid regimes

For the purposes of this text, the Hubbard model on the isotropic triangular lattice ($t_1 = t_2 = 1$) will serve as a showcase model, in order to observe the behavior of the collective mode of the charge excitations above and below T_{coh} in DMFT approximation. To this end, these regimes are firstly identified in the local spin susceptibility $\chi^z_{\omega=0}$ of the impurity model[11], as well as in the quasiparticle weight Z and in the total energy E_{tot}. The local spin susceptibility is shown in the left panel of Fig. 4.7 for three values of the interaction, $U = 4, 8, 10$, that all lie below the critical value of the Mott transition of $U_c \sim 12 - 15$ predicted by DMFT[12]. At small interaction $U = 4$ the Pauli paramagnetism is stable over a wide temperature range, which corresponds to an uncorrelated metal without local moments. Then χ^z begins to bend towards a Curie-Weiss law at very high T. On the other hand, at $U = 10$, which is much closer to U_c, a Curie regime is already reached at a moderate temperature of $T \gtrsim 0.4$. This is also visible in $\frac{d\langle n\rangle}{d\mu} = -X^c_{q=0}$ in the right panel of Fig. 4.7, which develops a minimum at this temperature and between $U = 8$ and $U = 10$, that is not there at small interaction. This suggests that at $U = 10$ there is an intermediate temperature regime bounded from below by roughly $T \sim 0.4$, where local

---

[11] As discussed in Sec. C.2, there is an ambiguity with respect to the local susceptibility one should consider, since in DMFT $X^z_{\text{loc}} \neq \chi^z$ [see also Fig. 4.3]. In principle, both quantities should show the transition from Pauli to Curie paramagnetism but due to the divergence of X^z at low temperature this option is ruled out.

[12] See supplemental material of [62] for a comprehensive list of values predicted for U_c.
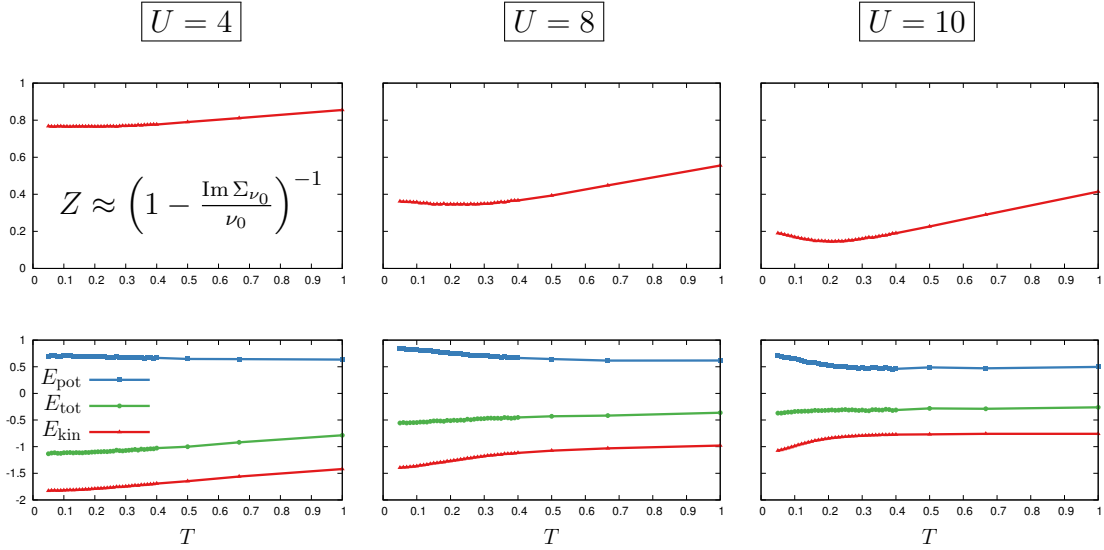
FIGURE 4.8: Top: Approximate quasiparticle weight Z (top) as a function of temperature. Z is of order ~ 1 at $U = 4$ and approaches its value at $T = 0$ monotonically, while for $U = 10$, which is near $U_c \sim 12 - 15$, Z is small and shows a change in slope at $T \sim 0.2$. Bottom: Kinetic, potential, and total energy corresponding to the top. At $U = 10$ both E_{kin} (red) and E_{pot} (blue) both show a change in slope and magnitude, whose onset corresponds to the change in slope of Z above. Above the crossover $T \sim 0.2$ local moments begin to form (see Fig. 4.7).

moments are formed, since the Kondo screening is undermined by thermal excitations. The green line in the right panel of Fig. 4.7 further shows that one leaves this regime upon lowering the temperature, where $\frac{d\langle n \rangle}{d\mu}$ shows a rather strong upturn at $T \sim 0.2$. It finally begins to saturate around $T \sim 0.05$, indicating that the coherent regime is reached. The coherence temperature of the Fermi liquid should lie between the saturated coherent and the saturated local moment regime.

In order to further confirm the existence of a crossover at $T \sim 0.2$ between two temperature regimes for $U = 10$, the approximate quasiparticle weight Z and the total energy are shown in Fig. 4.8. In DMFT the quasiparticle weight does not depend on the momentum. Since it is a real axis quantity, it is not directly available in the CTQMC calculations performed here (see implementation notes below). Instead, it is computed using the approximate formula Eq. (D.54) from chapter 3 for the scattering rate, such that the quasiparticle weight is given to a first approximation as $Z \approx (1 - \text{Im}\,\Sigma_{\nu_0}/\nu_0)^{-1}$. This approximation becomes exact in the limit $T \to 0$, but has a systematic error. In the top right panel of Fig. 4.8 it can be seen that at $U = 10$ the quasiparticle weight indeed shows a change in slope at $T \sim 0.2$. Although Z is only coarsely approximated by the self-energy on the Matsubara axis, one can be rather certain about the existence of a crossover at this point, since such a

strong bend is not there at $U = 4$, and still not clearly developed at $U = 8$.[13] Finally, the bottom panels of Fig. 4.8 show the total energy computed according to Eq. (C.12). The trend from small to large interaction is, of course, that the absolute value of the kinetic energy E_{kin} shrinks, since the punishment for the creation of double occupancies becomes larger. Also the potential energy $E_{\mathrm{pot}} = Ud$ is slightly reduced from $U = 8$ to $U = 10$, since localization begins to set in, such that the increase in U is overcompensated by a decrease in the double occupancy d. While the overall temperature dependence of E_{kin} and E_{pot} at $U = 4$ is weak and monotonous, the bottom right panel of Fig. 4.8 for $U = 10$ signals a rapid delocalization of the charge carriers below $T \sim 0.2$, where both E_{kin} and E_{pot} grow to values that are comparable to those at smaller interaction. The location $T \sim 0.2$ of this presumed crossover coincides with the change in slope of the quasiparticle weight Z in the top right panel of Fig. 4.8, with the upturn in $\frac{d\langle n \rangle}{d\mu}$ on the right of Fig. 4.7, and also with the bend in χ^z between the Pauli and the Curie-Weiss regime on the left of the same figure. It can therefore be concluded that DMFT predicts at $U = 10$ a crossover from a Fermi liquid with a coherence temperature $0.05 \lesssim T_{\mathrm{coh}} \lesssim 0.4$ to a bad metal regime with local moments, that is best realized from roughly $T \gtrsim 0.4$ upwards.

E.3   Revival of the collective mode

Let us now come back to the collective mode of the charge excitation spectrum near the Γ-point, whose spectral weight was explained earlier to decline with $d\langle n \rangle/d\mu$ upon an increase of U, until they vanish together in the Mott phase. According to the right panel of Fig. 4.7, the value of $d\langle n \rangle/d\mu$ roughly doubles when going from $T = 0.4$ in the bad metal to $T = 0.05$ in the Fermi liquid, it is to be expected that this has an effect on the shape of the collective mode. Black circles in Fig. 4.7 mark three values of the temperature, $T = 0.4, 0.1, 0.05$, where CTQMC calculations were performed that are sufficiently accurate to allow an analytical continuation of $X^c_{\mathbf{q}\omega}$ to the real axis via a Pade approximation (see implementation notes below). At least at small values of $\mathbf{q}$, where all spectral features of the excitation spectrum are located at small energies, and which is also the region that is of interest here, a qualitative discussion of the spectral line shapes is possible: Fig. 4.9 shows $\mathrm{Im}\, X^c_{\mathbf{q}_x}(E + \imath\delta)$ at $\mathbf{q}_x = x\mathbf{M}_3/N_k$, $x = 1, ..., 6$, where the path from Γ to the high-symmetry point $\mathbf{M}_3 = (\pi, -\pi/\sqrt{3})$ has been discretized into $N_k = 64$ steps. The figure shows that the temperature regime has indeed a significant influence on the spectrum of charge excitations near the Γ-point. While in the bad metal regime at $T = 0.4$ the spectrum is incoherent and has only a tiny spectral weight (see scale on the left panel of Fig. 4.9), the magnitude of the spectral lines increases by one order of magnitude on the way to $T = 0.1$, and by a further order of magnitude to $T = 0.05$, which is in the Fermi liquid regime. At the same time, the spectral lines are considerably sharpened as T is lowered, marking the revival of a well-defined collective mode in the Fermi liquid. This proves the working hypothesis of this section qualitatively, and shows that the fate of the collective mode near the Mott phase

QP

---

[13] It should be mentioned that the minima of Z in the center and in the right panel of Fig. 4.8 are probably an artifact of the approximation to the scattering rate, since accurate real axis calculations usually reveal a $Z(T)$ that is constant below T_{coh} and which increases monotonously above it [27, 155].
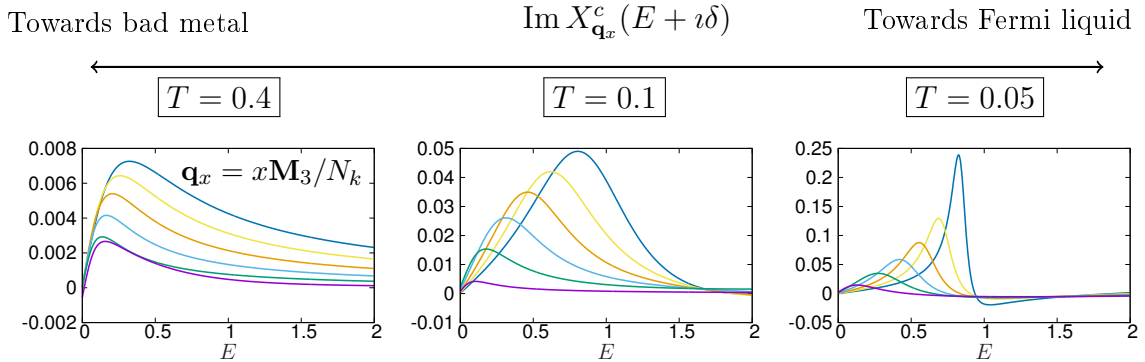
FIGURE 4.9:   Spectral lines of the charge excitations around the Γ-point for $U = 10$ at the six smallest increments of the discretized path to the M_3-point (see text, larger magnitude corresponds to larger $\mathbf{q}$, the blue lines are at $x = 6$). Between $T = 0.4$ and $T = 0.05$ lies the coherence temperature T_{coh} of the Fermi liquid. The excitation spectrum is incoherent in the bad metal and there is almost no spectral weight at the Γ-point. In the Fermi liquid regime the spectral lines are sharpened and their amplitude has increased by two orders of magnitude. This shows that in the DMFT picture the temperature is an important player around the fate of the collective mode near the Mott phase.

is determined to a large degree by the temperature. It seems plausible that the width, shape, and possibly also the position of the spectral lines in Fig. 4.9 is determined by the temperature at high T and by Fermi liquid parameters at low T. While this result seems to be sufficiently reliable for the qualitative statements above, a quantitative analysis of the spectral lines is certainly not possible, at least with the data at hand, since the uncertainty around the Pade spectra is too high (see artifacts in Fig. 4.9 with negative spectral weight). A quantitative analysis would be of interest, however, since the spectral features contain valuable information, such as about the memory and the relaxation functions [17, 44]. The results of this section are encouraging enough to attempt a quantitative analysis of the line shapes in the future, where great emphasis will have to be put on a tight error control of the analytical continuation.

E.4   Implementation notes and acknowledgments

F Application II: Approximation to the T-matrix in a strongly magnetized regime

While in the last two sections collective excitations in disordered phases were discussed, in this section the 2P excitations of an ordered phase will be considered. It will be shown that deep inside the antiferromagnetic phase of the Hubbard model on the hypercubic lattice a Ward identity can be used in order to simplify the DMFT susceptibility. The latter is then given in terms of single-particle properties, which could potentially be of significance in DMFT calculations for realistic systems, where it is typically not feasible to calculate four-point correlation functions. The results of this section are due for publication [137].

$\quad$ To make a start, let us recall that none of the gapless modes of the 2P spectrum discussed so far in this section are Goldstone modes. The latter are gapless excitations of ordered phases and their importance for the two-dimensional Hubbard models considered above *should* be their absence: As soon as an order sets in at $T > 0$ that breaks a continuous symmetry of a system with dimensionality $d < 3$, such as the SU(2) symmetry, Goldstone excitations of arbitrarily small energy undermine it, and these energies can be so small because the Goldstone modes are gapless. This is the essence of the Mermin-Wagner theorem, which is unfortunately violated in DMFT (with exceptions for, e.g., frustrated systems). In both applications in Secs. D and E of DMFT to the two-dimensional Hubbard model above, one would find spurious phase transitions to antiferromagnetism if the spin susceptibility was considered at moderately low temperature. If one allows these transitions to happen, one can, in fact, observe the Goldstone excitations of the antiferromagnet. These, however, should have undermined the spontaneous symmetry breaking that is the reason for their very occurrence. In this context it is of little help that DMFT satisfies the Ward identity, since this merely guarantees that the Goldstone excitations are gapless (cf. chapter 3, Sec. D), while they should not have been there from the very beginning. Although these are textbook facts, this story is reiterated here in order to set the stage for the application of DMFT to the Hubbard model in the limit of infinite dimensions, where proper Goldstone excitations do not occur for an entirely different reason. The introduction below relies on Ref. [32] and references therein, as well as on the definitions of correlation functions for bipartite ordered phases in Sec. C.6 of chapter 3.

F.1 The Hubbard model on the hypercubic lattice

Let us consider the half-filled Hubbard model on the hypercubic lattice in infinite dimensions, $d \to \infty$ (the unscaled hopping t is set to unity),

$$H = -(2d)^{-\frac{1}{2}} \sum_{\langle ij \rangle \sigma} c_{i\sigma}^{\dagger} c_{j\sigma} + U \sum_{i} n_{i\uparrow} n_{i\downarrow}, \tag{F.1}$$

where the summation over i and j runs over nearest neighbors. The dispersion relation of the hypercube is given as $\varepsilon_{\mathbf{k}} = -\sqrt{2/d} \sum_{i=1}^{d} \cos(k_i)$, which corresponds to a Gaussian density of states (DOS) of the noninteracting system, $D(\epsilon) = (2\pi)^{-1/2} e^{-\epsilon^2/2}$ [32]. At low

temperatures this system favors antiferromagnetic order over paramagnetism. It should be noted that other types of order may have an even smaller free energy than the AFM, but it seems impossible to find with certainty the phase with the lowest free energy. Nevertheless, one may probe, as a particular choice, the simple bipartite AFM phase on the hypercube by applying a staggered magnetic field h_σ^a, where a denotes the sublattice index that is either A or B. In practice this means that numerical calculations are started with a finite h_σ^a, which is set to zero after some iterations. The calculation may then lead to a finite staggered magnetization that is oriented in opposite ways on each sublattice, $\langle m^A \rangle = -\langle m^B \rangle = \langle m \rangle$. Likewise, Green's function G^{ab} becomes a two-by-two matrix in the sublattice indices $a = A, B$, see Eq. (C.34) of chapter 3. By symmetry, an exchange of the sublattice indices $A \leftrightarrow B$ is equivalent to a flip of the spin label $\sigma \leftrightarrow \bar{\sigma}$, the sublattice indices can therefore often be dropped.

In DMFT the Hubbard model in infinite dimensions is mapped exactly to a single-site Anderson impurity model (AIM), where impurity and local lattice Green's function G_{loc} are tied via the prescription $g_{\nu\sigma}^{ab} = \delta_{ab} G_{\text{loc},\nu\sigma}^{ab} \equiv g_{\nu\sigma}^a$. Therefore, the problem is reduced again to an effective single-impurity model, as in single-site DMFT for phases with one atom per unit cell. Furthermore, the self-energy becomes local, which is now not an approximation anymore, and Green's function can be written as follows [32],

$$\hat{G}_{\mathbf{k}\nu\sigma} = \begin{pmatrix} \zeta_{\nu\bar{\sigma}} & -\varepsilon_{\mathbf{k}} \\ -\varepsilon_{\mathbf{k}} & \zeta_{\nu\sigma} \end{pmatrix}^{-1}, \tag{F.2}$$

where $\zeta_{\nu\sigma} = i\nu + \mu - \Sigma_{\nu\sigma}$ and $\mathbf{k}$ is a vector of the *reduced* Brillouin zone. Performing the matrix inversion and taking the local part ($G_{\text{loc}} = \sum_{\mathbf{k}}' G_{\mathbf{k}}$) leads to the following formulation of the DMFT self-consistency condition,

$$\hat{G}_{\text{loc},\nu\sigma} = \hat{g}_{\nu\sigma} = \int_{-\infty}^{\infty} \frac{D(\epsilon)d\epsilon}{\zeta_{\nu\sigma}\zeta_{\nu\bar{\sigma}} - \epsilon^2} \begin{pmatrix} \zeta_{\nu\bar{\sigma}} & 0 \\ 0 & \zeta_{\nu\sigma} \end{pmatrix}, \tag{F.3}$$

where the momentum summation was already transferred to an integral over the noninteracting DOS. It was also made use of the fact that the off-diagonal elements of G_{loc} lead to integrals with an integrand that is odd in ϵ, and that therefore vanish due to the mirror symmetry of the noninteracting DOS. As usual, the prescription is satisfied by fixing the dynamical Weiss field $\mathcal{G}_{\nu\sigma}^{-1} = G_{\text{loc},\nu\sigma}^{-1} + \Sigma_{\nu\sigma}$ of the AIM self-consistently.

F.2   Phase diagram

QP Before turning to the 2P excitations of this model, let us briefly consider the phase diagram of the half-filled Hubbard model on the hypercubic lattice in infinite dimensions $d \to \infty$, which is shown in Fig. 4.10. This shows the Slater regime with an exponential onset of the
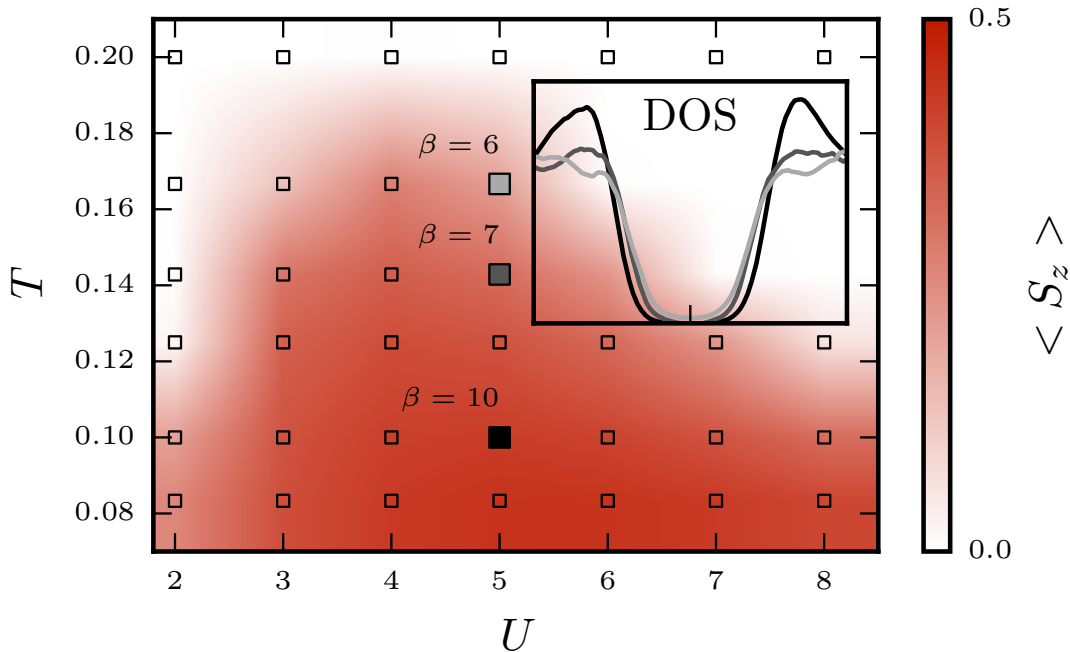
FIGURE 4.10: The antiferromagnetic phase of the half-filled Hubbard model on the hypercubic lattice in $d \to \infty$. The color code corresponds to the magnitude of the magnetic moment $\langle S_z \rangle = \langle m \rangle / 2$. The inset shows the widening of the gap $\sim U \langle m \rangle$ in the density of states at $U = 5$ as the temperature is lowered, the gray level of the lines corresponds to the three data points at $\beta = 1/T = 6, 7$ and 10, respectively. Note that AFM is the only instability probed in the calculations. I kindly thank M. Harland for providing this phase diagram, see also implementation notes below.

Néel temperature T_N for small U, and the Heisenberg regime at large U, where $T_N \sim 1/U$ (see, e.g., [135, 114, 30]).

   Other than in the paramagnetic phase, which features the Mott physics at intermediate U this model is so famous for, a gap in the DOS can occur in the AFM phase already for small U, given a sufficiently large staggered magnetization $\langle m \rangle$. The physics of this insulator is much different from the one in the Heisenberg regime at large U, which is characterized by an *interaction*-driven localization similar to that of the paramagnet. In the Slater regime hoppings are discouraged due to the staggered magnetization: Since on the bipartite lattice the sites of a given sublattice are not directly connected, the movement of the charge carriers against the antiferromagnetic background is discouraged energetically. They remain trapped on the sublattice whose magnetization is aligned with their magnetic moment when the staggered magnetization is sufficiently large. This effect can be observed in the inset of Fig. 4.10, albeit at the intermediate interaction $U = 5$, which lies already in the strongly correlated regime. The inset shows the DOS at three different temperatures that are also marked in the phase diagram. As the temperature is lowered from $T = 1/6$

to $T = 1/10$, the staggered magnetization increases from $\langle m \rangle \approx 0.42$ to 0.84, while at the same time the gap in the DOS becomes broader. However, due to the elevated interaction it is not guaranteed that one sees a pure Slater-regime here.

Since an insulator of the Slater-type may occur already in the weakly correlated regime, it is not a phenomenon directly related to the strong correlations at intermediate to large U, and lies therefore in reach of perturbative approximations. It was indeed predicted by J.C. Slater on the grounds of the Hartree-Fock approximation [135]. An interesting distinction between the two regimes was found in Ref. [30]: In the Slater regime the AFM state favors a relative localization compared to the paramagnet, while in the Heisenberg regime it does the opposite.

F.3   Susceptibility of the ordered state

The generalized susceptibility $X^{abcd}_{kk'q}$ of a bipartite ordered state is a four-index tensor in the sublattice indices A and B [cf. Eq. (C.41) of chapter 3]. This means that in principle the Bethe-Salpeter equation $\hat{X} = \hat{X}^0 + \hat{X}^0 \hat{\gamma} \hat{X}$ is a matrix equation involving 4×4 matrices in the sublattice indices, where the bubble is given as the tensor product $\hat{X}^0 = \hat{G} \otimes \hat{G}^{T}$[14]. However, in DMFT the 2P self-energy is given by the local 2P self-energy γ of the impurity model, such that of the tensor γ^{abcd} only the two elements $\gamma^{AAAA} \equiv \gamma^A$ and $\gamma^{BBBB} \equiv \gamma^B$ are nonzero. Furthermore, one is usually only interested in $X^{aabb}_{kk'q}$, in order to obtain the susceptibility X^{ab}_q by tracing out k and k'. In order to calculate $X^{aabb}_{kk'q}$, the Bethe-Salpeter equation can be solved in a 2×2 subspace, since in DMFT this channel is decoupled from matrix elements of the type X^{ABAB} or X^{AAAB}, due to the locality of γ. In this subspace the bubble is given by the element-wise matrix product $\hat{X}^0 = \hat{G} \circ \hat{G}^T$ and the 2P self-energy as $\gamma^{ab} = \gamma^a \delta_{ab}$.

In the following, the transversal spin susceptibility $X^{\overline{\sigma}\sigma,ab}_q$ in the antiferromagnetically ordered phase of the Hubbard model on the hypercubic lattice will be considered. Since this is an exact limit of DMFT, the T-matrix of this model is given exactly by the Bethe-Salpeter Eq. (B.15), which reads in a suitable notation for the transversal spin channel,

$$\hat{F}^{\overline{\sigma}\sigma}_{\nu\nu'q} = \hat{f}^{\overline{\sigma}\sigma}_{\nu\nu'\omega} + \sum_{\nu''}{}' \hat{f}^{\overline{\sigma}\sigma}_{\nu\nu''\omega} \hat{\tilde{X}}^{0,\sigma\bar{\sigma}}_{\nu''q} \hat{F}^{\overline{\sigma}\sigma}_{\nu''\nu'q}. \tag{F.4}$$

It should be noted that here the matrix notation implies 2×2 matrices in the sublattice indices. Eq. (F.4) uses the formulation of the DMFT susceptibility in terms of the local T-matrix $f^{ab} = f^a \delta_{ab}$ of the impurity, instead of the 2P self-energy γ (cf. Sec. B.2). In this

---

[14]

$$\hat{G} \otimes \hat{G}^T = \begin{pmatrix} G^{AA} \hat{G}^T & G^{AB} \hat{G}^T \\ G^{BA} \hat{G}^T & G^{BB} \hat{G}^T \end{pmatrix}.$$

formulation the building block of the Bethe-Salpeter equation is the nonlocal bubble from Eq. (B.13), which is given here as

$$\tilde{X}_{\nu\omega\mathbf{q}}^{0,\sigma\bar{\sigma},ab} = \sum_{\mathbf{k}}' X_{kq}^{0,\sigma\bar{\sigma},ab} - \chi_{\nu\omega}^{0,\sigma\bar{\sigma},ab} = \sum_{\mathbf{k}}' G_{\mathbf{k}+\mathbf{q},\nu+\omega,\bar{\sigma}}^{ab} G_{\mathbf{k}\nu\sigma}^{ba} - g_{\nu+\omega,\bar{\sigma}}^{a} g_{\nu\sigma}^{a} \delta_{ab}. \tag{F.5}$$

In infinite dimensions this object has rather peculiar properties. It turns out that the summation over $\mathbf{k}$ can be performed on both Green's functions separately, as long as the wave vector $\mathbf{q}_g$ is 'generic', meaning that it is a randomly chosen vector from the infinite-dimensional reduced Brillouin zone. This is shown in Ref. [32] for the paramagnetic case but it still holds in the ordered phase. Using the self-consistency condition $\sum_{\mathbf{k}}' G = g$, the nonlocal bubble therefore vanishes exactly at any generic wave vector, $\tilde{X}_{\mathbf{q}_g}^0 = 0$.

The nonlocal bubble is finite only for non-generic vectors $\mathbf{q}$, which are a zero-dimensional subset of the vectors in the reduced Brillouin zone. Of interest in the following is the non-generic wave vector $\mathbf{q}_0 = (0, ..., 0)$, where the momentum summation in Eq. (F.5) leads to the following expressions for the bubble X^0 [32],

$$\hat{X}_{\nu\omega\mathbf{q}_0}^{0,\sigma\bar{\sigma}} = \int_{-\infty}^{\infty} d\epsilon \frac{D(\epsilon)}{(\zeta_{\nu+\omega,\bar{\sigma}}\zeta_{\nu+\omega,\sigma} - \epsilon^2)(\zeta_{\nu\sigma}\zeta_{\nu\bar{\sigma}} - \epsilon^2)} \begin{pmatrix} \zeta_{\nu+\omega,\sigma}\zeta_{\nu,\bar{\sigma}} & \epsilon^2 \\ \epsilon^2 & \zeta_{\nu+\omega,\bar{\sigma}}\zeta_{\nu,\sigma} \end{pmatrix}. \tag{F.6}$$

Given a converged DMFT calculation, and given the local T-matrix f of the impurity, one can solve the integral in Eq. (F.6) numerically, and then proceed to calculate the T-matrix F of the lattice from the Bethe-Salpeter Eq. (F.4). In order to obtain the susceptibility, one then calculates the nonlocal corrections $X_q'^{\sigma\bar{\sigma}}$, as in Eq. (B.27), which are given in the suitable notation for the transversal spin channel as[15],

$$\hat{X}_q'^{\overline{\sigma\sigma}} = \text{Tr} \left(\hat{\lambda}_\omega^{\overline{\sigma\sigma},l} \left[\hat{\tilde{X}}_q^{0,\sigma\bar{\sigma}} + \hat{\tilde{X}}_q^{0,\sigma\bar{\sigma}} \hat{F}_q^{\overline{\sigma\sigma}} \hat{\tilde{X}}_q^{0,\sigma\bar{\sigma}} \right] \hat{\lambda}_\omega^{\overline{\sigma\sigma},r} \right). \tag{F.7}$$

It should be noted that X' on the LHS of this relation is a 2×2 matrix in the sublattice indices, while the matrices on the RHS are supermatrices in the sublattice indices and in the fermionic Matsubara frequencies. The trace denotes a summation over the outer fermionic frequencies. In Eq. (F.7) proper right- and left-sided triangular vertices for the transversal spin channel are needed, the right-sided one is given in analogy to Def. (B.24) as

$$\lambda_{\nu\nu'\omega}^{\overline{\sigma\sigma},r} = \beta\delta_{\nu\nu'} + f_{\nu\nu'\omega}^{\overline{\sigma\sigma}} g_{\nu'\sigma} g_{\nu'+\omega,\bar{\sigma}}, \tag{F.8}$$

while the left-sided triangular vertex $\lambda^{\overline{\sigma\sigma},l}$ instead has a left pair of legs $g_{\nu\sigma}g_{\nu+\omega,\bar{\sigma}}$. Like all other impurity quantities, λ is here a diagonal matrix in the sublattice indices, $\lambda^{\overline{\sigma\sigma},l,ab} = \lambda^{\overline{\sigma\sigma},l,a}\delta_{ab}$.

---

[15] Note that no factor of 2 occurs here, since Eq. (B.27) uses the notation for SU(2) symmetric cases, compare also Defs. (A.46) and (A.51) in chapter 2.

As a last step, the transversal spin susceptibility is then obtained analogous to Eq. (B.20) as the sum of the local impurity susceptibility $\chi_\omega^{\overline{\sigma\overline{\sigma}},ab} = \chi_\omega^{\overline{\sigma\overline{\sigma}},a}\delta_{ab}$ and the nonlocal corrections in Eq. (F.7),

$$\hat{X}_q^{\overline{\sigma\overline{\sigma}}} = \hat{\chi}_\omega^{\overline{\sigma\overline{\sigma}}} + \hat{X}_q'^{\overline{\sigma\overline{\sigma}}}, \tag{F.9}$$

where all quantities are 2×2 matrices. This is the exact susceptibility of the Hubbard model on the hypercubic lattice in infinite dimensions. Since the nonlocal bubble $\hat{\tilde{X}}^0$ vanishes at any generic vectors $\mathbf{q}_g$, it is immediately clear that the nonlocal corrections in Eq. (F.7) vanish as well. As a consequence, the susceptibility in Eq. (F.9) is given at these vectors by the impurity susceptibility $\hat{\chi}^{\overline{\sigma\overline{\sigma}}}$. For this reason, the Hubbard model in infinite dimensions does not have a proper magnon spectrum, since the generic vectors make up almost the entire reduced Brillouin zone, including the region around the Γ-point.

F.4   Ward identity in the ordered phase

QP   The computational bottleneck in the calculation of the susceptibility formulated in the last subsection is the measurement of the local T-matrix $f^{\overline{\sigma\overline{\sigma}}}$. In a CTQMC solver this requires a measurement of the four-point correlation function $g^{(2),\overline{\sigma\overline{\sigma}}}$ of the impurity model, cf. Eq. (B.3), which is several orders of magnitude more costly than the measurement of two-point correlation functions, and at the present time hardly even feasible for a two-band impurity model. It is certainly desirable to approximate f in a physically sound way that requires less computational cost. In the following, it will be shown in detail that this is indeed possible within a strongly magnetized regime by virtue of the Ward identity of the Anderson impurity model, which reads under broken SU(2) symmetry [cf. chapter 3, Eq. (E.9)],

$$\Sigma_{\nu+\omega,\bar{\sigma}} - \Sigma_{\nu\sigma} = \sum_{\nu'}{}' \gamma_{\nu\nu'\omega}^{\overline{\sigma\overline{\sigma}}} \left[g_{\nu'+\omega,\bar{\sigma}} - g_{\nu'\sigma} \right]. \tag{F.10}$$

 Firstly, let us confirm numerically that this Ward identity is indeed satisfied by the Anderson impurity model. To this end, the four-point correlation function $g^{(2),\overline{\sigma\overline{\sigma}}}$ was measured using a CTQMC solver that features a suitable measurement routine (see implementation notes). This was done at $U = 5$ and $\beta = 6$, using the converged hybridization function Δ_σ of a DMFT calculation at these parameters for the half-filled Hubbard model on the hypercubic lattice. This corresponds to the light gray data point in the phase diagram in Fig. 4.10, near the maximum of the Néel temperature. At these parameters the magnetization takes the moderate value $\langle m \rangle \approx 0.42$, such that the converged hybridization function is spin-dependent, which is therefore also the case for the quantities g_σ, Σ_σ, and $\gamma^{\overline{\sigma\overline{\sigma}}}$ in the Ward identity. The 2P self-energy γ was obtained from the inverted Bethe-Salpeter equation of the impurity model, analogous to Eq. (B.5). Although the summation in Eq. (F.10)
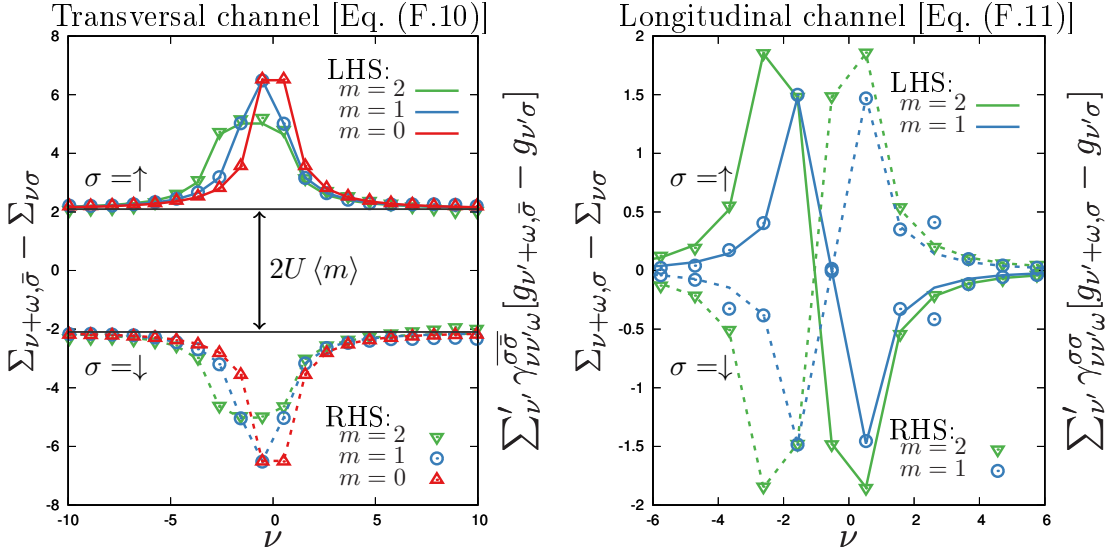
FIGURE 4.11:   Left: Real part of the LHS (lines) and of the RHS (symbols) of the Ward identity Eq. (F.10) in the transversal channel as a function of ν at the bosonic frequencies ω_m, $m = 0, 1, 2$. Solid lines show the LHS for $\sigma =\uparrow$, dashed lines show $\sigma =\downarrow$, these relations are separated for large $|\nu|$ by the gap $2U \langle m \rangle$. Right: The Ward identity Eq. (F.11) in the longitudinal channel for $\sigma = \sigma'$. Conventions as in the left panel. I kindly thank J.Otsuki for providing a CTQMC solver [98] that features a measurement of the T-matrix in the transversal channel.

converges rather slowly, such that the four-point correlation function has to be measured accurately at a sizable number of Matsubara frequencies, it is possible to confirm the validity of the Ward identity at these parameters to good accuracy.

This validation can be seen in Fig. 4.11, which shows the real part of both the LHS and of the RHS of Eq. (F.10), which coincide within the margin of numerical error. One can observe in the left panel of Fig. 4.11 that the LHS and RHS of Eq. (F.10) approach $\pm U \langle m \rangle$ at large frequency ν. This is the case, because the 1P self-energy at large ν approaches the Hartree energy, $\Sigma_{\nu\sigma} \to U \langle n_{\bar\sigma} \rangle$. In this limit the bosonic frequency ω on the LHS of the Ward identity Eq. (F.10) can be neglected, and the LHS therefore approaches $\Sigma_{\nu+\omega,\bar\sigma} - \Sigma_{\nu\sigma} \to U \langle n_\sigma \rangle - U \langle n_{\bar\sigma} \rangle = \sigma U \langle m \rangle$.

While the left panel of Fig. 4.11 shows the Ward identity in the transversal spin channel, a further Ward identity holds in the longitudinal channel [cf. chapter 3, Eq. (E.8)],

$$(\Sigma_{\nu+\omega,\sigma'} - \Sigma_{\nu\sigma})\delta_{\sigma\sigma'} = \sum_{\nu'}{}' \gamma^{\sigma\sigma'}_{\nu\nu'\omega} \left[g_{\nu'+\omega,\sigma'} - g_{\nu'\sigma} \right]. \tag{F.11}$$

If $\sigma = -\sigma'$, this Ward identity implies a nontrivial cancellation of the RHS, which was validated numerically to hold (not shown). The right panel of Fig. 4.11 shows Eq. (F.11)

for $\sigma = \sigma'$, where the LHS is finite. In the paramagnet the real part of the self-energy does not depend on the spin anymore and is simply given by the Hartree energy $U \langle n \rangle / 2$. As a consequence, the real parts of Eqs. (F.10) and (F.11) that are shown in Fig. 4.11 vanish in the paramagnetic phase. The imaginary parts of these relations are shown in Appendix C.

F.5   Approximation to the T-matrix

Q The idea is now to approximate the local T-matrix f that is needed in order to calculate the DMFT susceptibility in Eq. (F.7) by using the Ward identity in Eq. (F.10). To this end, that equation needs to be reformulated in terms of f, instead of γ, which leads to Eq. (D.43) of chapter 3,

$$\Sigma_{\nu+\omega,\bar{\sigma}} - \Sigma_{\nu\sigma} = \sum_{\nu'}^{'} \left([g^0_{\nu'\sigma}]^{-1} - [g^0_{\nu'+\omega,\bar{\sigma}}]^{-1} \right) f^{\overline{\sigma\bar{\sigma}}}_{\nu\nu'\omega} g_{\nu'\sigma} g_{\nu'+\omega,\bar{\sigma}}. \tag{F.12}$$

The goal is to obtain an approximation to f from this relation, even though it was clarified in Sec. E.2 of chapter 3 that the integral Ward identity does not allow to obtain the full information about the 2P self-energy γ, or equivalently f, from the 1P self-energy Σ. However, in a strongly magnetized setting this may actually be done to good accuracy: At large magnetization $\langle m \rangle$, the low-energy physics is dominated by spin excitations of long wave lengths, i.e., spin waves. When the magnetization axis is the z-axis, the susceptibility that describes these excitations is the transversal spin susceptibility $X^{\overline{\sigma\bar{\sigma}}}_{\mathbf{q}\omega}$, and the wave vector and frequency associated to the spin waves are $\mathbf{q}$ and ω, respectively. One may therefore expect that at large $\langle m \rangle$ the dynamics of three-frequency quantities is dominated by the bosonic frequency ω, and therefore neglect the dependence on the fermionic frequencies of the T-matrix, $f_{\nu\nu'\omega} \approx f_{\langle\nu\nu'\rangle\omega}$, as an ansatz for a simplification. However, if f does not depend on the fermionic frequencies, then it can be obtained from the Ward identity in Eq. (F.12) as,

$$f^{\overline{\sigma\bar{\sigma}}}_{\nu\nu'\omega} \approx f^{\overline{\sigma\bar{\sigma}}}_{\langle\nu\nu'\rangle\omega} = \frac{\Sigma_{\nu+\omega,\bar{\sigma}} - \Sigma_{\nu\sigma}}{\sum_{\nu'}^{'} \left([g^0_{\nu'\sigma}]^{-1} - [g^0_{\nu'+\omega,\bar{\sigma}}]^{-1} \right) g_{\nu'\sigma} g_{\nu'+\omega,\bar{\sigma}}}. \tag{F.13}$$

Here, $g^0_{\nu\sigma} = [\nu + \mu - \Delta_{\nu\sigma}]^{-1}$ is the noninteracting Green's function and Δ_σ is the self-consistent (and spin-dependent) hybridization function. It is understood that, in order for this approximation to yield accurate results, the dependence of the RHS on ν must be negligible, since $f^{\overline{\sigma\bar{\sigma}}}_{\langle\nu\nu'\rangle\omega}$ should not depend on fermionic frequencies. This may be used as a criterion for the applicability of the approximation.

The *ad-hoc* ansatz in Eq. (F.13) will now be put to a test in the Hubbard model on the hypercubic lattice by a comparison of its RHS to a direct measurement of f on its LHS. To this end, f was measured for $U = 5$ at three values of the temperature, $T = 1/6, 1/7$, and $1/10$, which are the three data points that are emphasized in the phase diagram in Fig. 4.10. The T-matrix is shown in Fig. 4.12, where $f^{\overline{\uparrow\downarrow}}_{\nu\nu'\omega}$ is plotted as a function of ν for
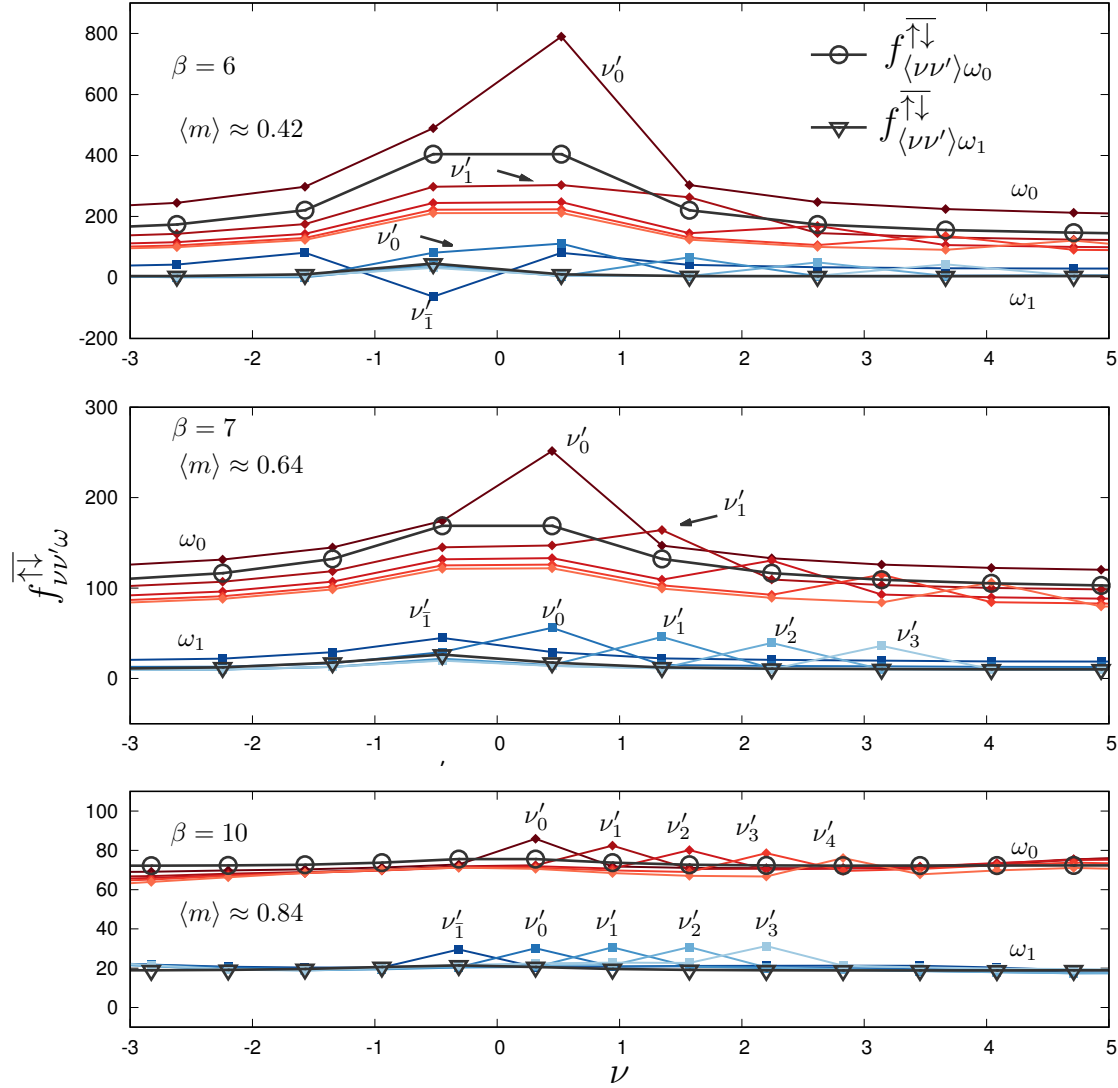
FIGURE 4.12: Real part of the T-matrix $f^{\overline{\uparrow\downarrow}}_{\nu\nu'\omega}$ at $U = 5$ for three different temperatures (cf. marked points in Fig. 4.10). The plot shows f as a function of ν for fixed ω and ν'. Red Diamonds and blue squares show data for $\omega = \omega_0$ and ω_1, respectively, lighter colors indicate larger ν'. Lines serve as guides to the eye. Black symbols show the ansatz $f^{\overline{\uparrow\downarrow}}_{\langle\nu\nu'\rangle\omega}$ from Eq. (F.13) at ω_0 (circles) and at ω_1 (triangles). The ansatz *a priori* depends on ν, but not on ν'. At the lowest temperature in the bottom panel the dependence of the ansatz on ν becomes negligible, at the same time it becomes a good approximation to the T-matrix.

several fixed ν' and at ω_0 and ω_1. At the highest temperature $T = 1/6$ in the top panel, the T-matrix depends quite strongly on ν. In particular, it changes with ν more strongly than with ω (compare the distance between the blue and red lines to the features due to the ν-dependence). Therefore, at $T = 1/6$ it is certainly not justified to neglect the dependence of f on ν and ν'.

However, upon lowering the temperature from $T = 1/6$ to $T = 1/10$, the magnetization increases from $\langle m \rangle \approx 0.42$ to 0.84, which lies closer to the regime where the ansatz in Eq. (F.13) is expected to become viable. The bottom panel of Fig. 4.12 shows that this is indeed the case, since at $T = 1/10$ the T-matrix depends only weakly on ν and ν' and much more strongly on ω. At the same time, the ansatz (see black symbols) becomes a good approximation to f. Importantly, although the RHS of the ansatz in Eq. (F.13) formally depends on ν, this dependence becomes negligible at strong magnetization. As a consequence, $f^{\overline{\sigma\bar{\sigma}}}_{\langle \nu\nu' \rangle \omega}$ indeed does not depend on fermionic frequencies anymore, which means that the ν and ν' labels are dropped on equal footing.

F.6 Simplification of the DMFT susceptibility

Using the ansatz in Eq. (F.13), the calculation of the transversal spin susceptibility of DMFT in Eq. (F.9) can be simplified in several ways:

(i) Since the fermionic labels of f can be dropped, the T-matrix F of the lattice does also not depend on the fermionic frequencies anymore. The solution of the Bethe-Salpeter Eq. (F.4) simplifies to a mere inversion of 2×2 matrices,

$$\hat{F}^{\overline{\sigma\bar{\sigma}}}_{\langle \nu\nu' \rangle q} = \hat{f}^{\overline{\sigma\bar{\sigma}}}_{\langle \nu\nu' \rangle \omega} + \hat{f}^{\overline{\sigma\bar{\sigma}}}_{\langle \nu\nu' \rangle \omega} \left(\sum_{\nu'}^{'} \hat{\hat{X}}^{0,\sigma\bar{\sigma}}_{\nu' q} \right) \hat{F}^{\overline{\sigma\bar{\sigma}}}_{\langle \nu\nu' \rangle q}. \tag{F.14}$$

(ii) The triangular vertex λ in Eq. (F.8) can be approximated as,

$$\lambda^{\overline{\sigma\bar{\sigma}},r}_{\nu\nu'\omega} \approx \beta \delta_{\nu\nu'} + f^{\overline{\sigma\bar{\sigma}}}_{\langle \nu\nu' \rangle \omega} g_{\nu'\sigma} g_{\nu'+\omega,\bar{\sigma}}, \tag{F.15}$$

such that in applications neither four- nor three-point correlation functions need to be measured.

(iii) Furthermore, in many CTQMC solvers a measurement of the transversal spin susceptibility $\chi^{\overline{\sigma\bar{\sigma}}}$ of the impurity is not implemented, since the measurement of this two-point correlation function is rather challenging. However, the generalized susceptibility that corresponds to this object is related to the local T-matrix f [cf. Eq. (D.47) of chapter 3], using the approximation in Eq. (F.13) leads to,

$$\chi^{\overline{\sigma\bar{\sigma}}}_{\nu\nu'\omega} \approx g_{\nu\sigma} g_{\nu+\omega,\bar{\sigma}} \left(\beta \delta_{\nu\nu'} + f^{\overline{\sigma\bar{\sigma}}}_{\langle \nu\nu' \rangle \omega} g_{\nu'\sigma} g_{\nu'+\omega,\bar{\sigma}} \right). \tag{F.16}$$

One may then obtain the transversal susceptibility of the impurity as $\chi^{\overline{\sigma\bar{\sigma}}}_{\omega} = \sum_{\nu\nu'}^{'} \chi^{\overline{\sigma\bar{\sigma}}}_{\nu\nu'\omega}$.

Making use of the simplifications (i)-(iii), the DMFT susceptibility can be obtained approximately by mere knowledge of Green's function g_σ and of the 1P self-energy Σ_σ.

F.7 Calculation of the DMFT susceptibility

In the bottom panel of Fig. 4.12 it can be seen that the simplifying ansatz from Eq. (F.13) for the local T-matrix seems to be a rather accurate approximation at the parameters $U = 5$ and $T = 1/10$, where the magnetization takes the moderately large value $\langle m \rangle \approx 0.82$ [cf. black data point in the phase diagram in Fig. 4.10]. At these parameters the measurement of f in a CTQMC calculation is already rather expensive and it is desirable to avoid it entirely. In the following, the simplifying ansatz for f will be exploited in order to calculate the DMFT susceptibility from single-particle quantities. Since DMFT becomes exact in the considered model (including its susceptibility [32]), Eq. (F.13) is the only approximation in the calculation of the susceptibility, such that any artifact of the results can be traced back to it.

The calculation of the simplified DMFT susceptibility is done as follows: Firstly, a DMFT calculation is converged, such that the impurity Green's function g_σ and its self-energy Σ_σ are known. After that, the nonlocal bubble $\tilde{X}^0$ in Eq. (F.5) is evaluated at the non-generic vector $\mathbf{q}_0 = \mathbf{0}$ by solving the integral for the bubble X^0 in Eq. (F.6) numerically. Making use of the ansatz in Eq. (F.13) for the local T-matrix f, the simplified Bethe-Salpeter Eq. (F.14) can be solved for the T-matrix F of the lattice. Furthermore, the triangular vertex λ and the impurity susceptibility χ can be calculated from Eqs. (F.15) and (F.16). Finally, the transversal spin susceptibility is obtained from Eq. (F.9).

The latter is a 2×2 matrix in the sublattice indices A and B. As shown in Sec. C.6 of chapter 3, the wave vector $\mathbf{q}_0 = \mathbf{0}$ of the reduced Brillouin zone maps to the two vectors $\tilde{\mathbf{q}}_0 = \mathbf{q}_0 = \mathbf{0}$ and $\tilde{\mathbf{q}}_\pi = \mathbf{q}_0 + \mathbf{Q} = \mathbf{Q}$ of the regular Brillouin zone[16], where on the hypercubic lattice the ordering vector is $\mathbf{Q} = (\pi, ..., \pi)$. However, in the ordered phase the susceptibility of the reduced Brillouin zone is not diagonalized by the mapping to the regular Brillouin zone anymore, since the offdiagonal element $X_{\tilde{\mathbf{q}}_0, \omega}^\pm$ does not vanish [cf. chapter 3, Eq. (C.45)].

Let us discuss the results found for the static transversal spin susceptibility, starting with a divergence that was found in one of its channels: When approaching the phase boundary to the AFM from the paramagnetic phase, the spin susceptibility diverges in the regular Brillouin zone at $\mathbf{Q}$ and $\omega = 0$. *Within* the ordered phase, where the magnetization is aligned with the z-axis, it seems plausible that the transversal susceptibility remains divergent. This can be expected, because even within the ordered phase the application of a small outer magnetic field should lead to a reorientation of the magnetization axis, which is signaled, as usual, by a divergent susceptibility. Since only the orientation of $\langle m \rangle$ changes, while the magnetic unit cell remains the same, this divergence should still happen at $\tilde{\mathbf{q}}_\pi = \mathbf{Q}$. It is therefore not surprising to find a divergent result when mapping the transversal spin susceptibility $X_{\mathbf{q}_0, \omega=0}^{\overline{\sigma}\overline{\sigma}}$ of the *reduced* Brillouin zone back to the wave vector $\tilde{\mathbf{q}}_\pi = \mathbf{Q}$ of the *regular* Brillouin zone, $X_{\tilde{\mathbf{q}}_\pi, \omega=0}^{\overline{\sigma}\overline{\sigma}} \to \infty$. For this reason, one of the two eigenvalues of the simplified Bethe-Salpeter Eq. (F.14) is expected to be unity. In the

---
[16]Note that in the discussion of bipartite phases vectors of the regular Brillouin zone are consistently marked with a tilde.
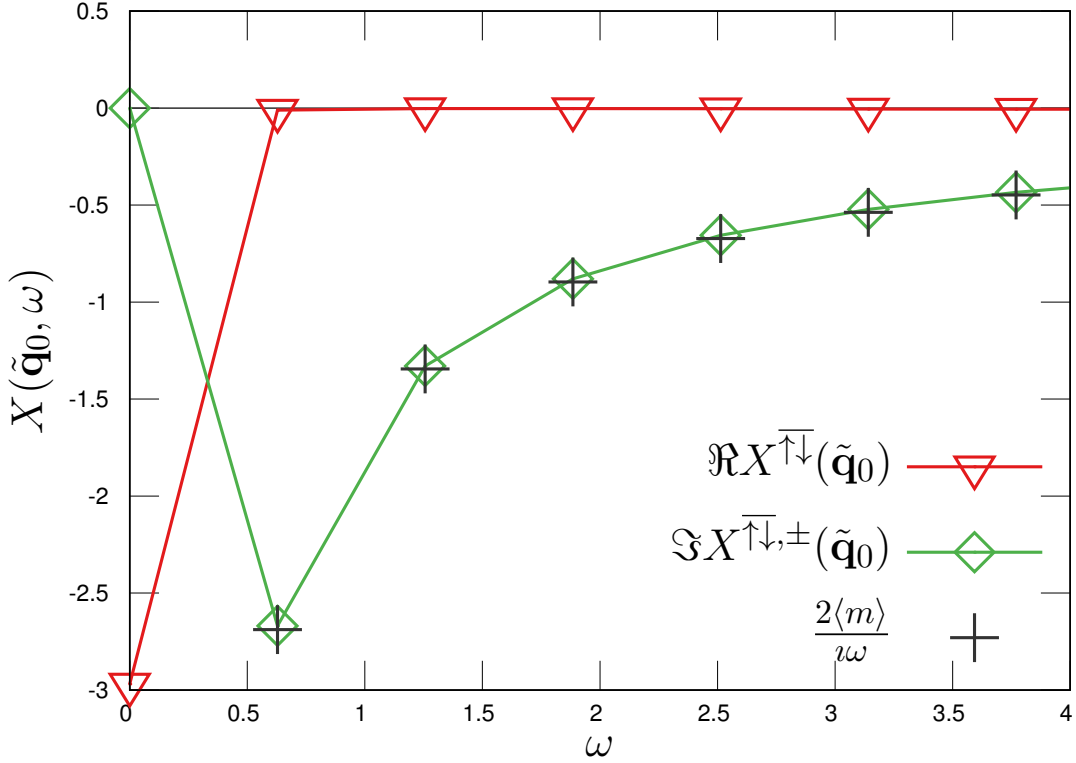
FIGURE 4.13: The homogeneous susceptibility in the regular Brillouin zone as a function of the Matsubara frequency (triangles). Global spin conservation requires that $X^{\overline{\uparrow\downarrow}}(\tilde{\mathbf{q}}_0, \omega > 0)$ vanishes, while $X^{\overline{\uparrow\downarrow},\pm}(\tilde{\mathbf{q}}_0, \omega > 0)$ must be equal to $\frac{2\langle m\rangle}{\imath\omega}$, which is marked by crosses. The parameters of this figure correspond to the black data point in the phase diagram Fig. 4.10 and to the bottom panel of Fig. 4.12.

calculation for $U = 5$ and $T = 1/10$ it is found that the eigenvalue that belongs to $\tilde{\mathbf{q}}_\pi$ is $|\lambda_\pi| \approx 0.993$, where I interpret the small deviation from unity to be a consequence of the simplifying ansatz Eq. (F.13) for the local T-matrix f. The second eigenvalue of the Bethe-Salpeter equation remains finite, at the considered parameters it is $|\lambda_0| \approx 0.715$, this eigenvalue belongs to the static homogeneous susceptibility $X^{\overline{\sigma\sigma}}_{\tilde{\mathbf{q}}_0, \omega=0}$ of the regular Brillouin zone.

Now to the findings regarding the dynamical susceptibility, which are remarkable: Fig. 4.13 shows the diagonal element $X^{\overline{\uparrow\downarrow}}$, as well as the offdiagonal element $X^{\overline{\uparrow\downarrow},\pm}$ of the homogeneous transversal spin susceptibility in the regular Brillouin zone [for their definitions cf. (C.45)]. As was shown in Eqs. (D.10) and (D.11) of chapter 3, these quantities are subjected to exact constraints at finite ω, which follow from global spin conservation. Namely, the diagonal element must vanish identically, while the offdiagonal element is given

by the magnetization,

$$X^{\overline{\uparrow\downarrow}}(\tilde{\mathbf{q}}_0, \omega > 0) = 0, \qquad\qquad X^{\overline{\uparrow\downarrow},\pm}(\tilde{\mathbf{q}}_0, \omega > 0) = \frac{2\langle m\rangle}{\iota\omega}. \qquad\qquad \text{(F.17)}$$

Fig. 4.13 reveals that the approximate susceptibility is in virtually exact agreement with these two constraints.

F.8   Conclusions

The transversal spin susceptibility of the Hubbard model on the hypercubic lattice in infinite dimensions was calculated in the antiferromagnetic phase using DMFT. A prerequisite to obtain the DMFT susceptibility is the calculation of the local T-matrix of the impurity, which is a computationally intense task. It was found that by virtue of a Ward identity the T-matrix can be approximated by single-particle quantities if the magnetization is large enough, which drastically reduces the computational cost. The physical motivation for this approximation is that the low-energy spin excitations deep in the antiferromagnetic regime are dominated by spin waves, which leads to a simplification in the frequency dependence of the T-matrix. Although an infinite-dimensional model does not have a proper spin wave dispersion, it was found that the decisive simplification in the T-matrix is indeed justified at a magnetization of $\langle m\rangle \approx 0.84$. As a consequence, it was possible to calculate the transversal susceptibility from mere knowledge of Green's function and of the self-energy of the impurity model. Remarkably, an evaluation of the homogeneous susceptibility shows an agreement with two exact constraints that follow from global spin conservation. It seems plausible that the presented approximation owes its conserving features to the fact that it is derived from the Ward identity of the Anderson impurity model, which was shown in Sec. A.3 to ultimately guarantee the satisfaction of local conservation laws in DMFT.

It should be noted that the application to the Hubbard model in infinite dimensions in this section was chosen because it is an exact limit of DMFT, such that the ansatz for the local T-matrix in Eq. (F.13) is the only approximation. It seems likely that this ansatz remains applicable when DMFT is used as an approximation in finite dimensions. Here lies the main potential of the presented approximation, since it greatly reduces the computational cost, such that a calculation of the susceptibility is feasible in a realistic setting with several orbitals. The conserving features of the approximation are of particular importance in finite dimensions, since global spin conservation guarantees a gapless spin wave spectrum in accord with Goldstone's theorem [see also Sec. D.1 of chapter 3]. This allows a physically sound description of spin waves in the strongly correlated regime, far away from the limit of large interaction, where the Hubbard model maps to the Heisenberg model. It is shown in Ref. [137] that the approximation used here can be related to an effective classical Heisenberg model, which has been used with great success in applications to realistic systems [72, 73, 59]. The added benefit here is that an effective classical model is not needed, since a spin wave spectrum may also be obtained from the DMFT susceptibility. It remains a task for the future to validate that the simplifying ansatz for the T-matrix remains a good approximation in a realistic setting.

F.9   Implementation notes and acknowledgments

Chapter 5

Two-particle self-consistency

"E voltei prá minha nota, como eu volto prá você
Vou contar com a minha nota, como eu gosto de você
E quem quer todas as notas, Ré, Mi, Fá, Sol, Lá, Si, Dó
Fica sempre sem nenhuma, fique numa nota só"

- Tom Jobim

In this section the concept of two-particle self-consistency will be motivated in two ways: **Q**
In Sec. A as a way to incorporate long-ranged interactions into DMFT and in Sec. C as
a means to reestablish the Mermin-Wagner theorem in diagrammatic extensions of DMFT
and to allow for a feedback of collective modes on the effective impurity model.

A   Long-ranged interactions

In DMFT many things fit perfectly together. One of its more accidental features is that   **Q**
the interaction Hamiltonian of the effective local impurity model is the same as the one
of the lattice model. This is the case in infinite dimensions, but also in finite dimensions,
where DMFT is an approximation. This is a unique feature of the local interaction of the
Hubbard model and it is not the case for nonlocal interactions.

A.1   Nonlocal interactions in infinite dimensions

Although the Hubbard model, in particular with several orbitals, is a suitable Hamiltonian   **Q**
for the description of many realistic materials, in some cases long-ranged interactions have
to be taken into account. This can be the case in ad-atom systems, where the interactions
between nearest neighbors can be as large as half the size of the local interaction [11, 41,
89]. It is then important to account for such interactions, since they may screen the local
interaction considerably, up to the point where a charge density wave state (charge order)
is favored.

Attempts have been made early on to account for nonlocal interactions, in the same way
as for the Hubbard model, by learning from the instructive limit of infinite dimensions [94,

123]. However, compared to the revolutionary success of DMFT, the advances in this direction are overshadowed, which is mainly due to the fact that a nonlocal interaction can not be absorbed into an effective local impurity model, as is the case for the Hubbard interaction. If the intention is nevertheless to use a local reference system, one is faced with the problem that the local and the nonlocal parts of the interactions can not be treated on equal footing. For example, in the limit of infinite dimensions the local part of the interaction need not be scaled with the coordination number z, whereas nonlocal interactions have to be scaled. There are even different ways to do that, namely, the nonlocal interaction may be scaled with z^{-1} [94] or with $z^{-1/2}$ [123, 129, 136], like the hopping. The first option, in fact, leads back to an effective Anderson impurity model, the difference to DMFT is then merely that a Hartree (not Fock) diagram arises, which is the only surviving effect of the nonlocal potential in infinite dimensions [147, 113]. This approach, however, neglects the screening of the local by the nonlocal interaction. Scaling the interaction with $z^{-1/2}$, on the other hand, leads to an effective impurity model with a retarded interaction [136], which is the motivation for the *extended* DMFT (EDMFT).

The retarded interaction of EDMFT is the effective interaction that arises in its local impurity model due to the nonlocal potential and that leads to a dynamical screening of the local interaction. If the nonlocal potential acts in the charge channels, $V_{ij}^c n_i n_j$, the retarded interaction will likewise couple charge densities, which reads in the action formalism as $\Lambda^c(\tau - \tau')n(\tau)n(\tau')$ [136]. Hence, the nonlocal and static interaction V^c of the lattice model is mapped to the local and dynamic interaction Λ^c of the effective impurity model. Similar to the hybridization function, the value of the retarded interaction must be fixed, in this case via a two-particle self-consistency condition. Fortunately, taking a retarded interaction between charge densities in CTQMC into account is well doable, both in interaction- and in hybridization-expansion solvers [153, 33].

On the other hand, a nonlocal interaction between spins, $V_{ij}^s \mathbf{S}_i \mathbf{S}_j$, leads to a retarded spin-spin interaction, $\Lambda^s(\tau - \tau')\mathbf{S}(\tau)\mathbf{S}(\tau')$ [123], this model is known as the Bose-Fermi-Kondo model [or spin-boson model, compare chapter 3, Eq. (F.28)]. In the limit of an infinitely large Hubbard repulsion, this is the effective impurity model that arises from the t-J model[1] in the limit of large coordination number [103]. Such a mapping of a system with an exchange interaction V^s to an impurity model with a retarded spin-spin interaction Λ^s is done more rarely than the analogous mapping of a charge-charge interaction V^c to Λ^c. One reason for this may be, in fact, that compared to an impurity model with a retarded charge-charge interaction it is much more difficult to solve the Bose-Fermi-Kondo model. Gross simplifications had to be accepted before a numerically exact solution of the Bose-Fermi-Kondo model became possible [98], which finally allowed an exact solution of the t-J model with random exchange couplings in infinite dimensions [101].

---

[1] In order to obtain a nontrivial limit of the t-J model in $d \to \infty$, the exchange couplings have to be randomly distributed [103, 101].

A.2 From Hartree to Hartree-Fock to anomalous Ward identities

The developments described above allowed the exact solution of several lattice models in infinite dimensions, the Hubbard model, the extended Hubbard model with charge-charge couplings, and the *t-J* model with random exchange couplings. However, only one of these solutions, the one for the Hubbard model, led to the sweeping success of DMFT as an approximation in *finite* dimensions. Certainly, this is not due to a lack of motivation to develop approaches for nonlocal interactions, since, for example, with ad-atom systems there exist applications for nonlocal charge-charge interactions on the one side, while the *t-J* model and the Heisenberg model are applications for nonlocal exchange couplings on the other. It is therefore an obvious question why it was not possible in the context of nonlocal interactions to develop a dynamical mean-field approximation that is able to catch up with the development of DMFT.

One reason for this is very simple: Even the lowest order approximation to the Luttinger-Ward functional of a system with a nonlocal interaction, the Hartree-Fock approximation, leads to a $\mathbf{k}$-dependent self-energy, while the Hartree approximation to the Hubbard model is local. The same is the case for the 2P self-energy [cf. Sec. B.4 of chapter 3]. Thus, while DMFT naturally recovers the Hartree self-energy, any local approximation to an extended Hubbard model neglects by construction the (nonlocal) Fock diagram, one of the two very first contributions to the Luttinger-Ward functional [cf. Fig. 3.1]. Although the Hartree-Fock approximation merely amounts to an interaction-dependent renormalization of the hopping [6], the $\mathbf{k}, \mathbf{k}'$-dependence of its 2P self-energy gravely complicates calculations on the two-particle level (see Fig. 3.2). At least in a conserving approximation to an extended Hubbard model, the momentum dependencies of Σ and Γ go hand in hand, as an explicit insertion of the Hartree-Fock approximation into the Ward identity in Sec. E.2 of chapter 3 shows.

Complications do not only arise when going from local to nonlocal interactions, but also when going from interactions in the charge channel to spin-dependent interactions. It was demonstrated in in Sec. F of chapter 3 that it is by far more challenging to satisfy the Ward identity in the spin channels when the interaction is spin-dependent, since the non-commutativity of the spin operators leads to an anomaly in the Ward identity [cf. conclusions I of chapter 3].

Certainly, the satisfaction of the Ward identity is only one of many viable goals that one may have. However, it seems fair to say that along the hierarchy of challenges listed above, the dynamical mean-field approaches that were developed in the past can be measured in their success: DMFT has become an established tool for modeling realistic systems, followed by EDMFT and EDMFT+GW approaches [139, 21], which find frequent applications to nonlocal charge-charge interactions, down to EDMFT for exchange interactions, also called spin-DMFT. It seems that especially for nonlocal spin-spin interactions there exists up to this point in time no satisfactory framework to obtain a dynamical mean-field approach for finite dimensions from the exact solution in infinite dimensions. Consequently, applications of single-site dynamical mean-field approaches to exchange systems are rare, although there are exceptions [100, 42, 113].

A.3   DMFT+RPA

Q   If one intends to calculate the susceptibility in a system with a nonlocal interaction, one is faced with the fundamental dilemma that the derivation of an approximation in the standard way from the Luttinger-Ward functional immediately leads to a $\mathbf{k}, \mathbf{k}'$-dependence of the 2P self-energy $\Gamma_{kk'q}$. It is therefore in general not feasible to account for vertex corrections in such systems, see also Fig. 5.1. On the other hand, it is feasible to account for vertex corrections in DMFT. Thanks to the locality of the 2P self-energy $\gamma_{\nu\nu'\omega}$ in DMFT, the solution of the Bethe-Salpeter equation merely requires the inversion of matrices in the indices ν and ν'. It is therefore desirable to *augment* DMFT, such that a nonlocal interaction potential can be incorporated, without leading to the problem of having to invert supermatrices in the indices $k = (\mathbf{k}, \nu)$ and $k' = (\mathbf{k}', \nu')$. It is clear that, in order to make progress, compromises have to be made. With respect to conservation laws, some compromises are more severe than others: It was seen in chapter 3 that a number of exact statements follow from the Ward identity, some of which are listed in Sec. D.12. Since the goal is eventually not to satisfy the Ward identity but to profit from its implications for the two-particle spectrum and for thermodynamic consistency, it seems acceptable as a starting point to consider such extensions of DMFT first that preserve the qualitatively most important features implied by the Ward identity.

A first step in this direction may be dubbed "DMFT+RPA", which is an appropriate name for an approach suggested by Pruschke et al. for a dynamical mean-field description of the *t*-*J* model [113]. Instead of *vertex corrections* due to the nonlocal interaction (such as in the Hartree-Fock approximation), a DMFT+RPA approach introduces *RPA corrections* (see Fig. 5.1), which do not lead to a complication of the Bethe-Salpeter equation. Let us consider such an approach for the case of a single-band extended Hubbard model with charge-charge interactions, whose interaction Hamiltonian is $H_{\text{int}} = U \sum_i n_{i\uparrow} n_{i\downarrow} + \frac{1}{2} \sum_{ij} V_{ij}^c n_i n_j$. A dynamical mean-field approach for this model *à la* Pruschke et al. is to ignore the nonlocal potential V_{ij}^c first, and to calculate the DMFT susceptibility X_q^c of the Hubbard model for $V^c = 0$. At the end of the calculation, RPA corrections to the susceptibility are included via a geometric series,

$$X_q^{c,\text{DRPA}} = \frac{X_q^c}{1 - V_q^c X_q^c}, \tag{A.1}$$

where $V_q^c = V_{\mathbf{q}}^c$ is the Fourier transform of the nonlocal potential V_{ij}^c. This approach is able to account for the occurrence of charge order, since the denominator of this expression can introduce divergences in $X_q^{c,\text{DRPA}}$ that do not originate from the DMFT susceptibility X^c. It is easy to see that this approach maintains several features of the conserving DMFT susceptibility, most importantly, the two-particle spectrum of $X_q^{c,\text{DRPA}}$ remains ungapped if the spectrum of X_q^c is ungapped. This is due to the relation $\imath\omega X_{\mathbf{q}=0,\omega}^c = 0$, which is satisfied in DMFT, and which follows from global charge conservation (cf. chapter 3, Sec. D.1). From this and the definition in Eq. (A.1) it follows that also $\imath\omega X_{\mathbf{q}=0,\omega}^{c,\text{DRPA}} = 0$.
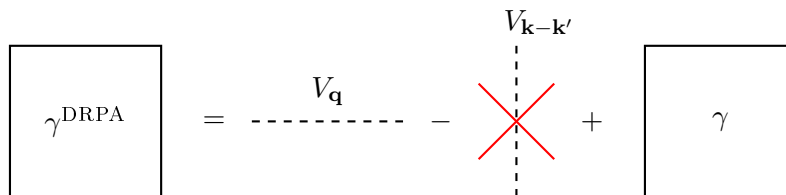
FIGURE 5.1: 2P self-energy of a 'DMFT+RPA' approach. It is computationally feasible to account for RPA corrections ($V_{\mathbf{q}}$) to the Bethe-Salpeter equation, since they depend only on the transferred momentum $\mathbf{q}$. For a reasonably dense discretization of the Brillouin zone, which is necessary to extrapolate to the thermodynamic limit, vertex corrections ($V_{\mathbf{k}-\mathbf{k}'}$) become unfeasible, unless the interaction is local (cf. Fig. 3.2). Vertex corrections are relevant for local conservation laws and arise already at the Hartree-Fock level (cf. chapter 3, Sec. B.4). Note that inserting γ^{DRPA} (without $V_{\mathbf{k}-\mathbf{k}'}$) instead of γ into the Bethe-Salpeter equation is equivalent to Eq. (A.1) [113].

Likewise, X_q^c and $X_q^{c,\mathrm{DRPA}}$ share the same ω^{-2} coefficient,

$$\lim_{\omega\to\infty}(\imath\omega)^2 X_{\mathbf{q}\omega}^{c,\mathrm{DRPA}} = \lim_{\omega\to\infty}(\imath\omega)^2 \frac{X_{\mathbf{q}\omega}^c}{1 - V_{\mathbf{q}}^c X_{\mathbf{q}\omega}^c} = \lim_{\omega\to\infty}(\imath\omega)^2 X_{\mathbf{q}\omega}^c. \tag{A.2}$$

This is desirable, since according to Eq. (F.39) of chapter 3 the susceptibility of an extended Hubbard model with charge-charge couplings and the susceptibility of the Hubbard model should have the same asymptotic coefficient,

$$\lim_{\omega\to\infty}(\imath\omega)^2 X_{\mathbf{q}\omega}^{c,\mathrm{DRPA}} = \sum_{\mathbf{k}}{}' \langle n_{\mathbf{k}}\rangle (\varepsilon_{\mathbf{k}+\mathbf{q}} + \varepsilon_{\mathbf{k}-\mathbf{q}} - 2\varepsilon_{\mathbf{k}}), \tag{A.3}$$

which is nothing but the f-sum rule (see Eq. (D.22) of chapter 3, [65]). Therefore, although a DMFT+RPA approach violates the Ward identity (see argument below regarding the dual boson approach), it preserves several qualitative features of the two-particle spectrum[2]. This, in turn, is a consequence of the fact that the DMFT susceptibility $X_{\mathbf{q}\omega}^c$ satisfies the Ward identity of the Hubbard model and because the DMFT+RPA susceptibility is related to it via the simple geometric series in Eq. (A.1).

A.4 Dynamical screening of the local interaction - EDMFT

The DMFT+RPA approach above accounts for an effect of the nonlocal interaction on the two-particle spectrum, while the single-particle spectrum remains unaffected. However, this

---

[2] In fact, in the DMFT+RPA approach to the t-J-model in Ref. [113] the f-sum rule is not satisfied, since $\lim_{\omega\to\infty}(\imath\omega)^2 X_{\mathbf{q}\omega}^{s,\mathrm{DRPA}}$ should have a contribution from the exchange interaction. This is *similar* to chapter 3, Eq. (D.19), which has such a contribution. Note that in the t-J-model asymptotic formulae have to be derived by taking the limit $U \to \infty$ before the limit $\omega \to \infty$.

neglects the effect of screening of the local interaction U by the nonlocal interaction V. One way to account for screening is to modify the effective impurity problem, which is done in *extended* DMFT [129, 100, 123, 134, 136, 25] by an additional dynamical mean-field, the retarded interaction. The action of this impurity problem is given by the action S_{AIM} of the Anderson impurity model, Eq. (F.22) of chapter 3, augmented by retarded interactions Λ^α,

$$S = S_{\mathrm{AIM}} + \frac{1}{2} \sum_{\omega\alpha} \rho^\alpha_{-\omega} \Lambda^\alpha_\omega \rho^\alpha_\omega. \tag{A.4}$$

In EDMFT there is a one-to-one correspondence between the nonlocal interactions acting on the lattice and the retarded interaction on the impurity[3],

$$V^c_{\mathbf{q}} \leftrightarrow \Lambda^c_\omega,$$
$$V^{x,y,z}_{\mathbf{q}} \leftrightarrow \Lambda^{x,y,z}_\omega.$$

The susceptibility is approximated in EDMFT via a severe simplification. Expressing the susceptibility in terms of the polarization Π, $X^{\alpha,-1}_{\mathbf{q}\omega} = -\Pi^{\alpha,-1}_{\mathbf{q}\omega} - (U + V^\alpha_{\mathbf{q}})$, one arrives at the EDMFT by approximating $\Pi^\alpha_{\mathbf{q}\omega} \approx \pi^\alpha_\omega$, where π is the polarization of the local impurity problem. The latter is defined analogously as $\chi^{\alpha,-1}_\omega = -\pi^{\alpha,-1}_\omega - (U + \Lambda^\alpha_\omega)$. This leads to the following simple expression for the EDMFT susceptibility,

$$X^{\alpha,\mathrm{EDMFT}}_{\mathbf{q}\omega} = \frac{\chi^\alpha_\omega}{1 - (V^\alpha_{\mathbf{q}} - \Lambda^\alpha_\omega)\chi^\alpha_\omega}. \tag{A.5}$$

The retarded interaction is fixed in EDMFT via the two-particle self-consistency condition $X^{\alpha,\mathrm{EDMFT}}_{\mathrm{loc},\omega} = \chi^\alpha_\omega$, where χ is the susceptibility of the impurity model. This is combined with the local approximation to the 1P self-energy that is known from DMFT, $G^{-1}_k = \imath\nu + \mu - \varepsilon_{\mathbf{k}} - \Sigma_\nu$, and with the DMFT self-consistency condition $G_{\mathrm{loc},\nu} = g_\nu$.

While EDMFT is able to capture a dynamical screening effect of the local interaction by the nonlocal one, its susceptibility does evidently not recover a qualitatively sound spectrum of collective excitations. In particular, the 2P spectrum is gapped, since $\imath\omega X^{\alpha,\mathrm{EDMFT}}_{\mathbf{q}=0,\omega}$ is not zero, which leads to a divergence of the plasma frequency [39].

A.5   RPA corrections + dynamical screening: Dual bosons

Q   The poor description of collective excitations in EDMFT shows that the limit of infinite coordination number of the extended Hubbard model, where EDMFT becomes exact, is much less valuable for approximations in finite dimensions than the analogous limit of the Hubbard model. While in DMFT one uses a local approximation to the 1P self-energy, $\Sigma_k \approx \Sigma_\nu$, EDMFT also introduces a local approximation on the 2P level by approximating

---

[3] Note that EDMFT is sometimes called 'spin-DMFT' when it is applied to a Heisenberg model [123, 100].

the polarization of the lattice with that of the impurity, $\Pi_q \approx \pi_\omega$. However, a local approximation to the polarization automatically leads to a gapped excitation spectrum, since the susceptibility $X_{\mathbf{q}\omega}^{\alpha,-1} \approx -\pi_\omega^{\alpha,-1} - (U + V_{\mathbf{q}}^\alpha)$ violates the condition $\imath\omega X_{\mathbf{q}=0,\omega}^\alpha = 0$ by construction.

Let us attempt to derive a dynamical mean-field approach for the extended Hubbard model in the same way as DMFT, which was derived in Sec. A.3 of chapter 4. To this end, let us consider the Ward identity of the extended Hubbard model with charge-charge interactions, $H_{\text{int}} = U \sum_i n_{i\uparrow} n_{i\downarrow} + \frac{1}{2} \sum_{ij} V_{ij}^c n_i n_j$. This model shares the same Ward identity with the Hubbard model, since the nonlocal charge-charge interaction does not lead to anomalous currents (cf. Sec. F of chapter 3),

$$\Sigma_{k+q} - \Sigma_k = \sum_{k'} \Gamma_{kk'q}^\alpha \left[G_{k'+q} - G_{k'} \right]. \tag{A.6}$$

Since the goal is to account for a dynamical screening effect of the local interaction, a retarded charge-charge interaction is introduced on the impurity,

$$S = S_{\text{AIM}} + \frac{1}{2} \sum_\omega \rho_{-\omega}^c \Lambda_\omega^c \rho_\omega^c. \tag{A.7}$$

The Ward identity of this impurity model is in turn given by Eq. (F.35) of chapter 3, where all quantities are replaced by their impurity counterparts,

$$\Sigma_{\nu+\omega} - \Sigma_\nu = \sum_{\nu'} \gamma_{\nu\nu'\omega}^\alpha \left[g_{\nu'+\omega} - g_{\nu'} \right]. \tag{A.8}$$

Therefore, in complete analogy to DMFT, it is possible to satisfy the Ward identity of the extended Hubbard model with charge-charge couplings if the 1P and 2P self-energies are approximated as $\Sigma_k = \Sigma_\nu$ and $\Gamma_{kk'q}^\alpha = \gamma_{\nu\nu'\omega}^\alpha$ and when the self-consistency condition $G_{\text{loc}} = g$ holds. These steps are independent of the value of the retarded interaction and hence, remarkably, this approximation satisfies the Ward identity for *any value* of Λ^c, provided that the 1P self-consistency condition holds.

Then, how should Λ^c be determined if is not fixed by the requirement of local conservation laws? A suitable starting point may be to determine its value using EDMFT: One converges the EDMFT scheme presented in Sec. A.4, which guarantees that $G_{\text{loc}} = g$ holds, and subsequently uses the 1P and 2P self-energies Σ and γ to calculate the susceptibility in the same way as in DMFT[4], using one of the four equivalent formulations presented in Sec. B of chapter 4, e.g.,

$$\hat{X}_q^\alpha = \hat{X}_q^0 + \hat{X}_q^0 \hat{\gamma}_\omega^\alpha \hat{X}_q^\alpha. \tag{A.9}$$

However, some ingredients are still missing for a suitable generalization of the dynamical

---

[4]It should be noted that the susceptibility obtained from Eq. (A.9) is *not* the DMFT susceptibility that corresponds to $V^c = 0$, as in the DMFT+RPA approach in Sec. A.3, since Λ^c acts on the impurity.

mean-field picture to the extended Hubbard model: The local approximation to the 2P self-energy $\Gamma \approx \gamma$ by the one of the impurity model neglects RPA corrections due to $V_{\mathbf{q}}^c$, which are included in the DMFT+RPA approach in Sec. A.3 and also in EDMFT in Sec. A.4. The RPA corrections allow for divergences of the charge susceptibility that signal a transition to charge order. On the other hand, the impurity problem *does* account for RPA corrections due to the retarded interaction Λ_ω^c, an interaction which is not present in the lattice model. In this respect the EDMFT susceptibility in Eq. (A.5) is instructive in that it cancels out the RPA corrections due to Λ^c and inserts the ones due to V^c instead. Within the dual boson formalism [121, 85] it can be shown rigorously that it is indeed sound to cancel out and insert the RPA corrections in this way from the susceptibility in Eq. (A.9), respectively,

$$X_q^{c,\mathrm{DB}} = \frac{X_q^c}{1 - (V_q^c - \Lambda_\omega^c)X_q^c}. \tag{A.10}$$

This approach therefore combines the best features of DMFT+RPA and EDMFT. (i) It accounts for RPA corrections and preserves an ungapped 2P spectrum (cf. Sec. A.3), (ii) it allows for the dynamical screening of the local interaction in the impurity model due to the nonlocal interaction.

The dual boson approach in Eq. (A.10) has been used successfully to describe plasmons in systems with long-ranged charge-charge interactions [78, 80]. The plasmon energy remains finite in the dual boson approach, since the condition $\imath\omega X_{\mathbf{q}=0,\omega}^{c,\mathrm{DB}} = 0$ holds [138]. The dual boson approach is thus a natural generalization of the dynamical mean-field picture to nonlocal charge-charge interactions. Of course, the neglect of vertex corrections also has some downsides: Although the 2P spectrum remains ungapped, the Ward identity is violated, also at the homogeneous wave vector $\mathbf{q} = 0$. This is the case, because the susceptibility in Eq. (A.10) is not fully consistent with the charge response $\frac{dn}{d\mu}$, which was found in Ref. [83]. However, as shown in Sec. D.6 of chapter 3, $X_{\mathbf{q}=0,\omega=0}^{c,\mathrm{DB}}$ and $-\frac{dn}{d\mu}$ would be exactly equal if the Ward identity was satisfied at $\mathbf{q} = 0$[5]. At the same time, Ref. [83] showed only small violations of thermodynamic consistency, such that the violation of the Ward identity is apparently negligible at least in the parameter regimes considered in this publication. It would be important to consider the consistency of the charge response at a phase transition to charge order, since a strong violation may lead to one of the scenarios shown on the left and right of Fig. 3.8.

The dual boson approach presented here has a local self-energy, and therefore neglects the nonlocal Fock diagram, which can be recovered by including nonlocal corrections to the self-energy [85]. This, however, will in general undermine the conserving features of the approximation. The tradeoff is therefore to either obtain a realistic description of collective

---

[5] The violation of the Ward identity at $\mathbf{q} = 0$ must happen, since by construction it is $\hat{X}_q^\alpha$ in Eq. (A.9) that satisfies the Ward identity, and that is therefore consistent with $\frac{dn}{d\mu}$, rather than $X_q^{c,\mathrm{DB}}$ from Eq. (A.10). The deviations between $X_q^{c,\mathrm{DB}}$ and $\frac{dn}{d\mu}$ are therefore due to $(V_q^c - \Lambda_\omega^c)X_q^c$ in the denominator of Eq. (A.10), and they may become large near a phase transition to charge order. It was found in Ref. [83] that in order to establish consistency of $X_q^{c,\mathrm{DB}}$ with $\frac{dn}{d\mu}$ one has to take three- and four-particle vertices of the impurity model into account. Consequently, such contributions are also needed in order to satisfy the Ward identity.

modes, and to accept the restriction to the local self-energy of the impurity model, or to include nonlocal corrections to the self-energy at the expense of conservation laws.

A.6 Complications in the spin channels

Motivated by the very successful application of the dual boson approach to nonlocal charge-charge interactions, one may hope for a straightforward generalization of this approach to exchange interactions. Against the expectation, severe complications arise: It is inherently more difficult to extend the dynamical mean-field picture to the spin channels. It will be documented here why this is the case, in order to help fostering the development of such an approach in the future.

Let us consider an extended Hubbard model with nonlocal interactions in all channels $\alpha = c, x, y, z$, $H_{\text{int}} = U \sum_i n_{i\uparrow} n_{i\downarrow} + \frac{1}{2} \sum_\alpha \sum_{ij} V_{ij}^\alpha \rho_i^\alpha \rho_j^\alpha$. The Ward identity of this model was derived in Sec. F of chapter 3,

$$\Sigma_{k+q} - \Sigma_k = \sum_{\underline{k}} \Gamma_{k\underline{k}q}^\alpha [G_{\underline{k}+q} - G_{\underline{k}}] - \sum_{\underline{k}k'k''p\beta\gamma} V_p^\beta (\hat{X}^{\alpha,-1})_{k\underline{k}q} X_{\underline{k}k'k''qp}^{\alpha\beta\gamma}, \qquad (A.11)$$

which is an anomalous Ward identity. The anomaly is the second term on the RHS of this relation and it is due to the exchange couplings $V^{x,y,z}$, it does not arise in the charge channel. The anomaly introduces the chiral six-point correlation function $X^{\alpha\beta\gamma}$ into the Ward identity, which is defined in Eq. (F.8) of chapter 3, such that the Ward identity is not merely a relation between the 1P and 2P level anymore. A straightforward generalization of the dual boson approach would begin by introducing retarded couplings $\Lambda^{c,x,y,z}$ on the impurity, which correspond to the charge-charge and exchange couplings $V^{c,x,y,z}$, respectively. This leads to the action of the Bose-Fermi-Kondo model,

$$S = S_{\text{AIM}} + \frac{1}{2} \sum_{\alpha\omega} \rho_{-\omega}^\alpha \Lambda_\omega^\alpha \rho_\omega^\alpha. \qquad (A.12)$$

The Ward identity of this model was derived in chapter 3, Sec. F as well, it reads,

$$\Sigma_{\nu+\omega} - \Sigma_\nu = \sum_{\nu'} \gamma_{\nu\nu'\omega}^\alpha [g_{\nu'+\omega} - g_{\nu'}] - \sum_{\underline{\nu}\nu'\nu''\omega'\beta\gamma} \Lambda_{\omega'}^\beta (\hat{\chi}^{\alpha,-1})_{\nu\underline{\nu}\omega} \chi_{\underline{\nu}\nu'\nu''\omega\omega'}^{\alpha\beta\gamma}. \qquad (A.13)$$

Here, the analogous chiral six-point correlation function of the impurity arises, which is defined in Eq. (F.32) of chapter 3.

It is now obvious that the equivalence of the lattice Ward identity in Eq. (A.11) to the impurity Ward identity in Eq. (A.13) is not simply established by approximating Σ and Γ with their respective counterparts of the impurity model and satisfying the self-consistency condition $G_{\text{loc}} = g$. Instead, in order to achieve the equivalence of Eqs. (A.11) and (A.13), one also has to make sure that the anomalies in these Ward identities are equal. It seems that, if this is at all possible, it can only be done using a suitable two-particle self-consistency condition in order to fix $\Lambda^{x,y,z}$. The charge and spin channels are

thus fundamentally different: In the charge channel no anomaly arises and one may fix the retarded charge-charge interaction to an arbitrary value. In the spin channels, on the other hand, the Ward identity will always be violated, unless one is able to fix the retarded spin-spin interaction by a suitable two-particle self-consistency condition. The reason for this is that exchange interactions, other than interactions in the charge channel, lead to anomalous currents, as discussed in Sec. I of chapter 3. In order to obtain a conserving approximation, one has to fix the current due to the hopping, which is done by the 1P self-consistency condition, as well as the anomalous spin currents. Unfortunately, up to the present day a suitable two-particle self-consistency condition is unknown.

A.7   Conclusions

Q   The dual boson approach was introduced in Sec. A.5, which combines advantageous features of a "DMFT+RPA" approach by Pruschke et al. and of EDMFT. It was shown that the dual boson approach to nonlocal charge-charge interactions can be motivated from the Ward identity. Although the latter is eventually violated, since RPA but not vertex corrections of the nonlocal potential are accounted for, several features of the 2P spectrum are recovered. In particular, the spectrum remains ungapped at the Γ-point. On the other hand, an attempt to derive a dual boson approach for exchange interactions reveals that these introduce an anomaly into the Ward identity. This prohibits a straightforward extension of the dual boson approach to the spin channel, unless a proper two-particle self-consistency condition can be found.

These considerations may also have implications for other approximations: It was shown in chapter 3 that in systems with exchange couplings the derivation of the 2P self-energy from the Luttinger-Ward functional is not sufficient to satisfy the Ward identity, since it does in general not account for anomalous currents. In a functional formulation these currents are not easily visible, although they may undermine local conservation laws if they are not properly accounted for. It seems that not only dynamical mean-field approaches, and not merely approaches using retarded interactions, could be affected by this. For example, in self-consistent cluster approaches, one usually accounts for inter-cluster hoppings, which represent the current between the clusters that is caused by the hopping. However, since exchange interactions lead to further anomalous spin currents, it seems that any approach to an exchange system that accounts merely for inter-cluster hoppings but not for anomalous inter-cluster currents most likely violates the Ward identity. Even if the Ward identity should hold in such approaches, for reasons that are arguably not obvious, it seems that much could be learned about spin conservation from these approximations if they were examined from the viewpoint of the integral Ward identity. This would make the anomalous currents explicitly visible.

B Application I: Exact diagonalization solver for EDMFT

Q The extended dynamical mean-field theory presented in Sec. A.4 is a computationally feasible approach, also in a multi-orbital context, that allows to take nonlocal interactions into account. Without question, this approach comes with a number of severe downsides: Qualitative features of the 2P spectrum are lost, and the Ward identity is violated [39]. This violation is severe, and as is clear from the considerations in Sec. D.6 of chapter 3, the violation of the Ward identity leads to thermodynamic inconsistency. For this reason, second order phase transitions may appear in this approximation as first order, or worse, there may be no stable phase. Both scenarios indeed occur in spin-DMFT (i.e., EDMFT for Heisenberg model), as investigated thoroughly in Ref. [100], compare also Fig. 3.8. Moreover, all nonlocal corrections to the self-energy are dropped, including the nonlocal Fock diagram. It was shown in Ref. [6] that the Fock diagram has a large influence on the phase diagram of the extended Hubbard model, in particular, neglecting the Fock diagram strongly favors the Mott insulator over charge order. It was further seen in a recent DCA study of the two-dimensional extended Hubbard model that nonlocal corrections to the self-energy are relevant [140]. On many lattices the screening predicted by EDMFT does not depend on the sign of the nonlocal interaction, which should make a large difference.

At the same time, EDMFT is the stepping stone for the dual boson approach presented in Sec. A.5, which rectifies many of these issues: The 2P spectrum is ungapped [39], thanks to the vertex corrections, thermodynamic consistency holds to good approximation [83], nonlocal corrections may be included into the self-energy [121, 85], which also recovers the nonlocal Fock diagram (see Appendix G2 of Ref. [85]), and, finally, the sign of the nonlocal interaction can also affect the effective screening [138, 79]. It seems, therefore, that the EDMFT approximation as such gives a false impression of the potential that it has as a stepping stone, and it is worthwhile to continue its development.

B.1 Exact diagonalization solvers for effective impurity problems

In dynamical mean-field approaches the impurity problem is solved often using CTQMC **Q** solvers, which have seen considerable improvements in the last years [33, 133]. The incorporation of retarded density-density interactions into the impurity model, which is necessary in EDMFT, is often possible without a numerical overhead [153]. Another possibility to account for these interactions is the numerical renormalization group [56, 23, 60]. One method of solution, however, which was one of the earliest to be used to solve the Anderson impurity model of DMFT, is absent from this list, the exact diagonalization (ED) [75, 24]. In ED the Hamiltonian of the impurity model is solved exactly, which is only possible if the Hamiltonian is small. In DMFT this can be dealt with by discretizing the hybridization function, which should in the thermodynamic limit represent a coupling of the impurity to a continuous bath. After the discretization the continuous bath is replaced typically by a handful of bath sites, which is a surprisingly reliable method to solve the effective impurity problem of DMFT [32, 24].

However, the retarded interaction that is introduced in EDMFT is represented in the Hamiltonian picture by a coupling of the impurity to a bosonic bath, as introduced in Sec. F.3 of chapter 3, which in principle leads to an infinite Hilbert space for the bosons. Since the exact diagonalization is applicable at small or even zero temperature and is directly applicable on the real axis, it is certainly desirable to have this method available as an alternative to CTQMC solvers. In this section an exact diagonalization solver for EDMFT will be presented briefly, together with an application to the half-filled extended Hubbard model on the square lattice with nearest neighbor hoppings and charge-charge interactions. The results of this section have been published in Ref. [90]. The reader should note that only in this section X^c will denote the EDMFT susceptibility in Eq. (A.5), $X^c_{\mathbf{q}\omega} \equiv X^{c,\text{EDMFT}}_{\mathbf{q}\omega}$, which does *not* take vertex corrections into account.

B.2   Truncation of the Hilbert space

In applications of EDMFT to the extended Hubbard model with charge-charge couplings, $H_{\text{int}} = U \sum_i n_{i\uparrow} n_{i\downarrow} + \frac{1}{2} \sum_{ij} V^c_{ij} n_i n_j$, a retarded interaction is introduced in the charge channel of the impurity model, which leads to the action in Eq. (A.7). In the Hamiltonian picture the hybridization function Δ and the retarded interaction Λ^c are represented by a coupling of the impurity to a fermionic and a bosonic bath, respectively,

$$H_{\text{imp}} = H_{\text{at}} + H^0_\Delta + H_\Delta + H^0_{\Lambda^c} + H_{\Lambda^c}. \tag{B.1}$$

Here, the impurity is represented by $H_{\text{at}} = -\mu n + U n_\uparrow n_\downarrow$, whereas the remaining operators H^0_Δ H_Δ, $H^0_{\Lambda^c}$, and H_{Λ^c} are defined in Eqs. (C.16), (C.17), (F.15), and (F.17) of chapter 3, considering only the channel $\alpha = c$ for the bosons. The Hamiltonian in Eq. (B.1) is also known as the Holstein-Anderson model. In order to obtain a finite Hamiltonian, one needs to restrict the size of the Hilbert space of H_{imp}. In case of the fermionic bath this can be done by considering only a finite number of K bath sites, such that the hybridization function [cf. Eq. (C.20) of chapter 3] of EDMFT is approximated as,

$$\Delta_\nu \approx \Delta^K_\nu = \sum_{k=1}^K \frac{|v_k|^2}{i\nu - \epsilon_k}. \tag{B.2}$$

Including the impurity, the single-band Hamiltonian in Eq. (B.1) therefore has $K + 1$ fermionic orbitals, which leads to a basis of the fermionic Hilbert space $\mathcal{H}_f$ with length 2^{2K+2}.

In the occupation number basis one conveniently labels the basis states with the binary numbers between 0 and $2^{2K+2} - 1$. For example, from 0000 to 1111 for $K = 1$, where 0 denotes empty and 1 filled states, respectively. It is advantageous to assign the first half of the digits to spin-$\uparrow$ states and the second half to spin-$\downarrow$ states, in the example $n_{1\uparrow} n_{2\uparrow} n_{1\downarrow} n_{2\downarrow}$, and to sort the binary numbers (i) by the occupation number and (ii) by the spin quantum number. In Python such a sorted list can be generated in a single line of code:

```
>>> K=1
>>> Kp1=K+1
>>> sorted(xrange(4**Kp1),key=lambda state:(lambda N:[N,2*bin(state>>Kp1).count("1")-N])(bin(state).count("1")))
[0, 1, 2, 4, 8, 3, 5, 6, 9, 10, 12, 7, 11, 13, 14, 15]
```

In binary format this list then reads as follows:

	↑	↓	N	M
0	00	00	0	0
1	00	01		-1
2	00	10	1	
4	01	00		
8	10	00		1
3	00	11		-2
5	01	01		
6	01	10	2	0
9	10	01		
10	10	10		
12	11	00		2
7	01	11		-1
11	10	11	3	
13	11	01		
14	11	10		1
15	11	11	4	0

If the Hamiltonian matrix is constructed from an occupation number basis that is ordered in this way, it will automatically be block-diagonal with respect to the total occupation number N and with respect to the total magnetic moment M (provided the Hamiltonian conserves N and M). The largest block of the Hamiltonian occurs at half-filling, $N = K + 1$, and at minimal M. Without the bosons, the number of basis states that span this block is then $\binom{K+1}{[K+1]/2}^2$ [that is 4 in the example][6]. The mapping of fermionic states to binary numbers is a perfect one and the action of operators may be implemented at the machine level using bit-wise operations [51].

The bosonic Hilbert space $\mathcal{H}_b$ is more delicate. Firstly, just like the fermionic bath, the bosonic spectrum has to be discretized into P energy levels. The retarded charge-charge interaction [cf. Eq. (F.29) of chapter 3] then takes the form,

$$\Lambda_\omega^c \approx \Lambda_\omega^{c,P} = \sum_{p=1}^{P} \frac{2|w_p^c|^2 \Omega_p^c}{(i\omega)^2 - (\Omega_p^c)^2}. \tag{B.3}$$

However, other than the fermions, the occupation number of the bosonic states is in principle not bounded. This leads to an infinite Hamiltonian already for a single bosonic energy level. To make any progress in an exact diagonalization, there has to be an upper bound N_p on

---

[6] K is odd here. For even K there are two largest blocks of equal size.

the number of bosons that can occupy the energy level with index p^7. Even then, the length of the basis grows considerably in combination with the fermionic Hilbert space. Overall, the largest block of the Hamiltonian has rank $\binom{K+1}{[K+1]/2}^2 (N_1+1)(N_2+1)\cdots(N_P+1)$, where the mixed fermion-boson Hilbert space $\mathcal{H}_f \otimes \mathcal{H}_b$ is constructed from basis states of the form,

$$|\psi\rangle = \underbrace{|m_1, m_2, \ldots, m_p, \ldots, m_P\rangle}_{\text{bosonic part}} \otimes \underbrace{|n_\uparrow, n_{1\uparrow}, \ldots, n_{k\uparrow} \ldots n_{K\uparrow}, n_\downarrow, n_{1\downarrow}, \ldots, n_{k\downarrow}, \ldots, n_{K\downarrow}\rangle}_{\text{fermionic part}}.$$

Here, n_σ is the occupancy of the impurity level, $n_{k\sigma}$ is the occupancy of the bath level k, and m_p is the bosonic occupancy in the level p. Of course, it becomes easily unfeasible to calculate all eigenvalues and eigenstates of the largest block. However, since the Hamiltonian is sparse, the eigenstates that belong to the smallest eigenvalues may be calculated using the Arnoldi method [69]. A feasible example for applications is $K = 7$ and $P = 3$.

It is clear that P must be a rather small number, and it is *a priori* not clear if $P = 3$ is sufficient for an accurate solution of the EDMFT equations. Detailed benchmarks in Ref. [90] show that P may indeed be chosen small. In fact, a number of $P = 2$ bosonic energy levels is usually sufficient, except in extreme regimes which feature charge excitations of both large and small energies, such as at an insulator to charge-order boundary. Since a handful of fermionic bath levels already describe the Mott transition with good accuracy [24], the application of ED as a quantum impurity solver for EDMFT is feasible.

B.3   EDMFT cycle

The usual progression to obtain the self-consistent EDMFT solution is to choose an appropriate initial guess for the hybridization function Δ_ν and the retarded interaction Λ_ω^c and to solve the impurity model. Then, Green's function g_σ and the charge susceptibility χ_ω^c of the impurity are known, in ED they are computed from the respective Lehmann formulae [90]. One further calculates the lattice Green's function as in DMFT, $G_k^{-1} = g_\nu^{-1} - \Delta_\nu + \varepsilon_{\mathbf{k}}$, as well as the EDMFT susceptibility in Eq. (A.5), $X_q^{c,-1} = \chi_\omega^{c,-1} - \Lambda_\omega^c + V_{\mathbf{q}}^c$. Using the local parts of the correlation functions, $G_{\text{loc},\nu} = \sum_{\mathbf{k}}' G_k$, and $X_{\text{loc},\omega}^c = \sum_{\mathbf{q}}' X_q^c$, a new hybridization function and a new retarded interaction can be obtained from the update formulae,

$$\begin{aligned}
\Delta_\nu^{\text{new}} &= \Delta_\nu^{\text{old}} + \xi_1[g_\nu^{-1} - G_{\text{loc},\nu}^{-1}], \\
\Lambda_\omega^{c,\text{new}} &= \Lambda_\omega^{c,\text{old}} + \xi_2[\chi_\omega^{c,-1} - X_{\text{loc},\omega}^{c,-1}].
\end{aligned} \tag{B.4}$$

Here, $0 < \xi_1, \xi_2 \leq 1$ are suitable mixing parameters. This process is repeated until the self-consistency conditions $G_{\text{loc}} = g$ and $X_{\text{loc}}^c = \chi^c$ are satisfied.

In an application of the ED as a solver for EDMFT, this cycle must be modified slightly: Even when starting with discrete initial guesses for Δ and Λ^c according to Eqs. (B.2) and (B.3), the input for the next iteration from Eq. (B.4) need not be representable in

---

[7] While the fermionic basis states are suitably labeled by numbers in the base 2, one may label the bosonic basis states by numbers in the base $N_p + 1$. This is obviously less useful than for the fermions, since N_p is variable and does not map as perfectly to the low level architecture of computers.
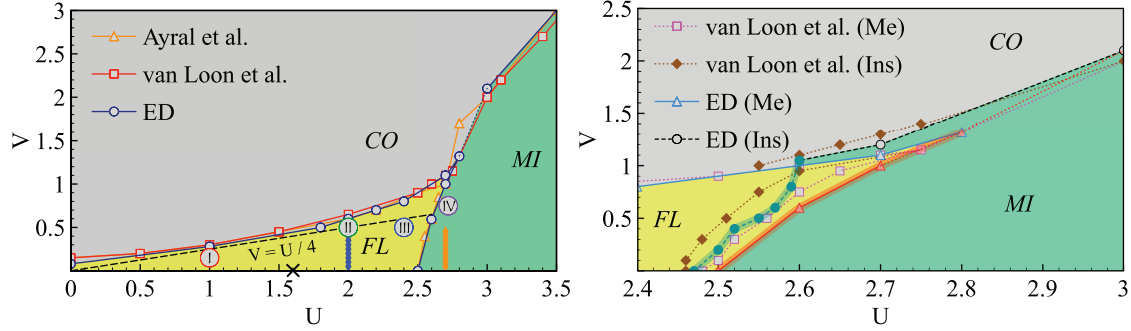
FIGURE 5.2: Left: EDMFT phase diagram of the extended Hubbard model in the *U-V* plane. Shown are the phase boundaries obtained from ED (circles), as well as those from van Loon et al. (squares, [85]) and Ayral et al. (triangles, [5]). Roman numerals indicate where benchmarks with CTQMC were performed, which show a very good agreement with ED on the Matsubara axis [90]. The dashed line shows $V = U/4$, a rough estimate of the FL-CO boundary. Right: Closeup of the FL-MI boundary. The ED data are compared to van Loon et al., who calculated the transition from the FL (squares) and from the insulator (diamonds), which reveals the FL-MI coexistence region. The coexistence region was also determined using ED, starting from metallic (triangles) and insulating seeds (circles).

terms of only K fermionic and P bosonic energy levels anymore. For this reason, the updated hybridization function Δ^{new} and retarded interaction $\Lambda^{c,\mathrm{new}}$ need to be projected into the subspace of solutions that is indeed representable in this way. This can be done by fitting the bath parameters in Eqs. (B.2) and (B.3) using a least squares fit, which minimizes the expressions,

$$c_f^2 = \frac{1}{N_\nu + 1} \sum_{n}^{N_\nu} \left[\Delta_{\nu_n}^{\mathrm{new}} - \Delta_{\nu_n}^{K,\mathrm{new}} \right]^2 ,$$

$$c_b^2 = \frac{1}{N_\omega + 1} \sum_{m}^{N_\omega} \left[\Lambda_{\omega_m}^{c,\mathrm{new}} - \Lambda_{\omega_m}^{c,P,\mathrm{new}} \right]^2 .$$

Here, $\Delta^{K,\mathrm{new}}$ and $\Lambda^{P,\mathrm{new}}$ are the desired discretized functions for the next iteration. The fit is performed for a finite number of N_ν fermionic and N_ω bosonic Matsubara energies, respectively.

B.4 Phase diagram of the extended Hubbard model on the square lattice

The ED solver described above was used to calculate EDMFT phase diagram in Fig. 5.2 of the half-filled extended Hubbard model with nearest neighbor hoppings and charge-charge couplings. The nearest neighbor hopping is set to $t = 0.25$ and the temperature to the low value $T = 0.01$. The phases that occur are the Fermi liquid (FL,yellow), the Mott insulator (MI,green), and the charge-ordered (CO,gray) phase at large V. In single-site
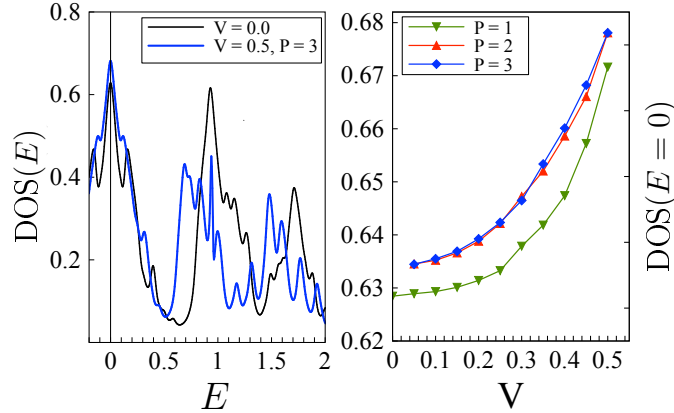
FIGURE 5.3: Left: Quasiparticle peak and the upper Hubbard band at $U = 2$ for $V = 0$ and $V = 0.5$. Right: DOS at the Fermi level as a function of V (cf. blue diamonds in the left panel of Fig. 5.2). P indicates the number of bosonic bath levels, the broadening of the DOS was chosen as $\delta = \pi/\beta$.

EDMFT calculations the CO phase can not be entered, since the charge susceptibility X_q^c is divergent at $\mathbf{q} = (\pi, \pi)$, which corresponds on the square lattice to a charge density wave that forms a checkerboard pattern. The divergence of X_q^c was used to determine the FL-CO and MI-CO boundaries. The boundary between FL and MI is estimated from a change in the slope of g_ν at small Matsubara energies. The left panel of Fig. 5.2 also shows the phase boundaries found by Ayral et al. [5] and van Loon et al. [85], who solved the effective impurity model via CTQMC.

The right panel of Fig. 5.2 is a closeup of the FL-MI boundary. This shows the coexistence region of the first order FL-MI transition. There is also a stripe above the yellow region where MI solutions can be converged while one encounters a transition to CO when coming from the FL. Although this suggests a coexistence of the MI and CO phases, the credibility of EDMFT in distinguishing first and second order transitions is questionable, since it violates the Ward identity. Compared to the CTQMC results of Ayral et al. and van Loon et al., the coexistence region of FL and MI is shifted to slightly larger values of U in ED. This can be attributed to the odd number of $K = 5$ fermionic bath levels that were used in the calculations: In ED an even number of bath levels favors the MI phase, since a symmetric discrete bath with an even number of peaks is 'gapped', while an odd number favors the Fermi liquid, because the bath then has a peak at the real energy $E = 0$. However, the error due to the bath discretization is much smaller than the error introduced by the EDMFT approximation: A black cross in the left panel of Fig. 5.2 shows the FL-MI transition at $V = 0$ obtained from DCA calculations [34], where $U_c \approx 1.6$.

Apparently, ED can be used as a reliable solver for the local reference system of EDMFT, at least at low temperature. However, the EDMFT approximation as such is not reliable in the estimation of the phase boundaries due to the deficiencies mentioned in the beginning.
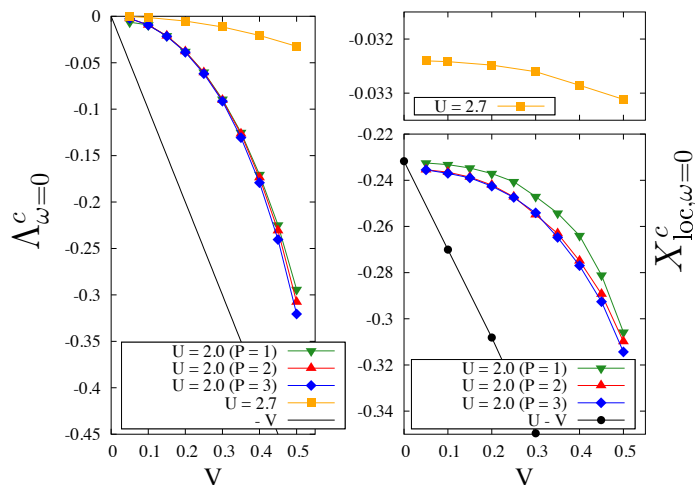
FIGURE 5.4: Left: Dynamic interaction $\Lambda^c_{\omega=0}$ as a function of V in the FL (triangles and diamonds) and in the insulator (yellow squares, compare yellow symbols at $U = 2.7$ on the left of Fig. 5.2). The line $-V$ indicates the linear screening predicted by the variational principle [127]. Top right: Local susceptibility $X^c_{\mathrm{loc},\omega=0}$ in the insulator. Bottom right: $X^c_{\mathrm{loc},\omega=0}$ in the FL, black symbols show calculations at $U^* = U - V$. Calculations in the MI were done at $P = 1$, in the FL at $P = 1, 2$ and 3 bosonic bath levels.

Nonlocal correlations could be accounted for by considering several sublattices, which would also give access to the charge-ordered phase. Further options for improvement lie in nonlocal extensions to EDMFT like GW+EDMFT [21] or in the dual boson approach [121].

B.5 Dynamical screening

Fig. 5.3 shows the effect of V on the density of states $\mathrm{DOS}(E) = -\frac{1}{\pi} \sum'_{\mathbf{k}} G_{\mathbf{k}}(E + \imath\delta)$ in the moderately correlated FL at $U = 2$. If the local interaction U is screened by the nonlocal one, an increase of V should enhance the quasiparticle peak. The right panel of Fig. 5.3 shows indeed an increase of the spectral weight at the Fermi level with V in a series of calculations that are marked with blue points in the left panel of Fig. 5.2. In order to examine the effect of the discretization of the bosonic spectrum (cf. Sec. B.2), these calculations were performed with $P = 1, 2$ and 3 bosonic energy levels, while the number $K = 5$ of the fermionic levels was kept fixed. There is a clear convergence trend and it seems that $P = 2$ is already sufficient. The reason that more than one level is needed is that in the FL this one level has to account for a relatively broad spectrum of charge excitations. Already at $P = 2$ one energy level accounts for high energy excitations and the second level for the excitations at low energies [90]. Since the latter play a more important role in the screening of the single-particle spectrum, the density of states at the Fermi level is slightly higher at $P = 2$ than at $P = 1$. The left panel of Fig. 5.3 shows the density of

states near $E = 0$ for $V = 0$ and $V = 0.5$, where the redistribution of spectral weight from the right Hubbard band to the quasiparticle peak is visible.

In EDMFT one considers $U_\omega = U + \Lambda^c_{\omega=0}$ as the screened interaction. The retarded interaction Λ^c is determined from the two-particle self-consistency condition $X^c_{\text{loc}} = \chi^c$, the spectrum of Λ^c is thus determined by the charge excitation spectrum of the impurity. If this spectrum has only features at high energies, this will also be the case for the spectrum of Λ^c. In the insulator charge excitations are indeed shifted to high energies, such that the screening described by EDMFT is very weak in this region, except in the vicinity of the MI-CO boundary. However, it is intuitively not immediately clear why this should be the case: In the half-filled insulator the creation of a double occupancy is disfavored energetically by the large local interaction U, but also incentivized by the nonlocal interaction V. A simple estimate from a viariational principle indeed predicts a linear screening mechanism, with the screened interaction $U^* = U - V$ [127]. In disagreement with the EDMFT picture, this scenario of strong and linear screening should be realized best in the insulating phase [81].

This discrepancy can be seen in the left panel of Fig. 5.4, which shows $\Lambda^c_{\omega=0}$ as a function of V for $U = 2$ and $U = 2.7$. In the Fermi liquid the screening is rather strong and comparable to the linear screening predicted by the variational principle, but nowhere linear. In the insulator at $U = 2.7$ $\Lambda^c_{\omega=0}$ is minuscule. This is due to the absence of low energetic charge excitations, which can be seen on the right panel of Fig. 5.4. In the insulator $X^c_{\text{loc},\omega=0}$ is roughly one order of magnitude smaller than in the FL, and receives virtually no enhancement as V is increased. In EDMFT the effect of screening is thus very strongly determined by the magnitude of U, and it can only happen at finite V when at $V = 0$ there are sizable low energetic charge excitations to work with. These results are in agreement with those in Ref. [48]. There seem to be conflicting viewpoints at the moment if screening in the insulator is indeed suppressed drastically or if it is better described by the variational principle. It is worth noting that a linear screening in the FL is predicted by the self-consistent dual boson approach [138].

B.6   Implementation notes

The ED solver is based on the open source exact-diagonalization library [49], which uses the core libraries [31] of the open source ALPS package [14].

C   Diagrammatic extensions of DMFT

Q The local reference frame of DMFT neglects nonlocal interactions on the one side and nonlocal correlations on the other. Early on, there have been attempts to augment DMFT on both ends, in order to cope with situations where one or the other can not be neglected (cf. Sec. A w.r.t. nonlocal interactions). Long-ranged nonlocal correlations are of importance, e.g., close to instabilities, such as superconductivity [99] or near magnetic phase transitions [80], where the correlation length even diverges at the critical point. Short-ranged nonlocal correlations, on the other hand, are of particular importance in low-dimensional

systems (cf. Fig. 4.1) and for Mott physics [12]. This is the case, since single-site DMFT replaces, what might be short-ranged singlet formations, by the Kondo-screening of the impurity by the structureless bath. This can lead to a strong overestimation of U_c by DMFT, for example, in the half-filled Hubbard model on the square lattice, compared to the DCA result that is drawn into the phase diagram in Fig. 5.2.

Two main branches have formed that address either long- or short-ranged correlations very well: (i) There are diagrammatic extensions of single-site DMFT [119] that aim to reinstate long-ranged correlations, while it is difficult to account for the short-ranged ones [99], due to the non-perturbative nature of the singlet state. Examples of methods under active development are the DΓA (dynamical vertex approximation, [141]) and dual fermion approach [122]. In these approaches one obtains an approximation to the T-matrix F from the (possibly dressed) Bethe-Salpeter equation, and then calculates a **k**-dependent 1P self-energy from the Schwinger-Dyson equation[8]. In both of these methods the 2P self-energy of the impurity model (or its T-matrix) is the fundamental building block of the Bethe-Salpeter equation. (ii) A way to include short-ranged correlations are self-consistent cluster approximations, such as cluster or cellular DMFT [71, 63], the variational cluster approach [108], or the dynamical cluster approximation [45]. Cluster approaches account very well for short-ranged correlations, but break the translational symmetry of the lattice. The distinction between these two categories is not sharp, and the tendency has become to unify aspects of both branches. For example, cluster versions of the dual fermion approach have been developed [156, 50].

C.1 Retarded interactions: From long-ranged interactions to a feedback of collective modes

The methods described above to take nonlocal correlations into account also allow to consider nonlocal interactions. Here, however, the diagrammatic extensions have the advantage that the interaction may be truly long-ranged, while its reach is limited in cluster methods, and interactions are cut off between sites on neighboring clusters. In diagrammatic approaches to long-ranged interactions one often brings retarded couplings on the impurity into the picture, as in EDMFT, that account for the screening of the local by the nonlocal interaction (see Sec. A.4). This picture implies that the retarded interactions should be zero when the nonlocal interaction vanishes, $V^\alpha = 0 \leftrightarrow \Lambda^\alpha = 0$. Indeed, the EDMFT self-consistency condition $X_{\text{loc}} = \chi$ is satisfied by default when V and Λ vanish [cf. Eq. (A.5)].

A recent trend has become to question this direct correspondence between the nonlocal and the retarded interactions. There are at least two intuitive arguments in favor of introducing such interactions, e.g., into a dynamical mean-field approach to the Hubbard model: (i) Although the interaction of the Hubbard model is not screened by a nonlocal interaction, it may be renormalized effectively, due to a feedback of collective charge and spin excitations. (ii) The dynamical interaction is fixed by a two-particle self-consistency

Q

---

[8] This amounts to closing the 'circle of fifths' in Fig. 3.6, typically at the cost of violating conservation laws.

condition, which may be chosen in a favorable way in order to satisfy physically relevant sum rules.

An example for the second point is the ambiguity of the potential energy in DMFT (see Sec. C.2 of chapter 4), which originates from the inconsistency of the local susceptibility of the lattice with the impurity susceptibility, $X_{\mathrm{loc}}^{\alpha} \neq \chi^{\alpha}$. It seems that if one was able to satisfy the self-consistency condition $X_{\mathrm{loc}}^{\alpha} = \chi^{\alpha}$ this ambiguity would be removed. Furthermore, a theorem in Ref. [157] states that any approximation that predicts a bounded double occupancy d will also suppress a divergence of the spin susceptibility in two dimensions, as required by the Mermin-Wagner theorem. This is the case, since the local spin susceptibility $X_{\mathrm{loc}}^{z} = \sum_{\mathbf{q}}' X_{\mathbf{q}}^{z}$ is related to the double occupancy, $d \sim X_{\mathrm{loc},\tau=0}^{z}$, as in Eq. (C.15) of chapter 4. In case of a divergence of X^{z} at some wave vector $\mathbf{Q}$ it assumes the Ornstein-Zernike form in the vicinity, $X_{\mathbf{q}\approx\mathbf{Q},\omega=0}^{z} \sim [(\mathbf{q}-\mathbf{Q})^{2} + \xi^{-2}]^{-1}$. In Ref. [157] it is shown that the integral $\sum_{\mathbf{q}}' X_{\mathbf{q}}^{z}$ over such an integrand leads to a divergence in one and two dimensions, while it remains finite for larger dimensionality. This means that if the double occupancy d remains finite in $d < 3$, which should be the case, then X^{z} can not have such a divergence[9].

There is thus definitely an incentive to make DMFT two-particle self-consistent. Given a suitable constraint on the two-particle level, such as $X_{\mathrm{loc}}^{\alpha} = \chi^{\alpha}$, retarded interactions may provide the necessary degrees of freedom to fix it. A number of approaches make attempts along this line, such as the TRILEX [9, 8] and QUADRILEX [7] approaches, a variant of the $D\Gamma A$ [119], as well as the self-consistent dual boson approach [138]. It may also straightforwardly be done in GW approaches, such as GW+DMFT [21].

C.2   Suitable effective impurity models for the Hubbard model

QP   The two-particle self-consistent extensions of DMFT described above relate to a highly interesting question: What may be 'the best' effective impurity model for the Hubbard model in *finite* dimensions? I will argue in the following that only the Anderson impurity model is the best local reference model, both with respect to local conservation laws (i) and in terms of one-particle self-consistency (ii). The main results of this section were published in Ref. [65].

(i) Like in Sec. A.3 of chapter 4 and in Secs. A.5 and A.6 of this chapter, let us approach the first of these points by considering the Ward identity of the lattice model in question, in case of the Hubbard model,

$$\Sigma_{k+q} - \Sigma_{k} = \sum_{k'} \Gamma_{kk'q}^{\alpha} \left[G_{k'+q} - G_{k'} \right]. \tag{C.1}$$

The goal of the methods described above is to introduce retarded interactions into the Anderson impurity model, such that a yet unspecified two-particle self-consistency condition

---

[9] This may be seen as a 'poor man's Mermin-Wagner theorem', but in this anecdotal version the physical background of this theorem is absent (cf. Sec. F of chapter 4).
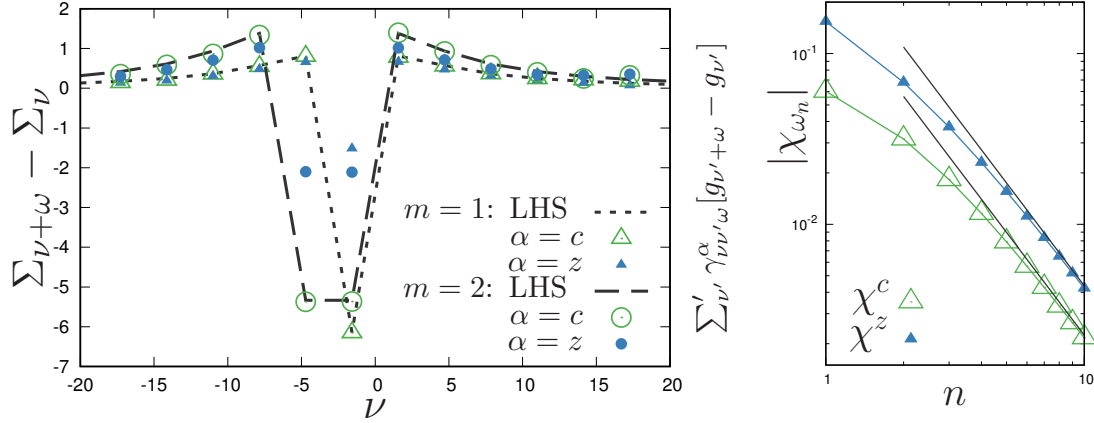
FIGURE 5.5: Left: In the Bose-Fermi-Kondo model an anomaly arises in the spin channel (blue circles) of the Ward identity [cf. Eq. (C.2)], which manifests in the difference between $\Sigma_{\nu+\omega} - \Sigma_\nu$ (dashed lines) and $\sum_{\nu'} \gamma^z_{\nu\nu'\omega} [g_{\nu'+\omega} - g_{\nu'}]$ (blue symbols). There is no anomaly in the charge channel (green triangles). ω_1 (circles) and ω_2 (triangles) are shown. Right: The asymptotes of the charge (green) and spin (blue) susceptibilities of the Bose-Fermi-Kondo model. The asymptotic constants (black lines) are calculated from Eqs. (C.4) and (C.5), respectively. Charge and spin susceptibility approach the same asymptotes when $\Lambda^{x,y,z} = 0$, compare Fig. 4.3. The left and right panel belong to the same parameters $U = 6, \beta = 2$, a conducting bath Δ_ν and sizable Λ^α_ω were used.

may be fixed. While the proposed QUADRILEX approach introduces a dynamical interaction $\Lambda_{\nu\nu'\omega}$, which depends on three frequencies, let us consider first interactions that depend only on ω. The impurity action then reads $S = S_{\mathrm{AIM}} + \frac{1}{2} \sum_{\alpha\omega} \rho^\alpha_{-\omega} \Lambda^\alpha_\omega \rho^\alpha_\omega$, as in the case of EDMFT in Eq. (A.4), which is the Bose-Fermi-Kondo model (see Sec. F.3 of chapter 3). The Ward identity of this impurity model hence has anomalies in the spin channels,

$$\Sigma_{\nu+\omega} - \Sigma_\nu = \sum_{\nu'} \gamma^\alpha_{\nu\nu'\omega} [g_{\nu'+\omega} - g_{\nu'}] - \sum_{\underline{\nu}\nu'\nu''\omega'\beta\gamma} \Lambda^\beta_{\omega'} (\hat{\chi}^{\alpha,-1})_{\nu\underline{\nu}\omega} \chi^{\alpha\beta\gamma}_{\underline{\nu}\nu'\nu''\omega\omega'}. \qquad (\mathrm{C.2})$$

The left panel of Fig. 5.5 shows the LHS and the first term on the RHS of this relation in a numerical example. They indeed coincide in the charge channel but not in the spin channels, due to the anomaly, the second term on the RHS.

The simplest way one could try to make use of this impurity model is by performing a local approximation to the 1P and 2P self-energies of the Hubbard model, $\Sigma_k = \Sigma_\nu$ and $\Gamma^\alpha_{kk'q} = \gamma^\alpha_{\nu\nu'\omega}$, and imposing one-particle self-consistency, $G_{\mathrm{loc}} = g$. Then, Eqs. (C.1) and (C.2) are equivalent in the charge channel, while they differ in the spin channels by the anomaly in Eq. (C.2). Apparently, the coincidence of the lattice and impurity Ward identities holds also in the spin channels when the anomaly vanishes, which is satisfied when $\Lambda^{x,y,z}$ are identically zero. Assuming the highly desirable situation that the solution for Λ^α is unique, no two-particle self-consistency condition can be fixed in the spin channels: An

impurity model with retarded spin-spin interactions is apparently an inappropriate local reference system to satisfy the Ward identity of the Hubbard model.

There are ways to attack this argument: (a) Maybe there is a second solution for $\Lambda^{x,y,z}$, such that the anomaly vanishes? It seems that then a conserving approximation is not uniquely defined. Furthermore, there seems to be nothing that stops $\Lambda^{x,y,z}$ from assuming values that lead to a violation of the Ward identity, unless the disappearance of the anomaly *is* the self-consistency condition. (b) The approximation chosen here is too simple, maybe conservation laws can be restored when Σ and Γ are nonlocal and obtained from the impurity model via, e.g., a parquet approach?

It is difficult to refute these objections in general, but it is possible in case of the self-consistency condition $X_{\text{loc}}^{\alpha} = \chi^{\alpha}$: Let us consider this self-consistency condition at high frequencies,

$$\lim_{\omega \to \infty} (\imath \omega)^2 X_{\text{loc},\omega}^{\alpha} = \lim_{\omega \to \infty} (\imath \omega)^2 \chi_{\omega}^{\alpha}. \tag{C.3}$$

On the LHS of this relation is the asymptote of the local lattice susceptibility of the Hubbard model. It was shown in Eq. (D.19) of chapter 3 that the Ward identity of the Hubbard model in Eq. (C.1) requires that the asymptotes of the charge and spin susceptibilities are the same, $\lim_{\omega \to \infty} (\imath \omega)^2 X_{\text{loc},\omega}^{c} = \lim_{\omega \to \infty} (\imath \omega)^2 X_{\text{loc},\omega}^{x,y,z}$. However, in an impurity model with retarded spin-spin interactions the asymptote of the charge and spin susceptibility are different, as can be seen in the right panel of Fig. 5.5. It was shown in Eq. (F.44) of chapter 3 that in the charge channel one has

$$\lim_{\omega \to \infty} (\imath \omega)^2 \chi_{\omega}^{c} = -4 \sum_{\nu}' g_{\nu} \Delta_{\nu}, \tag{C.4}$$

whereas the asymptote in the spin channels ($\alpha = x, y, z$) is

$$\lim_{\omega \to \infty} (\imath \omega)^2 \chi_{\omega}^{\alpha} = -4 \sum_{\nu}' g_{\nu} \Delta_{\nu} + 4 \sum_{\omega', \beta \neq \alpha}' \Lambda_{\omega'}^{\beta} \chi_{\omega'}^{\beta}. \tag{C.5}$$

Hence, the LHS of Eq. (C.3) must be the same in the charge and spin channels, otherwise the Ward identity of the Hubbard model is violated, while the RHS of Eq. (C.3) assumes different values for $\alpha = c$ and $\alpha = x, y, z$. It is therefore not possible to satisfy the self-consistency condition without violating the Ward identity. The last escape option here is that the second summand on the RHS of Eq. (C.5) is zero. However, χ in that sum does not change its sign ($\chi_{\omega} < 0$), such that a cancellation can only occur when Λ_{ω} has a sign change, which is unphysical for a bosonic function. It should be noted that this proof is independent of the respective approximation to Σ and Γ: Using retarded spin-spin interactions, it is in principle not possible to impose self-consistency between X_{loc}^{α} and χ^{α} and to satisfy the Ward identity at the same time.

Rather than trying to find more escape routes, let us consider the root cause for the

violation of the Ward identity: An impurity model with retarded spin-spin couplings features anomalous spin currents, whereas the Hubbard model does not. There is hence no motivation to introduce such currents into its local reference model. Since the anomalous spin currents arise due to the non-commutativity of the spin operators with the retarded spin-spin coupling, it is clear that an introduction of a three-frequency interaction $\Lambda_{\nu\nu'\omega}$, as has been proposed in the QUADRILEX approach [7], does not improve the situation but makes it worse: This interaction is the impurity analogue to a lattice interaction of the type $V_{1234}c_1^\dagger c_2^\dagger c_4 c_3$, which comprises not only exchange interactions but also pair-hoppings. Such an interaction commutes neither with the spin densities nor with the charge density, such that anomalies arise in all channels $\alpha = c, x, y, z$ of the impurity Ward identity.

Lastly, let us see how the violation of spin conservation occurs in practice, on the example of the approximation introduced above. Σ and γ are then the 1P and 2P self-energies of the Bose-Fermi-Kondo model and the 1P self-consistency condition is $G_{\mathrm{loc}} = g$. Like in DMFT the susceptibility X_q^α is obtained from Σ and γ via the Bethe-Salpeter equation. Finally, RPA corrections of Λ_ω^α are canceled from the lattice susceptibility, $X_q^{\alpha,\mathrm{DB}} = X_q^\alpha/(1+\Lambda_\omega^\alpha X_q^\alpha)$, which is reminiscent of the dual boson approach presented in Eq. (A.10). In the following example the retarded interactions are fixed via the two-particle self-consistency condition $W_{\mathrm{loc},\omega}^\alpha = w_\omega^\alpha$, which is known from GW approximations[10]. As in the TRILEX approach [9], this requires a splitting of the Hubbard interaction according to Eq. (C.17) of chapter 2, which is chosen here as $V^c = U/2$ and $V^{x,y,z} = -U/6$. The screened interactions of lattice and impurity are then given as $W_{\mathbf{q},\omega}^\alpha = V^\alpha + V^\alpha X_{\mathbf{q},\omega}^{\alpha,\mathrm{DB}} V^\alpha$ and $w_\omega^\alpha = (V^\alpha + \Lambda_\omega^\alpha) + (V^\alpha + \Lambda_\omega^\alpha)\chi_\omega^\alpha(V^\alpha + \Lambda_\omega^\alpha)$.

The center panels of Fig. 5.6 show the spin excitation spectrum $\mathrm{Im}\, X_{\mathbf{q}}^{z,\mathrm{DB}}(E + \imath\delta)$ in this approximation for the half-filled Hubbard model on the square lattice near the Γ-point. The nearest neighbor hopping was chosen as $t = 1$ and the inverse temperature as $\beta = 2$, three values of the interaction are shown. The top left panel of Fig. 5.6 shows $\chi_\omega^z \tilde{\Pi}_{\mathbf{q}=0,\omega}^z$, where $\tilde{\Pi}$ is the self-energy of the dual bosons [compare Eq. (B.28) of chapter 4]. This can be used to quantify a violation of global spin conservation, since it should be exactly equal to -1 when it holds. Indeed, at $U = 1$ this is satisfied, accordingly the excitation spectrum in the top center panel remains ungapped. At $U = 4$ a slight deviation from $\chi_\omega^z \tilde{\Pi}_{\mathbf{q}=0,\omega}^z = -1$ is visible, although it does not cause a visible gap in the spin excitation spectrum in the center yet. Finally, at $U = 8$ the violation is strong and the spectrum in the bottom center panel is clearly gapped. This value of the interaction is close to the Mott crossover, where localization sets in.

In the right panel of Fig. 5.6 the retarded spin-spin coupling Λ^z is shown. Obviously, its magnitude corresponds to the quantitative violation of global spin conservation, as expected. On the other hand, the magnitude of Λ^z grows with U. Apparently, the approximation does what it is supposed to do: It introduces a feedback of the spin excitations into the impurity model where these begin to dominate the physics. However, this is inevitably accompanied by the violation of spin conservation, since the anomalous spin currents on

---

[10]The self-consistency condition $W_{\mathrm{loc}}^\alpha = w^\alpha$ is used, since $X_{\mathrm{loc}}^{\alpha,\mathrm{DB}} = \chi^\alpha$ in combination with a SU(2)-symmetric coupling $\Lambda^x = \Lambda^y = \Lambda^z$ causes a severe sign problem in the CTQMC solver.
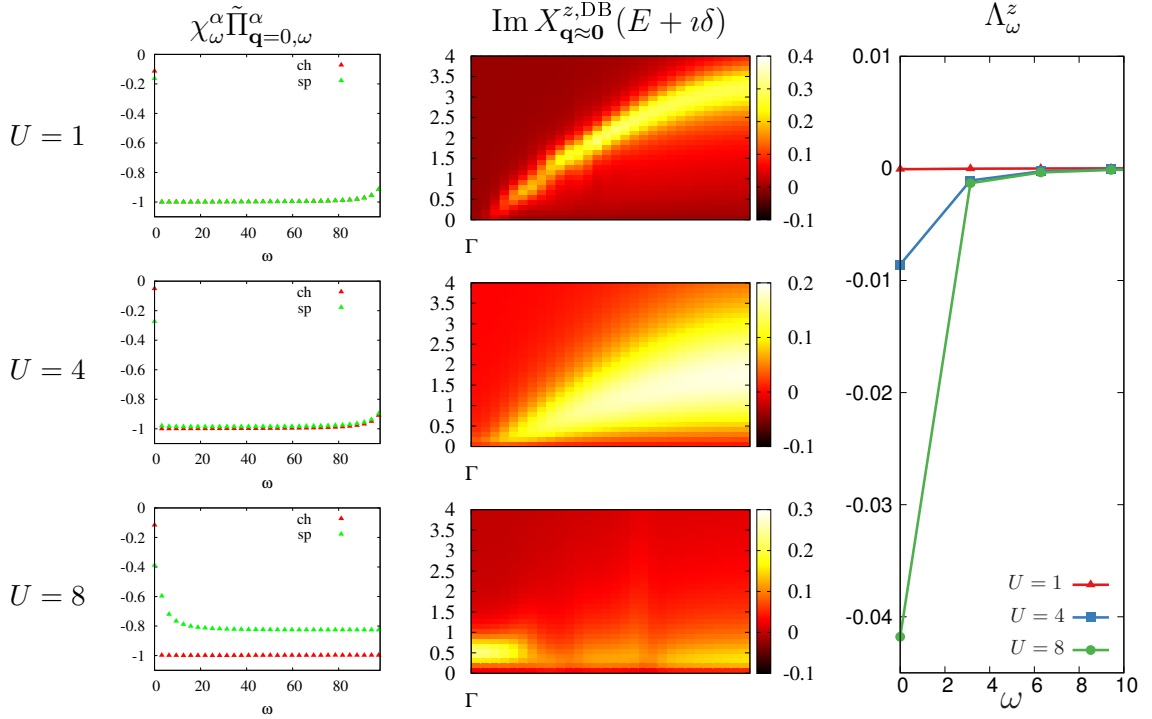
FIGURE 5.6:   Center: The spectrum of spin excitations of the Hubbard model on the high-symmetry path near the Γ-point for different values of U. In this approximation the prescription $W_{\text{loc}}^{\alpha} = w^{\alpha}$ (see text) is fixed using retarded interactions $\Lambda^z = \Lambda^x = \Lambda^y$ and Λ^c. At $U = 8$ global spin conservation is violated, which results in a gapped spectrum at Γ (bottom center). Left: Global conservation requires that $\chi_{\omega}^{\alpha}\tilde{\Pi}_{\mathbf{q}=0,\omega}^{\alpha} = -1$, which holds in the charge channel (red) but is violated in the spin channels (green) at elevated interaction. Right: The retarded spin-spin interaction Λ^z corresponding to the results on the left. The violation of global spin conservation is strong when Λ^z is large.

the impurity become large. Global charge conservation, on the other hand, holds for all interactions, the red data points in the left panels of Fig. 5.6 show that $\chi_{\omega}^{c}\tilde{\Pi}_{\mathbf{q}=0,\omega}^{c} = -1$ is satisfied, notwithstanding cutoff effects at large Matsubara energies.

(ii) Retarded interactions do not only undermine conservation laws but also one-particle in favor of two-particle self-consistency. Let us recall again that the introduction of retarded interactions is supposed to improve thermodynamic consistency, which is desirable, e.g., to resolve the ambiguity of the potential energy in DMFT (see Sec. C.2 of chapter 4). While it seems intuitive that two instead of one self-consistency condition should improve the situation, the opposite is the case for a subtle reason: In DMFT there are four ways to obtain the double occupancy, either from the 1P and 2P level of the impurity or from the 1P and 2P level of the lattice. Of these four values, three are equivalent, $d_{\text{1P}}^{\text{imp}} = d_{\text{2P}}^{\text{imp}} = d_{\text{1P}}^{\text{lat}}$, where the first equality originates from the numerically exact solution of the AIM, which is thermodynamically consistent, and the second equality originates from the 1P

self-consistency condition [cf. Eqs. (C.9) and (C.10) of chapter 4]. The fourth value is d_{2P}^{lat}, which is not equivalent to the other three.

Considering the self-consistency condition $X_{\text{loc}}^{\alpha,\text{DB}} = \chi^\alpha$, it seems to remove this inconsistency, since by construction it will lead to $d_{2P}^{\text{lat}} = d_{2P}^{\text{imp}}$ [compare Eqs. (C.15) and (C.16) of chapter 4]. Against the expectation, this does not lead to the equivalence of all four double occupancies. This is because the equivalence of $d_{1P}^{\text{lat}} = d_{1P}^{\text{imp}}$ in DMFT is grounded on the Migdal-Galitzkii formula $d_{1P}^{\text{imp}} = \frac{1}{U} \sum_\nu' g_\nu \Sigma_\nu$. However, retarded interactions invalidate this formula. Instead, the double occupancy is given as [65],

$$d_{\text{imp}}^{1P} = \frac{1}{2U} \left[2 \sum_\nu' g_\nu \Sigma_\nu + \sum_{\omega,\alpha}' \Lambda_\omega^\alpha (\chi_\omega^\alpha - \beta \langle \rho^\alpha \rangle^2 \delta_\omega) \right]. \tag{C.6}$$

The appearance of Λ^α is intuitively clear, since the potential energy of the impurity model is altered by the retarded interactions. Instead of achieving full consistency, one then has $d_{1P}^{\text{imp}} = d_{2P}^{\text{imp}} = d_{2P}^{\text{lat}}$, while it is now d_{1P}^{lat} that assumes a different value: One- and two-particle self-consistency are mutually exclusive. The numerical application in the next section shows that when $X_{\text{loc}}^{\alpha,\text{DB}} = \chi^\alpha$ is imposed the difference between the two inconsistent values of d is, in fact, *larger* than in DMFT.

Lastly, the retarded interactions also alter the first asymptotic coefficient of the self-energy. In the paramagnetic Anderson impurity model the self-energy is given to first order as [120],

$$\Sigma_\nu^{\text{AIM}} = \frac{U \langle n \rangle}{2} + U^2 \frac{\langle n \rangle}{2} \left(1 - \frac{\langle n \rangle}{2} \right) \frac{1}{\iota\nu} + \mathcal{O}[\nu^{-2}]. \tag{C.7}$$

Due to the close relation of the AIM with the Hubbard model in infinite dimensions, this is the exact ν^{-1}-coefficient of the Hubbard model. The self-energy of the latter is, of course, **k**-dependent in finite dimensions, but this dependence only enters at the second order in ν^{-2}. One can therefore write for the exact self-energy of the Hubbard model,

$$\Sigma_{\mathbf{k}\nu} = \Sigma_\nu^{\text{AIM}} + \mathcal{O}_{\mathbf{k}}(\nu^{-2}), \tag{C.8}$$

where $\mathcal{O}_{\mathbf{k}}(\nu^{-2})$ denotes **k**-dependent corrections of order ν^{-2}. It is therefore desirable to leave the self-energy of the Anderson impurity model intact to order $\mathcal{O}(\nu^{-1})$. However, retarded interactions *change* the ν^{-1}-coefficient, which is shown in Ref. [38] for a charge-charge interaction. In fact, once the ν^{-1}-coefficient has been tampered with, its correct form can not be recovered within the dual boson approach, even when corrections to the impurity self-energy are taken into account. This is because in this formalism the self-energy is given by [85],

$$\Sigma_{\mathbf{k}\nu} = \Sigma_\nu^{\text{BFK}} + \Sigma_{\mathbf{k}\nu}', \tag{C.9}$$

where Σ_ν^{BFK} is the self-energy of the Bose-Fermi-Kondo model and $\Sigma_{\mathbf{k}\nu}'$ are corrections to

the self-energy of order ν^{-2}. This means that the ν^{-1}-coefficient remains the same as in the impurity model, the modification due to the retarded interactions can not be reconciled[11].

C.3   Conclusions

QP   A class of dynamical mean-field approximations for the Hubbard model was discussed. These have in common that a two-particle self-consistency condition is fixed by introducing retarded interactions into the local reference model. This is motivated by the appealing perspective of improved thermodynamic consistency and by the account of screening effects due to collective excitations. However, it was seen that retarded interactions prove unsuitable to describe the Hubbard model, since they degrade a number of exact features of the original Anderson impurity model, which include its potential energy, the asymptotic coefficient of the self-energy, and its Ward identity. The latter guarantees local conservation in DMFT, as shown in Sec. A.3 of chapter 4, and it takes the particularly simple form $\mathbf{d\Sigma} = \hat{\Gamma}^{\alpha}\mathbf{dG}$ in the Hubbard model and in the Anderson impurity model. Introducing retarded spin-spin interactions into the impurity model gives rise to an anomaly in the spin channels of the impurity Ward identity, which is a similar situation as in lattice models with exchange couplings (cf. Sec. F of chapter 3). This opens a backdoor for complications that usually only arise when the lattice model in question is indeed an exchange model (see Sec. A.6). It was shown that this can make a satisfaction of the lattice Ward identity impossible on principle grounds. For these reasons, it seems desirable to avoid the introduction of anomalous currents into an approximation for the Hubbard model entirely.

Since these are of and by themselves negative statements, they do not deserve a detailed discussion, unless they convey an instructive message to make progress in the future. But such instructive conclusions can be made:

(a) Next to retarded interactions that arise from phonons or via downfolding [4], they are well suited to capture screening effects due to nonlocal interactions. This is because retarded interactions arise naturally in the $d \to \infty$ limit of extended Hubbard models (see Sec. A.1). While applications to nonlocal charge-charge interactions are ubiquitous, a satisfying dynamical mean-field approach for exchange models is yet absent (cf. Sec. A.2). In this context retarded interactions could play a crucial role in constructing conserving approximations. This was seen in Sec. A.6, where it became apparent that the effective dynamical mean-field of an exchange model *should* feature retarded spin-spin interactions. These need to be adjusted via a yet unknown 2P self-consistency condition, in order to fix the anomalous spin currents of the lattice model. This is a clear and promising path to pursue in the future and it could lead to a natural generalization of the dynamical mean-field to exchange models, such as the Heisenberg model and the t-J model. These insights also hint at natural applications for the QUADRILEX approach, whose impurity model is presumably ideal for lattice models with a full Coulomb matrix, including exchange interactions and pair hoppings.

---

[11] This is the case when only four-point vertices are considered in the dual potential as in Ref. [85]. When six-point vertices are included, the ν^{-1}-coefficient of the self-energy can be changed [116]. For practical purposes it is desirable to restrict oneself to four-point vertices.

(b) It was seen above that the numerically exact 1P and 2P self-energy of the Bose-Fermi-Kondo model violate the Ward identity of the Hubbard model. This is the case, even when the self-consistency condition $G_{\mathrm{loc}} = g$ holds, which guarantees local conservation in DMFT. This is surprising, since one would expect the 1P and 2P self-energies to arise from a local Luttinger-Ward functional of the Bose-Fermi-Kondo model, which seems to imply that the resulting approximation should be conserving. Let us consider in this light the functional derivation of DMFT again, which was stated in Sec. A.2 of chapter 4: In DMFT the 1P self-energy Σ is the first functional derivative of the Luttinger-Ward functional of the Anderson impurity model, $\Sigma = \delta\phi[g]/\delta g$, while its 2P self-energy $\gamma = \delta^2\phi[g]/dg^2$ is its second functional derivative. Combined with the self-consistency condition $G_{\mathrm{loc}} = g$, DMFT is a conserving approximation according to Baym [15]. While this argument is correct in case of DMFT, it is false in the present case: When Σ and γ are not obtained from the Anderson impurity model but from the Bose-Fermi-Kondo model, as above, one must not conclude on the grounds of Ref. [15] that the resulting approximation is conserving. Neither retarded nor spin-dependent interactions lie within the scope of this work. Since the violation of the Ward identity arises only in the spin channels, the crucial point is the spin-dependence of the interaction, not the retardation. For the same reason, the Hartree-Fock approximation violates spin conservation in an exchange model [see Sec. H of chapter 3]. This shows that conservation laws have to be reconsidered in an entirely new way for impurity or lattice models that lie outside the scope of Ref. [15]. A possible starting point for such considerations is the integral Ward identity, along the lines of Sec. A.6.

C.4   Implementation notes

A modified implementation [85] of the dual boson approach by H.Hafermann and E.G.C.P. van Loon was used to calculate the susceptibility in Fig. 5.6. The impurity model for the data in Figs. 5.5 and 5.6 was solved using the CTQMC algorithm presented in Ref. [98].

D   Application II: Two-particle self-consistent DMFT

Although it was seen above that retarded spin-spin interactions are unsuitable for a conserving description of the Hubbard model, one can make use of the peculiar commutation relations of the spin density operators to make partial progress. To this end, let us consider again the Ward identity of the Bose-Fermi-Kondo model, Eq. (C.2),

$$\Sigma_{\nu+\omega} - \Sigma_{\nu} = \sum_{\nu'} \gamma^{\alpha}_{\nu\nu'\omega} \left[g_{\nu'+\omega} - g_{\nu'} \right] - \sum_{\underline{\nu}\nu'\nu''\omega'\beta\gamma} \Lambda^{\beta}_{\omega'} (\hat{\chi}^{\alpha,-1})_{\nu\underline{\nu}\omega} \chi^{\alpha\beta\gamma}_{\underline{\nu}\nu'\nu''\omega\omega'}. \tag{D.1}$$

The anomaly on the RHS has the special property that in a given channel α of the Ward identity it only introduces contributions of retarded interactions $\Lambda^{\beta\neq\alpha}$. This is related to the fact that in the Hamiltonian representation of the Bose-Fermi-Kondo model the boson-fermion coupling that gives rise to Λ^{α} commutes with the spin-density ρ^{α} (see chapter 3,
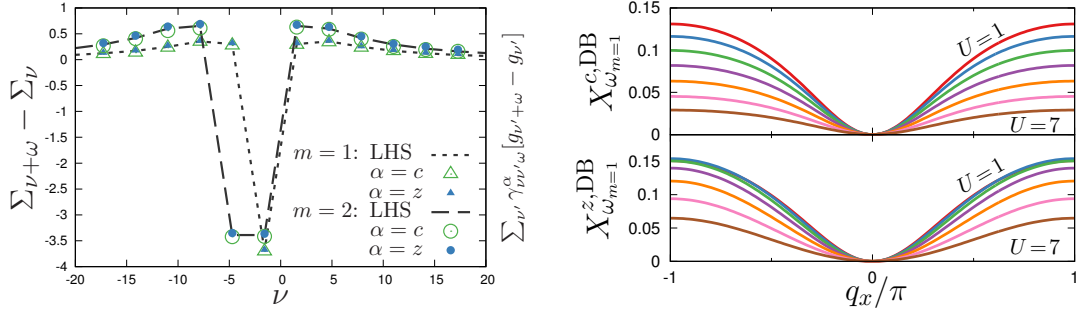
FIGURE 5.7: Left: Test of the Ward identity in Eq. (D.2) in the channels $\alpha = c$ and $\alpha = z$. The conventions are the same as in Fig. 5.5. This calculation corresponds to the two-particle self-consistent DMFT ($U = 6$), where retarded interactions Λ^c and Λ^z act on the impurity. Note that $\Lambda^x = \Lambda^y = 0$. Right: Susceptibility of the two-particle self-consistent DMFT at the first Matsubara frequency for several values of U. The panels show the charge (top) and spin (bottom) susceptibility obtained from Eq. (D.4) at small $\mathbf{q} = (q_x, 0)$. $X^{\alpha,\mathrm{DB}}_{\mathbf{q},\omega>0}$ vanishes at $\mathbf{q} = \mathbf{0}$ and satisfies a $|\mathbf{q}|^2$-law, both are required by global charge an spin conservation (see text). In these calculations the nearest neighbor hopping is $t = 1$ and the inverse temperature $\beta = 2$.

Sec. F.3). Hence, only the couplings that belong to $\Lambda^{\beta \neq \alpha}$ create anomalous currents in the channel α.

For this reason, one may restrict oneself to retarded interactions Λ^c in the charge channel and, w.l.o.g., Λ^z in the spin channel, while setting $\Lambda^{x,y} = 0$. Inserting this into Eq. (D.1) leads to

$$\Sigma_{\nu+\omega} - \Sigma_\nu = \sum_{\nu'} \gamma^{c,z}_{\nu\nu'\omega} [g_{\nu'+\omega} - g_{\nu'}] \tag{D.2}$$

in the channels $\alpha = c, z$, whereas for $\alpha = x$ the Ward identity reads,

$$\Sigma_{\nu+\omega} - \Sigma_\nu = \sum_{\nu'} \gamma^x_{\nu\nu'\omega} [g_{\nu'+\omega} - g_{\nu'}] - \sum_{\underline{\nu}\nu'\nu''\omega'} \Lambda^z_{\omega'} (\hat{\chi}^{x,-1})_{\nu\underline{\nu}\omega} \chi^{xzy}_{\underline{\nu}\nu'\nu''\omega\omega'}. \tag{D.3}$$

Likewise, the respective relation for $\alpha = y$ follows by exchanging x and y in this relation. While it is certainly not elegant to break the SU(2) symmetry, it now becomes possible again to satisfy the Ward identity in Eq. (C.1), at least in the channels $\alpha = c$ and $\alpha = z$. Namely, by setting $\Sigma_k = \Sigma_\nu$ and $\Gamma^\alpha_{kk'q} = \gamma^\alpha_{\nu\nu'\omega}$ and satisfying the self-consistency condition $G_{\mathrm{loc}} = g$. For $\alpha = c, z$ this leads to the coincidence of lattice and impurity Ward identity, Eqs. (C.1) and (D.2), respectively.

The susceptibility is then obtained as in the dual boson approach, by calculating the susceptibility from the Bethe-Salpeter equation, $\hat{X}^\alpha_q = \hat{X}^0_q + \hat{X}^0_q \hat{\gamma}^\alpha_\omega \hat{X}^\alpha_q$, and finally cancelling
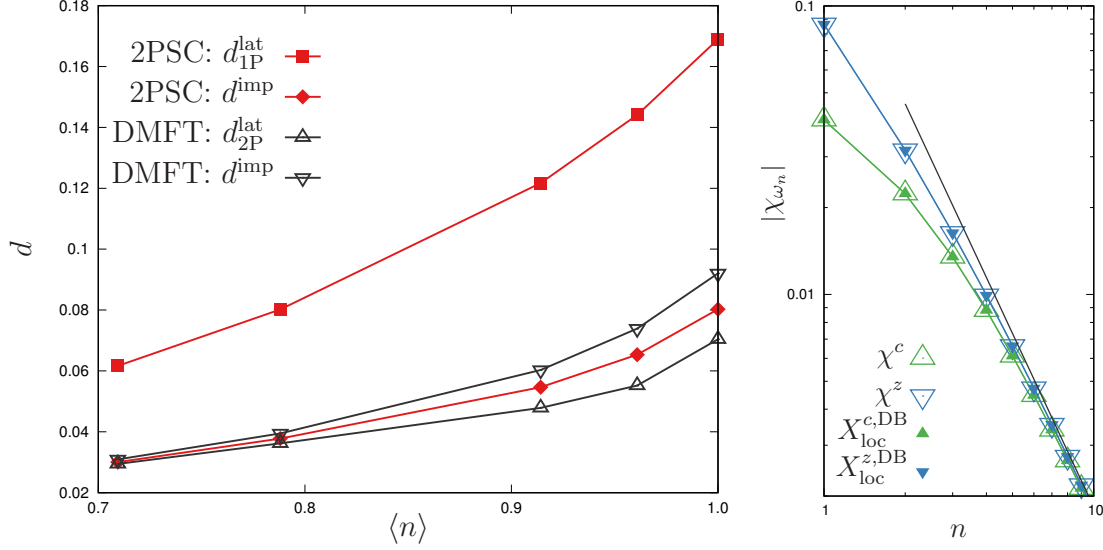
FIGURE 5.8: Left: The double occupancy as a function of filling in DMFT (black) and in two-particle self-consistent DMFT (red). The approximations are 1P or 2P self-consistent, respectively, but neither is 1P *and* 2P self-consistent (see text). Notably, the inconsistency is worse in the two-particle self-consistent method. Right: The local lattice susceptibility $X_{\text{loc}}^{\alpha,\text{DB}}$ (filled triangles) and the impurity susceptibility χ^{α} (open triangles) in two-particle self-consistent DMFT. These are equal for $\alpha = c$ (green) and $\alpha = z$ (blue) due to the self-consistency condition, which is not the case in DMFT (see Fig. 4.3). The asymptote (black line) is given by the kinetic energy, as in DMFT (see Eq. (C.5) of chapter 4, [65]).

the RPA contributions due to Λ^c and Λ^z,

$$X_q^{\alpha,\text{DB}} = \frac{X_q^{\alpha}}{1 + \Lambda_{\omega}^{\alpha} X_q^{\alpha}}, \ (\alpha = c, z). \tag{D.4}$$

The retarded interactions Λ^c and Λ^z may now be fixed by imposing the self-consistency conditions $X_{\text{loc}}^{c,\text{DB}} = \chi^c$ and $X_{\text{loc}}^{z,\text{DB}} = \chi^z$ (not for $\alpha = x, y$). This approximation may be called a 'two-particle self-consistent DMFT'.

D.1 Application to the Hubbard model

This approximation maintains several aspects of global charge and spin conservation and is also two-particle self-consistent. Firstly, the validity of the Ward identity Eq. (D.2) in the channels $\alpha = c, z$ is verified in the left panel of Fig. 5.7. The LHS and RHS of Eq. (D.2) are indeed equal within the margin of numerical error[12]. As a consequence, the susceptibility

---

[12] Note that due to Λ^z the Ward identity is violated in the spin channels x and y (not shown), which is clear from Eq. (D.3). The solver used in these calculations does not feature a measurement of the T-matrix in the transversal channel, such that this violation can not be demonstrated explicitly.

in Eq. (D.4) satisfies $\imath\omega X_{\mathbf{q}=0,\omega}^{\alpha,\mathrm{DB}} = 0$, which leads to an ungapped two-particle spectrum [cf. Eq. (D.3) of chapter 3][13]. In an application to the half-filled Hubbard model on the square lattice one can see in Fig. 5.7 that $X_{\mathbf{q},\omega_1}^{\alpha,\mathrm{DB}}$ indeed vanishes at $\mathbf{q} = \mathbf{0}$ and satisfies a $|\mathbf{q}|^2$-law in the vicinity, as it should [39]. The approximation also satisfies the f-sum rule (cf. Eq. (D.22) of chapter 3 and Ref. [65]). However, conservation laws are violated in the channels x and y, since the anomalous Ward identity in Eq. (D.3) is not equivalent to the Ward identity of the Hubbard model Eq. (C.1) in these channels.

The effects of the two-particle self-consistency can be seen in Fig. 5.8. The right panel shows that the self-consistency condition $X_{\mathrm{loc}}^{\alpha,\mathrm{DB}} = \chi^\alpha$ is indeed satisfied for $\alpha = c, z$. According to the discussion near Eq. (C.6) this implies that the double occupancy is consistent between the impurity and the 2P level of the lattice, $d_{2P}^{\mathrm{lat}} = d^{\mathrm{imp}}$. On the same note, however, the consistency of the 1P level to the impurity is undermined $d_{1P}^{\mathrm{lat}} \neq d^{\mathrm{imp}}$, which is the opposite situation compared to DMFT (cf. Sec. C.2 of chapter 4). This is because the Migdal-Galitzkii formula is modified due to the retarded interactions and takes the form of Eq. (C.6). The left panel of Fig. 5.8 shows the inconsistent double occupancies in DMFT and in the two-particle self-consistent DMFT in Eq. (D.4) as a function of filling ($U = 6$ and $\beta = 2$).

D.2   Conclusions

A two-particle self-consistent modification of DMFT was presented, which is also known as the self-consistent dual boson approach [138]. This approximation maintains features of global conservation laws in the charge and spin-z channel, as long as the two-particle self-consistency condition $X_{\mathrm{loc}}^{\alpha,\mathrm{DB}} = \chi^\alpha$ is only established in these channels ($\alpha = c, z$). An extension of this approach to an SU(2)-symmetric coupling is not possible (see. Sec. A.6). An interesting option, that was not considered here yet, is to perform a rotation of the z-axis and to average over all possible directions, which is a commonly used method to reestablish SU(2) symmetry [158]. It was shown in Ref. [84] that the double occupancy computed from the 2P level is in good agreement with DCA results.

However, the approximation has a number of problems. One- and two-particle self-consistency are mutually exclusive, the inconsistency of the double occupancy is, in fact, worse than in DMFT. Furthermore, although the self-consistency condition promises to suppress a divergence of $X^{z,\mathrm{DB}}$ in accord with the Mermin-Wagner theorem, calculations at low temperature do not lead to satisfying results: The divergence of $X^{z,\mathrm{DB}}$ is not suppressed due to a reduction of the leading eigenvalue of the Bethe-Salpeter equation but by a cutoff [65]. This is because the susceptibility $X_q^{\alpha,\mathrm{DB}} = (1/X_q^{\alpha,-1} + \Lambda_\omega^\alpha)^{-1}$ does not diverge at a divergence of X^α when Λ^α is finite. This form of the susceptibility is reminiscent of the Moriya-λ correction in DΓA [141, 120]. While Λ_ω^α is a dynamical quantity, the Moriya-λ is

---

[13] It should be noted that this does not mean that $X_q^{\alpha,\mathrm{DB}}$ satisfies the Ward identity. This is only certain to be the case for X_q^α, from which $X_q^{\alpha,\mathrm{DB}}$ is calculated via the geometric series in Eq. (D.4). A violation of the Ward identity in this approximation is likely, since it is known that the charge susceptibility $X_{\mathbf{q}=0,\omega=0}^{c,\mathrm{DB}}$ of the dual boson approach is not fully consistent with $\frac{d\langle n\rangle}{d\mu}$ [83]. See also Sec. D.6 of chapter 3 and Sec. A.5 of this chapter.

static, the self-consistency condition of DΓA arises by summing the one of the two-particle self-consistent DMFT over the Matsubara frequencies.

In DΓA this leads to the correct scaling law of the spin susceptibility with the temperature in two dimensions [58]. This is not the case in the two-particle self-consistent DMFT. The reason for this is that upon a divergence of $X_{\mathbf{q}\omega}^z$, the susceptibility is given as $X_{\mathbf{q}\omega}^{z,\mathrm{DB}} = \Lambda_\omega^{z,-1}$, which does not depend on the momentum $\mathbf{q}$. However, at temperatures below the mean-field instability $X_{\mathbf{q}\omega}^z$ diverges at more and more $\mathbf{q}$-points near the ordering vector of the spurious phase transition. This means that $X_{\mathbf{q}\omega}^{z,\mathrm{DB}}$ assumes the same value $\Lambda_\omega^{z,-1}$ at all of the divergences of $X_{\mathbf{q}\omega}^z$, forming a plateau. Via the 2P self-consistency condition Λ_ω^z then depends on the number of divergences, which in turn leads to an unphysical scaling of $X^{z,\mathrm{DB}}$ with the temperature. Although the Moriya-λ presumably also leads to a plateau in the spin susceptibility of DΓA, the correct scaling is recovered, since the self-consistency condition is summed over all Matsubaras.

The DΓA has been used to verify a new scenario for an insulating state of the two-dimensional Hubbard model at small interaction [124]. The proposed mechanism is that strong scattering arises at low temperature, due to long-ranged paramagnons related to the suppressed Slater antiferromagnetism. On the other hand, a recent dual fermion study [82] at small U predicted a significantly lower temperature for a possible crossover to an insulator than Ref. [124]. Other than in DΓA, the divergence of the spin susceptibility is suppressed in dual fermion because the leading eigenvalue of the Bethe-Salpeter equation is below unity [99]. Among the possible causes for this discrepancy in the results is therefore the difference in which both methods handle the mean-field divergence of the Bethe-Salpeter equation.

D.3 Implementation notes

A modified implementation of the dual boson approach was used [85]. The impurity problem was solved using the ALPS library [13] with improved estimators [40].

A   Integrating out bosons from a path integral

Integrating out bosonic degrees from a path integral is done in a slightly different way than for fermions [61]. A mixed boson-fermion action may be written as,

$$
\begin{aligned}
S_b[c^*, c, b^*, b] &= \int_0^\beta d\tau \left[\frac{1}{2}(b^*, b) \begin{pmatrix} 0 & \partial_\tau + \Omega \\ \partial_\tau - \Omega & 0 \end{pmatrix} (b^*, b)^T + w(\rho, \rho)^T (b^*, b)^T \right] \\
&= \frac{1}{2} \int_0^\beta \int_0^\beta d\tau d\tau' (b^*, b) \begin{pmatrix} 0 & D_+^{-1}(\tau - \tau') \\ D_-^{-1}(\tau - \tau') & 0 \end{pmatrix} (b^*, b)^T \\
&+ w \int_0^\beta d\tau (\rho, \rho)^T (b^*, b)^T
\end{aligned}
\tag{A.1}
$$

Other than for fermions, one needs to account for the fact that the emission of a boson with energy Ω and the absorption of a boson with energy $-\Omega$ have to be treated on equal footing, which is the reason that matrices appear in the Gaussian. The propagation of a non-interacting boson with energy $\pm\Omega$ is represented by the bosonic propagator $D_\pm^{-1}(\tau) = \partial_\tau \pm \Omega$. The bosonic system is coupled to a fermionic density $\rho = c^*c$ via the coupling matrix element w. The bosons may be integrated out from Eq. (A.1) using a standard Gaussian integral [61, 96], $\int D[b^\dagger, b] e^{-S_b[c^*, c, b^*, b]} = e^{-S_{\text{eff}}[c^*, c]}$, leaving the effective action,

$$
\begin{aligned}
S^{\text{eff}}[c^*, c] &= \frac{w^2}{2} \int_0^\beta \int_0^\beta d\tau d\tau' (\rho^*, \rho) \begin{pmatrix} 0 & D_-(\tau - \tau') \\ D_+(\tau - \tau') & 0 \end{pmatrix} (\rho^*, \rho)^T \\
&= \frac{w^2}{2} \int_0^\beta \int_0^\beta d\tau d\tau' \rho(\tau) D(\tau - \tau') \rho(\tau'), \qquad D(\tau) = D_-(\tau) + D_+(\tau).
\end{aligned}
$$

The remaining action represents a retarded coupling of the fermionic density $\rho(\tau)$ with itself, mediated by the bosonic function $D(\tau) = \langle [b^\dagger(\tau) + b(\tau)][b^\dagger(0) + b(0)] \rangle$. Transformed to Matsubara frequencies the bosonic propagator reads,

$$
D_\omega = \frac{2\Omega}{(\imath\omega)^2 - \Omega^2}.
\tag{A.2}
$$

B   Inserting the three-particle bubble into the Ward identity

The contribution of the three-particle bubble to the Ward identity is calculated. The three-particle bubble is given by the expression [cf. Eq. (G.11) of chapter 3],

$$
\begin{aligned}
X^{0,\alpha\beta\gamma}_{11'22'33'} &= 2\varepsilon^2_{\alpha\beta\gamma}\left[X^{\alpha}_{11'23'}G_3\delta_{32'} - X^{\alpha}_{11'32'}G_2\delta_{23'}\right]\\
&+ 2\varepsilon^2_{\alpha\beta\gamma}G_1 G_{1'}\left\{(G_3 F^{\beta}_{31'22'}\delta_{13'} - G_{3'}F^{\beta}_{13'22'}\delta_{31'})G_{2'}G_2\right.\\
&+ \left.(G_{2'}F^{\gamma}_{12'33'}\delta_{21'} - G_2 F^{\gamma}_{21'33'}\delta_{12'})G_{3'}G_3\right\}.
\end{aligned}
\tag{B.1}
$$

In order to go back to the momentum notation one replaces $1 = \underline{k}, 1' = \underline{k}+q, 2 = k'+p, 2' = k', 3 = k''+q-p, 3' = k''$. The relation between the four-label notation and the three-label notation is,

$$
X_{11'22'} \leftrightarrow X_{1,2',1'-1}.
\tag{B.2}
$$

Performing this replacement for the generalized susceptibilities X^{α} and the T-matrices F^{α} in Eq. (B.1) leads to,

$$
\begin{aligned}
X^{\alpha}_{11'23'}\delta_{32'} &= X^{\alpha}_{\underline{k},k'',q}\delta_{k'',k'+p-q}N\beta,\\
X^{\alpha}_{11'32'}\delta_{23'} &= X^{\alpha}_{\underline{k},k'',q}\delta_{k'',k'+p}N\beta,\\
F^{\beta}_{31'22'}\delta_{13'} &= F^{\beta}_{\underline{k}+q-p,k',p}\delta_{k'',\underline{k}}N\beta,\\
F^{\beta}_{13'22'}\delta_{31'} &= F^{\beta}_{\underline{k},k',p}\delta_{k'',\underline{k}+p}N\beta,\\
F^{\gamma}_{12'33'}\delta_{21'} &= F^{\gamma}_{\underline{k},k'',q-p}\delta_{k',\underline{k}+q-p}N\beta,\\
F^{\gamma}_{21'33'}\delta_{12'} &= F^{\gamma}_{\underline{k}+p,k'',q-p}\delta_{k',\underline{k}}N\beta.
\end{aligned}
$$

A factor $N\beta$ has been inserted for each Kronecker symbol. The three-particle bubble enters the Ward identity as the following expression,

$$
\begin{aligned}
\sum_{k'k''p\beta\gamma} V^{\beta}_p X^{0,\alpha\beta\gamma}_{\underline{k}k'k''qp} &= 2\sum_{k'p\beta\gamma}\varepsilon^2_{\alpha\beta\gamma}V^{\beta}_p\left[X^{\alpha}_{\underline{k},k',q}(G_{k'+q-p} - G_{k'-p})\right.\\
&+ G_{\underline{k}}G_{\underline{k}+q}\left\{\left(G_{\underline{k}+q-p}F^{\beta}_{\underline{k}+q-p,k',p} - G_{\underline{k}+p}F^{\beta}_{\underline{k},k',p}\right)G_{k'}G_{k'+p}\right.\\
&+ \left.\left.\left(G_{\underline{k}+q-p}F^{\gamma}_{\underline{k},k',q-p} - G_{\underline{k}+p}F^{\gamma}_{\underline{k}+p,k',q-p}\right)G_{k'}G_{k'+q-p}\right\}\right].
\end{aligned}
\tag{B.3}
$$

The three-particle bubble enters the Ward identity Eq. (H.3) of chapter 3 as

$$
\sum_{\underline{k}k'k''p\beta\gamma} V^{\beta}_p(\hat{X}^{\alpha,-1})_{k\underline{k}q}X^{0,\alpha\beta\gamma}_{\underline{k}k'k''qp} = \sum_{\underline{k}}(\hat{X}^{\alpha,-1})_{k\underline{k}q}\sum_{k'k''p\beta\gamma}V^{\beta}_p X^{0,\alpha\beta\gamma}_{\underline{k}k'k''qp}
$$

The second sum on the RHS is given in Eq. (B.3). The contribution of the term depending

on X^α in Eq. (B.3) is discussed in the text below Eq. (H.8) of chapter 3. The terms depending on F^β and F^γ contribute as follows,

$$2 \sum_{\underline{k}k'p\beta\gamma} \varepsilon^2_{\alpha\beta\gamma} V_p^\beta (\hat{X}^{\alpha,-1})_{k\underline{k}q} G_{\underline{k}} G_{\underline{k}+q}$$

$$\times \left\{ \left(G_{\underline{k}+q-p} F^\beta_{\underline{k}+q-p,k',p} - G_{\underline{k}+p} F^\beta_{\underline{k},k',p} \right) G_{k'} G_{k'+p} \right.$$

$$\left. + \left(G_{\underline{k}+q-p} F^\gamma_{\underline{k},k',q-p} - G_{\underline{k}+p} F^\gamma_{\underline{k}+p,k',q-p} \right) G_{k'} G_{k'+q-p} \right\}.$$

By shifting the summation index p and using inversion symmetry of the interaction, $V_p = V_{-p}$, this can be brought into the form,

$$\sum_{\underline{k}} (\hat{X}^{\alpha,-1})_{k\underline{k}q} G_{\underline{k}+q} G_{\underline{k}} T^\alpha_{\underline{k}q},$$

where

$$T^\alpha_{\underline{k}q} = 2 \sum_{k'p\beta\gamma} \varepsilon^2_{\alpha\beta\gamma} G_{\underline{k}+p} G_{k'} \left\{ G_{k'+q-p} (V^\beta_{q-p} F^\beta_{\underline{k}+p,k',q-p} - V^\beta_p F^\gamma_{\underline{k}+p,k',q-p}) \right.$$

$$\left. + G_{k'+p} (V^\beta_{q-p} F^\gamma_{\underline{k},k',p} - V^\beta_p F^\beta_{\underline{k},k',p}) \right\}. \tag{B.4}$$

This simplifies to Eq. (H.9) of chapter 3 for $F^\beta = F^\gamma$.

C Imaginary part of the Ward identity in the ordered phase

Fig. 9 shows the imaginary part of the Ward identities Eqs. (F.10) and (F.11) of chapter 4.
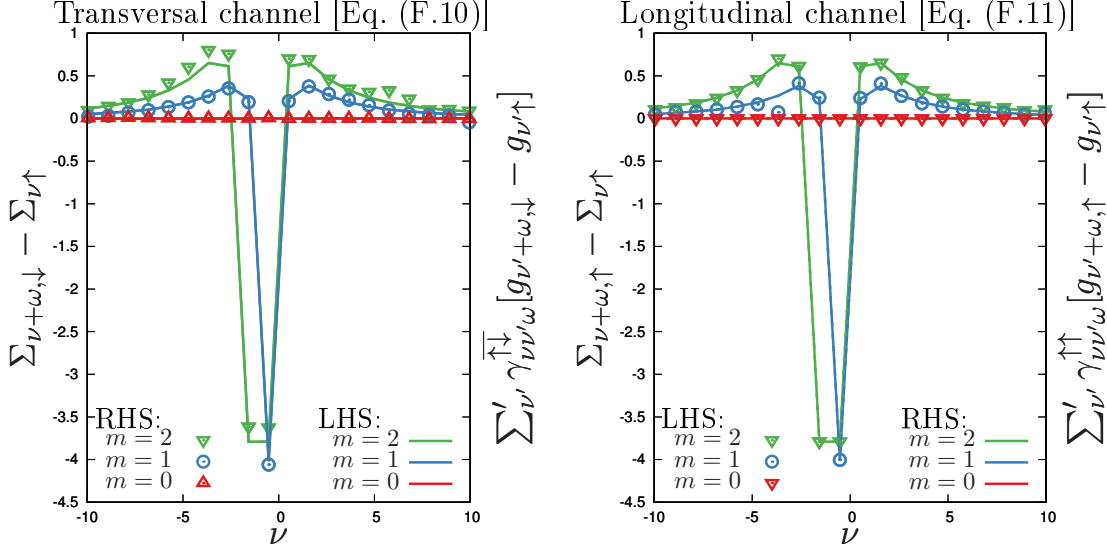
FIGURE 9: Left: Imaginary part of the Ward identity Eq. (F.10) in the transversal channel. Lines show the LHS, symbols the RHS. $\sigma = \uparrow$ is shown. Right: Imaginary part of the Ward identity Eq. (F.11) in the longitudinal channel for $\sigma = \sigma' = \uparrow$. Conventions as in the left panel. The imaginary part of the Ward identities Eqs. (F.10) and (F.11) do not depend on the spin label σ, therefore the left and right panels show the same functions. However, the data for the respective RHSs of the Ward identities are obtained from different four-point correlation functions $g^{\overline{\sigma}\overline{\sigma}}$ and $g^{\sigma\sigma'}$, respectively. Note that there may be deviations between LHS and RHS due to the large statistical error in the measurement of the four-point correlation function, and due to a cutoff error in the summation over Matsubara frequencies on the RHS of the Ward identity. It is worth noting that the Ward identity may be used to validate quantum impurity solvers, since it is a nontrivial summation rule that is sensitive to broken symmetries and that involves both 1P and 2P correlation functions.

Bibliography

[1]   Eva Pavarini, Erik Koch, Richard Scalettar, and Richard Martin, eds. *The Physics of Correlated Insulators, Metals, and Superconductors*. Vol. 7. Schriften des Forschungszentrums Jülich Reihe Modeling and Simulation. Jülich: Forschungszentrum Jülich GmbH Zentralbibliothek, Verlag, Sept. 25, 2017, 450 p. ISBN: 978-3-95806-224-5. URL: http://juser.fz-juelich.de/record/837488.

[2]   V I Anisimov, A I Poteryaev, M A Korotin, A O Anokhin, and G Kotliar. "First-principles calculations of the electronic structure and spectra of strongly correlated systems: dynamical mean-field theory". In: *Journal of Physics: Condensed Matter* 9.35 (1997), p. 7359. URL: http://stacks.iop.org/0953-8984/9/i=35/a=010.

[3]   Louis-François Arsenault, Patrick Sémon, and A.-M. S. Tremblay. "Benchmark of a modified iterated perturbation theory approach on the fcc lattice at strong coupling". In: *Phys. Rev. B* 86 (8 Aug. 2012), p. 085133. DOI: 10.1103/PhysRevB.86.085133. URL: https://link.aps.org/doi/10.1103/PhysRevB.86.085133.

[4]   F. Aryasetiawan, M. Imada, A. Georges, G. Kotliar, S. Biermann, and A. I. Lichtenstein. "Frequency-dependent local interactions and low-energy effective models from electronic structure calculations". In: *Phys. Rev. B* 70 (19 Nov. 2004), p. 195104. DOI: 10.1103/PhysRevB.70.195104. URL: https://link.aps.org/doi/10.1103/PhysRevB.70.195104.

[5]   Thomas Ayral, Silke Biermann, and Philipp Werner. "Screening and nonlocal correlations in the extended Hubbard model from self-consistent combined *GW* and dynamical mean field theory". In: *Phys. Rev. B* 87 (12 Mar. 2013), p. 125149. DOI: 10.1103/PhysRevB.87.125149. URL: http://link.aps.org/doi/10.1103/PhysRevB.87.125149.

[6]   Thomas Ayral, Silke Biermann, Philipp Werner, and Lewin Boehnke. "Influence of Fock exchange in combined many-body perturbation and dynamical mean field theory". In: *Phys. Rev. B* 95 (24 June 2017), p. 245130. DOI: 10.1103/PhysRevB.95.245130. URL: https://link.aps.org/doi/10.1103/PhysRevB.95.245130.

[7]   Thomas Ayral and Olivier Parcollet. "Mott physics and collective modes: An atomic approximation of the four-particle irreducible functional". In: *Phys. Rev. B* 94 (7 Aug. 2016), p. 075159. DOI: 10.1103/PhysRevB.94.075159. URL: http://link.aps.org/doi/10.1103/PhysRevB.94.075159.

[8]   Thomas Ayral and Olivier Parcollet. "Mott physics and spin fluctuations: A functional viewpoint". In: *Phys. Rev. B* 93 (23 June 2016), p. 235124. DOI: 10.1103/PhysRevB.93.235124. URL: http://link.aps.org/doi/10.1103/PhysRevB.93.235124.

[9]   Thomas Ayral and Olivier Parcollet. "Mott physics and spin fluctuations: A unified framework". In: *Phys. Rev. B* 92 (11 Sept. 2015), p. 115109. DOI: 10.1103/PhysRevB.92.115109. URL: http://link.aps.org/doi/10.1103/PhysRevB.92.115109.

[10]   Thomas Ayral, Jaksa Vučičević, and Olivier Parcollet. "Fierz Convergence Criterion: A Controlled Approach to Strongly Interacting Systems with Small Embedded Clusters". In: *Phys. Rev. Lett.* 119 (16 Oct. 2017), p. 166401. DOI: 10.1103/PhysRevLett.119.166401. URL: https://link.aps.org/doi/10.1103/PhysRevLett.119.166401.

[11]   D. I. Badrtdinov, S. A. Nikolaev, M. I. Katsnelson, and V. V. Mazurenko. "Spin-orbit coupling and magnetic interactions in Si(111): C,Si,Sn,Pb". In: *Phys. Rev. B* 94 (22 Dec. 2016), p. 224418. DOI: 10.1103/PhysRevB.94.224418. URL: http://link.aps.org/doi/10.1103/PhysRevB.94.224418.

[12]   M. Balzer, B. Kyung, D. Sénéchal, A.-M. S. Tremblay, and M. Potthoff. "First-order Mott transition at zero temperature in two dimensions: Variational plaquette study". In: *EPL (Europhysics Letters)* 85.1 (2009), p. 17002. URL: http://stacks.iop.org/0295-5075/85/i=1/a=17002.

[13]   B Bauer, L D Carr, H G Evertz, A Feiguin, J Freire, S Fuchs, L Gamper, J Gukelberger, E Gull, S Guertler, A Hehn, R Igarashi, S V Isakov, D Koop, P N Ma, P Mates, H Matsuo, O Parcollet, G Pawłowski, J D Picon, L Pollet, E Santos, V W Scarola, U Schollwöck, C Silva, B Surer, S Todo, S Trebst, M Troyer, M L Wall, P Werner, and S Wessel. "The ALPS project release 2.0: open source software for strongly correlated systems". In: *Journal of Statistical Mechanics: Theory and Experiment* 2011.05 (2011), P05001. DOI: 10.1088/1742-5468/2011/05/P05001.

[14]   B Bauer, L D Carr, H G Evertz, A Feiguin, J Freire, S Fuchs, L Gamper, J Gukelberger, E Gull, S Guertler, A Hehn, R Igarashi, S V Isakov, D Koop, P N Ma, P Mates, H Matsuo, O Parcollet, G Pawłowski, J D Picon, L Pollet, E Santos, V W Scarola, U Schollwöck, C Silva, B Surer, S Todo, S Trebst, M Troyer, M L Wall, P Werner, and S Wessel. "The ALPS project release 2.0: open source software for strongly correlated systems". In: *Journal of Statistical Mechanics: Theory and Experiment* 2011.05 (2011), P05001. DOI: 10.1088/1742-5468/2011/05/P05001.

[15]   Gordon Baym. "Self-Consistent Approximations in Many-Body Systems". In: *Phys. Rev.* 127 (4 Aug. 1962), pp. 1391–1401. DOI: 10.1103/PhysRev.127.1391. URL: http://link.aps.org/doi/10.1103/PhysRev.127.1391.

[16]   Gordon Baym and Leo P. Kadanoff. "Conservation Laws and Correlation Functions". In: *Phys. Rev.* 124 (2 Oct. 1961), pp. 287–299. DOI: 10.1103/PhysRev.124.287. URL: http://link.aps.org/doi/10.1103/PhysRev.124.287.

[17] R. Beck, W. Götze, and P. Prelovšek. "Theory for the transition to self-trapping in spin-phonon systems". In: *Phys. Rev. A* 20 (3 Sept. 1979), pp. 1140–1151. DOI: 10.1103/PhysRevA.20.1140. URL: https://link.aps.org/doi/10.1103/PhysRevA.20.1140.

[18] Dominic Bergeron, Vasyl Hankevych, Bumsoo Kyung, and A.-M. S. Tremblay. "Optical and dc conductivity of the two-dimensional Hubbard model in the pseudogap regime and across the antiferromagnetic quantum critical point including vertex corrections". In: *Phys. Rev. B* 84 (8 Aug. 2011), p. 085128. DOI: 10.1103/PhysRevB.84.085128. URL: https://link.aps.org/doi/10.1103/PhysRevB.84.085128.

[19] N. E. Bickers. "Self-Consistent Many-Body Theory for Condensed Matter Systems". In: *Theoretical Methods for Strongly Correlated Electrons*. Ed. by David Sénéchal, André-Marie Tremblay, and Claude Bourbonnais. New York, NY: Springer New York, 2004, pp. 237–296. ISBN: 978-0-387-21717-8. DOI: 10.1007/0-387-21717-7_6. URL: https://doi.org/10.1007/0-387-21717-7_6.

[20] N. E. Bickers, D. J. Scalapino, and S. R. White. "Conserving Approximations for Strongly Correlated Electron Systems: Bethe-Salpeter Equation and Dynamics for the Two-Dimensional Hubbard Model". In: *Phys. Rev. Lett.* 62 (8 Feb. 1989), pp. 961–964. DOI: 10.1103/PhysRevLett.62.961. URL: http://link.aps.org/doi/10.1103/PhysRevLett.62.961.

[21] S. Biermann, F. Aryasetiawan, and A. Georges. "First-Principles Approach to the Electronic Structure of Strongly Correlated Systems: Combining the *GW* Approximation and Dynamical Mean-Field Theory". In: *Phys. Rev. Lett.* 90 (8 Feb. 2003), p. 086402. DOI: 10.1103/PhysRevLett.90.086402. URL: https://link.aps.org/doi/10.1103/PhysRevLett.90.086402.

[22] Adel Bilal. *Lectures on Anomalies*. 2008. eprint: arXiv:0802.0634.

[23] Ralf Bulla, Theo A. Costi, and Thomas Pruschke. "Numerical renormalization group method for quantum impurity systems". In: *Rev. Mod. Phys.* 80 (2 Apr. 2008), pp. 395–450. DOI: 10.1103/RevModPhys.80.395. URL: http://link.aps.org/doi/10.1103/RevModPhys.80.395.

[24] Michel Caffarel and Werner Krauth. "Exact diagonalization approach to correlated fermions in infinite dimensions: Mott transition and superconductivity". In: *Phys. Rev. Lett.* 72 (10 Mar. 1994), pp. 1545–1548. DOI: 10.1103/PhysRevLett.72.1545. URL: http://link.aps.org/doi/10.1103/PhysRevLett.72.1545.

[25] R. Chitra and Gabriel Kotliar. "Effective-action approach to strongly correlated fermion systems". In: *Phys. Rev. B* 63 (11 Mar. 2001), p. 115110. DOI: 10.1103/PhysRevB.63.115110. URL: http://link.aps.org/doi/10.1103/PhysRevB.63.115110.

[26]   Anne-Marie Daré, Liang Chen, and A.-M. S. Tremblay. "Comparisons between Monte
        Carlo simulations and a simple crossing-symmetric approach to the Hubbard model
        at low density". In: *Phys. Rev. B* 49 (6 Feb. 1994), pp. 4106–4118. DOI: 10.1103/
        PhysRevB.49.4106. URL: http://link.aps.org/doi/10.1103/PhysRevB.49.4106.

[27]   Xiaoyu Deng, Jernej Mravlje, Rok Žitko, Michel Ferrero, Gabriel Kotliar, and An-
        toine Georges. "How Bad Metals Turn Good: Spectroscopic Signatures of Resilient
        Quasiparticles". In: *Phys. Rev. Lett.* 110 (8 Feb. 2013), p. 086401. DOI: 10.1103/
        PhysRevLett.110.086401. URL: https://link.aps.org/doi/10.1103/PhysRevLett.
        110.086401.

[28]   Wenxin Ding, Rok Žitko, Peizhi Mai, Edward Perepelitsky, and B. Sriram Shastry.
        "Strange metal from Gutzwiller correlations in infinite dimensions". In: *Phys. Rev.
        B* 96 (5 Aug. 2017), p. 054114. DOI: 10.1103/PhysRevB.96.054114. URL: https:
        //link.aps.org/doi/10.1103/PhysRevB.96.054114.

[29]   Qiaoyuan Dong, Igor Krivenko, Joseph Kleinhenz, Andrey E. Antipov, Guy Cohen,
        and Emanuel Gull. "Quantum Monte Carlo solution of the dynamical mean field
        equations in real time". In: *Phys. Rev. B* 96 (15 Oct. 2017), p. 155126. DOI: 10.1103/
        PhysRevB.96.155126. URL: https://link.aps.org/doi/10.1103/PhysRevB.96.
        155126.

[30]   L. Fratino, P. Sémon, M. Charlebois, G. Sordi, and A.-M. S. Tremblay. "Signatures
        of the Mott transition in the antiferromagnetic state of the two-dimensional Hubbard
        model". In: *Phys. Rev. B* 95 (23 June 2017), p. 235109. DOI: 10.1103/PhysRevB.
        95.235109. URL: https://link.aps.org/doi/10.1103/PhysRevB.95.235109.

[31]   A. Gaenko, A.E. Antipov, G. Carcassi, T. Chen, X. Chen, Q. Dong, L. Gamper, J.
        Gukelberger, R. Igarashi, S. Iskakov, M. Könz, J.P.F. LeBlanc, R. Levy, P.N. Ma,
        J.E. Paki, H. Shinaoka, S. Todo, M. Troyer, and E. Gull. "Updated core libraries of
        the ALPS project". In: *Computer Physics Communications* 213 (2017), pp. 235–251.
        ISSN: 0010-4655. DOI: https://doi.org/10.1016/j.cpc.2016.12.009. URL:
        http://www.sciencedirect.com/science/article/pii/S0010465516303885.

[32]   Antoine Georges, Gabriel Kotliar, Werner Krauth, and Marcelo J. Rozenberg. "Dy-
        namical mean-field theory of strongly correlated fermion systems and the limit of
        infinite dimensions". In: *Rev. Mod. Phys.* 68.1 (Jan. 1996), p. 13. DOI: 10.1103/
        RevModPhys.68.13. URL: http://dx.doi.org/10.1103/RevModPhys.68.13.

[33]   Emanuel Gull, Andrew J. Millis, Alexander I. Lichtenstein, Alexey N. Rubtsov,
        Matthias Troyer, and Philipp Werner. "Continuous-time Monte Carlo methods for
        quantum impurity models". In: *Rev. Mod. Phys.* 83 (2 May 2011), pp. 349–404. DOI:
        10.1103/RevModPhys.83.349. URL: https://link.aps.org/doi/10.1103/
        RevModPhys.83.349.

[34] Emanuel Gull, Olivier Parcollet, and Andrew J. Millis. "Superconductivity and the Pseudogap in the Two-Dimensional Hubbard Model". In: *Phys. Rev. Lett.* 110 (21 May 2013), p. 216405. DOI: 10.1103/PhysRevLett.110.216405. URL: http://link.aps.org/doi/10.1103/PhysRevLett.110.216405.

[35] O. Gunnarsson, G. Rohringer, T. Schäfer, G. Sangiovanni, and A. Toschi. "Breakdown of Traditional Many-Body Theories for Correlated Electrons". In: *Phys. Rev. Lett.* 119 (5 Aug. 2017), p. 056402. DOI: 10.1103/PhysRevLett.119.056402. URL: https://link.aps.org/doi/10.1103/PhysRevLett.119.056402.

[36] G. S. Guralnik, C. R. Hagen, and T. W. B. Kibble. "Global Conservation Laws and Massless Particles". In: *Phys. Rev. Lett.* 13 (20 Nov. 1964), pp. 585–587. DOI: 10.1103/PhysRevLett.13.585. URL: http://link.aps.org/doi/10.1103/PhysRevLett.13.585.

[37] H. Hafermann. *Numerical Approaches to Spatial Correlations in Strongly Interacting Fermion Systems.*

[38] Hartmut Hafermann. "Self-energy and vertex functions from hybridization-expansion continuous-time quantum Monte Carlo for impurity models with retarded interaction". In: *Phys. Rev. B* 89 (23 June 2014), p. 235128. DOI: 10.1103/PhysRevB.89.235128. URL: http://link.aps.org/doi/10.1103/PhysRevB.89.235128.

[39] Hartmut Hafermann, Erik G. C. P. van Loon, Mikhail I. Katsnelson, Alexander I. Lichtenstein, and Olivier Parcollet. "Collective charge excitations of strongly correlated electrons, vertex corrections, and gauge invariance". In: *Phys. Rev. B* 90 (23 Dec. 2014), p. 235105. DOI: 10.1103/PhysRevB.90.235105. URL: http://link.aps.org/doi/10.1103/PhysRevB.90.235105.

[40] Hartmut Hafermann, Kelly R. Patton, and Philipp Werner. "Improved estimators for the self-energy and vertex function in hybridization-expansion continuous-time quantum Monte Carlo simulations". In: *Phys. Rev. B* 85 (20 May 2012), p. 205106. DOI: 10.1103/PhysRevB.85.205106. URL: http://link.aps.org/doi/10.1103/PhysRevB.85.205106.

[41] P. Hansmann, T. Ayral, L. Vaugier, P. Werner, and S. Biermann. "Long-Range Coulomb Interactions in Surface Systems: A First-Principles Description within Self-Consistently Combined *GW* and Dynamical Mean-Field Theory". In: *Phys. Rev. Lett.* 110 (16 Apr. 2013), p. 166401. DOI: 10.1103/PhysRevLett.110.166401. URL: http://link.aps.org/doi/10.1103/PhysRevLett.110.166401.

[42] K. Haule, A. Rosch, J. Kroha, and P. Wölfle. "Pseudogaps in the $t - J$ model: An extended dynamical mean-field theory study". In: *Phys. Rev. B* 68 (15 Oct. 2003), p. 155119. DOI: 10.1103/PhysRevB.68.155119. URL: https://link.aps.org/doi/10.1103/PhysRevB.68.155119.

[43]   Kristjan Haule. "Quantum Monte Carlo impurity solver for cluster dynamical mean-field theory and electronic structure calculations with adjustable cluster base". In: *Phys. Rev. B* 75 (15 Apr. 2007), p. 155113. DOI: 10.1103/PhysRevB.75.155113. URL: https://link.aps.org/doi/10.1103/PhysRevB.75.155113.

[44]   J. Herbrych, R. Steinigeweg, and P. Prelovšek. "Spin hydrodynamics in the $S = \frac{1}{2}$ anisotropic Heisenberg chain". In: *Phys. Rev. B* 86 (11 Sept. 2012), p. 115106. DOI: 10.1103/PhysRevB.86.115106. URL: https://link.aps.org/doi/10.1103/PhysRevB.86.115106.

[45]   M. H. Hettler, M. Mukherjee, M. Jarrell, and H. R. Krishnamurthy. "Dynamical cluster approximation: Nonlocal dynamics of correlated electron systems". In: *Phys. Rev. B* 61 (19 May 2000), pp. 12739–12756. DOI: 10.1103/PhysRevB.61.12739. URL: https://link.aps.org/doi/10.1103/PhysRevB.61.12739.

[46]   B. Horváth, B Lazarovits, and G. Zaránd. "Fluctuation-exchange approximation theory of the nonequilibrium singlet-triplet transition". In: *Phys. Rev. B* 84 (20 Nov. 2011), p. 205117. DOI: 10.1103/PhysRevB.84.205117. URL: https://link.aps.org/doi/10.1103/PhysRevB.84.205117.

[47]   Kerson Huang and H. Arthur Weldon. "Bound-state wave functions and bound-state scattering in relativistic field theory". In: *Phys. Rev. D* 11 (2 Jan. 1975), pp. 257–278. DOI: 10.1103/PhysRevD.11.257. URL: http://link.aps.org/doi/10.1103/PhysRevD.11.257.

[48]   Li Huang, Thomas Ayral, Silke Biermann, and Philipp Werner. "Extended dynamical mean-field study of the Hubbard model with long-range interactions". In: *Phys. Rev. B* 90 (19 Nov. 2014), p. 195114. DOI: 10.1103/PhysRevB.90.195114. URL: http://link.aps.org/doi/10.1103/PhysRevB.90.195114.

[49]   S. Iskakov and M. Danilov. "Exact Diagonalization library for quantum electron models". In: *ArXiv e-prints* (Jan. 2017). arXiv: 1701.05645 [cond-mat.str-el].

[50]   Sergei Iskakov, Hanna Terletska, and Emanuel Gull. *Momentum-Space Cluster Dual Fermion Method*. 2017. eprint: arXiv:1712.03295.

[51]   S. A. Jafari. "Introduction to Hubbard Model and Exact Diagonalization". In: (2008). eprint: arXiv:0807.4878.

[52]   J. Jaklič and P. Prelovšek. "Charge dynamics in the planar t-J model". In: *Phys. Rev. B* 52 (9 Sept. 1995), pp. 6903–6912. DOI: 10.1103/PhysRevB.52.6903. URL: https://link.aps.org/doi/10.1103/PhysRevB.52.6903.

[53]   V. Janiš. "Parquet approach to nonlocal vertex functions and electrical conductivity of disordered electrons". In: *Phys. Rev. B* 64 (11 Aug. 2001), p. 115115. DOI: 10.1103/PhysRevB.64.115115. URL: https://link.aps.org/doi/10.1103/PhysRevB.64.115115.

[54]   Václav Janiš, Anna Kauch, and Vladislav Pokorný. "Thermodynamically consistent description of criticality in models of correlated electrons". In: (2016). DOI: 10.1103/PhysRevB.95.045108. eprint: arXiv:1604.01678.

[55] M. Jarrell and Th. Pruschke. "Anomalous properties of the Hubbard model in infinite dimensions". In: *Phys. Rev. B* 49 (2 Jan. 1994), pp. 1458–1461. DOI: 10.1103/PhysRevB.49.1458. URL: https://link.aps.org/doi/10.1103/PhysRevB.49.1458.

[56] Gun Sang Jeon, Tae-Ho Park, and Han-Yong Choi. "Numerical renormalization-group study of the symmetric Anderson-Holstein model: Phonon and electron spectral functions". In: *Phys. Rev. B* 68 (4 July 2003), p. 045106. DOI: 10.1103/PhysRevB.68.045106. URL: http://link.aps.org/doi/10.1103/PhysRevB.68.045106.

[57] A. A. Katanin. "Fulfillment of Ward identities in the functional renormalization group approach". In: *Phys. Rev. B* 70 (11 Sept. 2004), p. 115109. DOI: 10.1103/PhysRevB.70.115109. URL: http://link.aps.org/doi/10.1103/PhysRevB.70.115109.

[58] A. A. Katanin, A. Toschi, and K. Held. "Comparing pertinent effects of antiferromagnetic fluctuations in the two- and three-dimensional Hubbard model". In: *Phys. Rev. B* 80 (7 Aug. 2009), p. 075104. DOI: 10.1103/PhysRevB.80.075104. URL: http://link.aps.org/doi/10.1103/PhysRevB.80.075104.

[59] M. I. Katsnelson and A. I. Lichtenstein. "First-principles calculations of magnetic interactions in correlated systems". In: *Phys. Rev. B* 61 (13 Apr. 2000), pp. 8906–8912. DOI: 10.1103/PhysRevB.61.8906. URL: https://link.aps.org/doi/10.1103/PhysRevB.61.8906.

[60] Stefan Kirchner, Kevin Ingersent, and Qimiao Si. "Quantum criticality of the sub-Ohmic spin-boson model". In: *Phys. Rev. B* 85 (7 Feb. 2012), p. 075113. DOI: 10.1103/PhysRevB.85.075113. URL: https://link.aps.org/doi/10.1103/PhysRevB.85.075113.

[61] H. Kleinert. *Path Integrals in Quantum Mechanics, Statistics, Polymer Physics, and Financial Markets*. EBL-Schweitzer. World Scientific, 2009. ISBN: 9789814273572. URL: https://books.google.de/books?id=VJ1qNz5xYzkC.

[62] J. Kokalj and Ross H. McKenzie. "Thermodynamics of a Bad Metal-Mott Insulator Transition in the Presence of Frustration". In: *Phys. Rev. Lett.* 110 (20 May 2013), p. 206402. DOI: 10.1103/PhysRevLett.110.206402. URL: https://link.aps.org/doi/10.1103/PhysRevLett.110.206402.

[63] Gabriel Kotliar, Sergej Y. Savrasov, Gunnar Pálsson, and Giulio Biroli. "Cellular Dynamical Mean Field Approach to Strongly Correlated Systems". In: *Phys. Rev. Lett.* 87 (18 Oct. 2001), p. 186401. DOI: 10.1103/PhysRevLett.87.186401. URL: https://link.aps.org/doi/10.1103/PhysRevLett.87.186401.

[64]   Evgeny Kozik, Michel Ferrero, and Antoine Georges. "Nonexistence of the Luttinger-Ward Functional and Misleading Convergence of Skeleton Diagrammatic Series for Hubbard-Like Models". In: *Phys. Rev. Lett.* 114 (15 Apr. 2015), p. 156402. DOI: 10.1103/PhysRevLett.114.156402. URL: http://link.aps.org/doi/10.1103/PhysRevLett.114.156402.

[65]   Friedrich Krien, Erik G. C. P. van Loon, Hartmut Hafermann, Junya Otsuki, Mikhail I. Katsnelson, and Alexander I. Lichtenstein. "Conservation in two-particle self-consistent extensions of dynamical mean-field theory". In: *Phys. Rev. B* 96 (7 Aug. 2017), p. 075155. DOI: 10.1103/PhysRevB.96.075155. URL: https://link.aps.org/doi/10.1103/PhysRevB.96.075155.

[66]   I. Krivenko. "TRIQS-based Stochastic Optimization Method for Analytic Continuation". In: *https://github.com/krivenko/som* (2016). URL: https://github.com/krivenko/som.

[67]   Yoshio Kuramoto and Noboru Fukushima. "Dynamical Effective Medium Theory for Quantum Spins and Multipoles". In: *Journal of the Physical Society of Japan* 67.2 (1998), pp. 583–593. DOI: 10.1143/JPSJ.67.583. eprint: https://doi.org/10.1143/JPSJ.67.583. URL: https://doi.org/10.1143/JPSJ.67.583.

[68]   L.D. Landau, E.M. Lifshitz, and L.P. Pitaevskij. *Statistical Physics: Part 2 : Theory of Condensed State*. Landau and Lifshitz Course of theoretical physics. Oxford, 1980. URL: https://books.google.de/books?id=dEVtKQEACAAJ.

[69]   R. Lehoucq, D. Sorensen, and C. Yang. *ARPACK Users' Guide*. Society for Industrial and Applied Mathematics, 1998. DOI: 10.1137/1.9780898719628. eprint: http://epubs.siam.org/doi/pdf/10.1137/1.9780898719628. URL: http://epubs.siam.org/doi/abs/10.1137/1.9780898719628.

[70]   A. I. Lichtenstein and M. I. Katsnelson. "Ab initio". In: *Phys. Rev. B* 57 (12 Mar. 1998), pp. 6884–6895. DOI: 10.1103/PhysRevB.57.6884. URL: https://link.aps.org/doi/10.1103/PhysRevB.57.6884.

[71]   A. I. Lichtenstein and M. I. Katsnelson. "Antiferromagnetism and d-wave superconductivity in cuprates: A cluster dynamical mean-field theory". In: *Phys. Rev. B* 62 (14 Oct. 2000), R9283–R9286. DOI: 10.1103/PhysRevB.62.R9283. URL: https://link.aps.org/doi/10.1103/PhysRevB.62.R9283.

[72]   A. I. Liechtenstein, M. I. Katsnelson, and V. A. Gubanov. "Exchange interactions and spin-wave stiffness in ferromagnetic metals". In: *Journal of Physics F: Metal Physics* 14.7 (1984), p. L125. URL: http://stacks.iop.org/0305-4608/14/i=7/a=007.

[73]   A.I. Liechtenstein, M.I. Katsnelson, and V.A. Gubanov. "Local spin excitations and Curie temperature of iron". In: *Solid State Communications* 54.4 (1985), pp. 327–329. ISSN: 0038-1098. DOI: https://doi.org/10.1016/0038-1098(85)90007-9. URL: http://www.sciencedirect.com/science/article/pii/0038109885900079.

[74] E. M. Lifshitz and L. P. Pitaevskii. *Statistical Physics: Theory of the Condensed State: 009 (Course of Theoretical Physics Vol. 9)*. Butterworth-Heinemann, 2013. URL: https://www.amazon.com/Statistical-Physics-Theory-Condensed-Theoretical-ebook/dp/B0026IUOQO?SubscriptionId=0JYN1NVW651KCA56C102&tag=techkie-20&linkCode=xm2&camp=2025&creative=165953&creativeASIN=B0026IUOQO.

[75] H. Q. Lin and J. E. Gubernatis. "Exact Diagonalization Methods for Quantum Systems". In: *Computers in Physics* 7.4 (1993), pp. 400–407. DOI: 10.1063/1.4823192. URL: http://www.phy.cuhk.edu.hk/hqlin/paper/033ComPhys7_400.pdf.

[76] David E. Logan, Adam P. Tucker, and Martin R. Galpin. "Common non-Fermi liquid phases in quantum impurity physics". In: *Phys. Rev. B* 90 (7 Aug. 2014), p. 075150. DOI: 10.1103/PhysRevB.90.075150. URL: https://link.aps.org/doi/10.1103/PhysRevB.90.075150.

[77] David E. Logan, Christopher J. Wright, and Martin R. Galpin. "Correlated electron physics in two-level quantum dots: Phase transitions, transport, and experiment". In: *Phys. Rev. B* 80 (12 Sept. 2009), p. 125117. DOI: 10.1103/PhysRevB.80.125117. URL: https://link.aps.org/doi/10.1103/PhysRevB.80.125117.

[78] E. G. C. P. van Loon, H. Hafermann, A. I. Lichtenstein, A. N. Rubtsov, and M. I. Katsnelson. "Plasmons in Strongly Correlated Systems: Spectral Weight Transfer and Renormalized Dispersion". In: *Phys. Rev. Lett.* 113 (24 Dec. 2014), p. 246407. DOI: 10.1103/PhysRevLett.113.246407. URL: http://link.aps.org/doi/10.1103/PhysRevLett.113.246407.

[79] E. G. C. P. van Loon and M. I. Katsnelson. *The extended Hubbard model with attractive interactions*. 2017. eprint: arXiv:1709.06379.

[80] E. G. C. P. van Loon, M. Rösner, G. Schönhoff, M. I. Katsnelson, and T. O. Wehling. *Competition of strong charge and spin fluctuations in monolayer NbS$_2$*. 2017. eprint: arXiv:1707.05640.

[81] E. G. C. P. van Loon, M. Schüler, M. I. Katsnelson, and T. O. Wehling. "Capturing nonlocal interaction effects in the Hubbard model: Optimal mappings and limits of applicability". In: *Phys. Rev. B* 94 (16 Oct. 2016), p. 165141. DOI: 10.1103/PhysRevB.94.165141. URL: https://link.aps.org/doi/10.1103/PhysRevB.94.165141.

[82] Erik G. C. P. van Loon, Hartmut Hafermann, and Mikhail Katsnelson. *Precursors of the insulating state in the square lattice Hubbard model*. 2017. eprint: arXiv:1712.08379.

[83]   Erik G. C. P. van Loon, Hartmut Hafermann, Alexander I. Lichtenstein, and Mikhail I. Katsnelson. "Thermodynamic consistency of the charge response in dynamical mean-field based approaches". In: *Phys. Rev. B* 92 (8 Aug. 2015), p. 085106. DOI: 10.1103/PhysRevB.92.085106. URL: http://link.aps.org/doi/10.1103/PhysRevB.92.085106.

[84]   Erik G. C. P. van Loon, Friedrich Krien, Hartmut Hafermann, Evgeny A. Stepanov, Alexander I. Lichtenstein, and Mikhail I. Katsnelson. "Double occupancy in dynamical mean-field theory and the dual boson approach". In: *Phys. Rev. B* 93 (15 Apr. 2016), p. 155162. DOI: 10.1103/PhysRevB.93.155162. URL: http://link.aps.org/doi/10.1103/PhysRevB.93.155162.

[85]   Erik G. C. P. van Loon, Alexander I. Lichtenstein, Mikhail I. Katsnelson, Olivier Parcollet, and Hartmut Hafermann. "Beyond extended dynamical mean-field theory: Dual boson approach to the two-dimensional extended Hubbard model". In: *Phys. Rev. B* 90 (23 Dec. 2014), p. 235135. DOI: 10.1103/PhysRevB.90.235135. URL: http://link.aps.org/doi/10.1103/PhysRevB.90.235135.

[86]   J. M. Luttinger and J. C. Ward. "Ground-State Energy of a Many-Fermion System. II". In: *Phys. Rev.* 118 (5 June 1960), pp. 1417–1427. DOI: 10.1103/PhysRev.118.1417. URL: http://link.aps.org/doi/10.1103/PhysRev.118.1417.

[87]   Gerald D. Mahan. *Many-Particle Physics*. Springer US, 2000. DOI: 10.1007/978-1-4757-5714-9. URL: https://doi.org/10.1007/978-1-4757-5714-9.

[88]   Atsushi Masumizu and Kiyoshi Sogo. "Ward-Takahashi relations for SO(4) symmetry in the Hubbard model". In: *Phys. Rev. B* 72 (11 Sept. 2005), p. 115107. DOI: 10.1103/PhysRevB.72.115107. URL: https://link.aps.org/doi/10.1103/PhysRevB.72.115107.

[89]   V. V. Mazurenko, A. N. Rudenko, S. A. Nikolaev, D. S. Medvedeva, A. I. Lichtenstein, and M. I. Katsnelson. "Role of direct exchange and Dzyaloshinskii-Moriya interactions in magnetic properties of graphene derivatives: C_2F and C_2H". In: *Phys. Rev. B* 94 (21 Dec. 2016), p. 214411. DOI: 10.1103/PhysRevB.94.214411. URL: http://link.aps.org/doi/10.1103/PhysRevB.94.214411.

[90]   Darya Medvedeva, Sergei Iskakov, Friedrich Krien, Vladimir V. Mazurenko, and Alexander I. Lichtenstein. "Exact diagonalization solver for extended dynamical mean-field theory". In: *Phys. Rev. B* 96 (23 Dec. 2017), p. 235149. DOI: 10.1103/PhysRevB.96.235149. URL: https://link.aps.org/doi/10.1103/PhysRevB.96.235149.

[91]   W. Metzner, C. Castellani, and C. Di Castro. *Fermi Systems with Strong Forward Scattering*. 1997. eprint: arXiv:cond-mat/9701012.

[92]   Walter Metzner and Dieter Vollhardt. "Correlated Lattice Fermions in $d = \infty$ Dimensions". In: *Phys. Rev. Lett.* 62 (3 Jan. 1989), pp. 324–327. DOI: 10.1103/PhysRevLett.62.324. URL: http://link.aps.org/doi/10.1103/PhysRevLett.62.324.

[93] A. S. Mishchenko, N. V. Prokof'ev, A. Sakamoto, and B. V. Svistunov. "Diagrammatic quantum Monte Carlo study of the Fröhlich polaron". In: *Phys. Rev. B* 62 (10 Sept. 2000), pp. 6317–6336. DOI: 10.1103/PhysRevB.62.6317. URL: https://link.aps.org/doi/10.1103/PhysRevB.62.6317.

[94] E. Müller-Hartmann. "Correlated fermions on a lattice in high dimensions". In: *Zeitschrift für Physik B Condensed Matter* 74.4 (Dec. 1989), pp. 507–512. ISSN: 1431-584X. DOI: 10.1007/BF01311397. URL: https://doi.org/10.1007/BF01311397.

[95] Yosuke Nagaoka. "Ferromagnetism in a Narrow, Almost Half-Filled s Band". In: *Phys. Rev.* 147 (1 July 1966), pp. 392–405. DOI: 10.1103/PhysRev.147.392. URL: https://link.aps.org/doi/10.1103/PhysRev.147.392.

[96] John W. Negele and Henri Orland. *Quantum Many-Particle Systems*. Addison-Wesley Publishing Company, 1988. ISBN: 0-201-12593-5.

[97] Junya Otsuki. "Competing d-Wave and p-Wave Spin-Singlet Superconductivities in the Two-Dimensional Kondo Lattice". In: *Phys. Rev. Lett.* 115 (3 July 2015), p. 036404. DOI: 10.1103/PhysRevLett.115.036404. URL: http://link.aps.org/doi/10.1103/PhysRevLett.115.036404.

[98] Junya Otsuki. "Spin-boson coupling in continuous-time quantum Monte Carlo". In: *Phys. Rev. B* 87 (12 Mar. 2013), p. 125102. DOI: 10.1103/PhysRevB.87.125102. URL: http://link.aps.org/doi/10.1103/PhysRevB.87.125102.

[99] Junya Otsuki, Hartmut Hafermann, and Alexander I. Lichtenstein. "Superconductivity, antiferromagnetism, and phase separation in the two-dimensional Hubbard model: A dual-fermion approach". In: *Phys. Rev. B* 90 (23 Dec. 2014), p. 235132. DOI: 10.1103/PhysRevB.90.235132. URL: http://link.aps.org/doi/10.1103/PhysRevB.90.235132.

[100] Junya Otsuki and Yoshio Kuramoto. "Dynamical mean-field theory for quantum spin systems: Test of solutions for magnetically ordered states". In: *Phys. Rev. B* 88 (2 July 2013), p. 024427. DOI: 10.1103/PhysRevB.88.024427. URL: http://link.aps.org/doi/10.1103/PhysRevB.88.024427.

[101] Junya Otsuki and Dieter Vollhardt. "Numerical Solution of the $t-J$ Model with Random Exchange Couplings in $d=\infty$ Dimensions". In: *Phys. Rev. Lett.* 110 (19 May 2013), p. 196407. DOI: 10.1103/PhysRevLett.110.196407. URL: https://link.aps.org/doi/10.1103/PhysRevLett.110.196407.

[102] Olivier Parcollet, Michel Ferrero, Thomas Ayral, Hartmut Hafermann, Igor Krivenko, Laura Messio, and Priyanka Seth. "TRIQS: A toolbox for research on interacting quantum systems". In: *Computer Physics Communications* 196.Supplement C (2015), pp. 398–415. ISSN: 0010-4655. DOI: https://doi.org/10.1016/j.cpc.2015.04.023. URL: http://www.sciencedirect.com/science/article/pii/S0010465515001666.

[103]   Olivier Parcollet and Antoine Georges. "Non-Fermi-liquid regime of a doped Mott in-
        sulator". In: *Phys. Rev. B* 59 (8 Feb. 1999), pp. 5341–5360. DOI: 10.1103/PhysRevB.
        59.5341. URL: http://link.aps.org/doi/10.1103/PhysRevB.59.5341.

[104]   Pierbiagio Pieri and Giancarlo Calvanese Strinati. "Luttinger theorem and imbal-
        anced Fermi systems". In: *The European Physical Journal B* 90.4 (Apr. 2017), p. 68.
        ISSN: 1434-6036. DOI: 10.1140/epjb/e2017-80071-2. URL: https://doi.org/10.
        1140/epjb/e2017-80071-2.

[105]   V. N. Popov and S. A. Fedotov. "The functional-integration method and diagram
        technique for spin systems". In: *JETP Letters* 67 (3 1988), p. 535.

[106]   M. Potthoff. "Non-perturbative construction of the Luttinger-Ward functional". In:
        Condensed Matter Physics 9 (3 2006), p. 557. DOI: 10.5488/CMP.9.3.557.

[107]   M. Potthoff. "Self-energy-functional approach to systems of correlated electrons". In:
        The European Physical Journal B - Condensed Matter and Complex Systems 32.4
        (2003), pp. 429–436. DOI: 10.1140/epjb/e2003-00121-8. URL: http://dx.doi.
        org/10.1140/epjb/e2003-00121-8.

[108]   M. Potthoff, M. Aichhorn, and C. Dahnken. "Variational Cluster Approach to Corre-
        lated Electron Systems in Low Dimensions". In: *Phys. Rev. Lett.* 91 (20 Nov. 2003),
        p. 206402. DOI: 10.1103/PhysRevLett.91.206402. URL: http://link.aps.org/
        doi/10.1103/PhysRevLett.91.206402.

[109]   Michael Potthoff. "Self-Energy-Functional Theory". In: *Strongly Correlated Systems:
        Theoretical Methods*. Ed. by Adolfo Avella and Ferdinando Mancini. Berlin, Heidel-
        berg: Springer Berlin Heidelberg, 2012, pp. 303–339. ISBN: 978-3-642-21831-6. DOI:
        10.1007/978-3-642-21831-6_10. URL: https://doi.org/10.1007/978-3-642-
        21831-6_10.

[110]   P. Prelovšek. personal communication. Nov. 2017.

[111]   P. Prelovšek and A. Ramšak. "Spectral functions and the pseudogap in the $t - J$
        model". In: *Phys. Rev. B* 63 (18 Apr. 2001), p. 180506. DOI: 10.1103/PhysRevB.
        63.180506. URL: https://link.aps.org/doi/10.1103/PhysRevB.63.180506.

[112]   Nikolay Prokof'ev and Boris Svistunov. "Bold Diagrammatic Monte Carlo Tech-
        nique: When the Sign Problem Is Welcome". In: *Phys. Rev. Lett.* 99 (25 Dec. 2007),
        p. 250201. DOI: 10.1103/PhysRevLett.99.250201. URL: http://link.aps.org/
        doi/10.1103/PhysRevLett.99.250201.

[113]   Th Pruschke, Q Qin, Th Obermeier, and J Keller. "Magnetic properties of the t - J
        model in the dynamical mean-field theory". In: *Journal of Physics: Condensed Matter*
        8.18 (1996), p. 3161. URL: http://stacks.iop.org/0953-8984/8/i=18/a=009.

[114]   Th Pruschke and R Zitzler. "From Slater to Mott–Heisenberg physics: the antiferro-
        magnetic phase of the Hubbard model". In: *Journal of Physics: Condensed Matter*
        15.46 (2003), p. 7867. URL: http://stacks.iop.org/0953-8984/15/i=46/a=006.

[115]   M. Revzen, T. Toyoda, Y. Takahashi, and F. C. Khanna. "Baym-Kadanoff criteria and the Ward-Takahashi relations in many-body theory". In: *Phys. Rev. B* 40 (1 July 1989), pp. 769–771. DOI: 10.1103/PhysRevB.40.769. URL: http://link.aps.org/doi/10.1103/PhysRevB.40.769.

[116]   T. Ribic, P. Gunacker, S. Iskakov, M. Wallerberger, G. Rohringer, A. N. Rubtsov, E. Gull, and K. Held. "Role of three-particle vertex within dual fermion calculations". In: *Phys. Rev. B* 96 (23 Dec. 2017), p. 235127. DOI: 10.1103/PhysRevB.96.235127. URL: https://link.aps.org/doi/10.1103/PhysRevB.96.235127.

[117]   T. Ribic, G. Rohringer, and K. Held. "Nonlocal correlations and spectral properties of the Falicov-Kimball model". In: *Phys. Rev. B* 93 (19 May 2016), p. 195105. DOI: 10.1103/PhysRevB.93.195105. URL: http://link.aps.org/doi/10.1103/PhysRevB.93.195105.

[118]   G. Rohringer. *New routes towards a theoretical treatment of nonlocal electronic correlations*.

[119]   G. Rohringer, H. Hafermann, A. Toschi, A. A. Katanin, A. E. Antipov, M. I. Katsnelson, A. I. Lichtenstein, A. N. Rubtsov, and K. Held. "Diagrammatic routes to nonlocal correlations beyond dynamical mean field theory". In: *preprint arXiv:1705.00024* (2017). arXiv: 1705.00024 [cond-mat]. URL: https://arxiv.org/abs/1705.00024.

[120]   G. Rohringer and A. Toschi. "Impact of nonlocal correlations over different energy scales: A dynamical vertex approximation study". In: *Phys. Rev. B* 94 (12 Sept. 2016), p. 125144. DOI: 10.1103/PhysRevB.94.125144. URL: http://link.aps.org/doi/10.1103/PhysRevB.94.125144.

[121]   A. N. Rubtsov, M. I. Katsnelson, and A. I. Lichtenstein. "Dual boson approach to collective excitations in correlated fermionic systems". In: *Annals of Physics* 327.5 (2012), p. 1320. ISSN: 0003-4916. DOI: 10.1016/j.aop.2012.01.002. URL: http://www.sciencedirect.com/science/article/pii/S0003491612000164.

[122]   A. N. Rubtsov, M. I. Katsnelson, and A. I. Lichtenstein. "Dual fermion approach to nonlocal correlations in the Hubbard model". In: *Phys. Rev. B* 77 (3 Jan. 2008), p. 033101. DOI: 10.1103/PhysRevB.77.033101. URL: http://link.aps.org/doi/10.1103/PhysRevB.77.033101.

[123]   Subir Sachdev and Jinwu Ye. "Gapless spin-fluid ground state in a random quantum Heisenberg magnet". In: *Phys. Rev. Lett.* 70 (21 May 1993), pp. 3339–3342. DOI: 10.1103/PhysRevLett.70.3339. URL: https://link.aps.org/doi/10.1103/PhysRevLett.70.3339.

[124]   T. Schäfer, F. Geles, D. Rost, G. Rohringer, E. Arrigoni, K. Held, N. Blümer, M. Aichhorn, and A. Toschi. "Fate of the false Mott-Hubbard transition in two dimensions". In: *Phys. Rev. B* 91 (12 Mar. 2015), p. 125109. DOI: 10.1103/PhysRevB.91.125109. URL: http://link.aps.org/doi/10.1103/PhysRevB.91.125109.

[125]   T. Schäfer, G. Rohringer, O. Gunnarsson, S. Ciuchi, G. Sangiovanni, and A. Toschi. "Divergent Precursors of the Mott-Hubbard Transition at the Two-Particle Level". In: *Phys. Rev. Lett.* 110 (24 June 2013), p. 246405. DOI: 10.1103/PhysRevLett.110.246405. URL: http://link.aps.org/doi/10.1103/PhysRevLett.110.246405.

[126]   B. Schrieffer. "Theory of Superconductivity". In: *Advanced Book Program, Perseus Books* (1999).

[127]   M. Schüler, M. Rösner, T. O. Wehling, A. I. Lichtenstein, and M. I. Katsnelson. "Optimal Hubbard Models for Materials with Nonlocal Coulomb Interactions: Graphene, Silicene, and Benzene". In: *Phys. Rev. Lett.* 111 (3 July 2013), p. 036601. DOI: 10.1103/PhysRevLett.111.036601. URL: http://link.aps.org/doi/10.1103/PhysRevLett.111.036601.

[128]   F. Schütz, P. Kopietz, and M. Kollar. "What are spin currents in Heisenberg magnets?" In: *The European Physical Journal B - Condensed Matter and Complex Systems* 41.4 (2004), pp. 557–560. ISSN: 1434-6036. DOI: 10.1140/epjb/e2004-00348-9. URL: http://dx.doi.org/10.1140/epjb/e2004-00348-9.

[129]   Anirvan M. Sengupta and Antoine Georges. "Non-Fermi-liquid behavior near a T=0 spin-glass transition". In: *Phys. Rev. B* 52 (14 Oct. 1995), pp. 10295–10302. DOI: 10.1103/PhysRevB.52.10295. URL: https://link.aps.org/doi/10.1103/PhysRevB.52.10295.

[130]   J. W. Serene and D. W. Hess. "Quasiparticle properties of the two-dimensional Hubbard model in a propagator-renormalized fluctuation-exchange approximation". In: *Phys. Rev. B* 44 (7 Aug. 1991), pp. 3391–3394. DOI: 10.1103/PhysRevB.44.3391. URL: https://link.aps.org/doi/10.1103/PhysRevB.44.3391.

[131]   Priyanka Seth, Igor Krivenko, Michel Ferrero, and Olivier Parcollet. "TRIQS/CTHYB: A continuous-time quantum Monte Carlo hybridisation expansion solver for quantum impurity problems". In: *Computer Physics Communications* 200.Supplement C (2016), pp. 274–284. ISSN: 0010-4655. DOI: https://doi.org/10.1016/j.cpc.2015.10.023. URL: http://www.sciencedirect.com/science/article/pii/S001046551500404X.

[132]   Y. Shimizu, K. Miyagawa, K. Kanoda, M. Maesato, and G. Saito. "Spin Liquid State in an Organic Mott Insulator with a Triangular Lattice". In: *Phys. Rev. Lett.* 91 (10 Sept. 2003), p. 107001. DOI: 10.1103/PhysRevLett.91.107001. URL: https://link.aps.org/doi/10.1103/PhysRevLett.91.107001.

[133]   H. Shinaoka, F. Assaad, N. Blümer, and P. Werner. "Quantum Monte Carlo impurity solvers for multi-orbital problems and frequency-dependent interactions". In: *The European Physical Journal Special Topics* 226.11 (July 2017), pp. 2499–2523. ISSN: 1951-6401. DOI: 10.1140/epjst/e2017-70050-x. URL: https://doi.org/10.1140/epjst/e2017-70050-x.

[134] Qimiao Si and J. Lleweilun Smith. "Kosterlitz-Thouless Transition and Short Range Spatial Correlations in an Extended Hubbard Model". In: *Phys. Rev. Lett.* 77 (16 Oct. 1996), pp. 3391–3394. DOI: 10.1103/PhysRevLett.77.3391. URL: http://link.aps.org/doi/10.1103/PhysRevLett.77.3391.

[135] J. C. Slater. "Magnetic Effects and the Hartree-Fock Equation". In: *Phys. Rev.* 82 (4 May 1951), pp. 538–541. DOI: 10.1103/PhysRev.82.538. URL: https://link.aps.org/doi/10.1103/PhysRev.82.538.

[136] J. Lleweilun Smith and Qimiao Si. "Spatial correlations in dynamical mean-field theory". In: *Phys. Rev. B* 61 (8 Feb. 2000), pp. 5184–5193. DOI: 10.1103/PhysRevB.61.5184. URL: http://link.aps.org/doi/10.1103/PhysRevB.61.5184.

[137] E. A. Stepanov, S. Brener, F. Krien, M. Harland, A. I. Lichtenstein, and M. I. Katsnelson. "Effective Heisenberg model and exchange interaction for strongly correlated systems". In: *t.b.p.* (2018).

[138] E. A. Stepanov, E. G. C. P. van Loon, A. A. Katanin, A. I. Lichtenstein, M. I. Katsnelson, and A. N. Rubtsov. "Self-consistent dual boson approach to single-particle and collective excitations in correlated systems". In: *Phys. Rev. B* 93 (4 Jan. 2016), p. 045107. DOI: 10.1103/PhysRevB.93.045107. URL: http://link.aps.org/doi/10.1103/PhysRevB.93.045107.

[139] Ping Sun and Gabriel Kotliar. "Extended dynamical mean-field theory and GW method". In: *Phys. Rev. B* 66 (8 Aug. 2002), p. 085120. DOI: 10.1103/PhysRevB.66.085120. URL: http://link.aps.org/doi/10.1103/PhysRevB.66.085120.

[140] Hanna Terletska, Tianran Chen, and Emanuel Gull. "Charge ordering and correlation effects in the extended Hubbard model". In: *Phys. Rev. B* 95 (11 Mar. 2017), p. 115149. DOI: 10.1103/PhysRevB.95.115149. URL: https://link.aps.org/doi/10.1103/PhysRevB.95.115149.

[141] A. Toschi, A. A. Katanin, and K. Held. "Dynamical vertex approximation: A step beyond dynamical mean-field theory". In: *Physical Review B (Condensed Matter and Materials Physics)* 75.4, 045118 (2007), p. 045118. DOI: 10.1103/PhysRevB.75.045118. URL: http://link.aps.org/abstract/PRB/v75/e045118.

[142] Tadashi Toyoda and Masamichi Okada. "Exact relations for the spin-correlation functions for an interacting electron gas in a nonuniform magnetic field". In: *Phys. Rev. B* 58 (3 July 1998), pp. 1210–1217. DOI: 10.1103/PhysRevB.58.1210. URL: http://link.aps.org/doi/10.1103/PhysRevB.58.1210.

[143] A.-M. S. Tremblay. "Two-Particle-Self-Consistent Approach for the Hubbard Model". In: (2011). Ed. by A. Avella and F. Mancini.

[144] André-Marie S. Tremblay. "Two-Particle-Self-Consistent Approach for the Hubbard Model". In: *Strongly Correlated Systems*. Ed. by Adolfo Avella and Ferdinando Mancini. Vol. 171. Springer Series in Solid-State Sciences. Springer Berlin Heidelberg, 2012, pp. 409–453. ISBN: 978-3-642-21830-9. DOI: 10.1007/978-3-642-21831-6_13. URL: http://dx.doi.org/10.1007/978-3-642-21831-6_13.

[145] H. J. Vidberg and J. W. Serene. "Solving the Eliashberg equations by means of N-point Padé approximants". In: *J. Low Temp. Phys.* 29 (3 1977), pp. 179–192. DOI: 10.1007/BF00655090.

[146] Y. M. Vilk, Liang Chen, and A.-M. S. Tremblay. "Theory of spin and charge fluctuations in the Hubbard model". In: *Phys. Rev. B* 49 (18 May 1994), pp. 13267–13270. DOI: 10.1103/PhysRevB.49.13267. URL: http://link.aps.org/doi/10.1103/PhysRevB.49.13267.

[147] D. Vollhardt, N. Blümer, K. Held, M. Kollar, J. Schlipf, and M. Ulmke. "Non-perturbative approaches to magnetism in strongly correlated electron systems". In: *Zeitschrift für Physik B Condensed Matter* 103.2 (June 1996), pp. 283–292. ISSN: 1431-584X. DOI: 10.1007/s002570050375. URL: https://doi.org/10.1007/s002570050375.

[148] D. Vollhardt and A. I. Lichtenstein. "Dynamical mean-field approach with predictive power for strongly correlated materials". In: *The European Physical Journal Special Topics* 226.11 (July 2017), pp. 2439–2443. ISSN: 1951-6401. DOI: 10.1140/epjst/e2017-70078-x. URL: https://doi.org/10.1140/epjst/e2017-70078-x.

[149] D. Vollhardt and P. Wölfle. "Diagrammatic, self-consistent treatment of the Anderson localization problem in $d \leq 2$ dimensions". In: *Phys. Rev. B* 22 (10 Nov. 1980), pp. 4666–4679. DOI: 10.1103/PhysRevB.22.4666. URL: http://link.aps.org/doi/10.1103/PhysRevB.22.4666.

[150] Dieter Vollhardt. "Normal ^{3}He: an almost localized Fermi liquid". In: *Rev. Mod. Phys.* 56 (1 Jan. 1984), pp. 99–120. DOI: 10.1103/RevModPhys.56.99. URL: https://link.aps.org/doi/10.1103/RevModPhys.56.99.

[151] J. C. Ward. "An Identity in Quantum Electrodynamics". In: *Phys. Rev.* 78 (2 Apr. 1950), pp. 182–182. DOI: 10.1103/PhysRev.78.182. URL: http://link.aps.org/doi/10.1103/PhysRev.78.182.

[152] X. G. Wen, Frank Wilczek, and A. Zee. "Chiral spin states and superconductivity". In: *Phys. Rev. B* 39 (16 June 1989), pp. 11413–11423. DOI: 10.1103/PhysRevB.39.11413. URL: https://link.aps.org/doi/10.1103/PhysRevB.39.11413.

[153] Philipp Werner and Andrew J. Millis. "Efficient Dynamical Mean Field Simulation of the Holstein-Hubbard Model". In: *Phys. Rev. Lett.* 99 (14 Oct. 2007), p. 146404. DOI: 10.1103/PhysRevLett.99.146404. URL: http://link.aps.org/doi/10.1103/PhysRevLett.99.146404.

[154] R. van Wesep. "A Brief Introduction to Linear Response Theory with Examples in Electromagnetic Response". In: *unpublished article* (2013).

[155] Wenhu Xu, Kristjan Haule, and Gabriel Kotliar. "Hidden Fermi Liquid, Scattering Rate Saturation, and Nernst Effect: A Dynamical Mean-Field Theory Perspective". In: *Phys. Rev. Lett.* 111 (3 July 2013), p. 036401. DOI: 10.1103/PhysRevLett.111.036401. URL: https://link.aps.org/doi/10.1103/PhysRevLett.111.036401.

[156] S.-X. Yang, H. Fotso, H. Hafermann, K.-M. Tam, J. Moreno, T. Pruschke, and M. Jarrell. "Dual fermion dynamical cluster approach for strongly correlated systems". In: *Phys. Rev. B* 84 (15 Oct. 2011), p. 155106. DOI: 10.1103/PhysRevB.84.155106. URL: https://link.aps.org/doi/10.1103/PhysRevB.84.155106.

[157] Y.M. Vilk and A.-M.S. Tremblay. "Non-Perturbative Many-Body Approach to the Hubbard Model and Single-Particle Pseudogap". In: *J. Phys. I France* 7.11 (1997), pp. 1309–1368. DOI: 10.1051/jp1:1997135. URL: http://dx.doi.org/10.1051/jp1:1997135.

[158] Farzaneh Zamani, Pedro Ribeiro, and Stefan Kirchner. "The functional integral formulation of the Schrieffer–Wolff transformation". In: *New Journal of Physics* 18.6 (2016), p. 063024. URL: http://stacks.iop.org/1367-2630/18/i=6/a=063024.

[159] M. M. Zemljič and P. Prelovšek. "Resistivity and optical conductivity of cuprates within the $t-J$ model". In: *Phys. Rev. B* 72 (7 Aug. 2005), p. 075108. DOI: 10.1103/PhysRevB.72.075108. URL: https://link.aps.org/doi/10.1103/PhysRevB.72.075108.

[160] Rok Žitko and Michele Fabrizio. "Non-Fermi-liquid behavior in quantum impurity models with superconducting channels". In: *Phys. Rev. B* 95 (8 Feb. 2017), p. 085121. DOI: 10.1103/PhysRevB.95.085121. URL: https://link.aps.org/doi/10.1103/PhysRevB.95.085121.

[161] Rok Žitko and Michele Fabrizio. "Z_2 gauge theory description of the Mott transition in infinite dimensions". In: *Phys. Rev. B* 91 (24 June 2015), p. 245130. DOI: 10.1103/PhysRevB.91.245130. URL: https://link.aps.org/doi/10.1103/PhysRevB.91.245130.

Hopping/hybridization	$\varepsilon_{\mathbf{k}}, \Delta_\nu$
Matsubara energy (bos./ferm.)	ω, ν
Momentum (bos./ferm.)	$\mathbf{q}, \mathbf{k}$
(Inverse) temperature	$(\beta), T$
Real energy	E
Chemical potential	μ
Magnetic field	h
Qasiparticle weight	Z
Double occupancy	d
Channel index	$\alpha = c, x, y, z$
Pauli matrices	$s^\alpha_{\sigma,\sigma'}, \hat{s}^c = \hat{1}$
Time-ordering operator	T_τ
Density operators (continuum/lattice)	$\varrho^\alpha_{\mathbf{r}}, \rho^\alpha_i$
Bosonic self-energy	$\widetilde{\Pi}_{\mathbf{q}\omega}$
Triangular vertex	$\lambda_{\nu\omega}$
Luttinger-Ward functional	Φ, ϕ
Hubbard repulsion	U
Nonlocal potential (charge/spin)	$V^c, V^{x,y,z}$
Retarded interaction	$\Lambda^c, \Lambda^{x,y,z}$
Bosonic energy	$\Omega^\alpha_{\boldsymbol{q}}$
Fermion-boson coupling	$w^\alpha_{\boldsymbol{q}}$
Bosonic propagator	$\mathcal{D}^\alpha_{\boldsymbol{q}\omega}$
Levi-Civita tensor	$\varepsilon_{\alpha\beta\gamma}$
1P Green's function	G_k, g_ν
2P Green's function	$G^{(2)}_{kk'q}, g^{(2)}_{\nu\nu'\omega}$
Susceptibility	X_q, χ_ω
Bubble	$X^0_{kq}, \chi^0_{\nu\omega}$
Bubble (matrix)	$X^0_{kk'q} = N\beta\delta_{kk'}X^0_{kq}, \chi^0_{\nu\nu'\omega} = \beta\delta_{\nu\nu'}\chi^0_{\nu\omega}$ or $\hat{X}^0_q, \hat{\chi}^0_\omega$
Bubble (summed)	$X^0_q = \sum_k X^0_{kq}, \chi^0_\omega = \sum'_\nu \chi^0_{\nu\omega}$
Nonlocal bubble (matrix)	$\tilde{X}^0_{kk'q}$ or $\hat{\tilde{X}}^0_q$
Gen. susceptibility	$X_{kk'q}, \chi_{\nu\nu'\omega}$ or $\hat{X}_q, \hat{\chi}_\omega$
1P self-energy	Σ_k, Σ_ν
2P self-energy	$\Gamma_{kk'q}, \gamma_{\nu\nu'\omega}$ or $\hat{\Gamma}_q, \hat{\gamma}_\omega$
T-matrix	$F_{kk'q}, f_{\nu\nu'\omega}$ or $\hat{F}_q, \hat{f}_\omega$
Chiral 3P correlation function	$X^{\alpha\beta\gamma}_{kk'k''qp}, \chi^{\alpha\beta\gamma}_{\nu\nu'\nu''\omega\omega'}$

List of Publications

Refereed publications:

- Darya Medvedeva, Sergei Iskakov, Friedrich Krien, Vladimir V. Mazurenko, and Alexander I. Lichtenstein. "Exact diagonalization solver for extended dynamical mean-field theory". In: *Phys. Rev. B* 96 (23 Dec. 2017), p. 235149. DOI: 10. 1103/PhysRevB.96.235149. URL: https://link.aps.org/doi/10.1103/PhysRevB. 96.235149

- Friedrich Krien, Erik G. C. P. van Loon, Hartmut Hafermann, Junya Otsuki, Mikhail I. Katsnelson, and Alexander I. Lichtenstein. "Conservation in two-particle self-consistent extensions of dynamical mean-field theory". In: *Phys. Rev. B* 96 (7 Aug. 2017), p. 075155. DOI: 10.1103/PhysRevB.96.075155. URL: https: //link.aps.org/doi/10.1103/PhysRevB.96.075155

- Erik G. C. P. van Loon, Friedrich Krien, Hartmut Hafermann, Evgeny A. Stepanov, Alexander I. Lichtenstein, and Mikhail I. Katsnelson. "Double occupancy in dynamical mean-field theory and the dual boson approach". In: *Phys. Rev. B* 93 (15 Apr. 2016), p. 155162. DOI: 10.1103/PhysRevB.93.155162. URL: http: //link.aps.org/doi/10.1103/PhysRevB.93.155162

Publications in preparation:

- E. A. Stepanov, S. Brener, F. Krien, M. Harland, A. I. Lichtenstein, and M. I. Katsnelson. "Effective Heisenberg model and exchange interaction for strongly correlated systems". In: *t.b.p.* (2018)

Eidesstattliche Erklärung

Hiermit versichere ich an Eides statt, die vorliegende Dissertationsschrift selbst verfasst und keine anderen als die angegebenen Hilfsmittel und Quellen benutzt zu haben.

Die eingereichte schriftliche Fassung entspricht der auf dem elektronischen Speichermedium.

Die Dissertation wurde in der vorgelegten oder einer ähnlichen Form nicht schon einmal in einem früheren Promotionsverfahren angenommen oder als ungenügend beurteilt.

Unterschrift:

_____

Datum:

_____

Acknowledgments

I like to thank my supervisor Alexander Lichtenstein for his kindness, his patience, and his advice during my years as a PhD student. These were there in the same way back then, when I knew nothing, and now that I know a little, which is something that I will keep in mind should I be responsible later myself. Then, there are the funding, the summer schools, conferences, and travels that he sponsored, that have all contributed to my growth and development as a physicist.

All the work presented here is based on, or inspired by, the solid body of work that Hartmut Hafermann and Erik van Loon have manufactured before me, the dual boson implementation, various scripts, their publications, to name the least bits. Beyond that I can say with confidence that if there is one proper argument in this text it is here thanks to the cathartic act of writing my paper with Hartmut. This was the exact thing I needed and it will help me for the rest of my life, regardless of what I will do in the future. Erik helped me immensely with his responsiveness over a long time, he was often the only one who knew the details and he always shared them. I thank Junya Otsuki for his advice that helped me to understand finally what is going on in the spin channels. It was only possible to develop the ideas that are presented here because I had access to his spin-boson CTQMC solver, he therefore greatly contributed to this work. I like to thank Alexey Rubtsov and Silke Biermann for their invitations to Moscow and Paris and Mikhail Katsnelson for his advice during the production of the paper on conservation laws and the invitation to his anniversary in Nijmegen. I am very grateful to Jindrich Kolorenč and Vaclav Janiš for the opportunity to present my work in Prague and to Jernej Mravlje, Rok Žitko, and Peter Prelovšek, who gave me a very warm welcome at the Jožef Stefan institute and who offered me to write there on my thesis. Then, I am delighted to have been invited to Trieste by Massimo Capone and Michele Fabrizio, and about the opportunity to work with them in the near future on Hund's metals. I knew that my six years of Latin would one day help me. It has been a pleasure to work with Sergey Iskakov and Darya Medvedeva using EDMFT and with Evgeny Stepanov and Sergey Brener, who found a nice application for the impurity Ward identity. I like to thank the whole work group in Hamburg for a wonderful time, including the multilateral discussions at lunch, we have been an enrichment to the law school, unfortunately never quite getting the due recognition by its students. Burkhard Sachs and Viktor Valmispild have been great office neighbors, thanks to inspiring conversations on just about anything, but also because I presumably leave the stage with a net plus in muffins and of approximately five nuts. It has also been a pleasure to visit from time to time the other offices, where Malte Harland, Daniel Hirschmeier, Aljoscha Wilhelm, Roberto Mozara, Yusuf Mohammed, Arthur Huber, Patryk Kubiczek, Mikhail Danilov and Oleg Kristanovski were readily available for (non-)work-related things. I also like to remember the times with Igor Krivenko and Maria Valentyuk, who were joined by

204